Assessing the Structure and Function of the Posterior Visual Pathway in Eye Disease

Holly Diane Brown

Doctor of Philosophy

Cognitive Neuroscience and Neuroimaging

University of York

Psychology

March 2021

Abstract

This thesis examines the consequences of partial vision loss, namely macular disease (MD), on both the structure and function of the posterior visual pathway. Using both cross-sectional and longitudinal analyses we explored how the anatomy of MD patients may change differently than in those aging naturally. The patient group showed reduced cortical thickness, which appears to largely impact the anatomical representation of central vision. However, they also showed reduced fractional anisotropy of the underlying white matter; but both the fiber bundles projecting to central *and* peripheral representations in early visual cortex were affected, suggesting broader deficits emerge in visual white matter. Our longitudinal assessments identified continued decline in cortical thickness and myelin density, even in long-standing vision loss, but individual case studies indicate the greatest changes in cortex likely emerge early in the disease following functional vision loss. We next assessed how partial vision loss may impact functional connectivity between striate and extrastriate cortex and found a selective reduction in functional connectivity between striate and the fusiform face area patients with central field loss. Finally, we used transient retinal lesions to test for responses in a 'simulated lesion projection zone' (sLPZ) in sighted participants, providing some evidence that peripheral visual stimulation can produce 'patient-like' responses in central representations in some individual controls while performing a task. This suggests LPZ responses - often deemed the 'signature of reorganization of visual processing' - may be driven by unmasked top-down feedback. Collectively, our findings add to growing evidence for atrophy in the posterior visual pathway in MD. Given that the viability of the visual brain may limit the success of visual restoration, development of neuroprotective strategies will benefit from a better understanding of the time scale and magnitude of changes observed in the brain following MD.

List of Contents

List of Tables

List of Figures

List of Appendices

Acknowledgements

I have many people to thank, who have in their own ways contributed to the success of this thesis, whether it be supporting the research directly, or simply providing support for me personally throughout the whole process.

To my family – thank you for putting up with all the talk of eyes and brains. Your unconditional love and support during my academic journey have been amazing, especially during times of hardship. We lost some incredible people since I started the PhD, and I would like to dedicate my thesis to them; my Grandad John and my stepmother Joan – the life and soul of any party who both taught me not to shy away from hard work, not to take myself too seriously and embrace every opportunity thrown my way. I love and miss you every day.

Professor Antony Morland – my supervisor and mentor for the last 6 years - it has been an absolute pleasure to work with you. You created such a warm and friendly atmosphere in which to work and provided so many opportunities for us to grow as researchers and as people. Your continued support, guidance and constructive criticism have been invaluable; thank you for believing in me and for helping to keep the imposter syndrome demons at bay.

I would like to thank my thesis advisory panel, Dr Heidi Baseler and Professor Tim Andrews. Having worked with you both prior to the PhD, I was so pleased you could continue to be a part of this journey. Thank you for your guidance, feedback, and continued support over the last few years.

To our collaborators, Professor Richard Gale, the Ophthalmology research team, and the R&D team at York Teaching Hospital – thank you for helping me navigate research within the NHS and for helping develop my research skills outside of the university environment. A special thanks also goes to the local organisations who I have had the pleasure of working with over the last few years, who have helped me engage with the sight loss community and find some budding volunteers. This includes Fight for Sight UK, the Macular Society groups in both York and Leeds, MySight York, Doncaster's Partially Sighted Society and Blind Veterans UK.

A heartfelt thanks goes out to all the wonderful people who engaged with and participated in my research; your enthusiasm for science, inquisitive nature and

commitment to the projects made the whole process so enjoyable. It was a privilege to get to know you all.

To my science family both past and present in the Department of Psychology and YNiC, with a special shout out to Rachel, Richard, Sam, Becky, Martin, Babs, Ellie, Elisa, Theo & Jamie - thank you for keeping me grounded, especially during the final year which can be difficult at the best of times, let alone when it coincides with a global pandemic. A special thanks also goes to Dr André Gouws - your generosity knows no bounds, and you have been such a patient and brilliant mentor throughout my time at York. I genuinely could not have gotten through some of the challenges faced without the unwavering support and kindness you have all shown me. I feel very fortunate to have worked alongside friends every day.

I am very lucky to have an equally brilliant group of friends outside of the university. To my netball teammates – I am so proud of how far we have come over the last 4 years, working our way up to higher divisions and more competitive netball leagues. Thank you for trusting me to be your captain last year, for giving me something to focus on outside of the PhD and for the many laughs both on and off court. I would also like to acknowledge our lab's favourite watering hole – the Rook and Gaskill - for putting up with our nonsense and always making us feel at home on a Thursday evening for several years. I look forward to returning for a celebratory pint once it is safe for us to do so.

Finally, a PhD can easily become all-consuming and having a good work/life balance is difficult enough at the best of times, but during multiple national lockdowns this became very difficult to manage, especially when living alone. I would like to thank Ben (New Leaf Physical Training) for being the lifeline I (and many others) needed during the pandemic. Without your infectious optimism and tough (but fun) virtual fitness classes, I would not have maintained a healthy lifestyle and my work would have suffered this past year as a result. To everyone who took the time to come on socially-distanced walks with me, reached out for extra virtual catchups, and to my social bubble – Becky and Phil – thank you for keeping me going.

Declaration

I declare that this thesis is a presentation of original work carried out under the supervision of Professor Antony B. Morland, and I am the sole author. This work has not previously been presented for an award at this, or any other, University. All sources are acknowledged as References.

Content from **Chapter 1** (notably Figure 1.3) were adapted for the publication below:

> Brown, HDH, Morland, AB. (2019) Consequences of ocular disease on the brain. *Optometry Today, (62-66)*

Structural MRI data for the first time point for 12 of the sighted controls (referred to as C1-C12) included in **Chapters 2 and 3** was collected prior to my PhD for a separate project completed with Rachel L. W. Hanson in 2016. Raw data were used for this thesis, and I analysed this separately alongside additional data I acquired on the same participants in 2018.

For **Chapters 2 and 3**, the structural MRI data for the first time point for 6 controls (referred to as C13-C18), as well as the two case studies (referred to as MD7 and MD13 in Chapters 2 and 3) were collected by researchers in Professor Jonathan Smallwood and Professor Elizabeth Jeffries teams in 2016 at the York Neuroimaging Centre. Permission was granted by the PI's for me to use the raw data and analyse separately along with the more recent data I acquired on these individuals myself. I recruited the same individuals through the participant pool following ethical approval from the York Neuroimage Centre ethics committee.

Visual Acuity measures for **Chapters 2 and 3** were collected by me, the Ophthalmology Research Team at York Teaching Hospital Foundation Trust under the supervision of Professor Richard Gale, and some were self-reported by the participants who were not recruited through the hospital directly.

Data reported in **Chapter 2** were presented at the European Conference of Visual Perception (2019), Leuven, Belgium and the abstract was published as:

> Brown, Holly DH; Gale, Richard P; Vernon, Richard JW; Gouws, Andre D; Baseler, Heidi A; Morland, Antony B; Assessing the Status of Visual Cortex in Macular Disease. *Perception(48), 172-172*

Data reported in **Chapter 2** were presented at the Applied Vision Association Christmas meeting (2019), Cardiff, UK, as:

Brown, Holly DH; Gale, Richard P; Vernon, Richard JW; Gouws, Andre D; Baseler, Heidi A; Morland, Antony B; *Assessing the Status of Visual Cortex in Macular Disease.*

Chapter 6 is currently under review (at the time of thesis submission) at Brain Structure and Function, as:

Brown, Holly DH; Gouws, André D; Vernon, Richard JW; Lawrence, Samuel JD; Donnelly, Gemma; Gill, Lorraine; Gale, Richard P; Baseler, Heidi A; Morland, Antony B (under review), Assessing functional reorganisation in visual cortex with simulated retinal lesions. *Brain Structure and Function.*

Chapter 1: A review of the neural and behavioural consequences of eye disease

1.1 Overview

The central aim of this thesis is to enhance our understanding of how the brain is impacted by eye disease, specifically in the visual cortex. The primary question in this field asks whether visual cortex remains dormant due to lack of visual input, deteriorates over time, or whether it undergoes some form of cortical reorganisation which may help patients process remaining vision more effectively. Whilst it is the eye that receives visual input, it is often forgotten that the brain processes and makes sense of incoming information. A great deal of clinical research on eye disease has focused on the physiological changes and degeneration of the eye with the aim of preventing, treating, and restoring functionally useful vision. Comparatively fewer studies are actively monitoring other aspects of vision, notably the consequences on basic visual perception such as face or object recognition, as well as the neural consequences of eye disease. Magnetic Resonance Imaging (MRI) has provided neuroscientists with a safe and non-invasive means of evaluating both the structure and function of the human brain. Approximately 20% of cortex within the human brain is recruited to process visual information, primarily occupying the occipital lobe, and extending to temporal and parietal regions (Wandell, Dumoulin, & Brewer, 2007). Given that sight ultimately takes place in the brain, structural and functional consequences of sight loss on both the anterior (eye) and posterior (brain) parts of the visual pathway should be explored together.

This review will explore different methods employed by researchers to assess the extent to which eye disease impacts on visual cortex, considering both neural and behavioural consequences. First, research concerning structural changes in the brain will be considered for different types of eye disease, primarily the leading causes of blindness - macular degeneration and glaucoma. Additionally, it will also provide an overview of an on-going debate within the literature concerning whether cortical reorganisation occurs following vision loss, a question that will be addressed further in Chapter 6. Finally, the review will discuss the importance of refining methods used with visually impaired individuals, and the impact this has on clinical research, for which efforts are currently focused on restoring visual function.

The focus of the review will be on studies investigating visual loss; however it must be acknowledged that fMRI is widely used to examine how the brain represents the visual world in normally-sighted individuals, which provides the necessary context for understanding how mechanisms underlying 'normal' visual function can be affected by eye disease. The opening section of this review will also discuss the structural changes associated with natural aging, to provide context particularly when discussing research investigating structural changes associated with vision loss in an aging population. Given that most studies investigate age-related visual diseases, it is important to know how the brain changes due to natural aging, enabling us to disentangle whether it is aging or eye disease that is driving any changes observed in visual cortex in visually impaired participants. Additionally, for the most part, degeneration of the eye is the cause of visual dysfunction, however there are cases where the eyes remain intact but damage to the visual brain (from trauma or disease) results in visual deficits (Brown, Woodall, Kitching, Baseler, & Morland, 2016). This review will focus on visual loss caused by eye disease, given that partially sighted individuals recruited for the empirical chapters have forms of eye disease only.

1.2 Overview of eye diseases

Throughout this review, literature relating to different forms of central and peripheral vision loss will be discussed in the context of what we already know about visual processing in normally sighted individuals. Primarily, macular degeneration (both age-related and inherited forms), glaucoma, and retinitis pigmentosa will be discussed. Whilst it is known that visual loss may have other underlying causes, they will not be covered in detail in this review.

1.2.1 Macular degeneration

Macular degeneration (MD) refers to a collection of disorders which cause a progressive loss of the central vision following damage to the macula, the central part of the retina. There are a sub-group of disorders which have an early onset and are commonly known as juvenile macular dystrophies (JMD), and those with a later onset are collectively referred to as age-related macular degeneration (AMD). Stargardt's disease and cone rod dystrophy (CRD) are among the most common inherited juvenile forms of MD. Like AMD, forms of JMD are progressive, with an earlier onset and typically, a faster progression. With Stargardt's disease, there is a

known mutation of the ABCA4 gene (Lois, Halfyard, Bird, Holder, & Fitzke, 2004). Fatty substances accumulate within the RPE which in turn causes the photoreceptors in the macular to degenerate. CRD refers to a collection of disorders causing progressive vision loss first affecting the cones and later in the disease, the rods. CRD is caused by mutations in multiple genes, some of which are linked to other diseases such as Stargardt's disease and retinitis pigmentosa (Gill, Georgiou, Kalitzeos, Moore, & Michaelides, 2019).

Currently, AMD is the leading cause of central visual loss in the western world (Rostron & McKibbin, 2012). In the UK, approximately 2.4% of individuals aged 50+ year, 4.8% aged over 65 years and 12.2% aged over 80 years are affected by late stage AMD (NICE, 2018). Whilst most forms of JMD are inherited, AMD as the name suggests, occurs later in life with a variety of different risk factors, most notably smoking (Lim, Mitchell, Seddon, Holz, & Wong, 2012). There are two forms of AMD as shown in Figure 1.1: neovascular or 'wet' AMD, and geographic atrophy or 'dry' AMD. Dry AMD is the most common form, characterised by the progressive build-up of drusen (waste products) in the retinal pigment epithelium (RPE), in turn damaging the photoreceptors and causing the loss of central vision. Wet AMD damages the macular in a different way; blood, lipids and fluid leak and cause swelling under the macula. Additionally, the breakthrough of new blood vessel growth to the neural retinal (choroidal neovascularisation) results in scarring. Dry AMD is currently the most common form of age-related vision loss, yet currently there is no cure. The wet form is more treatable, and patients are recommended to have anti-vascular endothelial growth factor drugs (anti-VEGF) which aim to prevent further leaks and prevent the growth of new blood vessels. This does not necessarily result in improved vision in all cases, but it does prevent the progression of the disease and stabilise vision, and so interventions should be administered at the earliest time in order to preserve more vision (Lim et al., 2012).
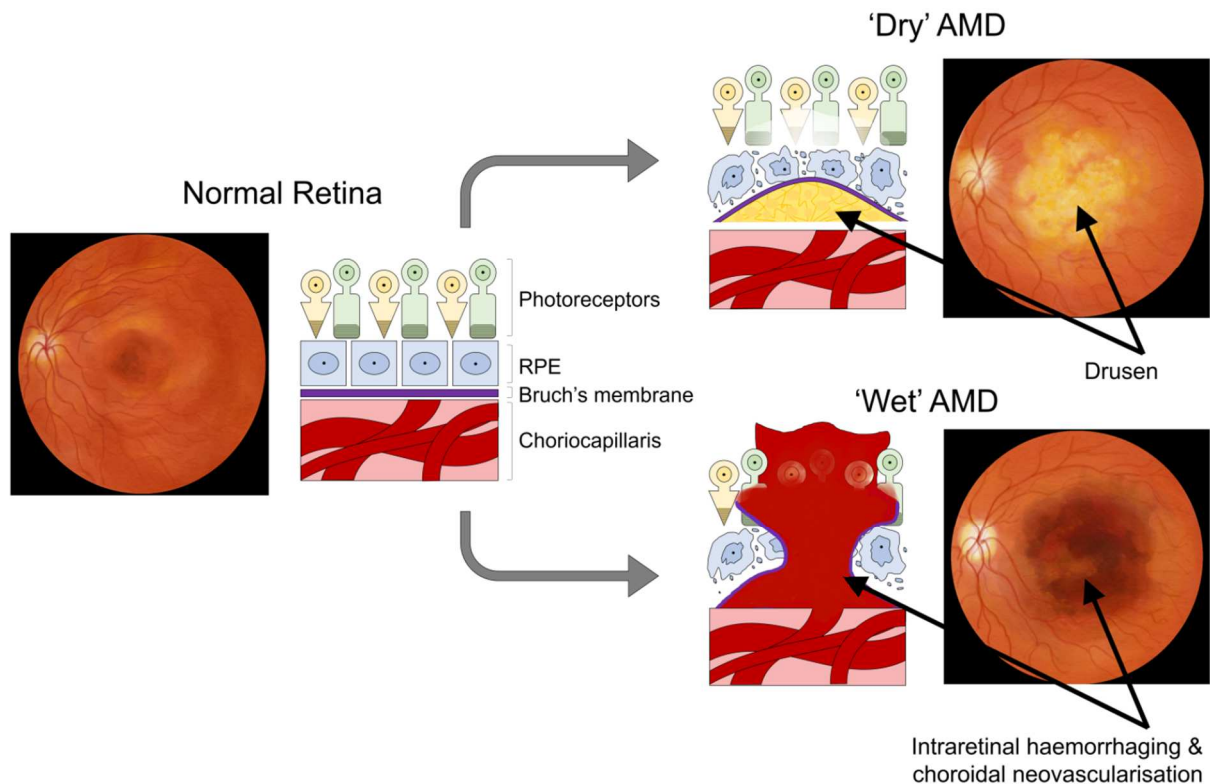
Figure 1.1. Illustrations of the retina and schematics of the outer layers of the retina in normally sighted individuals, dry AMD, and wet AMD. Both forms damage the retinal pigment epithelium (RPE) but through different mechanisms. In dry AMD, a fatty waste product – drusen - builds up and can be detected in retinal imaging (yellow substance appearing in the macula). The cross-sectional schematic of part of the retina shows the build-up of drusen which in turn damages the RPE and photoreceptors, largely the cones. In wet AMD, the damage is caused by the growth of leaky blood vessels, which if not treated with anti-VEGF drugs, will continue to haemorrhage (reddening of the macula in the retinal image) and damage multiple layers in the retina.

1.3. Structural changes associated with natural aging

It is known that as we age, our brains show signs of gradual structural decline. Structural changes refer to reductions in cortical thickness, volume and/or surface area, the extent to which increases with age. This happens gradually over the lifespan as a result of the natural aging process, notably after 50 years of age (Salat et al., 2004). However, in cases of neurological disease, eye disease or trauma to the eye or brain, changes can become more significant and can occur more rapidly, depending on the nature of the disease. Collectively, research has tried to establish three key points: (1) what the expected rate of change is in the human brain with normal aging, (2) determine whether any observed changes are uniform and constant across the whole brain, or (3) whether there are specific brain regions with more rapid changes.

For visual areas, evidence concerning structural changes is quite mixed; earlier studies found small changes in the occipital cortex, including the occipital pole (Fjell et al., 2009; Salat et al., 2004), while others have seen no significant change in primary visual cortex (Naftali Raz et al., 2005; Thambisetty et al., 2010). One study of interest examined visual cortex in more detail, parcellating visual cortex into 9 different regions of interest (ROIs), each representing a different mean eccentricity, ranging from < 1˚, up to 63.3˚ (Griffis, Burge, & Visscher, 2016). Different portions of the calcarine sulcus were examined, including the sulcal wall, gyral crown, as well as the sulcus depth. Results showed a significant interaction between age group and ROI whereby older participants exhibit a reduction in cortical thickness in the 4 ROIs representing the most eccentric parts of vision – the more anterior portions of the calcarine sulcus. No significant differences between age groups were observed for the more central representations (up to 7˚ eccentricity). Findings suggest that peripheral vision may be more affected by age-related decline in contrast to central vision (Griffis et al., 2016). Whilst this study did not acquire any measures of visual acuity or assess visual perception at different eccentricities, previous studies using tasks engaging peripheral vision have supported this conclusion. Distractor and attention-based tasks highlight a steep decline in performance, associated with aging (Ball, Edwards, & Ross, 2007; Owsley, 2011). Arguably, any attention-driven tasks will rely on central vision and sighted individuals will always opt to use their central vision to complete tasks successfully. Perhaps this biases us to use central vision, and by not utilising peripheral vision to the same extent, any deterioration in peripheral vision may go undetected. This may also explain how glaucoma can go unnoticed for many years. This work is of particular interest when determining how visual cortex changes as a result of disease versus natural aging; this will be explored further in this thesis.

Evidence has been largely mixed, primarily because of the varying methods used to parcellate the brain into different ROIs, but also because most studies use a cross-sectional design, incorporating data from a range of ages as opposed to conducting within-subject comparisons over time. Furthermore, it is known that in contrast to non-visual brain regions, visual cortex, particularly primary visual cortex is thin, and as such, some protocols or analysis techniques may not be sensitive enough to detect subtle changes in cortical thickness (Glasser, Goyal, Preuss, Raichle, & Van

Essen, 2014). Studies which interrogated the calcarine sulcus further by parcellating it into regions representing different parts of the visual field are more likely to detect subtle changes compared to those who opted for examining the calcarine sulcus as a whole. Due to cortical magnification, it is likely any subtle changes in more anterior calcarine sulcus are averaged out by the stability of central representations. To address this gap in the literature, a longitudinal study following patients with macular disease, as well as sighted controls, will be described Chapter 2.

Cortical myelin can also be assessed using in vivo MRI; areas of cortex known to be thinner such as the primary sensory regions are often highly myelinated, apart from motor cortex (Glasser & Van Essen, 2011). It has been suggested that regions with more myelin are often considered to be less 'plastic'; primary visual cortex is a good example as it is present in those who are congenitally blind and it develops without the need for visual experience (Glasser et al., 2014). Cortical regions deemed as being capable of greater plasticity are thought to be thicker and consist of more complex intracortical circuits (Glasser et al., 2014). With natural aging, degeneration is not limited to just cortical neurons, but also extends to myelin. Oligodendrocytes – cells within the central nervous system that produce myelin – are considered to be the most vulnerable cells within the brain (Peters, 2002).

Whilst cortical myelin is thought to be better preserved with age compared to myelin in the white matter, it is important to recognise that degeneration is not uniform across the whole brain (Fjell & Walhovd, 2010; Lu et al., 2011; Peters, 2002). Myelination in prefrontal and association areas continues well into our 40's whereas primary sensory regions such as the visual cortex are heavily myelinated in early life, commencing in utero, and appear to be least affected by natural aging (Fjell & Walhovd, 2010). Areas undergoing myelination later in life are the most vulnerable to aging and indeed are shown to degenerate first (Lu et al., 2011). A consequence of natural aging is cognitive decline; increased forgetfulness, poor short-term memory and taking longer to learn new things (Bartzokis, 2004; Peters, 2002). These are all exacerbated in age-related neurodegenerative diseases such as Alzheimer's Disease (Peters, 2002). The decline in myelin could explain this as the main role for myelin is to improve conduction speed and timing of neuronal circuits, which in turn boosts cognitive processing speeds (Bartzokis, 2004; Lu et al., 2011; Williamson & Lyons, 2018). Human stereological studies have also shown between 27-45%

reduction in the fast-conducting central nervous system axons as a result of natural aging. Visual cortex, the area of interest for this thesis, seems to be resistant to aging and some have proposed a '*first in, last out*' theory behind the regional variability of myelin degeneration (Davis et al., 2009; Fjell & Walhovd, 2010). Currently, little is known about the consequences of eye disease on cortical myelin. As mentioned previously, primary visual cortex develops and is heavily myelinated even in congenital blindness, but how this may change as a result of acquired vision loss is currently unknown. We will discuss cortical myelin density in macular disease and sighted controls in Chapter 2.

1.4. Structural changes associated with central vision loss

When present in both eyes, macular degeneration results in overlapping visual defects, and the cortical representation of this part of the visual field – referred to as the lesion projection zone (LPZ) – lacks normal visual input (Figure 1.2). Changes in cortical architecture have been observed in macular disease (MD) across multiple studies, particularly with hereditary forms such as Stargardt's disease (Beer, Plank, & Greenlee, 2020). Using whole brain and ROI based analyses, MD patients show reduced grey and white matter within visual cortex, mainly at the occipital pole (the anatomical location of the LPZ). There was also atrophy of the LGN, and within the optic radiations which connect the LGN and primary visual cortex. This suggests deficits extend far beyond the retina and impact on the posterior visual pathway (Hernowo et al., 2014). Results for age-related MD are quite similar, with patients exhibiting significantly reduced grey matter within the occipital lobe, largely at the occipital pole (Boucard et al., 2009). A larger scale anatomical study demonstrated very little difference between JMD and AMD populations, suggesting the overall consequences on cortical structure are consistent across forms of central vision loss, irrespective of aetiology and age of disease onset (Hernowo et al., 2014). However, notable differences emerged between the groups when assessing the state of white matter in frontal regions in AMD, which could be attributed to the age difference, or the comorbidity between AMD and mild cognitive impairment (Beer et al., 2020; Hernowo et al., 2014). Olivo and colleagues (Olivo et al., 2015) argued that previous methods were not sensitive enough to detect possible subtle changes in the white matter in cases of JMD. By using diffusion MRI as well as voxel-based morphometry (VBM), more subtle changes in white matter integrity and grey matter volume were

indeed detected in JMD participants. Results showed widespread reductions in grey matter volume and fractional anisotropy (suggesting a reduction in white matter integrity) in Stargardt's disease (a form of JMD), largely in more posterior areas, but these changes were not exclusively in the optic pathway. It is possible that the observed differences in JMD, despite being subtle, may be showing some form of protection against degeneration (Olivo et al., 2015).
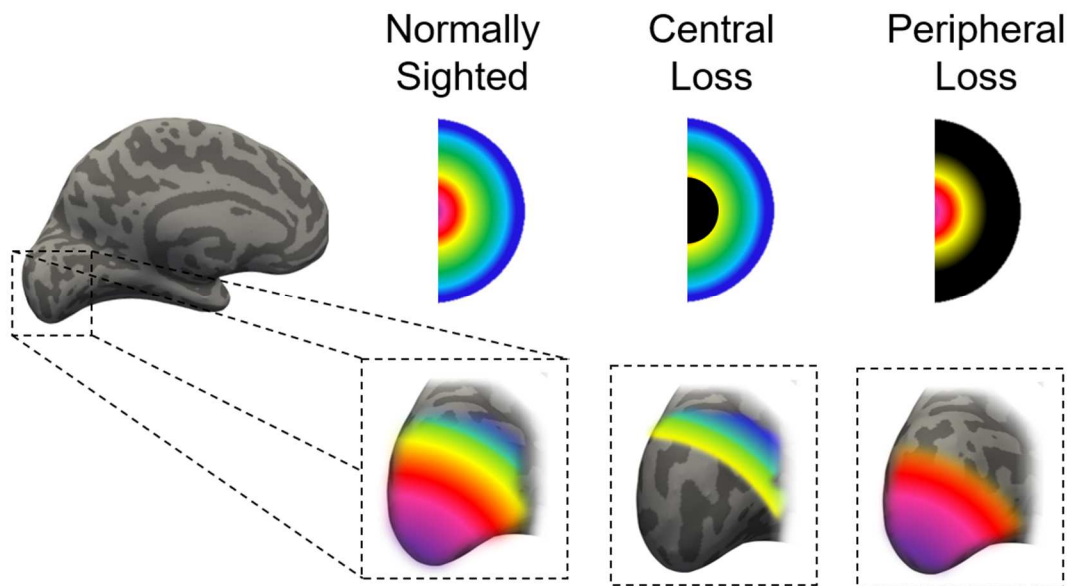
Figure 1.2: Schematic of the representation of the visual field in normally sighted individuals, central vision loss and peripheral vision loss. In normally sighted individuals you can see a larger representation of the entire visual field from the central representations (warmer colours), expanding to the more peripheral visual field representations (cooler colours). In individuals with visual field loss, there is an absence of activation in the part of visual cortex representing the retinal lesion – referred to as the lesion projection zone (LPZ). The remaining part of the visual field will elicit responses in the corresponding part of visual cortex - the intact projection zone – IPZ. In cases of central vision loss, the LPZ spans a larger region of cortex due to cortical magnification – given we use foveal vision for finer visual tasks, there is a larger representation within cortex, hence a larger region remains unstimulated. In cases of peripheral vision loss, the LPZ appear smaller given that a smaller amount of cortex is dedicated to peripheral visual fields, where vision is poorer.

In addition to the white matter changes in the frontal regions of AMD patients, using diffusion-weighted MRI (dMRI), others have shown that as well as reduced grey matter in visual cortex, patients with AMD also exhibit localised deficits within the optic radiations, specifically in the portion directly projecting to foveal representations - the LPZ (Yoshimine et al., 2018). This study examined individuals receiving treatment for neovascular AMD, for an undefined period of time. The optic radiation

was segmented into sections depending on where in primary visual cortex it projected to; fovea (0°- 3°), mid-periphery (15° - 30°) and far periphery (30° - 90°). Results showed tracts that projected to the foveal representation were the only ones significantly affected by the disease; other portions projecting to more peripheral representations in primary visual cortex did not differ significantly from the age-matched controls. At what stage in the disease progression these changes occur is still unknown as participants in this particular study appear to be in the later stages of the disease. To help address this question, we compare changes in a group of AMD patients with established bilateral AMD against sighted controls, as well as two cases of AMD before and after diagnosis in Chapter 3.

Assessments of the representations of the intact parts of the peripheral visual fields that remain unaffected by the disease – referred to as the intact projection zone (IPZ) - yield mixed results. The cortex in the calcarine sulcus is known to be thinner, meaning subtle changes are harder to detect. As described previously, any inconsistency may also be attributed to the differences in protocols, analysis methods and the way the cortex is parcellated into different ROIs. Some groups have suggested that there is evidence of thinning in this region in addition to the LPZ (Doety Prins et al., 2016), however others have reported the opposite pattern of results, and conclude central vision loss can even cause cortical thickening in the representation of the intact visual field (Burge et al., 2016). Burge and colleagues attribute this thickening to the increased reliance on remaining peripheral vision, arguing it may be indicative of cortex compensating for the lost vision. What is not clear, is why patients differ. It seems plausible that factors influencing the change in cortex in either direction could include the time since disease onset, extent of the vision loss and the diagnosis (JMD vs AMD for example). In Chapter 2 we will discuss cases for which we have measures of cortical thickness before and after AMD diagnosis alongside a group of MD patients with longstanding central vision loss. This offers some insights into how results may differ in individuals at different stages of the disease progression.

It is currently unknown whether treatment of the eye (anti-VEGF injections for wet AMD for example) would result in preserved cortical structure and prevent degeneration. Evidence from Hanson et al (2019) suggests that while visual acuity stabilises and, in some cases, slightly improves with such treatments in unilateral

wet AMD, visual cortex still reduces in volume – likely driven by reductions in cortical thickness in the LPZ. Whilst significant changes in visual cortex were not observed 3 months after the second eye was diagnosed with AMD, cortical atrophy was evident 5 years post diagnosis. This highlights why research into neuroprotective strategies needs to be considered. What also remains unclear is the relationship between structure and function of the retina and how changes in the retinal drive the cortical atrophy observed; this may prove important for the success of restorative treatments as if visual cortex continues to decline in spite of successful stabilisation of visual function in the eye, new incoming information may not be processed appropriately, therefore limiting the chances of patients gaining some form of functionally useful vision. This is a particularly pressing issue for the dry form of AMD, given there are no treatments currently available to slow the progression of the disease.

1.5. Assessing the function of visual cortex

A great deal of clinical research concerning eye disease focuses on monitoring physiological changes in the eye, with the overall aim of treating the eye, preventing further sight loss, and restoring functionally useful vision. However there is also evidence to suggest that further up the visual pathway, parts of visual cortex representing regions of the visual field which are no longer receiving input, are subject to change (Baker, Dilks, Peli, & Kanwisher, 2008; Baker, Peli, Knouf, & Kanwisher, 2005; Dilks, Julian, Peli, & Kanwisher, 2014; Hoffmann & Dumoulin, 2015). Results from visual assessments such as visual acuity and contrast sensitivity do not inform us about the consequences on higher-level visual processing, hence incorporating fMRI alongside other psychophysical based measures is important for determining the consequences of vision loss on the posterior visual pathway.

Reorganisation of function was first described in other modalities. Phantom limb syndrome is characterised by sensations, typically pain, coming from a limb that has been removed. Studies have found a correlation between the amount of cortical reorganisation observed from fMRI and the extent to which individuals experience phantom limb pain, as patients who do not experience pain show differential reorganisation in motor and somatosensory areas (Flor et al., 1994; Karl, Birbaumer, Lutzenberger, Cohen, & Flor, 2001). Similarly, in cases of tinnitus – where sounds are heard in the absence of any external auditory stimuli - the extent to which participants experience phantom sensations was related to the changes in cortical

organisation (Elbert & Flor, 1999). Collectively, this suggests cortical reorganisation may not always have an adaptive function, and in the case of sight loss, reorganisation is not always ideal if attempts to restore vision are to be successful.

1.5.1 Reorganisation of function in visual cortex following central vision loss

There is a debate in the literature concerning functional changes in visual cortex following central vision loss. Cortical reorganisation can refer to anatomical changes, but generally it concerns how neural activity, in response to a visual stimulus, changes as a result of eye damage or disease. FMRI in conjunction with clinical measures (visual acuity, contrast sensitivity and perimetry for example) allows researchers to determine the extent of the damage at various points along the visual pathway. Retinotopic mapping has been widely used in sighted populations and to an extent in those with visual deficits. Given that fixation instability is a common problem particularly in cases with central vision loss, researchers cannot rely on participants fixating steadily on a small central fixation point to map out visual cortex. Instead, a full field flickering checkerboard stimulus can be used to identify parts of visual cortex that are no longer receiving input – this is referred to as the lesion projection zone (LPZ). In addition to conflicting results concerning the status of the LPZ, definitions of what constitutes cortical reorganisation differ across research groups. Cortical reorganisation can be referred to as a change from what we know about the organisation of the visual system in normally sighted individuals but observing abnormal signals does not necessarily mean that any cortical reorganisation has occurred (Morland, 2015). Some research groups adopt a broader definition; if an individual with sight loss demonstrates a response that cannot be replicated in sighted individuals, it suggests reorganisation has occurred. Three overarching theories regarding the function within the LPZ will be discussed, outlined in Figure 1.3.
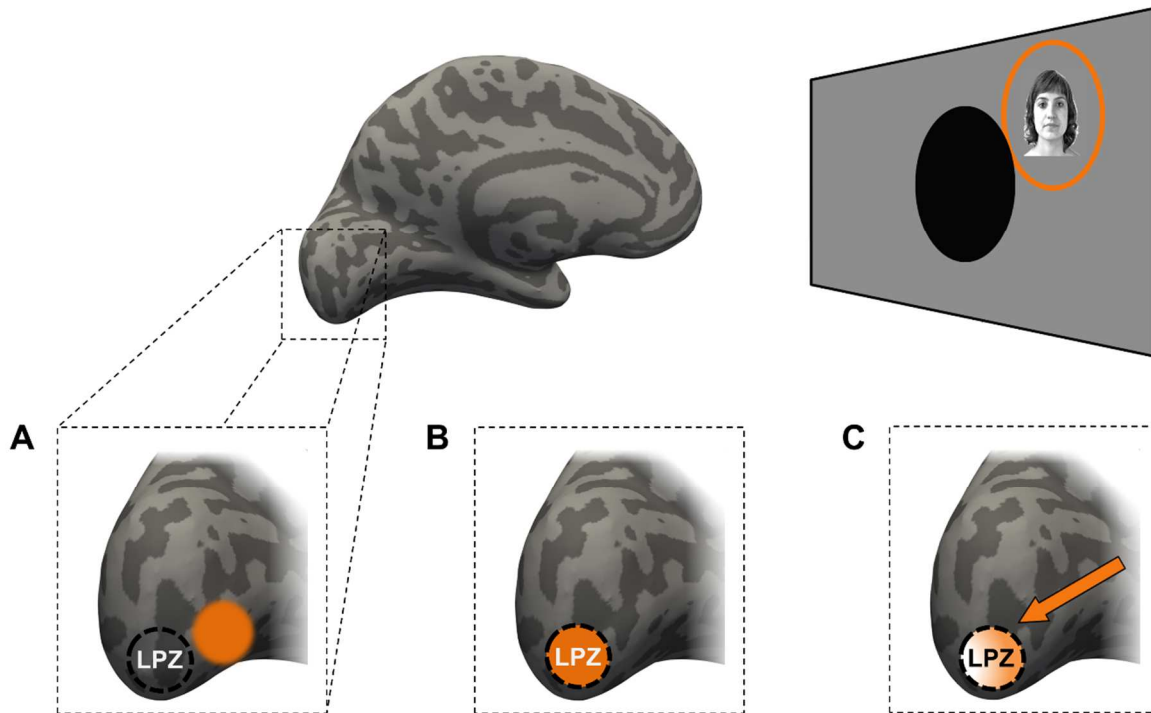
Figure 1.3: The reorganisation debate. An illustration of central vision loss; MD participant viewing an image of a face that falls within the intact part of the visual field and can be seen by the observer, abutting the central scotoma (black filled circle). The dotted line at the occipital pole denotes the lesion projection zone (LPZ), the representation of the scotoma. The unfilled arrow leaving the scotoma represents a lack of input coming from this part of the visual field. The orange filled arrows/shapes represent visual input that can be processed by the visual system. **A**: No reorganisation occurs – the LPZ remains silent and stimuli falling on intact parts of the visual field are processed as normal. **B:** Reorganisation occurs – the LPZ takes on the processing of information presented to the intact parts of the visual field. **C:** No reorganisation occurs but activity may be observed within the LPZ, perhaps evidence of unmasking of feedback from extrastriate areas, brought on by task demands (Masuda et al., 2008).

Firstly, it must be acknowledged that multiple research groups have not observed any evidence of reorganisation in patients with macular lesions, nor did they observe any notable activity in the LPZ – often taken as a signature of functional reorganisation of visual processing (Baseler et al., 2011; Smirnakis et al., 2005; Sunness, Liu, & Yantis, 2004). Furthermore, when contrasted with sighted control participants who had a simulated central lesion (presented a stimulus with a grey disc obscuring the central part of the image), no discernible differences were observed (Baseler et al., 2011). Collectively, the aforementioned studies suggest the LPZ lies dormant, showing no evidence of functional reorganisation.

There is evidence to suggest that cortical reorganisation might occur following central vision loss, however the mechanisms underlying it are largely speculative (Baker et al., 2008, 2005; Dilks, Baker, Peli, & Kanwisher, 2009). Some researchers have suggested following bilateral central vision loss, the function of the LPZ changes, and it begins processing information presented to intact parts of the visual field (Baker et al., 2005; Dilks et al., 2014). Sighted controls did not exhibit the same patterns of response, suggesting a change in cortical function associated with vision loss. It is difficult to establish what drives this observed LPZ activity, given that patients do not engage in the same viewing conditions for each experiment. One argument for why reorganisation is not observed in all patients, is because it relies on absolute bilateral loss with no evidence of foveal sparing (Dilks et al., 2014). This highlights the importance of acquiring careful measures of the scotoma using microperimetry for example, to establish the coordinates of visual space affected by the visual impairment and in turn, accurately map the representation in visual cortex (Morland, 2015).

A consequence of central vision loss is the natural development of a new fixation point; a preferred retinal locus (PRL). The PRL develops in a part of the intact peripheral retina, typically abutting the scotoma, usually within 6 months of diagnosis (Cheung & Legge, 2005; Schumacher et al., 2008). Researchers suggested that the establishment of a PRL might trigger reorganisation as the PRL is in theory taking on the role of the fovea, hence being used for fixation (Plank et al., 2017; Schumacher et al., 2008). However, others have demonstrated no significant difference in the extent of LPZ activation when presenting stimuli at the PRL compared to another peripheral location in the retina, equidistant from the boundary of the scotoma. Authors suggest conflicting results could simply be driven by attentional mechanisms, task and/or stimulus type (Dilks et al., 2009; Plank et al., 2017).

A third explanation suggests whilst the LPZ may not have been reorganised, signals can be observed under specific viewing conditions, when engaging in a stimulus related task. This may be due to the unmasking of feedback from extrastriate areas – a mechanism found in the normal visual system, which may be 'unlocked' by the absence of geniculo-cortical signals coming from the retina (see Figure 1.4). Masuda and colleagues observed LPZ responses in individuals with MD, as well as individuals with retinitis pigmentosa (Masuda, Dumoulin, Nakadomari, & Wandell,

2008; Masuda et al., 2010). Interestingly, this activity was observed when participants engaged in a stimulus-related task, but not when passively viewing the same stimulus (Masuda et al., 2008). This was observed in 3 out of 4 patients irrespective of stimulus type, and highlights that perhaps the reason different research groups have conflicting results may be due to the different paradigms used. Moreover, age-matched sighted control participants showed no evidence of task-related activity in their simulated LPZ, generated by obscuring the central vision with a uniform grey disc and presenting stimuli peripherally. Supporting this, Plank et al (2017) demonstrate that task and/or stimulus type can elicit responses in the LPZ, particularly when viewing naturalistic images at the PRL. Collectively, results suggest activity observed in the visually impaired might be due to the unmasking of a normal feedback mechanism from extrastriate cortex, brought on by task demands. The studies from Masuda and colleagues are of particular importance to the work presented in Chapter 6 of this thesis and therefore warranted a more detailed appraisal.

The reorganisation debate largely stems from the fact different research groups employ different stimulus types and experimental paradigms to investigate activity within the LPZ, but also can be attributed to the different ways in which reorganisation of visual function is defined (Morland, 2015). To determine under what viewing conditions LPZ responses can reliably be observed, experimental design should be systematically varied using the same participant cohort. Additionally, most patient studies examine LPZ responses at the individual level without explicitly testing the reliability of the responses and establishing if they are legitimate or due to noise. Studies with sighted participants have shown that when viewing a naturalistic scene that has been partially occluded, meaningful stimulus-related information can be decoded from the representation of the unstimulated region, suggesting it has been fed back from higher cortical areas (Muckli et al., 2015; Smith & Muckli, 2010; Williams et al., 2008). In cases of visual impairment, by correlating the pattern of responses of voxels within the LPZ across different scans using the same paradigm, researchers could assess the reliability of the responses in the LPZ. This technique will be implemented in Chapter 6 allowing us to determine whether responses observed in sighted individuals with simulated retinal lesions are reliable, but also to establish whether these were comparable to a patient with JMD

in terms of the reliability and magnitude of the responses. Thus far, studies have not detected such responses in the simulated LPZ of sighted participants, but also collectively, fewer than 50% of patients exhibit LPZ responses when examining the literature (Morland, 2015).

While it is beyond the scope of this review, it is worth noting there is evidence of cortical reorganisation in individuals with congenital vision loss. Individuals with rod achromacy (whose vision is dominated by rod function as they have no functioning cones and therefore a deficit in central vision) demonstrate LPZ responses when viewing stimuli under scotopic conditions. This is a surprising finding given they have no functioning cones, and only rods function under such viewing conditions (Baseler
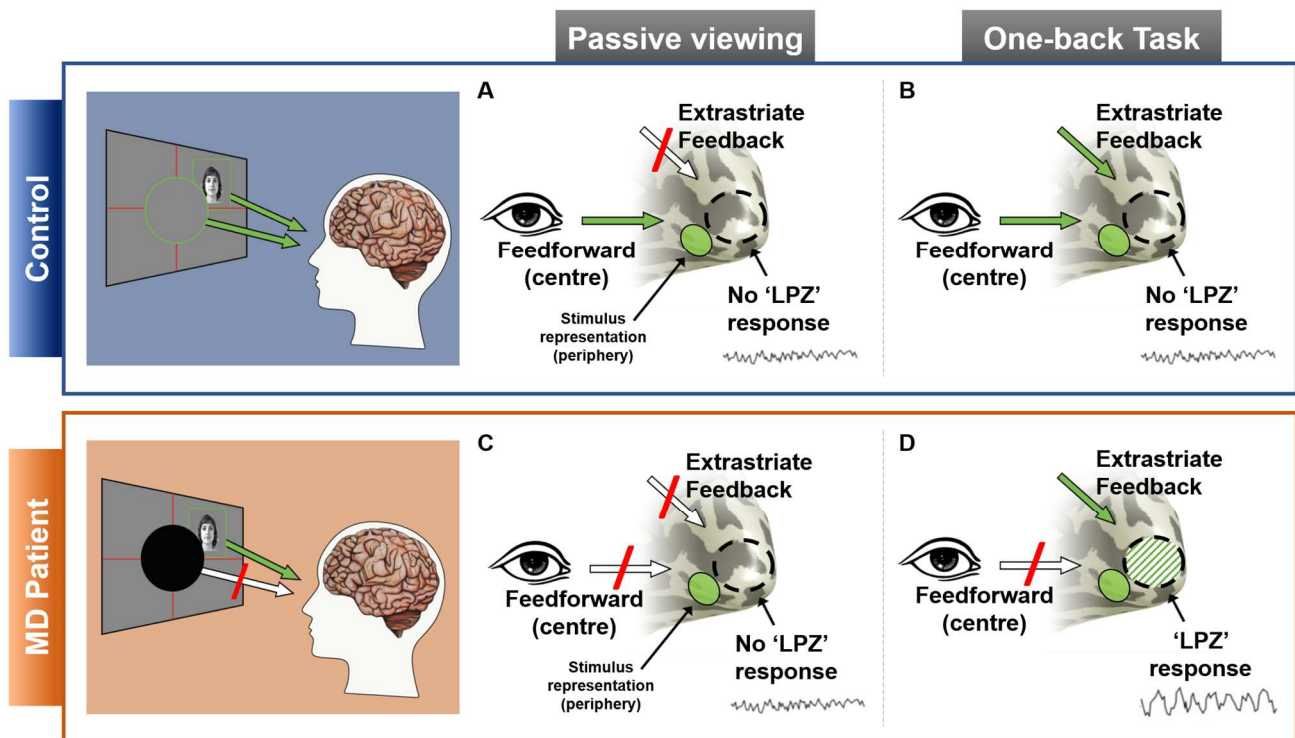
Figure 1.4. Illustration of the unmasking of feedback theory (Masuda et al., 2008). LPZ activity under different viewing conditions (passive viewing and engaging in a one-back task) for a sighted individual (upper panel) and an MD patient (lower panel). Sighted controls, when passively viewing a peripheral stimulus (**A**) do not exhibit a response in the simulated LPZ but there is a feedforward signal coming from the eye (green filled arrow), and a V1 response in area representing the stimulus (green oval). When completing a one-back task (**B**), there is a cortico-cortical feedback signal (green filled arrow) as well as the feedforward signal coming from the eye (green filled arrow); the combined signals do not result in sLPZ responses. MD patients do not exhibit feedforward signal from the macula but do have a V1 response to the peripheral stimulus (green oval). When passively viewing stimuli, no LPZ signals are evident (**C**), however when engaging in a task, as the cortico-cortical signals are not cancelled out by an incoming feedforward signal, feedback signals are unmasked and emerge in the LPZ (**D**).

et al., 2002). Sighted controls did not exhibit activity in the same zone under the same viewing conditions. This study clearly highlights that reorganisation of V1 in terms of the remapping of eccentricity is possible in certain visual disorders and is perhaps dependent on congenital loss. This is not necessarily a desirable result however, given that there is evidence gene therapy has been successful in restoring cone function in animal models (Lipinski, Thake, & MacLaren, 2013); cortical reorganisation will negatively impact on the success or restoration of visual function, unless visual cortex is capable of reorganising again to compensate for the change.

1.5.2 The impact of vision loss on higher-level visual processing

Until recently, the focus of vision loss research has been on cortical reorganisation and whether any discernible responses can be detected in the LPZ. There are comparatively fewer studies exploring the neural response to more complex visual stimuli, such as faces and scenes. Psychophysical work however is becoming more prevalent, building on standard visual assessments. Psychophysical studies will primarily be discussed since there is a notable absence of fMRI studies investigating higher-level visual processing following vision loss.

1.5.2.1 Face and object perception

Faces are highly complex stimuli with which we, as human observers, are very familiar. We are incredibly skilled when it comes to detecting changes in identity and expression in faces. Given the vast social cues a face can exhibit, it is understandable the inability to process faces is highly debilitating. Neuroimaging research has demonstrated that face processing recruits multiple interconnected neural regions, including the fusiform face area (FFA), occipital face area (OFA) and superior temporal sulcus (STS) (Haxby, Hoffman, & Gobbini, 2000). Most of the literature concerning face processing focuses on individuals with normal or corrected-to-normal vision, and individuals who demonstrate selective impairments with face processing, either through congenital or acquired disease or injury affecting the aforementioned cortical regions. The impact of visual impairment (resulting from eye disease of injury) on face-selective regions is not as well documented.

A common complaint among individuals with macular degeneration (MD) concerns face recognition. Individuals report they frequently struggle to identify familiar faces and rely on other information to establish a persons' identity. Given that faces

contain a lot of complex visual information, we utilise our central vision, where acuity is highest, hence MD will impact highly on face recognition. Despite developing a PRL, the diminished acuity means deficits cannot be overcome by simply stabilising eye movements. Various psychophysical studies have demonstrated a decline in performance in age-related MD (AMD) patients when categorising facial expressions and identity (Boucart et al., 2008; Tejeria, Harper, Artes, & Dickinson, 2002). Interestingly, it appears that patients generally perform better on tasks involving categorisation of emotions when compared to tasks requiring participants to state if the face is showing and expression or not (Boucart et al., 2008). To categorise the expression, patients could only rely on low spatial frequency information. Given that AMD patients struggle with higher spatial frequencies and rely on intact peripheral vision to see, this might explain why distinguishing the presence of a certain expression was more challenging. Mäkelä et al (2001) tested normally sighted individuals on face recognition, presenting stimuli to their periphery at varying degrees of eccentricity, but also removed luminance cues such as hairline, colouring, and clothing. Performance on face identification tasks was maintained by altering the contrast appropriately for the different eccentricities. It was shown that peripheral processing of faces was approximately 66% worse than at the fovea (Mäkelä et al., 2001). Not only do results support findings of the deficit in face processing in AMD, but they also indicate that altering the contrast of images may improve performance for AMD patients, rather than simply enlarging images. This has clinical implications as most AMD patients are recommended to use a magnifier, which will primarily benefit reading - a foveal task.

Currently, standard clinical assessments include visual acuity, perimetry (used to assess visual field function), and more rarely contrast sensitivity, all of which are simple and easy to administer. Researchers have debated whether simply reading letters of varying size and contrast is a representative measure of an individual's visual perception. For example, visual acuity assessments do not inform clinicians about many aspects of higher-level visual processing, which is more akin to day-to-day perception, having to process objects and faces and navigate obstacles for example. The Caledonian Face Test, an 'odd one out' task, can be used to assess face discrimination in a more controlled manner (Logan, Wilkinson, Wilson, Gordon, & Loffler, 2016). Using synthetic faces allowed for researchers to easily manipulate

the stimuli while testing in a quantifiable manner, as it considers participant's individual thresholds. Faces are rid of any non-face cues such as clothing, different postures etc but also highly discriminative features. Given that some individuals may use these additional factors as an alternative strategy to aid recognition, removing these has allowed Logan et al to generate a much more controlled assessment of face discrimination specifically. When individuals do use their own compensatory strategies, they can generate responses unrepresentative of their actual visual perception. The Caledonian Face Test has been primarily used to assess face discrimination in normally sighted individuals, but the flexibility of the stimulus set has wider implications for clinical populations, including the visually impaired. Paired with functional MRI, this paradigm has the potential to aid our understanding of the impact of visual loss on face processing throughout the visual hierarchy (Thibaut, Delerue, Boucart, & Tran, 2016).

1.5.2.2 Scene perception

Behavioural evidence suggests AMD patients can process scenes in a particular manner. Scene gist recognition is plausible with only peripheral vision intact, suggesting scenes can be recognised using low level features such as orientation and texture, without needing to identify objects within a scene, for example. Evidence from computer vision as well as AMD patients' ability to categorise scenes by naturalness supports this (Tran, Rambaud, Despretz, & Boucart, 2010). There is also evidence that scenes are processed implicitly in AMD; When objects were presented in a scene, either congruent or incongruent, participants performed better in congruent trials when asked to focus on the object, suggesting implicit scene processing was intact (Boucart, Moroni, Szaffarczyk, & Tran, 2013). The way in which a scene is explored also changes with sight loss; as well as performing significantly worse on an identification task compared to sighted controls, AMD patients show increased numbers of saccades and consequently, shorter fixation durations (Thibaut et al., 2016). Studies with sighted controls support this as when presented with an artificial scotoma, controls also showed increased number of saccades. Taken together, behavioural studies indicate that the manner in which AMD patients visually inspect, and process scenes is markedly different from controls, but they can still successfully do so. How this change in behaviour affects cortical responses is unknown.

Research on sighted individuals has unveiled a series of cortical regions dedicated to processing visual scenes; the parahippocampal place area (PPA), retrosplenial cortex (RSC) and occipital place area (OPA – formally known as the transverse occipital sulcus, TOS) (Epstein, 2008; R. Epstein & Kanwisher, 1998; Maguire, 2001; Maguire et al., 1998; Nakamura et al., 2000). A recent study used fMRI to explicitly assess neural underpinnings of scene perception following AMD (Ramanoël et al., 2018), but in a limited group (n = 4). Patients had to categorise scenes of high and low spatial frequencies as either indoor or outdoor; when images were presented with high spatial frequencies, patients showed an absence of activation in the PPA, as well as over a broad area of the occipital lobe, dedicated to both peripheral and central processing. Additionally, by increasing the luminance contrast of the images, performance with higher spatial frequencies improved and induced activation in occipital regions dedicated to peripheral processing (Ramanoël et al., 2018). This demonstrates that with improvements in visual perception (e.g., increasing contrast), higher order visual areas will respond as you would expect in sighted individuals, but this also refutes the idea of functional reorganisation further up the visual hierarchy.

Research should continue to investigate performance in tasks involving more complex stimuli such as faces and scenes, as visual acuity alone does not inform us of everyday difficulties patients deal with. Visual acuity did not correlate with number of saccades and fixation times (Thibaut et al., 2016) or performance on categorisation tasks (Tran et al., 2010); additionally, contrast sensitivity is another measure of importance but more frequently, a decrease in visual acuity is thought to be more debilitating by clinicians than a reduction in contrast sensitivity. It is important to note that both visual acuity and contrast sensitivity decline in normal aging populations, however the deficit is much more pronounced following vision loss. Evidence shows that contrast sensitivity is important when making judgements in face recognition tasks (Ramanoël et al., 2018). Adding to the building psychophysics literature and developing paradigms using fMRI will inform our understanding of the extent of deficits in visual processing across a broader range of tasks.

1.5.2.3 Resting state functional connectivity

One of the biggest challenges facing vision researchers is finding methods which allow us to measure neural responses in visual cortex when vision is limited. In

cases of anophthalmia, there are further difficulties assessing visual cortex when individuals have no form of light perception at all. Resting state fMRI allows for the opportunity to study the organisation of visual cortex in individuals without vision. Evidence from cases of microphthalmia (underdeveloped eyes) and anophthalmia (a condition in which the individuals never develop a functioning retina) have shown that the architecture underlying visual cortex remains largely the same, demonstrating typical retinotopic organisation despite no visual experience (Bock et al., 2015; Bridge, Cowey, Ragge, & Watkins, 2009; Striem-Amit et al., 2015). The consistency in organisation extends to representations of eccentricity, laterality, and elevation in primary and extrastriate visual cortices. This also extended to the higher-level visual areas, whereby face and place selective regions exhibited the expected eccentricity biases (Striem-Amit et al., 2015). However, there were notable changes in terms of functional connectivity between primary visual cortex and other brain areas which suggest that there may be critical periods during which these connections are established (Striem-Amit et al., 2015). In addition to the reduced overall functional connectivity within visual cortex, resting state fMRI revealed a different pattern between visual and non-visual areas. Within primary visual cortex, representations of the central visual field and the peripheral visual field were impacted differently in the congenitally blind group, with central V1 showing increased connectivity to the non-visual areas involved in language processing. Contrary to this, more anterior V1 representing peripheral portions of the visual field exhibited stronger functional connectivity with the dorsolateral prefrontal cortex.

Further support for this comes from a unique study examining functional connectivity within visual cortex in 27-day old neonates, and this study is of particular importance to the work presented in Chapter 5. Whilst research has shown that domain-specific connectivity is evident in the adult seeing brain, how it develops over time is unknown. Kamps et al., (2020) examined how primary visual cortex connects with higher-level visual areas such as FFA and PPA, given that these areas are shown to have specific retinotopic biases (Hasson, Andric, Atilgan, & Collignon, 2016; Kamps, Hendrix, Brennan, & Dilks, 2020; Levy, Hasson, Avidan, Hendler, & Malach, 2001). Face processing is largely biased toward central visual processing, and scenes biased towards peripheral visual processing. The nature of the stimulus types themselves are believed to be the driving force for these domain-specific networks.

Kamps et al have shown, however, that as early as 27-days old, domain-specific patterns of functional connectivity are observed in the face and scene networks, when examining functional connectivity between all combinations of FFA, OFA, PPA, RSC. Further to this, stronger functional connectivity was observed between OFA and the central representation in V1, and for PPA and RSC, functional connectivity was strongest with peripheral V1. Interestingly, the FFA - central V1 functional connectivity was not significant, but authors note there was a trend in the direction of a foveal bias. In Chapter 5 we will examine the same functional connections in individuals with either central or peripheral visual field defects, to see how the functional connections that are established early in life may be impacted by sight loss.

More recently, studies have been investigating functional connectivity in partially sighted individuals (Frezzotti et al., 2014). Whilst the architecture is largely the same in congenitally blind patients, there is evidence of structural degeneration in those losing sight later in life (AMD, glaucoma). In glaucoma, there is evidence of decreased functional connectivity between the visual and working memory networks, as well as showing increased functional connectivity between visual and executive networks (Frezzotti et al., 2014). Such broad changes mirror the structural changes observed across the whole brain; this lends support to the idea that glaucoma should be considered a neurodegenerative disorder and demonstrates how fMRI could aid our understanding of disease progression. Most of the work was largely exploratory, looking at connectivity over the whole brain, rather than just focusing on visual cortex. Considering visual deficits can be selective (as in AMD and glaucoma, affecting central and peripheral vision respectively) it would be informative to probe specific paths within visual cortex i.e., between the LPZ and other visual areas. Given that most of the work thus far has examined structure and function of visual cortex, primarily investigating the state of the LPZ, assessing connectivity between visual areas might be informative, particularly if fMRI shows deficits in higher-level visual areas. It may also help to explain why some individuals may exhibit LPZ responses, while others do not. A resting state fMRI paradigm was implemented in Chapter 5 to help address some of these outstanding questions.

1.6. Evidence of behavioural and neural consequences of peripheral vision loss

The focus of this thesis is on patients with forms of macular degeneration, however it is important to understand the consequences of peripheral vision loss on the posterior pathway as well, as it can tell us what is common across eye diseases, but also how they may differ. Glaucoma and retinitis pigmentosa will be discussed.

1.6.1 Glaucoma

Glaucoma describes a collection of neurodegenerative diseases which at first manifest as damage to the optic nerve, affecting both the retina and more anterior parts of the visual pathway. Like MD, glaucoma can manifest in different ways. Primary open-angle glaucoma (POAG) is characterised by raised intraocular pressure causing increased cupping of the optic disc (Figure 1.5), damaging the retinal ganglion cells and the optic nerve, causing loss of peripheral vision initially, and later extending to parafoveal regions. Normal-tension glaucoma is largely similar but characterised by optic nerve damage in the absence of elevated intraocular pressure. Due to the fact glaucoma impacts on the entire visual pathway, there are a wide range of deficits associated with the disease, affecting visual acuity, contrast sensitivity, as well as motion and colour processing. As the disease progresses, degeneration extends to posterior parts of the visual pathway including subcortical areas – the lateral geniculate nucleus (LGN) – and cortical visual areas. Despite being the second most common cause of blindness in the western world, if caught early, most cases of vision loss due to glaucoma could be prevented (Quigley, 2006). This highlights the importance of going for regular visual assessments.

1.6.2 Retinitis pigmentosa

Retinitis pigmentosa (RP) refers to a collection of rare inherited visual disorders, affecting approximately 1 in 4000 people worldwide (Berson, 1993; Machado et al., 2017). RP is characterised by the progressive and irreversible loss of both the rod and cone photoreceptors (Figure 1.5); initially it impacts on peripheral locations and causes problems seeing in low light conditions, extending to the fovea as the disease progresses (Brown et al., 2016). The symptoms emerge typically in childhood, but this can vary from infancy to adulthood (Ferreira et al., 2017). Vision loss progresses over time, with the periphery being first affected and inducing what is known colloquially as 'tunnel vision'. With time this progresses and causes night

blindness, blue blindness, loss of central vision, eventually resulting in complete blindness (Berson, 1993; Ferreira et al., 2017). Like AMD, there is currently no cure, however research has focused on the use of retinal implants and gene therapy as a means of stabilising or restoring visual function (Chow, Packo, Pollack, & Schuchard, 2003; Chow et al., 2004; Cunningham et al., 2015; Stingl et al., 2015; Tschernutter et al., 2005).
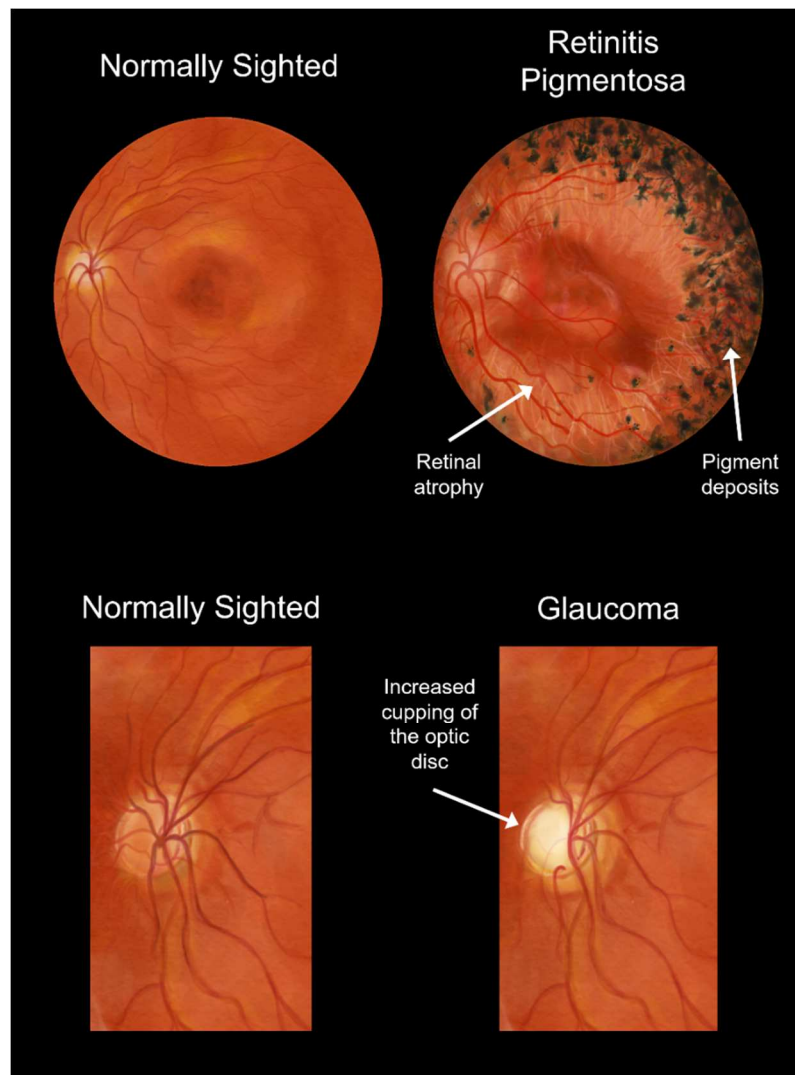
Figure 1.5. Illustrations of the retina for retinitis pigmentosa (RP, top) and glaucoma (bottom) in contrast to normally sighted retinae. In cases of RP, pigment deposits emerge (dark spots) alongside evidence of atrophy of the retina. The macula is relatively well preserved until the later stages of the disease. Glaucoma is the result of increased interocular pressure, causing increase cupping of the optic disc, in turn compressing the optic nerve.

1.6.3 Structural changes associated with peripheral vision loss

In contrast to MD, many studies have examined structural abnormalities in glaucoma (Brown et al., 2016). As mentioned previously, glaucoma often goes unnoticed until symptoms become more severe and damage irreversible; the disease manifests itself along the whole of the visual pathway, affecting anterior (eye) and posterior (brain) pathways significantly. Studies examining smaller structures in two forms of glaucoma (primary open-angle glaucoma and normal tension) have shown a reduction in size of the optic nerve and chiasm, as well a reduction in the LGN (Chen et al., 2013; Gupta et al., 2009; Zhang et al., 2012). Volumetric differences are also apparent in anterior and medial occipital lobe, encompassing representations of the peripheral vision which has been lost – the LPZ. Studies using diffusion MRI have revealed an overall decrease in fractional anisotropy and increase in mean diffusivity within white matter tracts of visual processing, irrespective of glaucoma subtype (Li et al., 2014). Chen et al (2013) showed specific reductions in diffusivity along the optic radiations in late-blind glaucoma patients, further highlighting a reduction in integrity of the white matter tracts, more extensive than that observed in AMD (Yoshimine et al., 2018). The degree of the degeneration seemed to be determined by the extent of visual impairment; this pattern of results is also apparent in AMD, with the LPZ being most affected. The literature examining the IPZ is a bit more consistent for glaucoma compared to AMD; multiple studies have found evidence of an increase in grey matter volume in the regions adjacent to the LPZ which could be evidence of reorganisation or compensation for lost vision. Finally, given evidence for increases in grey matter in multiple cortical regions, not all related to visual processing, suggests cortical changes associated with glaucoma are broad and complex (Williams et al., 2013).

Fewer studies examine the structural changes associated with retinitis pigmentosa (RP) and there are some discrepancies within the literature. Some studies involving late blind RP patients with evidence of residual vision either found subtle differences when compared to sighted controls, or no difference at all (Ferreira et al., 2017; Machado et al., 2017). Further to this, when comparing patients with different disease severity, patients with more severe visual field defects had a thicker V1, restricted to the portion representing the intact central visual field, suggesting some

form of compensation for the loss of retinal input. However, this did not emerge as significant when compared to the control group.

Contrary to some RP studies but in line with glaucoma research, some groups have shown a reduction in cortical thickness in individuals with RP (Castaldi, Cicchini, Falsini, Binda, & Morrone, 2019; Park et al., 2009). Castaldi et al (2019) found a decrease in cortical thickness in V1 (capturing ~20deg of visual angle) in RP patients compared to sighted controls, but given the groups were not age-matched, the structural decline cannot be assumed to be related to the disease. Park et al also observed a reduction in cortical thickness in the pericalcarine ROI in contrast to both the sighted controls and congenitally blind group. In addition to cortical thickness, decreases in grey matter volume in the occipital cortex were observed in RP patients, and correlated positively with visual field defect (Machado et al., 2017). Cortical areas identified included bilateral calcarine, lingual gyrus, cuneus, and right occipital superior gyrus. It is possible this reduction in volume may be driven by this reduction in cortical thickness, like in cases of AMD (Hanson et al., 2019). Whilst this shows there may be a direct link between the extent of visual field loss and cortical changes (Machado et al., 2017), Castaldi et al did not find a significant correlation between cortical thickness in V1 and the degree of visual impairment. Together, this highlights how the consequences of RP on the structural properties of visual cortex are still a source of debate. As with the aging studies, differences in results may be attributed in part due to the various ways V1 has been defined. Given cortical thickness is deemed by many research groups to be a possible predictor of treatment effectiveness in both central and peripheral forms of vision loss, understanding the link between disease severity and anatomical changes in the posterior visual pathway may prove important (Castaldi et al., 2019; Hanson et al., 2019; Plank et al., 2011).

1.6.4 Functional consequences of peripheral field loss

Deficits associated with glaucoma extend far beyond the retina, most notably involving the optic nerve, LGN and visual cortex (Boucard et al., 2009; Graham & Klistorner, 2013; Gupta & Yücel, 2007). Whilst most research has demonstrated structural changes in glaucoma, research investigating the functional consequences of the disease is somewhat lacking (Brown et al., 2016; Duncan, Sample, Weinreb, Bowd, & Zangwill, 2007; Miki, Nakajima, Takagi, Shirakashi, & Abe, 1996). Given the

extensive structural changes described previously, one would assume that this might lead to some changes in function as well. Previous studies have used checkerboard stimuli to map visual cortex in glaucoma, with responses in primary visual cortex corresponding with structural changes in the eye, revealing the location of the LPZ in peripheral representations of V1 (Borges, Danesh-Meyer, Black, & Thompson, 2015; Duncan et al., 2007). Primary visual cortex showed more severe deficits compared to higher order visual areas, and interestingly, in some cases the deficits in visual cortex were apparent before the visual field deficit (M. C. Murphy et al., 2016).

It is apparent that fMRI could be used to further assess the extent of damage caused by glaucoma (Duncan et al., 2007). While there is evidence that functional reorganisation is unlikely, some researchers have argued that in unilateral glaucoma, the fellow eye would compensate and perhaps prevent cortical reorganisation (Duncan et al., 2007). Additionally, Masuda and colleagues have already demonstrated that LPZ responses can be observed in retinitis pigmentosa because of task demands, which could be the case for glaucoma as well (Masuda et al., 2010). Given that it impacts on the entire visual pathway, it would be useful to determine whether functional reorganisation is likely to occur. As with any form of eye disease, visual cortex needs to be viable and ideally remain unchanged in function and structure, to allow for the best chance of successful restoration.

While evidence is also limited for RP, interesting results have emerged concerning functional changes. The anatomical changes associated with RP are quite mixed as described previously, therefore complicating our understanding of how disease progression impacts on the posterior visual pathway. Ferreira et al (2017) examined both structural and functional measures in primary visual cortex in RP patients and sighted controls. Interestingly, while they did not find any anatomical changes, they did provide evidence of visual field remapping in V1, whereby representations of spared central vision appear to be shifted to what were formally representations of peripheral visual fields. This may correspond with the thickening of representations of central vision in cases of advanced RP, but the link is not yet clear. Castaldi & colleagues examined a group of late-stage RP patients using a combination of methods to assess visual function. Patients exhibited minimal responses when presented with flashes of light and assessed using visual evoked potentials (VEP) and electroretinogram responses (ERG). However, when using fMRI to examine the

BOLD response to flashes of light, significant BOLD responses were detected in primary visual cortex, as well as in extrastriate cortex (Castaldi et al., 2019). This suggests fMRI may be a more sensitive tool when assessing the extent of visual sparing in late-stage RP patients, compared to more standard ophthalmological and electrophysiological tests such as VEP and ERG. The common theme among the few studies presented here is that the magnitude and extent of the BOLD response to visual images seems to correlate with the extent of the visual field defect but does not necessarily correlate with cortical thickness.

Individuals with glaucoma also report their quality of life is affected by the inability to recognise everyday objects and faces. Like MD, individuals in later stage glaucoma show deficits in face processing which could arguably be attributed to contrast sensitivity (Glen, Crabb, Smith, Burton, & Garway-Heath, 2012). Using the Cambridge Face Memory test, Glen et al found individuals with glaucoma had difficulties, particularly those with more advanced stage glaucoma. Despite this, patients with advanced forms of glaucoma tend to underestimate the extent of their deficits with face recognition, much like individuals with AMD (Friedman et al., 1999). In a study directly comparing performance on detection and categorisation tasks, Roux-Sibilon and colleagues observed impairments for both tasks with low contrast faces. Individuals with early stage glaucoma were not significantly different from sighted controls, however more advanced cases show stronger impairments (Roux-Sibilon et al., 2018). This is an important finding as it demonstrates that peripheral vision loss still impacts on processing of stimuli in the intact central visual field – a finding not observed using standard perimetry tests. In support of this, when presented objects in the central intact part of the visual field, glaucoma patients show a deficit in categorisation compared to sighted controls, but only in the lower contrast condition (Lenoble, Lek, & Mckendrick, 2016). This suggests patients with glaucoma have deficits beyond what is reported by standard clinical assessments and highlights the importance of including more complex visual tasks, as it seems regions of the visual field that are perimetrically intact are still affected by the disease.

1.7. Concluding comments

It is evident there are many outstanding questions concerning the impact of vision loss on the brain, particularly regarding the time course of both structural and

functional changes and how these vary throughout disease progression. With much clinical work currently aiming to restore the function of the eye, researchers must also consider whether the brain is viable and able to process incoming information, as this could limit the success of the restoration attempts. Determining what the functional consequences are, how it relates to structural abnormalities, and over what time course changes occur, is important. If visual cortex has reorganised, as some have proposed, how can the brain process new information? Studies directly addressing the reorganisation debate, systematically varying stimulus, task and viewing conditions would be highly valuable. This will also allow us to determine whether signals observed in the LPZ are not only reliable, but also meaningful, containing contextual information that has been fed back from higher cortical areas.

The aim of Chapter 2 is to better understand the extent of structural changes (focusing on cortical thickness and myelin density) occurring in visual cortex following bilateral central vision loss, but also to establish the time course of such changes in individuals who have had various forms of central loss for several years. It is evident from the literature that vision loss results in structural changes in both the grey and white matter when compared to sighted, age-matched control participants, however it is not known how structure changes within an individual, and whether changes progress at the same rate throughout the disease progression. Additionally, myelin has yet to be explored in the context of macular disease; the literature indicates myelin in the visual cortex remains stable even with natural aging, but the impact of vision loss remains unknown. We will also examine two cases before and after an AMD diagnosis which have given us a unique opportunity to explore how and when changes occur, but also how this relates to the extent of vision loss. In Chapter 3 white matter integrity - specifically in the optic radiations - will be explored over the same period in the same cohort of MD patients and sighted controls, to determine the rate at which white matter integrity declines both health and disease. Collectively, these chapters will further our understanding of when there might be an optimum time at which interventions should be implemented for AMD, during which restoration will be most successful.

There is some evidence to suggest higher-level visual processing such as face and scene processing are affected after losing sight. However, evidence is largely limited to psychophysical data and the impact on higher-level regions is yet to be explored

thoroughly in the visually impaired. As extrastriate regions receive input from earlier visual areas (referred to as feedforward connections), it is important to understand how and whether information is relayed to higher-order visual areas when earlier regions in the visual pathway no longer receive normal visual input. Regions dedicated to face and scene processing are known to have a central and peripheral eccentricity bias respectively and since visual impairment can result in selective deficits, it would be interesting to explore whether higher-level visual areas with eccentricity biases matching that which is lost in V1 (LPZ) also show diminished neural activity. This will be explored in Chapter 5 using resting-state fMRI in patients with either peripheral or central retinal lesions.

Finally, it is important to recognise the aging population, particularly within the UK. By 2037 almost a quarter of the population will be over 65 years old (Office for National Statistics, 2018). In turn, this will result in a rise in prevalence of the age-related macular degeneration as it primarily affects individuals over 50 years of age. To fully understand the disease progression, exploring both ophthalmological and neural consequences would be informative. It is important to acknowledge that the viability of the visual brain may limit the success of visual restoration. Research focused on treating the eye is currently gaining pace, examining the effects of gene therapy, stem cell therapy, as well as retinal prostheses, in a bid to restore functionally useful vision. There is an assumption that visual areas will be able to process the restored retinal signals in an appropriate manner, but if the visual brain is no longer viable due to prolonged sensory deprivation, or if there is evidence of reorganisation of function, success will likely be limited. With various MRI protocols, we can non-invasively tease apart the consequences of sight loss on both the structure and function of the entire visual pathway, from retina to cortex.

Chapter 2: Longitudinal effects of bilateral macular disease on cortical thickness and myelin density in visual cortex

2.1 Abstract

The focus of most ophthalmological research concerns physiological changes within the eye, aiming to treat eye disease and prevent further loss of vision. However, fewer studies have examined the consequences of eye disease on visual cortex. Macular Degeneration (MD) embodies a collection of disorders causing a progressive loss of central vision. Cross-sectional MRI studies have revealed structural changes in the grey and white matter in visual cortex in MD, however the rate at which changes occur is currently unknown. We explored the rate of change in cortical thickness and cortical myelin in four regions of interest in patients with bilateral MD and sighted controls. The occipital pole and central-V1 were used to capture the cortical representation of the retinal lesion. The calcarine sulcus and peripheral-V1 were used to represent the cortical representation of the intact visual field. Data acquired over a ~24month period revealed a decline in cortical thickness over time in all participants, presumably because of natural ageing. A significant reduction in grey matter was observed in patients in occipital pole, calcarine sulcus and central-V1. Whilst patients did not show a significant accelerated rate of change during this period, the pattern suggests a faster decline in the occipital pole and central-V1 in patients compared to controls. Myelin content, despite appearing to show higher values in the cross-sectional analysis for the patients compared to controls, showed a significant difference in the rate of change for both the occipital pole and central-V1, suggesting this too declines faster in MD. A unique opportunity to examine cortical thickness changes in two individuals before and after diagnosis of age-related MD unveiled that thinning is likely more acute early in the disease process. Taken together, our results support earlier work showing that MD leads to a thinning of visual cortex in the representation of visual field loss, but also highlights that cortical myelin is not immune to decline. Despite cross-sectional work appearing to show more myelin in the regions that have thinned, the rate of change suggests that on average, myelin reduces with time.

2.2 Introduction

It is known that as we age, changes in cortical architecture occur; changes observed include reductions in cortical thickness, volume and surface area as well as changes in myelin particularly in prefrontal and association areas (Fjell & Walhovd, 2010; Fjell et al., 2009; Lu et al., 2011; McGinnis, Brickhouse, Pascual, & Dickerson, 2011; Salat et al., 2004; Schaie, 2005; Thambisetty et al., 2010). Anatomical changes in the grey and white matter are also shown to be driven by sensory deprivation, for example in visual cortex in cases of vision loss (Boucard et al., 2009; Brown et al., 2016; Hanson et al., 2019; Hernowo, Boucard, Jansonius, Hooymans, & Cornelissen, 2011; Hernowo et al., 2014; Malania, Konra, Jägle, Werner, & Greenlee, 2017; Olivo et al., 2015; Doety Prins et al., 2016). The rate at which the structural changes occur in visual cortex is currently unknown in cases of longstanding bilateral macular disease (MD), but recent evidence has shown long-term changes in cases of unilateral wet MD (Hanson et al., 2019). Understanding the time course of changes in individuals with established bilateral vision loss may prove important for visual restoration; if visual cortex is no longer viable and capable of processing new incoming information, the success of interventions aiming to restore functionally useful vision may be limited. Currently, we do not know whether treatment of the eye would in turn cause visual cortex to resume normal functioning and therefore prevent further atrophy. Additionally, we do not know at what point during disease progression interventions would be most effective at slowing atrophy in the entire visual pathway, allowing patients to maintain some form of functionally useful vision.

Given the retinotopic organisation of visual cortex, when macular degeneration (MD) is present in both eyes, resulting in overlapping visual defects, the cortical representation of this part of the visual field lacks sensory input – this is referred to as the lesion projection zone (LPZ). Previous neuroimaging studies have reported a reduction in cortical thickness in the LPZ in both juvenile MD (JMD) and age-related MD (AMD) compared to age-matched sighted controls (Beer et al., 2020; Hernowo et al., 2014). Patients show a reduction in both grey and white matter within the posterior visual pathway, but primarily at the occipital pole - corresponding to the LPZ - the lateral geniculate nucleus (LGN) as well as the optic radiations which connect the two (Boucard et al., 2009; Burge et al., 2016; Hernowo et al., 2014;

Malania et al., 2017; Plank et al., 2011). Evidence concerning the state of the intact projection zone (IPZ) – more anterior parts of the calcarine sulcus representing intact peripheral vision in MD patients – is somewhat mixed. Some argue there is evidence of thinning in the IPZ (Doety Prins et al., 2016), however others report that an increased reliance on peripheral vision induces cortical thickening (Burge et al., 2016). As discussed in Chapter 1, some controversy remains however, concerning the nature of changes in visual cortex following retinal disease, and there is limited evidence assessing the time course of such changes as well as the impact of MD on cortical myelin content. We know primary visual cortex is highly myelinated and seems to be more resistant to the effects of aging than prefrontal and association areas (Fjell & Walhovd, 2010; Lu et al., 2011; Williamson & Lyons, 2018), but the impact of MD on cortical myelin is yet to be explored.

Our study aimed to track the decline in visual cortex in patients with bilateral MD (age-related and juvenile forms), compared to sighted controls, to extend the work of Hanson et al., (2019) who showed changes in the LPZ over time in cases of AMD with unilateral visual loss. We want to determine whether cortex continues to show a decline in thickness even in the later stages of disease progression, but also establish how cortical myelin is impacted by the disease. We measured cortical thickness and myelin over multiple time points in a ~24-month period, using structural MRI. Given the evidence from cross-sectional studies showing MD patients exhibit notable structural changes compared to sighted controls (Beer et al., 2020; Boucard et al., 2009; Burge et al., 2016; Malania et al., 2017; Doety Prins et al., 2016), we predicted an accelerated rate of decline in cortical thickness in the LPZ (the occipital pole) compared to regions of visual cortex representing spared vision (anterior calcarine sulcus). Regarding cortical myelin, we predicted that during this brief 24-month period that perhaps we would not observe any significant changes in the LPZ, given the literature indicates myelin appears to be robust to changes associated with aging in visual areas. However, other age-related diseases such as Alzheimer's disease do show degeneration in myelin within the prefrontal and association areas, but such changes may occur over a much broader timeframe than we are examining here (Bartzokis, 2004; Williamson & Lyons, 2018). It is possible that there is an interaction between the two measures of interest, as has been suggested in developmental work showing that in childhood, increases in myelin

caused apparent cortical thinning (Natu et al., 2019). If changes in cortical thickness drive any changes in myelin density, we may expect to see an increase in myelin over time, alongside the well-established thinning of grey matter in MD patients (Glasser & Van Essen, 2011).

Research focusing on visual impairments largely contrasts patients with sighted controls, comparing visual function and measures of both the structure and function of visual cortex (Boucard et al., 2009; Hernowo et al., 2014; Doety Prins et al., 2016). Whilst this allows researchers to determine how vision loss has impacted such measures in contrast to natural aging, something rarely reported are the changes that occur within individuals before and after a diagnosis affecting vision. Hanson et al (2019) established that in the first 3-4month period following diagnosis, there was no significant change in cortical thickness in the LPZ, but changes were found to have emerged ~5 years after diagnosis. It is therefore plausible any changes after 3 months were too small to detect. We have had the unique opportunity to assess structural changes in visual cortex in two individuals before and after bilateral AMD diagnosis, allowing us to determine how visual cortex is impacted at disease onset in two very different cases: the first with sudden bilateral vision loss, the second with an AMD diagnosis, but no vision loss. Such cases will provide insight into how early interventions should be in order to preserve the integrity of the posterior visual pathway, from eye to brain.

2.3 Methods

2.3.1 Participants
13 individuals with macular disease (MD) were recruited from the Ophthalmology department at York Teaching Hospital and through advertisements in sight loss support groups in York (referred to as MD1-MD13; mean age = 71.42 years, age range = 28–87 years, full MD patient demographics included in Table 2.1). MD patients all had a diagnosis of bilateral macular disease; time since disease onset at the time of enrolment ranged from 9 months to 23 years, mean = 11.2 years. MD12 was excluded from most analyses due to ill health preventing participation in follow up MRI sessions. 18 sighted controls (referred to as C1–C18, mean age = 55.33 years, age range = 24-73 years) were recruited for this study through advertisements at the York Neuroimaging Centre (YNiC), University of York.

We acquired additional MRI data for two MD patients, who will be referred to as patient MD7 and MD13 throughout. MD7 has bilateral AMD, with a secondary bleed to one eye causing more severe sight loss (hand movements only). MD7 had participated in an MRI study prior to diagnosis and therefore, we included an additional set of MRI scans for MD7 to compute a detailed assessment of how visual cortex changed after diagnosis (see Figure 2.1A for timeline). We recruited another individual who had also regularly participated in neuroimaging studies at YNiC prior to an AMD diagnosis. This individual, referred to as MD13 has bilateral dry AMD but does not experience any vision loss, as assessed by visual acuity (see Figure 2.1B for timeline).

Finally, an additional 15 sighted controls (referred to as C19-C33, mean age = 66.27 years, age range = 48 – 83 years) were recruited through advertisements at YNiC. Despite being scanned under a different MRI protocol, they were included in the cross-sectional analysis to assess the relationship between our two measures: cortical thickness and myelin density. It was important for us to use additional data here to try and understand the nature of the relationship between the measures in normal aging and provide us with the necessary context when assessing the outcome for the MD patient group. Written informed consent was obtained from all participants. This study followed the tenets of the Declaration of Helsinki with approval granted by YNiC Research, Ethics and Governance Committee and the NHS Research Ethics Committee (IRAS: 158456).

Table 2.1. MD participant demographics. Some missing data for time since diagnosis and visual acuity scores – participants were unable to provide this information, or we were unable to access it.

Group	Eye Disease	Receiving treatment	Age at enrolment (years)	Time since disease onset (years)	Visual Acuity ETDRS letters [logMAR] OD	Visual Acuity ETDRS letters [logMAR] OS	Number of MRI sessions	Time between first and last MRI session (years)
MD1	Wet AMD	Yes	85	-	40 [0.90]	76 [0.18]	3	0.57
MD2	Wet AMD	Yes	86	-	39 [0.92]	60 [0.50]	3	0.47
MD3	Wet AMD	Yes	76	3.6	69 [0.32]	54 [0.62]	5	1.68
MD4	Dry AMD	No	79	5	34 [1.02]	34 [1.02]	6	2.08
MD5	Wet AMD	Yes	87	-	55 [0.60]	79 [0.12]	3	0.47
MD6	JMD (Best's Disease)	No	51	20	85 [0.00]	85 [0.00]	6	2.07
MD7	Wet & Dry AMD	Yes	73	0.5	67 [0.36]	0 [2.20]	5	1.56
MD8	Dry AMD	No	78	14.9	0 [2.20]	44 [0.82]	4	1.02
MD9	Dry AMD	No	68	-	40 [0.90]	44 [0.82]	2	0.66
MD10	Dry AMD	No	65	21.2	65 [0.40]	65 [0.40]	4	1.61
MD11	JMD (Stargardt Disease)	No	28	1	90 [-0.10]	90 [-0.10]	4	0.98
MD12	Wet & Dry AMD	No	81	23.4	-	-	1	0
MD13	Dry AMD	No	72	1.42	-	-	2	2.2
Average (MD1 - MD12)			71.42	11.20			3.83	1.10

Table 2.2. Sighted control participant demographics.

Group	Age at enrolment (years)	Number of MRI sessions	Time between first and last MRI session (years)
C1	38	2	2.25
C2	63	2	2.5
C3	51	2	2.42
C4	64	2	2.25
C5	62	2	2.17
C6	24	2	2.17
C7	33	2	2.42
C8	29	2	2.42
C9	58	2	2.42
C10	69	2	2.42
C11	34	2	2.42
C12	73	2	2.42
C13	71	2	2
C14	70	2	2
C15	64	2	1.83
C16	72	2	1.67
C17	63	2	1.92
C18	58	2	1.83
Average	55.33	2.00	2.20
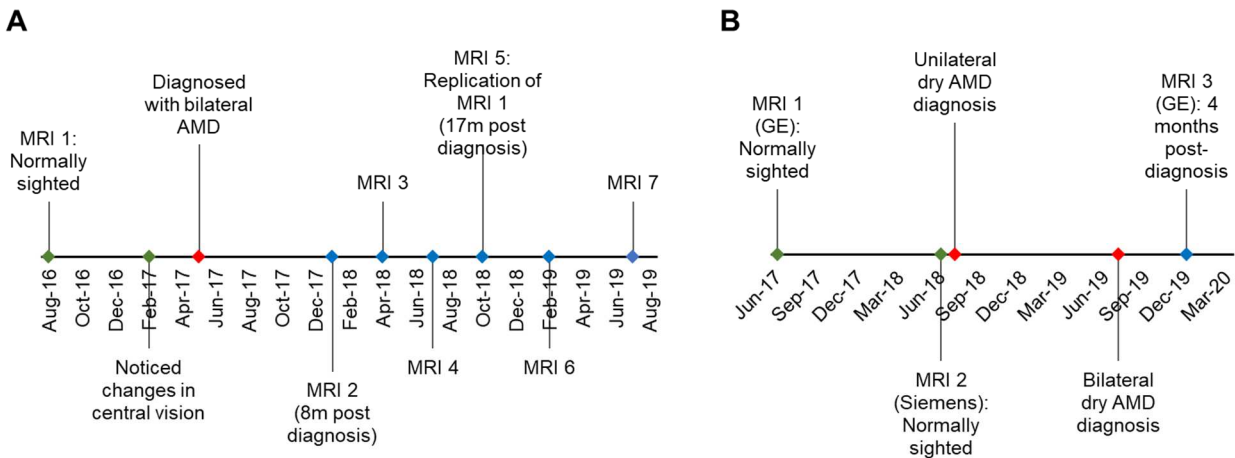
Figure 2.1. Timeline of events for two MD participants for whom data were acquired prior to AMD diagnosis. A: MD7 has bilateral AMD with severe vision loss after a secondary bleed to the left eye. B: MD13 has been diagnosed with bilateral dry AMD but has not reported any vision loss.

2.3.2 MRI data acquisition

Scanning was performed at the University of York Neuroimaging Centre using a 3 Tesla HD MRI system (GE Signa Excite 3.0T, High resolution brain array, MRI Devices Corp., Gainesville, FL) with an 8 channel whole head High Resolution Brain Array. Patients were scanned between one and six times over a ~24-month period, whereas controls were scanned twice, approximately ~24 months apart (See Table 2.1 for details). Some subgroups (C13-C18) have different T1 and T2 protocols due

to the fact we were replicating protocols from the first time points which were often conducted by different research groups. It was essential to keep protocols consistent within individuals to reduce the effect of scan type on the outcome measures. All T1 and T2 images were gradwarped to correct for nonlinearities in the gradients.

For our final set of control participants (C19-C33) scanning was performed on the 3T Magnetom Prisma MR scanner (Siemens Healthineers, Erlangen, Germany), using the 20-channel head / neck receive-array coil. Participants were scanned using the Human Connectome Project (HCP) recommended protocols.

2.3.2.1 For MD1-MD12 and C1-C12

For each time point for each participant, one 8-channel 3D T1-weighted anatomical image (TR = 7.88ms, TE = 2.99ms, TI = 600ms, voxel size = 1 x 1 x 1mm^3, flip angle = 10°, matrix size 256 x 256 x 176, FOV = 256mm) and one T2-weighted anatomical image was acquired (TR = 2500ms, TE = 75.48ms, voxel size = 1 x 1 x 1mm^3, flip angle = 90°, matrix size = 256 x 256 x 176, FOV = 256mm).

2.3.2.2 For MD7(2 time points), MD13 and C13-C18 (all time points)

At each time point for a subset of controls (n=6) and MD13 one 8-channel 3D FSPGR T1-weighted anatomical image was acquired (TR = 7.76ms, TE = 2.96ms, TI = 450ms, voxel size = 1.13 x 1.13 x 1mm^3, flip angle = 20°, matrix size = 256 x 256 x 176, FOV = 290mm).

2.3.2.3 For MD7(1 time point), MD13 (1 time point) and C13-C18 (1 time point)

One T2-weighted anatomical image was acquired (TR = 8940ms, TE = 201.704ms, voxel size = 1.13 x 1.13 x 1mm^3, flip angle = 90°, matrix size = 256 x 256 x 176, FOV = 290mm).

2.3.2.4 For C19-33

One T1-weighted anatomical image was acquired using a 3D-MPRAGE sequence (TR = 2400ms, TE = 2.28ms, TI = 1010ms, voxel size = 0.8 x 0.8 x 0.8mm^3, flip angle = 8°, matrix size = 320 x 320 x 208, FOV = 256mm) and one T2-weighted anatomical image was acquired (TR = 3200ms, TE = 563ms, voxel size = 0.8 x 0.8 x 0.8mm^3, flip angle = 120°, matrix size = 320 x 320 x 208, FOV = 256mm).

2.3.3 Longitudinal experiment
2.3.3.1 Study Design (MD1-MD12, C1-C18)

MD Participants were enrolled in the study for up to ~24 months with a maximum of 6 MRI scans in the time period. MD patients were given the option to opt in for the sessions they wished to attend, hence not all participants completed all sessions offered. Control participants only completed 2 MRI scans ~24 months apart. See Table 2.1 for details of the number of sessions completed by each participant. Figure 2.1 outlines the number of sessions and timeline for MD7 (Figure 2.1A) and MD13 (Figure 2.1B).

2.3.3.2 Cortical thickness analysis

Due to participant ill health and only having one time point, MD12 was excluded from the longitudinal analysis. All T1 and T2 weighted data (where possible) were analysed using the automatic longitudinal processing stream (Reuter, Schmansky, Rosas, & Fischl, 2012) in FreeSurfer analysis suite (version 6, available at: http://surfer.nmr.mgh.harvard.edu/). To compute reliable estimates of the rate of change in cortical thickness, several processing steps were completed. Each individual data set was processed automatically using FreeSurfer; Cortical reconstruction and volumetric segmentation was performed, and segmentations were inspected and manually corrected where applicable (e.g., when pial (grey matter) surface extended too far into the cerebellum). Once individual time points were checked and processed, an unbiased within-subjects template space and image was created (Reuter & Fischl, 2011) using robust inverse consistent registration (Reuter, Rosas, & Fischl, 2010). Next, skull stripping, Talairach transforms, atlas registration as well as spherical surface maps and parcellations were initialised using common information for the within-subject template created. This is known to significantly increase the reliability of cortical thickness measures and in turn increase the statistical power (Reuter et al., 2012). Our regions of interest (ROIs) were defined using FreeSurfer's Destrieux anatomical atlas (Destrieux, Fischl, Dale, & Halgren, 2010). Cortical thickness is calculated by taking the shortest distance (millimetres) between the white matter surface and the grey matter surface at each vertex across the cortex; measurements across all vertices within an ROI are then averaged (Figure 2.2). Rate of change in cortical thickness across all time points was calculated and plotted for all ROIs. ROIs taken from the Destrieux

anatomical atlas were the occipital pole (parcellation index = 42) and the calcarine sulcus (parcellation index = 44). Values were averaged across hemispheres. Given that both the occipital pole and calcarine sulcus ROIs defined here are not restricted to primary visual cortex, we generated a second set of ROIs by intersecting the occipital pole with V1 - Brodmann Area label created during initial recon-all processing (Fischl et al., 2008). This allowed us to generate two ROIs restricted to primary visual cortex which will be referred to as central-V1 (overlap between occipital pole and V1) and peripheral-V1 (areas of V1 not overlapping with occipital pole) throughout. The peripheral-V1 ROI includes more of the upper / lower meridian than the calcarine sulcus.
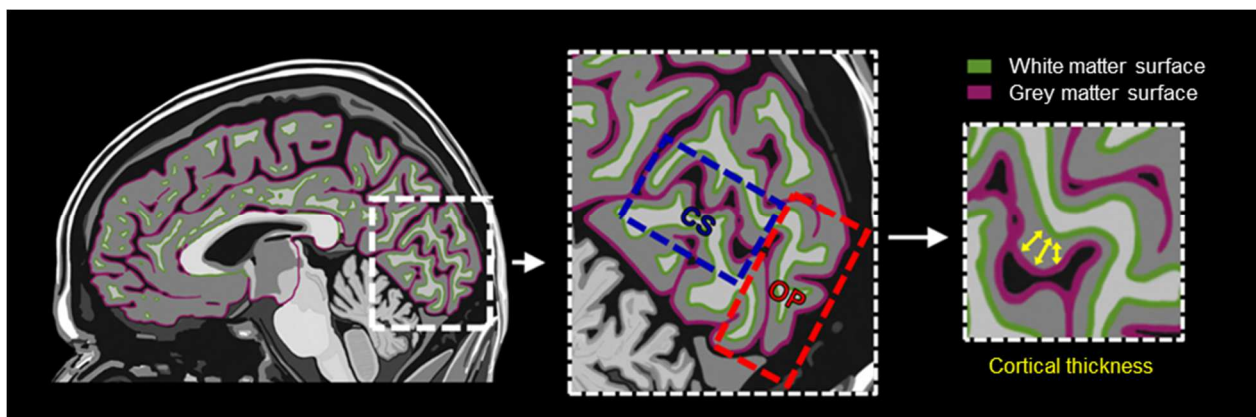
Figure 2.2. Illustration of processed anatomical data from the sagittal view. Cortical thickness (yellow arrows) is calculated by taking the shortest distance (millimetres) between the white matter surface (green) and the grey matter/pial surface (magenta). Two example regions of interest are indicated by the dashed boxes: calcarine sulcus (blue) and occipital pole (red).

2.3.3.3 Myelin Density analysis

To compute cortical myelin density, T1 and T2 data were processed using the automatic pipeline developed by the Human Connectome Project (HCP, version 4.0.0) which uses the T1w/T2w ratio to generate myelin maps (Glasser et al., 2014). The HCP MRI data pre-processing pipelines use tools from FreeSurfer (Van Essen, Glasser, Dierker, Harwell, & Coalson, 2012) and FSL (Jenkinson, Beckmann, Behrens, Woolrich, & Smith, 2012). The pipeline generates cortical myelin maps (example shown in Figure 2.3) in the subject's native space (Glasser & Van Essen, 2011). The ROIs used were the same as described above - occipital pole and calcarine sulcus from the Destrieux anatomical atlas and the central-V1 and

peripheral-V1. As myelin was calculated using the HCP processing stream, each time point was effectively processed as if it were a separate individual, as there is currently no comparable longitudinal processing stream for generating myelin maps. However, as this was a FreeSurfer based analysis, the same ROIs could be computed for this separate data analysis. MD1-M11 and C1-C12 were included in this analysis. No T2-weighted images were acquired for C13-C18, and therefore estimates of myelin density could not be computed for these individuals, nor could they be computed for the first time point pre-diagnosis for MD7 and MD13.

Rate of change was calculated for myelin density using the slope of a regression line based on the times measurements were taken (x-values), and what the myelin values were at each time point (y-values). This was done for every individual before the group result was calculated.
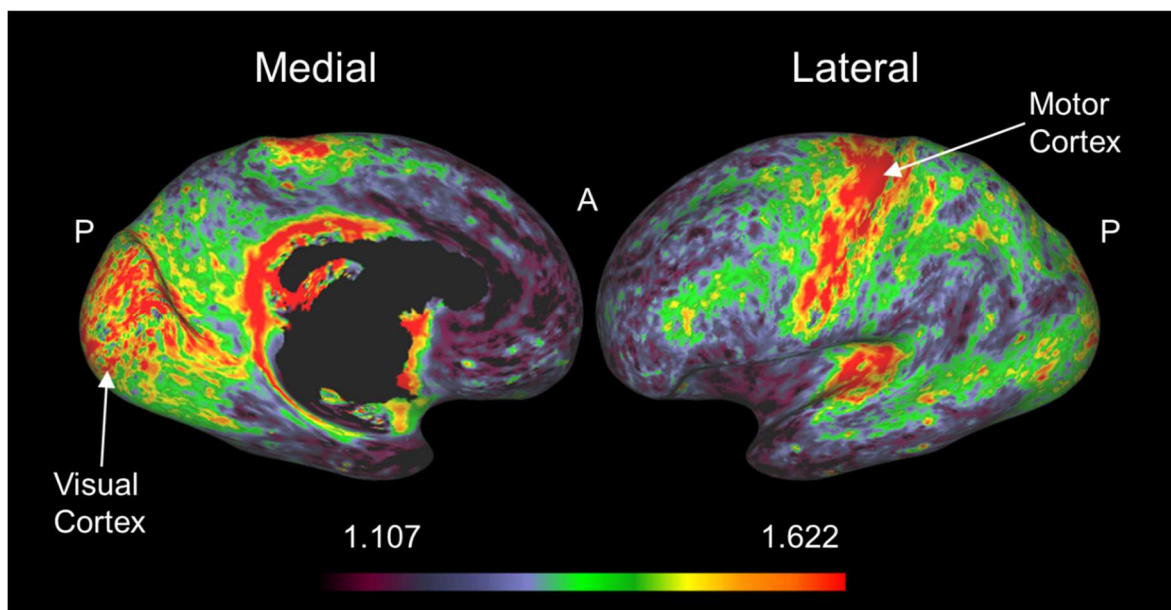
Figure 2.3. Example unsmoothed myelin map for the left hemisphere of a sighted control using the HCP minimal processing pipeline (Glasser et al., 2011). Hotter colours represent regions with higher myelin density values, notably the visual and motor cortices.

2.3.3.4 Longitudinal analysis of cortical thickness in MD7 and MD13

We calculated cortical thickness values for each time point in the within-subject template to visualise how cortical thickness changes over time, as well as computing the rate of change. Data were processed using the longitudinal stream as described above, but for this analysis for MD7, two additional time points were included. For MD13, only data acquired on the GE scanner was included in this analysis (MRI 1 and MRI 3). See Figure 2.1 for details.

2.3.3.5 Longitudinal analysis of myelin density in MD7

We also had the opportunity to examine myelin density in MD7 post-diagnosis. No T2-weighted scans were acquired at the first time point, however the 6 post-diagnosis timepoints did include a T2 scan. The 4th time point post-diagnosis (2.11 years post diagnosis) was removed from this analysis due to issues generating a myelin map. As such, only 5 post-diagnosis time points are presented. As described above, the HCP processing pipeline was used to generate myelin maps for MD7 and a mean value for each ROI was plotted. A rate of change value was also computed in the same was as described for group data.

2.3.4 Cross sectional cortical thickness and myelin density analysis

In order to visualise the impact of group on both myelin density and cortical thickness, as well as the relationship between measures, we calculated group mean values for MD patients (MD1-MD11) and controls (C1-C18 for cortical thickness and C1-C12 for myelin density) for all four ROIs. We simply averaged across timepoints for each individual, before then computing a group average.

C19-C13 were only scanned at a single time point and so do not contribute to the longitudinal analysis. Data were processed using the HCP minimal processing stream described above, after which the cortical thickness and myelin values were extracted from the subject's native space. The ROIs were computed as described previously. C19-C33 were only included in the scatterplots along with C1-C12. Myelin density and cortical thickness were converted to Z-scores for this due to the fact data were acquired on different MRI scanners, and given the difference in resolution, thickness and myelin values will differ.

2.3.5 Linear mixed effects for individual time points

To assess the difference in cortical thickness and myelin density between groups and over multiple time points, values for both measures at each time point were analysed using a linear mixed effects model (Winter, 2013a, 2013b). The model used for each ROI were as follows *(R syntax):*

$$(a) \; Thickness \sim 1 + Age + Group{:}Time + (1 \mid Participant)$$

$$(b) \; Myelin \sim 1 + Age + Group{:}Time + (1 \mid Participant)$$

Age at the time of recruitment, group and time were included as fixed effects, and participants as a random effect. By having this as a random effect, all participants have a different intercept, and this allows us to account for between-subject variability in cortical thickness and myelin density. We examined both measures for all four ROIs for both the MD and control groups. The model for each ROI was evaluated using restricted maximum likelihood (REML) estimation to ensure the model was robust. This is the optimal method for studies with smaller samples and uneven group sizes. The significance was assessed using t-tests which incorporated the Satterthwaite's method to calculate our degrees of freedom and in turn control for possible type-1 errors.

2.4 Results

2.4.1 Cross-Sectional analysis

2.4.1.1 Assessing the relationship between cortical thickness and myelin density in sighted group

In order to understand the possible impact of macular disease on both of our measures, we pooled together sighted control data across studies, to enable us to visualise how the two measures may be related. Given data were acquired using different MRI scanners, we converted cortical thickness and myelin density values to z-scores separately before combining them, to allow us to interrogate the data on the same scale. Figure 2.4 shows data for all four ROIs for our control data (n=27). It appears there is a hint of a negative correlation between cortical thickness and myelin density, but this is significant in the occipital pole only.
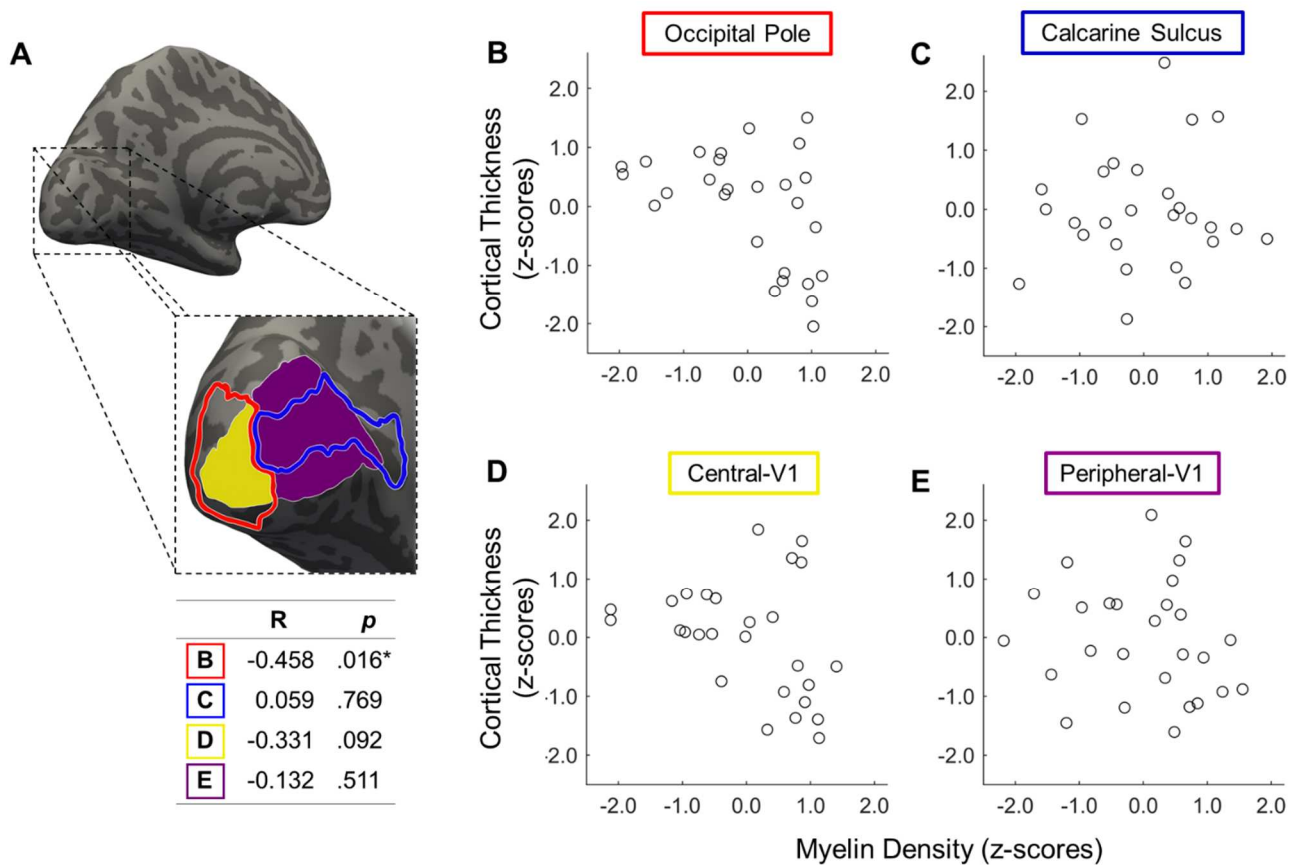
Figure 2.4. A: Regions of interest in visual cortex for all analyses shown on an inflated cortical surface. Occipital pole = red, calcarine sulcus = blue, central-V1 = yellow, peripheral-V1 = purple. The table below the inflated surface is a summary of the correlation (R) and corresponding p-values for each of our ROIs. The only significant correlation was for the occipital pole (**B**). **B-E**: Scatterplots plotting myelin density against cortical thickness (z-scores) for all sighted controls.

2.4.1.2 Mean cortical thickness

To establish whether results for this group of MD patients (MD1-M11) and sighted controls are consistent with previous cross-sectional studies, we calculated the mean cortical thickness values for each group for all ROIs. Values reported in Figure 2.5B-E and H-K were averaged across hemispheres and then averaged across time points for each individual, before a group mean was calculated. In Figure 2.5B and C, we have calculated the mean group cortical thickness for all MD patients and all 18 controls for the four ROIs. In Figure 2.5D and E we present just C1-C12 who have also contributed myelin data. Mean cortical thickness seems to be consistent across Figure 2.5B and D, even with fewer participants contributing to Figure 2.5D, with MD patients showing an overall thinner cortex than sighted controls, for both the occipital pole and calcarine sulcus. For our ROIs restricted to V1, while the figures

57

are lower overall in C and E, we generally see the same pattern, with MD patients having a thinner cortex. For E in particular, the difference between groups is far smaller. See Section 2.4.2.3 for the results of the linear mixed effects model. Table 2.2 summarises the results for the linear mixed effects models. In summary, a significant effect of group was shown for the occipital pole, calcarine sulcus, central-V1 but not peripheral-V1, indicating MD patients had, on average, a thinner cortex than sighted controls, particularly in the regions capturing the LPZ.

2.4.1.3 Mean Myelin density

For myelin density, we calculated the group means as described above. We observed a higher mean myelin density value for our MD patient groups compared to our sighted control group, and this occurred for all four ROIs (Figure 2.5F and G). Given the literature indicates that thinner regions of cortex often have a larger amount of myelin, this pattern of results seems unsurprising. Interestingly, as shown in Table 2.2, the linear mixed effects models revealed a significant effect of group for the calcarine sulcus and peripheral-v1 ROIs only, with MD patients having, on average, more myelin in the peripheral representation in visual cortex. Example myelin maps and cortical thickness for an MD patient and sighted control are shown in Figure 2.6. Looking at cortical thickness and myelin together, the group data seems to support the negative correlation shown in the sighted control cohort (Figure 2.4), whereby a reduction in cortical thickness appears to be accompanied by an increase in myelin.

Next, we wanted to explore what would happen to both cortical thickness and myelin density over a period of time. Cross-sectional results show a difference between our sighted and MD groups, but it is unknown (a) whether these two measures will change in the same way over time with natural aging and (b) whether eye disease will have an impact on these measures in a different manner to natural aging.
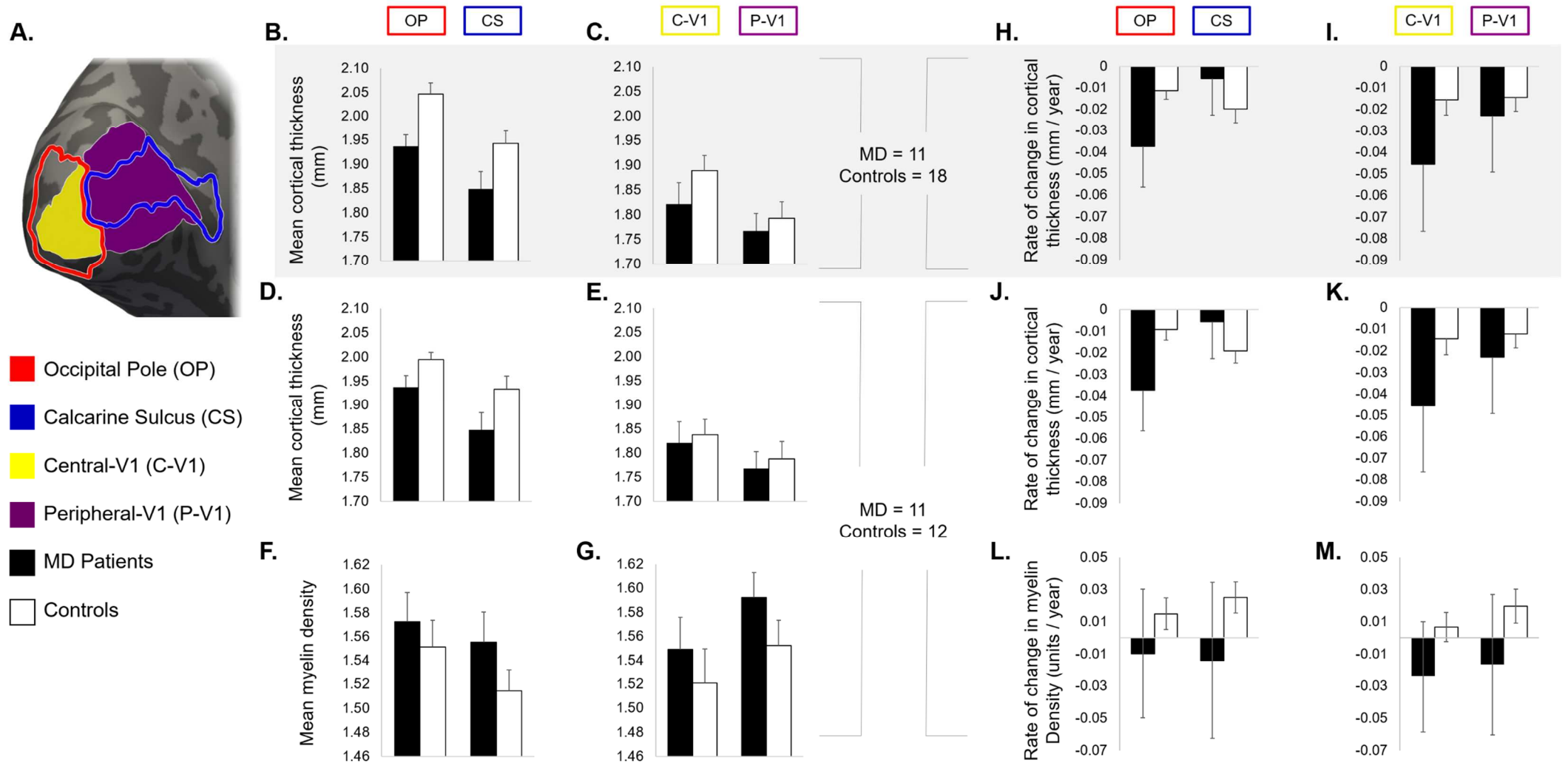
Figure 2.5. A: Regions of interest (ROIs) on the inflated cortical surface for MD patient (black bars) and sighted controls (white bars). Error bars = SEM. **B-E**: Mean cortical thickness (mm) for four ROIs as indicated at the top of each column. **B&C**: MD patients and C1-C18. **D&E**: MD patients and C1-C12, the subset of controls that contribute myelin data. **F&G**: Mean myelin density for MD patients and C1-C12 for all ROIs. **H-K**: Rate of change in cortical thickness (millimetres per year) for MD patients and C1-C18 (**H&I**) and MD patients and C1-C12 (**J&K**). **L&M**: Rate of change in myelin density (units per year) for MD patients and C1-C12.

Table 2.3: Results from the Linear Mixed Effects Models for cortical thickness and myelin density. Here we are reporting the fixed-effects 's with the standard error (SE) for the predictors we used for each ROI. Age refers to the age of participants at the first time point. Group refers to MD patients and sighted controls. T-test results determine the significance of each of the predictors reported here. All significant results are in bold.

Cortical Thickness

Predictor	Occipital Pole b (SE)	Occipital Pole t (df)	Calcarine Sulcus b (SE)	Calcarine Sulcus t (df)	Central-V1 b (SE)	Central-V1 t (df)	Peripheral-V1 b (SE)	Peripheral-V1 t (df)
Age	**0.002 (0.001)**	**2.09 (25.76)***	-0.001 (0.001)	-0.76 (25.96)	**0.003 (0.001)**	**2.19 (26.10)***	0.001 (0.001)	0.65 (26.00)
Group	**-0.14 (0.04)**	**-3.52 (27.76)***	**-0.10 (0.05)**	**-2.06 (26.92)***	**-0.12 (0.06)**	**-2.12 (28.11)***	-0.05 (0.06)	-0.85 (27.04)
Time	**-0.01 (0.01)**	**-2.34 (50.00)***	**-0.02 (0.005)**	**-4.30 (50.07)***	**-0.02 (0.01)**	**-2.28 (50.34)***	**-0.01 (0.01)**	**-2.32 (50.11)***
Group:Time	-0.02 (0.01)	-1.56 (50.54)	0.02 (0.01)	1.64 (50.32)	-0.02 (0.02)	-1.08 (50.88)	0.001 (0.01)	0.09 (50.39)

Myelin Density

Predictor	Occipital Pole b (SE)	Occipital Pole t (df)	Calcarine Sulcus b (SE)	Calcarine Sulcus t (df)	Central-V1 b (SE)	Central-V1 t (df)	Peripheral-V1 b (SE)	Peripheral-V1 t (df)
Age	0.001 (0.001)	0.83 (20.78)	-0.002 (0.001)	-1.61 (20.67)	0.001 (0.001)	0.83 (20.03)	-0.001 (0.001)	-0.57 (20.68)
Group	0.03 (0.04)	0.78 (26.90)	**0.11 (0.04)**	**2.71 (31.13)***	0.04 (0.05)	0.70 (24.55)	**0.09 (0.04)**	**2.05 (31.39)***
Time	0.02 (0.01)	1.48 (45.20)	**0.03 (0.01)**	**2.11 (45.58)***	0.01 (0.01)	0.67 (44.34)	0.02 (0.01)	1.63 (45.62)
Group:Time	**-0.04 (0.02)**	**-2.16 (46.93)***	-0.05 (0.02)	-1.94 (48.63)	**-0.05 (0.02)**	**-2.29 (45.66)***	-0.04 (0.02)	-1.85 (48.75)

$*p<.05, **p<.01, ***p<.001$; from t-tests, using Satterthwaite's method to correct degrees of freedom (df)
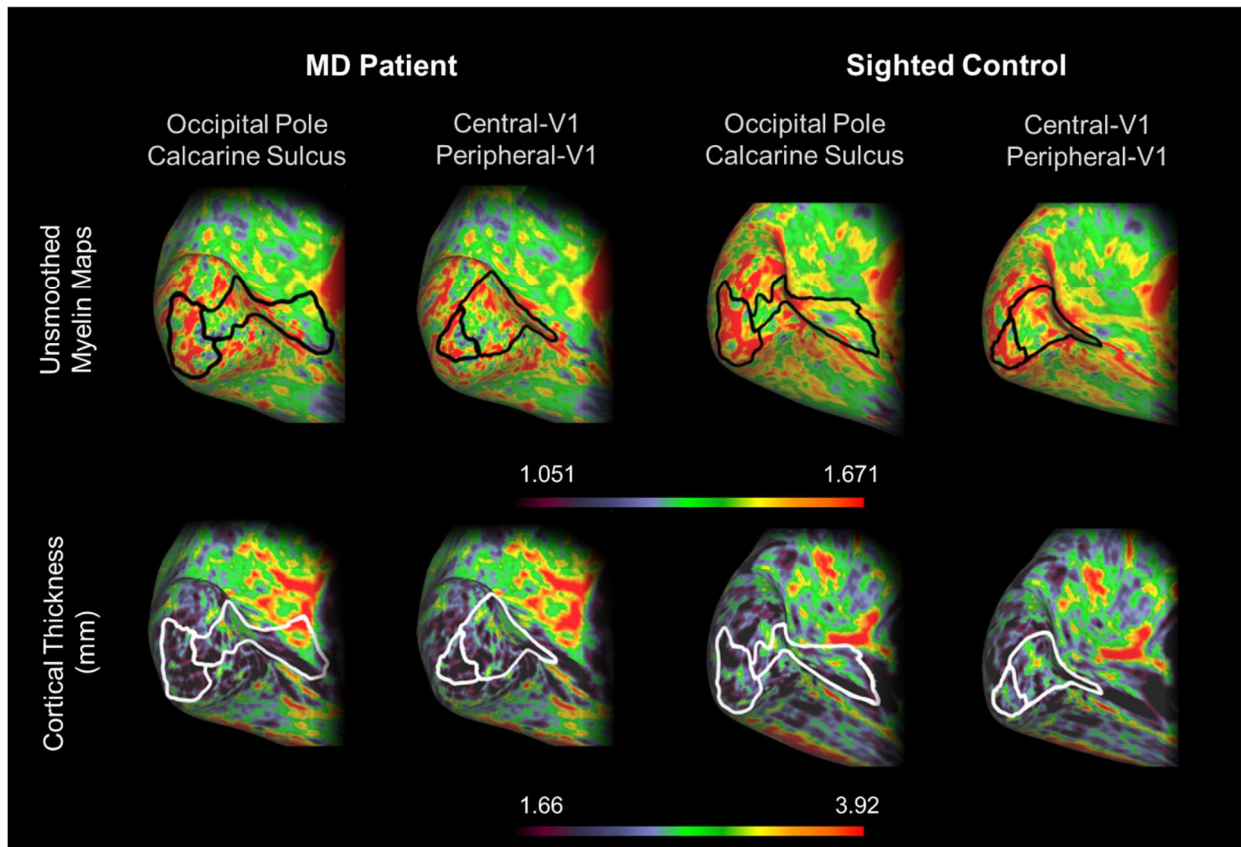
Figure 2.6. Example unsmoothed myelin maps (upper row) and cortical thickness maps (lower row) for an MD patient (column 1&2) and sighted control matched for age and gender (column 3&4). Regions of interest have been overlaid onto the myelin and thickness maps. Colour bars represent myelin density and cortical thickness, with hotter colours indicating higher values.

2.4.2 Longitudinal Analysis

2.4.2.1 Rate of change in cortical thickness

As part of the longitudinal pipeline, rate of change in cortical thickness was calculated for all ROIs, allowing us to determine how cortical thickness values may change over the ~24-month period in both groups. We predicted that patients would show an accelerated rate of decline in the occipital pole / central-V1 compared to controls given these ROIs capture the representation of the damaged visual field, but we did not predict a difference between groups for the calcarine sulcus, given that for both groups, this represents the intact projection zone. Figure 2.5 H & J show the rate of change in cortical thickness for our occipital pole and calcarine sulcus ROIs. Despite the reduced number of participants in Figure 2.5J, results are consistent. The general pattern observed is that irrespective of group, with time, cortical thickness declines. MD patients seem to show a faster decline in cortical thickness within the occipital pole and central-V1, whereas there seems to be a

smaller difference between groups in the calcarine sulcus and peripheral-V1. Differences between the groups were explored using a linear mixed effects model analysis (see Section 2.4.2.3). Again, the rate of change remained consistent for the sighted controls even when only including the 12 who also contributed myelin data (Figure 2.5I, K).

2.4.2.2 Rate of change in myelin density

The rate of change in myelin density was calculated for each ROI as shown in Figure 2.5 L-M. The data appear to show a decline in myelin over time in MD patients across all ROIs, more so in those restricted to V1, but in contrast, a small increase was observed for the control group. This result for the controls appears to compliment the cross-sectional findings between the two measures and the increase observed could simply be explained by an artefact caused by the decrease in cortical thickness. For MD patients, this is not the case. Differences between the groups were explored using a linear mixed effects model analysis (see Section 2.4.2.3).

2.4.2.3 Linear Mixed Effects Model: Cortical Thickness

All results for the linear mixed effects models are reported in Table 2.2. Given the difference in the average age of our two groups, we wanted to account for the role it may play in any observed findings by including it as a fixed effect in our model. Age had a significant effect on cortical thickness in the occipital pole (t(25.76)=2.09, p=.047), but not for the calcarine sulcus (t(25.96)= -0.76, p=.453) however despite this, we still find a significant effect of group, suggesting any group differences are likely attributed to visual impairment, not age. MD patients have a thinner cortex overall compared to controls (significant effect of group; occipital pole: $t(27.76)$= -3.52, p<.001, calcarine sulcus: $t(26.92)$= -2.06 p=.050). In line with previous literature, all participants irrespective of group, show a decline in cortical thickness over time (significant effect of time in the occipital pole: $t(50.00)$ = -2.34, p=.023 and calcarine sulcus: $t(50.07)$= -4.30, p<.001).

For our V1 ROIs, age also had a significant effect for our central representation (t(26.10)=2.19, p=.038), but not for the peripheral-V1 (t(26.00)= 0.65, p=.524). Our group effects still emerged as significant for central-V1 (t(28.11)= -2.12, p=.043), however no significant differences emerged between groups for peripheral-V1. Irrespective of group, we still see a decline in cortical thickness over time for both of our ROIs (central-V1: $t(50.34)$ = -2.28, p=.027 and peripheral-V1: $t(50.11)$= -2.32, p=.028). Finally, there was no significant interaction between group and time for any of our ROIs (see Table 2.2)

suggesting MD patients did not decline at a significantly faster rate than controls during this time period.

2.4.2.4 Linear Mixed Effects Model: Myelin Density

As with cortical thickness, age was entered as a predictor into our model, however age was not a significant predictor of myelin density for any of our ROIs (see Table 2.2). In terms of group differences, overall MD patients overall had a higher mean myelin density value for both our peripheral ROIs compared to controls (calcarine sulcus: $t(31.13)= 2.71$, $p=.011$, peripheral-V1: $t(31.39)= 2.05$ $p=.049$). Interestingly, time was only a significant predictor of myelin content for calcarine sulcus ($t(45.58)= 2.11$, $p=.041$), again showing a significant increase with time. Looking at our rate of change plots, this is likely driven by the control data. In terms of group x time interactions, a significant effect emerged for both of our central representations, whereby patients are shown to be changing at a significantly different rate to controls. The estimates for this predictor being negative (-0.04) indicates that MD patients decline faster than controls for both occipital pole ($t(46.93)= -2.16$, $p=.036$) and central-V1 $t(45.66)= -2.29$, $p=.027$). Whilst not significant, the calcarine sulcus result was close ($p=.058$), hinting that the decline in myelin may extend to regions beyond the representation of the lesion.

2.4.2.5 Case studies: MD7 & MD13

As well as assessing the group data, we also investigated changes in cortical thickness at each time point before and after an AMD diagnosis in our individual cases - MD7 and MD13. Figure 2.7 shows cortical thickness values for each individual time point for MD7 (Figure 2.7A), illustrating a decline in all four ROIs over time, with a slightly steeper decline for the occipital pole and central-V1. A decline, albeit slower, was also observed for all ROIs for MD13 (Figure 2.7B).

Rate of change was also calculated for both MD7 and MD13. Table 2.3 summarises the rate of change data from our MD patient group, sighted controls (n=18) and two cases for each of our ROIs. The rate of change for MD7 is most extreme, showing a faster decline compared to MD13 and both the MD patient and control groups. This was apparent for all ROIs indicating that cortical thickness may decline fastest in the earliest stages of the disease, but after vision is lost. Overall change is slower than MD7, which could be expected because MD13 reported no vision loss at the time. MD13 also shows a slower decline compared to the MD group for ROIs capturing the representation of central vision, however it is worth noting MD13 shows a faster decline in the peripheral representations

compared to the MD group, much like MD7. Whilst the general direction of change in cortical thickness for MD13 seems similar to the control group, it is interesting that MD13 does appear to decline faster than controls in all ROIs despite having functional vision.
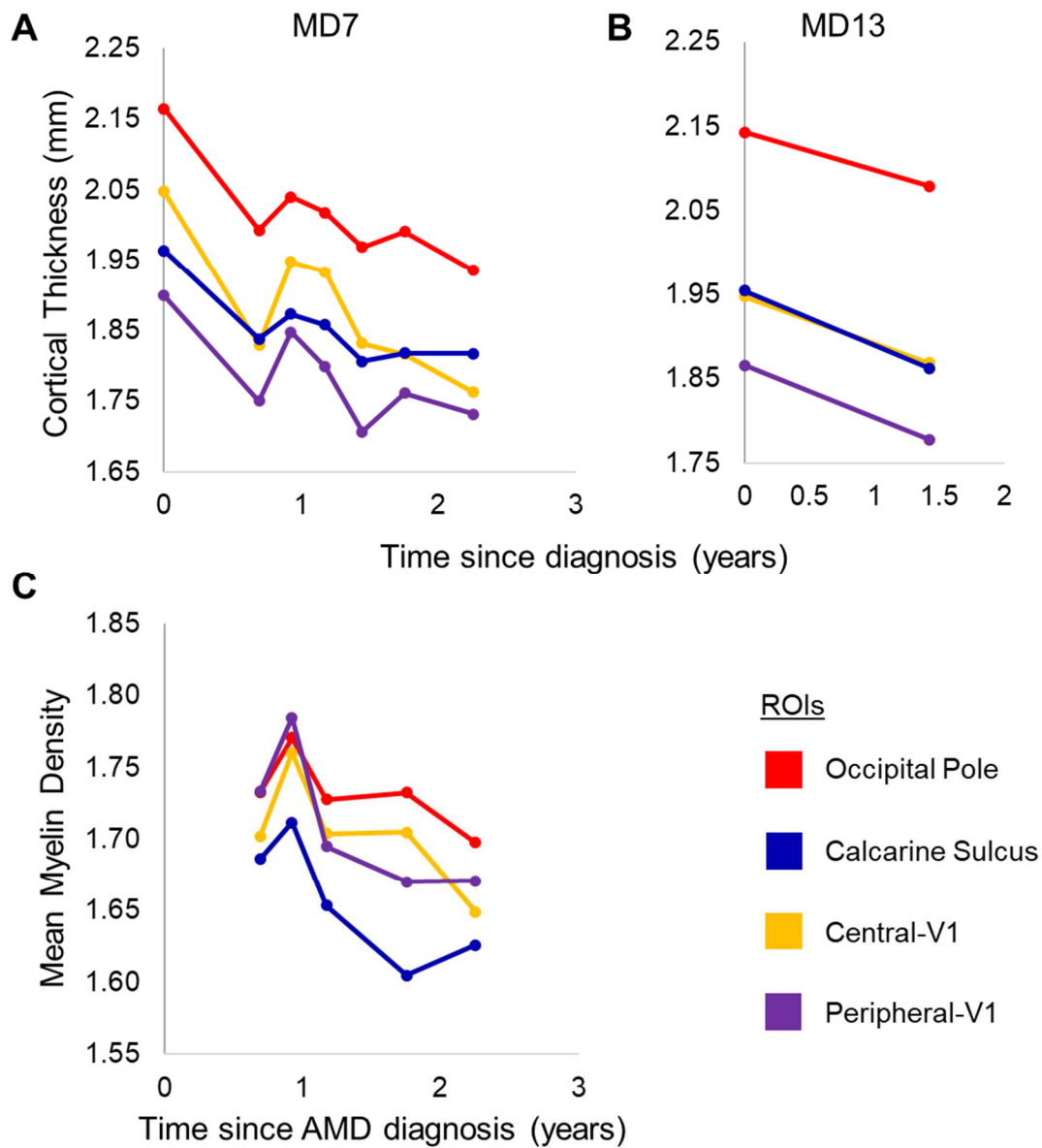
Figure 2.7. Mean cortical thickness measures (mm) in our 4 regions of interest for **A**: MD7 – bilateral AMD with bilateral vision loss and **B**: MD13 – bilateral AMD with no vision loss. Mean myelin density for the same ROIs for MD7 – post diagnosis timepoints only (**C**). Interestingly, all data show a decline.

Table 2.4. Summary of rate of change in cortical thickness for each ROI. Data presented for MD patient group, control group (n=18) and our two individual AMD cases. MD7 shows the greatest changes in all ROIs.

	Occipital Pole	Calcarine Sulcus	Central-V1	Peripheral-V1
MD group	-0.037	-0.006	-0.046	-0.023
Controls	-0.009	-0.019	-0.014	-0.012
MD7	-0.071	-0.055	-0.085	-0.060
MD13	-0.023	-0.036	-0.039	-0.03

Finally, we were able to assess cortical myelin for MD7 for 5 out of the 6 time points after diagnosis. Unfortunately, T2-weighted scans were not acquired during the first time point, however it is interesting to observe how the individual time point values post-diagnosis may change over time. The cross-sectional data seemed to indicate that areas that thinner tend to have more cortical myelin. Given this, one would expect to perhaps see a complimentary increase in myelin in MD7 over the 5 time points post-diagnosis. However, this does not appear to be the case. The group MD data show an overall significant change in myelin compared to controls, and in the negative direction. MD7's data seem to support this, showing a very slight decline in all regions over time which is supported by the rate of change values. Changes in cortical myelin appear to be more subtle than those shown in cortical thickness, but it provides additional insights to other anatomical structures that may be degenerating as a result of eye disease.

2.5 Discussion

Our study aimed to assess the status of visual cortex in macular disease, by acquiring two anatomical measures: cortical thickness and cortical myelin density. We assessed four atlas-based anatomical ROIs, capturing both intact and lesion projection zones over multiple time points in a ~24-month period. Our results show that irrespective of group, there is a decline in cortical thickness during the time period of the study in all ROIs. This was expected given cross-sectional studies have highlighted reductions associated with natural aging, but also that MD affects not only the physiology of the eye, but also largely supports a thinning of cortex and reduction in volume in the posterior visual pathway (Boucard et al., 2009; Brown et al., 2016; Hanson et al., 2019; Hernowo et al., 2011, 2014; Malania et al., 2017; Olivo et al., 2015; Doety Prins et al., 2016). In terms of group effects, our results indicate that overall, our MD patients have a thinner cortex, with 3 out of 4 of our ROIs emerging significant – both central representations, plus the calcarine sulcus.

Whilst at first glance our rate of change plots suggest MD patients appear to decline at a faster rate compared to sighted controls in both central representations, this result did not emerge as significant. However, rate of change data did support our second prediction that there would be no difference in the rate of change in cortical thickness between groups for the two peripheral ROIs, given that in patients, this captures the representation of the intact visual fields. The group data for cortical thickness support earlier work in our lab; Hanson et al (2019) followed a group of unilateral AMD patients and found a decline in cortical thickness in the occipital lobe, driven by changes in the occipital pole. Here, we

show cortical thinning has occurred in bilateral MD of different forms, even in patients who have had MD for several years, some spanning decades.

Our cross-sectional results indicate there may be an interplay between cortical thickness and myelin measures, whereby thinner regions of cortex are generally more heavily myelinated. This is further supported by the literature which suggests that thinner but heavily myelinated regions, such as V1 are more robust to the effects of natural aging. This is reflected in the rate of change data for our control group; the decrease in cortical thickness over time is complemented by a relative increase in cortical myelin over time (Fjell & Walhovd, 2010; Lu et al., 2011; Natu et al., 2019; Williamson & Lyons, 2018). Based on the cross-sectional findings and the hint of an interplay between our measures, one would predict to see a greater increase in myelin for MD patients compared to controls in the rate of change analysis, given that on average, ROIs were thinner for the MD patient group. The effect of time seems to suggest that irrespective of group, myelin progressively increases, but was only significant for our calcarine sulcus ROI and appeared to be driven by the control group. Regarding group effects, our MD patients appear to have more cortical myelin in all ROIs, but again this only emerged significant for the peripheral representations. Interestingly, a significant group and time interaction was reported for the central representations only, whereby the MD patients' myelin density declines more rapidly. Our cross-sectional data alone would lead one to believe that areas with a thinner cortex would have greater myelin density, but the longitudinal data highlights that while our MD group may appear to have more myelin, MD patients do appear to show a decrease with time, primarily in the representations of the lesion.

It is likely that the proportion of cortical myelin relative to grey matter may be high in MD patients due to the reduction in grey matter we observe in this group rather than MD patients showing an increase in cortical myelin for which there would be no apparent explanation. A similar age dependent atrophy of cortex is accompanied by a relative increase in myelin in the longitudinal myelin density control data. The observed reduction in myelin density over time in the MD patient data suggests therefore a likely pathological change in myelin density resulting from an absence of visual input. Figure 2.8 describes possible explanations for the interplay between total cortical thickness and myelin density. The developmental perspective (Figure 2.8B) shows how a decline in cortical thickness can be explained by a genuine increase in cortical myelin due to the shift in white matter
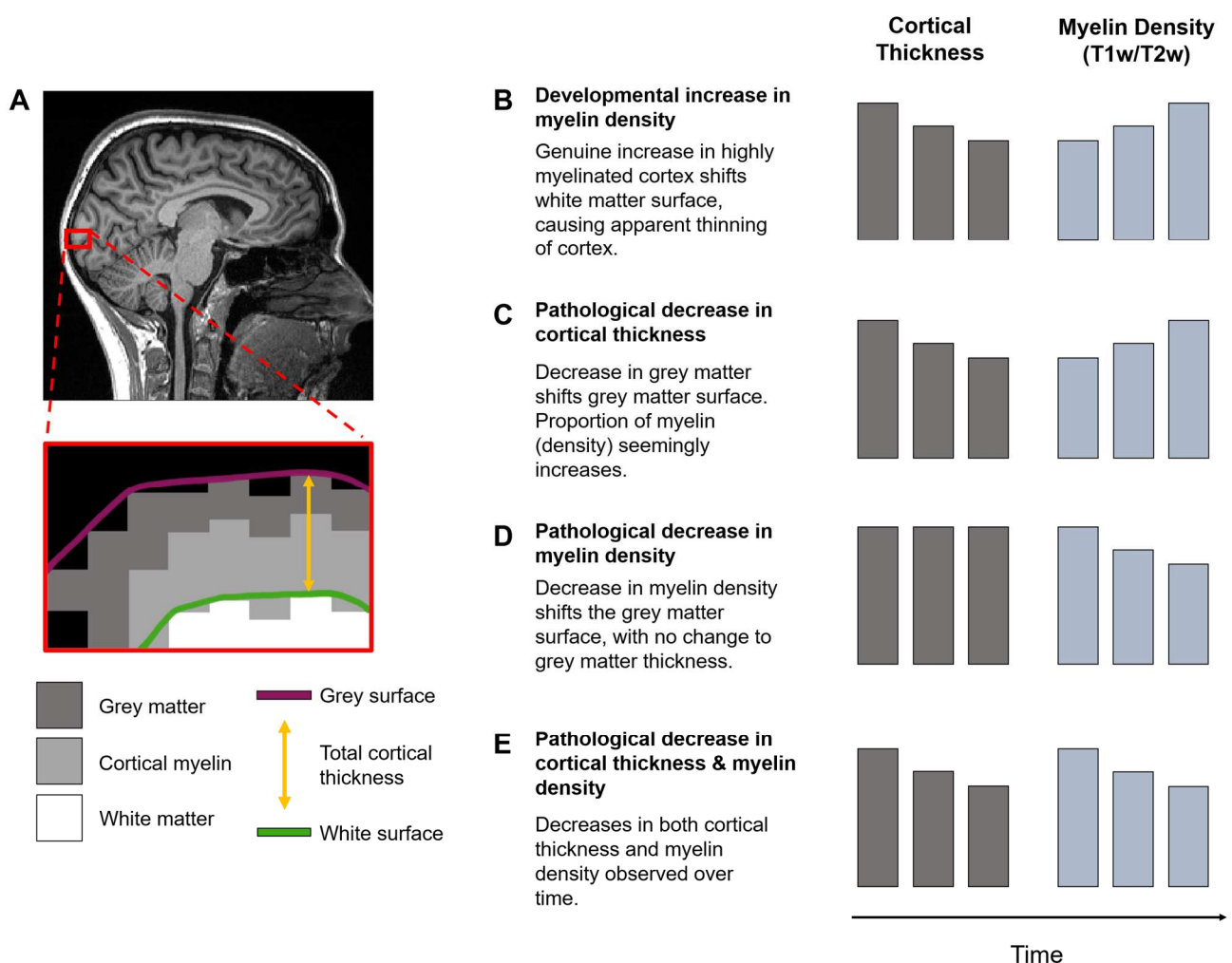
Figure 2.8. A: T1-weighted anatomical image with an illustration of the grey matter, cortical myelin, and white matter tissue. The grey and white matter boundaries are indicated by the purple and green lines respectively. **B-E:** Illustrations of possible observations over time with cortical thickness and myelin density. **B:** Illustration of the developmental increase in myelin observed in Natu et al., (2019), causing a shift in the white matter surface **C:** Illustration of the pathological decrease in grey matter thickness while myelin density appears to increase. **D:** Pathological decrease in myelin density causes a shift in the grey matter surface, while cortical thickness remains stable. **E:** Pathological decrease in both cortical thickness and myelin density.

boundaries. The pathological decrease in grey matter thickness (Figure 2.8C) shows how myelin may remain unchanged, but register an increase in density, resulting from the overall reductions in cortical thickness. It is possible that overall cortical thickness may be explained by a pathological decrease in cortical myelin and not other tissues (Figure 2.8D) and finally, pathological decreases in both grey matter thickness and myelin density may contribute to a reduction in total cortical thickness (Figure 2.8E). Our results would suggest that a combination of C and E can explain our findings; the cross-sectional data suggest a decrease cortical thickness could register an increase in myelin density (as in Figure 2.8C), but our rate of change data suggest that macular disease has a negative impact on both grey matter and cortical myelin density (as shown in Figure 2.8E).

Whilst reductions in cortical thickness and volume are well documented in the literature, the functional consequences of a reduction in myelin density in macular degeneration are unknown. In the animal literature, there is evidence of sensory deprivation leading to selective demyelination in cortex; adult rats deprived of visual input to one eye for several days showed a decrease in cortical myelination specifically in the deprived region of visual cortex (Hill, Patel, Goncalves, Grutzendler, & Nishiyama, 2014; Murphy, Mancini, Clayworth, Arbabi, & Beshara, 2020; Timmler & Simons, 2019; Xin & Chan, 2020). Evidence of demyelination of either grey or white matter following vision loss in humans is much more limited (Timmler & Simons, 2019). Myelin production is not uniform across cortex, and is regulated over the lifespan, with post-mortem work highlighting that the process of myelination occurs well into our 30's (de Hoz & Simons, 2015; Timmler & Simons, 2019). Areas involved in higher cognitive functions are the last to undergo myelination, with visual and other sensory areas myelinating early in life (de Hoz & Simons, 2015; Timmler & Simons, 2019). The main role of myelin is to regulate conduction speed, but it has also been implicated in metabolic processes and maintenance of fibers (Simons & Nave, 2016). A reduction in myelin may therefore negatively impact neural conduction, in turn causing a temporal delay. In multiple sclerosis, demyelination across the brain is thought to explain symptoms such as physical and cognitive decline (Bø, 2009). Evidence from the psychophysical and electrophysiological literature in individuals with multiple sclerosis or demyelinating optic neuritis highlight that a possible consequence of demyelination in cortex is a decline in temporal aspects of visual processing (Raz, Shear-Yashuv, Backner, Bick, & Levin, 2015; Young, Braich, & Haines, 2018). Studies using critical flicker-fusion frequency experiments to determine the threshold where a flickering light becomes indistinguishable from a constant light have shown reduced

responses in such patient groups. Other paradigms measuring visually evoked potentials (VEPs) report complementary findings, highlighting a possible loss of high temporal resolution of vision in demyelinating conditions. It may be possible to detect temporal delays in MD patients as well, for which there is some evidence already (Sabeti, James, Essex, & Maddess, 2013). Exploring possible myelin changes beyond early visual cortex, for example, assessing changes in motion perception and corresponding myelin in area V5 may provide further insights. Furthermore, in Chapter 5 we report a reduction in functional connectivity between central-biased portion of V1 and a ventral face-selective ROI; perhaps the reduced synchrony between these areas relates to structural changes, including those involving myelin. Knowing whether the decline in myelin (particularly in the grey matter) triggers changes in neural signalling or vice versa is yet to be fully understood in both natural and pathological aging.

The results from both the cross-sectional and longitudinal data raise the question of when changes are happening in cortex. In addition to the interplay between measures described above, a thinner cortex overall in patients across ROIs could have been explained by the age gap between our participant groups. However, we accounted for this by including age at the time of enrolment into our model which despite showing that age was a significant predictor for cortical thickness, our group and time effects still emerged and therefore age cannot solely explain the thinner cortex in MD patients. This then begs the question of how patients have a thinner cortex in all ROIs when during this time period, they did not decline significantly faster. Patient MD7 sheds some light on this; we captured the changes in cortical thickness in the period during which MD7 lost a substantial amount of vision, due to bilateral AMD and a secondary bleed in one eye. We compared the changes associated with longstanding bilateral MD against MD7, predicting greater changes in MD7, given that we were able to capture the window immediately before, and the first few years after diagnosis. The data show a sharper decline over the time points immediately after diagnosis, and the rate of change for this participant exceeded that of both controls and other MD patients. This gives us an indication that perhaps cortical thinning occurs at the early stage of the disease (after sight loss) but stabilises over time. Given that MD7 progressed quite rapidly compared to the MD patient group, it was important to assess the rate of change in MD13 who showed a much slower disease progression; despite a diagnosis of bilateral AMD, MD13 has retained vision and shows no deficit as yet. We therefore predicted changes akin to those observed in sighted controls, only showing signs of natural aging at this early stage in the disease. Despite results showing a more

accelerated rate of change, the pattern of results is more similar to the controls as calcarine sulcus declines faster than the occipital pole, and for our V1-restricted ROIs, the rate of change was quite similar. The trajectory for myelin appears to be similar; a steady decline emerged over time post diagnosis for MD7, further supporting the idea that while cortical myelin does seem more robust to change, there may be a pathological decline associated with macular disease.

In MD7, we observed a faster decline in cortical thickness in all ROIs compared to controls and other MD patients. The accelerated decline in peripheral representations however is an interesting finding; it may be that changes in the representation of the intact visual field occur in the early stages of MD, but with prolonged vision loss this may stabilise, hence in the group data, we do not see an accelerated decline, and if anything, a stabilisation of cortical thickness with mean rate of change being close to zero for the calcarine sulcus (-0.006 mm/year). Examining MD7's individual time points more closely, we can see that the slope starts to flatten in peripheral ROIs but shows a steady decline in the central ROIs, suggesting the representation of the intact visual field is starting to stabilise like our MD patient group appears to be. To fully understand the nature of the changes, it is important to continue collecting measurements on individuals like MD7 and MD13 and track changes over a greater period; data captured during the first 24 months post diagnosis will help us to better characterise the time course of changes in visual cortex, but severity of the disease must also be considered as MD7 and MD13 have progressed very differently since their AMD diagnoses. Collectively, it seems the loss of vision, rather than diagnosis of the disease itself, is what triggers more rapid changes in the posterior visual pathway.

We cannot ignore the fact patients with longstanding bilateral MD are still showing a decline in visual cortex. This tells us that interventions need to be implemented as early as possible as there is evidence that changes occur throughout the disease progression, even in the later stages. This also suggests perhaps late-stage individuals would not be ideal candidates for visual restoration; whilst a lot of research is geared towards curing eye disease and restoring the function of the eye, one must consider if the brain is even capable of processing new incoming information. Data from MD7 suggests that the optimum time to intervene would be as early as possible, given the steeper decline in cortical thickness in the pre and post diagnosis time points compared to post diagnosis time points only. Further to this, data from MD7 and MD13 suggest that structural and functional changes within the anterior visual pathway seem to be necessary to drive the greater changes in the posterior visual pathway, hence MD13 still has functionally normal

vision and appears not to have declined as fast as MD7. We have also shown that cortical myelin is affected, giving further reason to adopt more neuroprotective strategies going forward.

For this study, we included two sets of ROIs to capture the anatomical representations of the central retinal lesion and the intact peripheral fields. As discussed in Chapter 1, the way in which they have been defined does vary across studies, and we suspect this may explain some of the differing results, particularly concerning the intact representation. For some, these are defined functionally using retinotopic mapping procedures either on the patients themselves, or on a group of sighted controls which are then transformed into the appropriate subject space. Others have opted for anatomical based atlases. To keep consistent within our lab and to follow on from the work by Hanson et al. (2019), we used the occipital pole (lesion) and calcarine sulcus (intact visual field) from the Destrieux atlas in FreeSurfer. These ROIs are anatomical and are not restricted to primary visual cortex (V1). We reasoned that since previous work often uses V1 parcellated into central and peripheral representations, we should also restrict the occipital pole and calcarine sulcus to V1 and examine how the responses might vary. Our results were consistent across our two sets of ROIs; the pattern of the results remained the same, whereby increases or decreases in cortical thickness or myelin observed in the occipital pole and calcarine sulcus were generally seen in the central-V1 and peripheral-V1, and while the rate of change remained in the same direction, the absolute values did differ. This was to be expected given that for the occipital pole restricted to V1, we are reducing the size of the ROI. For the peripheral-V1, the ROI did not occupy the full length of the calcarine sulcus and so did not capture the far peripheral representations compared to the calcarine sulcus, but it did include more of the upper and lower bank of the calcarine, representing the vertical meridian.

Deciding on how to define ROIs can be difficult. Using anatomical atlases has many advantages, since they can be used in all participant groups, irrespective of whether they have sight or not. This ensures that we are indeed comparing data from the same regions of cortex across individuals and groups. Functional based ROIs do however allow for more accurate mapping of the representation of the lesion and can be corroborated with measures of retinal function too. Our MD patients vary considerably in terms of duration of disease and how advanced the vision loss is. We also have some patients undergoing treatment for wet-AMD while others have no treatment options available. With a longitudinal design, it is essential to ensure ROIs remain consistent across time points

within an individual so that we could get a reliable measure of the rate of change in cortical thickness and myelin density. Furthermore, measures of visual function could not be acquired for all participants, meaning we would not be able to use scotoma size to guide our measure of the lesion projection zone (LPZ). Using anatomical ROIs, as well as using the longitudinal within-subject processing stream for cortical thickness measures, allowed for greater consistency in both MD patients and controls.

As we are an aging population, we need to understand the nature of the eye and cortical changes in age-related diseases such as AMD. Recent reports indicate that by 2037, approximately 24% of the population will be over 65 years old (Office for National Statistics, 2018). Though changes in the eye in AMD are regularly monitored, determining what is causing changes in the posterior visual pathway is important to understand, as this will likely affect restoration attempts – something that will require more attention given the projections for increasing numbers of elderly population and in turn, the prevalence of AMD. We need to know whether it is sufficient to treat the eye alone, or whether we need to incorporate additional neuroprotective strategies to prevent or slow the cortical changes. Evidence already indicates the latter is necessary. Given that age-related changes are known to occur throughout the whole brain (Lu et al., 2011), it is fundamental to tease apart what is part of the normal aging process, and what may be a biomarker for age-related decline that is attributed to some form of pathology, as aging is a risk factor for AMD as well as Alzheimer's disease.

Recent advances in protocols for in vivo MRI allow for much more reliable data, as has the development of longitudinal processing streams, but what is also encouraging from this study is that non-HCP standard T1 and T2-weighted imaging protocols acquired on our GE scanner (1mm isotropic images) were processed adequately using the minimal processing pipeline. We verified this in our first analysis with our two control cohorts, one who had GE 1mm isotropic images, and one cohort with HCP protocols on the Siemens scanner with 0.8mm isotropic images. Despite the differences, we observed the same pattern of results and hence were able to verify the GE data. Going forward, it is highly desirable to continue to acquire data using the HCP protocols and compare in vivo MRI myelin maps with post-mortem data to give us further insights into the nature of the structural changes we are observing in health and disease. Histological studies assessing cortical myelin changes are largely limited to animals and in humans, to diseases associated with demyelination such as multiple sclerosis and optic neuritis. Multiple sclerosis affects both grey and white matter myelin and this therefore provides import insights into how demyelination affects

grey and white matter differently (Bø, 2009). Some argue histological work is less sensitive to changes in more superficial cortical layers, but studies are still able to provide sufficient evidence of demyelination. As yet, there are no histological studies exploring myelin density changes in eye disease in humans. Furthermore, a shift to more longitudinal designs to assess measures of change more reliably within individuals will help to shed more light on disease progression. We have already shown how it may differ in two individuals with a similar pathology.

Beyond the grey matter and cortical myelin, examining changes in the integrity of the white matter tracts, for example projections from the lateral geniculate nucleus (LGN) to the lesion and intact projection zones will provide a more complete picture of the changes in the posterior visual pathway, alongside measures of cortical thickness and myelin. There is a limited amount of cross-sectional evidence showing degradation of these white matter tracts – the optic radiations (Beer et al., 2020; Hernowo et al., 2014; Malania et al., 2017; Ogawa et al., 2014; D. Prins et al., 2011; Sullivan, Rohlfing, & Pfefferbaum, 2010; Yoshimine et al., 2018) - but those examining white matter using diffusion MRI (dMRI) do reveal changes specifically in the projections from the LGN to the lesion projection zone in primary visual cortex (Yoshimine et al., 2018). Most studies using traditional methods such as voxel-based morphometry are not sensitive enough to detect subtle changes in white matter integrity (Yoshimine et al., 2018). The time course of such changes is currently unknown, and this will be discussed further in Chapter 3 with the same participants included in this study.

Techniques such as magnetic resonance spectroscopy (MRS) will allow us to investigate neurochemical changes occurring in visual cortex in both health and disease, which may be able to indicate whether the cortical changes are reversible of not by looking for markers of types of cell death: necrosis versus apoptosis (Hanson et al., 2019). Collectively, such measures will allow us to capture the window in which the greatest changes occur, and where they occur, providing insight into the optimum intervention window for restoration to have the most chance of success.

We conclude that there is accumulating evidence of the thinning of visual cortex in individuals with MD, which continues throughout the disease progression, as shown in cases of long-standing bilateral macular disease in this study. We have provided new insights with two individual cases who we have had the unique opportunity to assess before and after diagnosis. Data indicate that changes occur more rapidly earlier in the

disease progression, but this appears to be largely triggered by the onset of visual loss. Cortical myelin is also showing possible signs of decline in visual cortex and more so in the representation of the lesion, something which has not been demonstrated before. Monitoring the entire visual pathway in individuals in the earliest stages of the disease will provide valuable insight into the time course of changes, as well as establishing the link between changes in the anterior and posterior visual pathways, further highlighting the need for neuroprotective interventions.

Chapter 3: Assessing the integrity of the optic radiations in bilateral macular disease

3.1 Abstract

The advent of diffusion MRI has allowed for in vivo assessments of the micro and macrostructure of the brain. Reductions in cortical thickness, volume and surface area have been widely observed in individuals with macular disease, however fewer investigations of the visual white matter have been conducted in this population. The aim of this study was to assess the structural integrity of the optic radiations in individuals with bilateral vision loss as a result of juvenile (JMD) and age-related (AMD) forms of macular disease. The optic radiations were divided into two bundles – fibers projecting to the occipital pole (anatomical representation of central vision) and fibers projecting to the calcarine sulcus (anatomical representation of peripheral vision). Recent work has shown selective deficits in only the fibers projecting to the location representing the visual field defect in largely unilateral AMD patients, and only in a portion of this tract. We replicate these findings in our bilateral patient group, observing reductions in fractional anisotropy (FA), and respective increases in radial diffusivity (RD), in middle portions of the tract projecting to the occipital pole. However, we also see this pattern in the calcarine sulcus projection, suggesting more widespread alterations in the white matter in bilateral MD. We also evaluated changes in FA over time in the portion of the tracts significantly reduced in our MD group; results indicate in the time window of the study, no significant changes occurred in either sighted controls or MD patients. The same measures were reported for two individuals before and after an AMD diagnosis; reductions in FA in the same portion of both projections in the optic radiations were evident for both cases before and after diagnosis, suggesting that perhaps structural changes in the posterior visual pathway emerge prior to functional vision loss. Finally, volume measures revealed no significant differences between groups or across time. Individual AMD cases however indicate reductions in projections to both central and peripheral representations may still occur in the early stages of the disease.

3.2 Introduction

In Chapters 1 and 2, the changes observed in cortical thickness, volume and surface area as a result of the natural ageing process were discussed (Salat et al., 2004). In cases of vision loss, multiple neuroimaging studies, including the work presented in Chapter 2, have reported atrophy of the posterior visual pathway, greater than that observed with ageing. Reductions in grey and white matter volume, as well as a reduction in cortical thickness in regions representing the visual field defect have been reported, with effects being more pronounced in cases of bilateral vision loss in both age-related and juvenile forms of macular degeneration (Baseler et al., 2011; Beer et al., 2020; Burge et al., 2016; Hanson et al., 2019; Hernowo et al., 2014; Lemaitre et al., 2012; Prins et al., 2011; Salat et al., 2004). Whilst a large proportion of structural changes observed in the literature concern the cortical representation of the retinal defect, there is some evidence of more widespread atrophy, particularly in age-related macular degeneration (AMD). Structural changes in AMD extend beyond primary visual cortex and appear to be more generalised, affecting both white and grey matter, even in frontal regions (Hernowo et al., 2014).

The development of diffusion weighted imaging has allowed for the evaluation of subtle changes in microstructure, macrostructure and anatomical connectivity in vivo, making it a valuable technique to use when exploring the impact of natural aging, disease and injury on the white matter tracts (Olivo et al., 2015; Reislev, Dyrby, Siebner, Kupers, & Ptito, 2016; Thomason & Thompson, 2011; Yeatman, Dougherty, Myall, Wandell, & Feldman, 2012; Yoshimine et al., 2018). Fractional anisotropy (FA) is used to measure the structural integrity of white matter tracts and allows inferences to be made about the alignment of fibers within a tract. Axial diffusivity (AD) concerns diffusion in the direction parallel to the tract - the principal orientation. Radial diffusivity (RD) is a measure diffusion in directions that are perpendicular to the tract's principal direction. Finally, mean diffusivity measures the average diffusion of water over all directions. A combination of diffusion properties can help clarify the state of white matter tracts in both health and disease (Rokem et al., 2017). The white matter tracts of most interest in vision loss research are the optic tracts, which project from the optic chiasm to the lateral geniculate nucleus (LGN), and the optic radiations, which project from the LGN to early visual cortex (Primarily V1 and V2).

Given there are far fewer diffusion studies exploring the effects of blindness, it is not surprising that there are some inconsistencies within the literature. Generally, it is agreed that the severity of the visual field defects correlate with diffusion properties, but age of onset is also an important consideration. Cases of early or congenital blindness such as

anophthalmia, where individuals are both without one or both eyes, indicate there are severe changes in both the optic radiations and the optic tracts, including a reduction in volume and increase in RD as a result of visual deprivation (Bridge et al., 2009; Pan et al., 2007; Reislev et al., 2016; Shu, Li, Li, Yu, & Jiang, 2009). Ogawa et al., (2014) have shown that the optic radiations are affected in rarer forms of central vision loss - leber hereditary optic neuropathy (LHON) and cone-rod dystrophy (CRD). Reductions in FA in the optic radiations and optic tracts were consistent across groups and did not depend on whether certain layers of the retina were damaged by the disease. LHON causes damage to the retinal ganglion cell layers whereas CRD affects the photoreceptor layer, but both lead to progressive loss of central vision (Ogawa et al., 2014). Others have reported greater changes in late onset vision loss compared to early and/or congenital cases, suggesting this is perhaps due to a reduction in plasticity in older patients. The important point is that regardless of age of onset, changes (to varying degrees) in the visual white matter can be observed, even in cases of partial vision loss (Dietrich, Hertrich, Kumar, & Ackermann, 2015; Hofstetter et al., 2019; Pan et al., 2007; Reislev et al., 2016; Wang et al., 2013).

Regarding acquired vision loss, multiple glaucoma studies have revealed an overall decrease in FA and increase in mean diffusivity and RD in visual white matter tracts; the extent of the change also seems to be correlated with disease severity and ophthalmic measures (Li et al., 2014; Tellouck et al., 2016). Furthermore, Chen et al., (2013) found specific reductions in diffusivity along the optic radiations in a group of late-blind glaucoma patients; the reduction in integrity of the white matter tracts was more extensive than that observed in AMD (Yoshimine et al., 2018). Whilst some report reduced FA in clusters (driven by an increase in RD) of the optic radiations and optic tracts in individuals with retinitis pigmentosa (RP) (Hofstetter et al., 2019; Ohno et al., 2015), others find no significant difference between RP patients and sighted controls (Schoth, Burgel, Dorsch, Reinges, & Krings, 2006). Differences in protocols, analysis techniques as well as the state of the disease in the RP patients can all contribute to such differences and highlights the need for consistency when addressing questions concerning structural changes, to ensure the results are meaningful and show legitimate changes associated with the disease.

Yoshimine et al., (2018) evaluated the integrity of the optic tracts and optic radiations in individuals with wet AMD (6/8 had unilateral AMD) and age-matched sighted controls (Yoshimine et al., 2018). While there were no significant differences between the groups

on any measures of the optic tracts, patients with AMD had localised deficits within the optic radiations, specifically in the fiber bundles projecting to foveal representations (0°- 3° visual angle) but no significant changes were observed in either the mid-periphery (15° - 30°) or far periphery (30° - 90°). Furthermore, it was only a subsection of the foveal fiber bundle that differed significantly between groups. Measures were taken at multiple locations along the tract from LGN to portions of V1, and the greatest difference between groups appeared to be in the middle of the tract, edging towards V1. This suggests that only fiber bundles projecting to the representations of the visual defect were significantly affected in the patient group.

Despite anatomical studies demonstrating few differences between juvenile MD (JMD) and AMD populations, Olivo and colleagues were also able to detect more subtle changes in both the grey and white matter in JMD compared to previous studies focusing more on volumetric changes. A reduction in FA was observed in more posterior regions of cortex but was not limited to purely visual areas. The reduction in FA suggests white matter integrity is somewhat compromised (Olivo et al., 2015). Furthermore, notable differences did emerge between groups when assessing white matter in frontal regions in AMD. This has been attributed to the difference in age, or perhaps the comorbidity between AMD and other age-related ailments such as mild cognitive impairment (Beer et al., 2020; Hernowo et al., 2014). There is growing evidence linking AMD with other neurodegenerative conditions such as Mild Cognitive Impairment and/or Alzheimer's disease, suggesting that perhaps the changes observed outside visual cortex may not be driven by sensory loss, but may reflect the overlap in diseases (Beer et al., 2020; Ikram, Cheung, Wong, & Chen, 2012).

What is currently unknown is over what time scale changes occur in the visual white matter in MD. As shown by Ogawa et al., (2015), while the outcome may be the same in terms of reductions in FA in the visual white matter across AMD and JMD, the extent of the damage differed between the groups. Whilst changes in the volume of visual cortex are well established in AMD, assessments of white matter in a larger group have been limited. It is generally accepted that atrophy of grey matter and the white matter tracts may limit the success of restorative treatments, particularly if such changes are irreversible. Assessing the long-term effects of MD on visual cortex will provide valuable insights into the biological changes in white matter as a result of eye disease; such methods have already been successfully implemented in other neurodegenerative diseases such as Alzheimer's disease (Thomason & Thompson, 2011; Yeatman et al., 2012).

Diffusion weighted imaging was utilised for the current study to reconstruct and measure the optic radiations, in the same group of MD patients and sighted controls described in Chapter 2. We have already found evidence of a decline in cortical thickness and myelin density in early visual cortex, which appears to emerge in the early stages of bilateral MD. Next, we wanted to assess whether alterations to the white matter could be observed in the same group of patients. We predicted that for the cross-sectional analysis, we would see a reduction in FA and increases in RD in the patient group in contrast to the sighted controls, but specifically in the fiber bundles projecting to the occipital pole - the anatomical representation of the retinal lesion (as described in Chapter 2). This is a different way of defining the foveal representations, but we anticipate replicating findings from Yoshimine et al., (2018). We also predict group differences in radial diffusivity and possible changes to AD; when RD increases or AD decreases, it indicates axons are less tightly packed together, therefore allowing for more free diffusion in the radial axis as shown in Figure 3.1. Since significant changes in AD are not always found, particularly in glaucoma and RP studies described (Hofstetter et al., 2019; Tellouck et al., 2016), it is likely if changes are observed, they may be subtle. In terms of the change over the ~24-month time window of the study, we may see subtle changes in the aforementioned direction in the patients, particularly for the individual case study (MD7 as described in Chapter 2) for whom we have data before AMD diagnosis, but we do not anticipate seeing age-related changes over this brief time window in the sighted controls, or MD13 - our second case for whom we also have before and after diagnosis data, but who has not experienced any functional vision loss. For volume, we predict changes in the same direction as described for FA whereby the MD patient group may exhibit selective reductions in volume, as well as accelerated changes over time for the occipital pole projection.
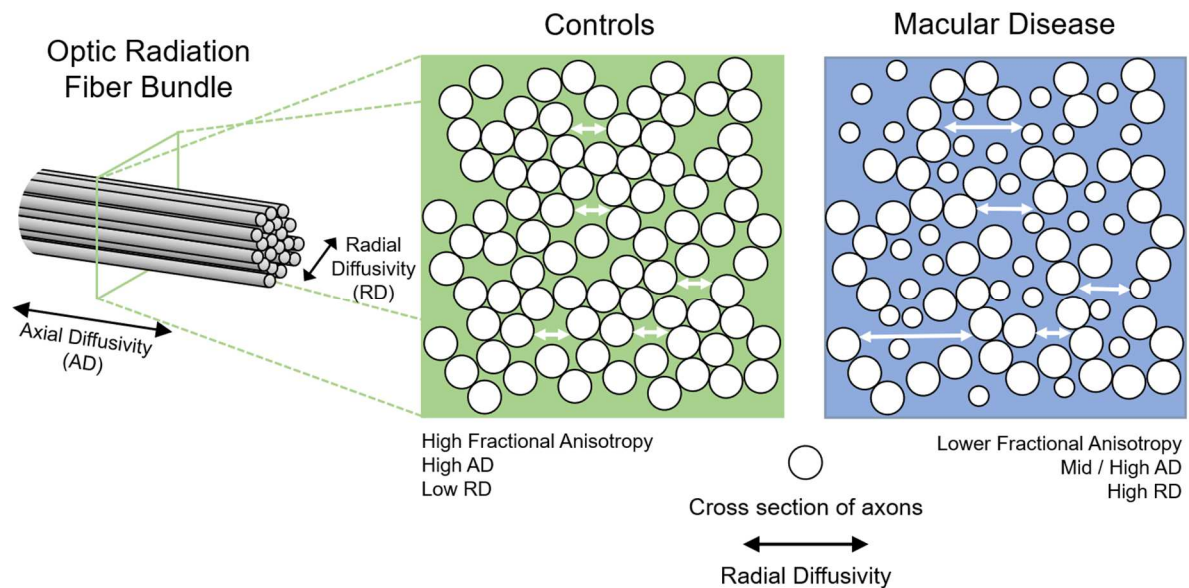
Figure 3.1. Schematic of our predictions for the fiber bundles in the optic radiations projecting to the occipital pole. Cross-section of a fiber bundle for controls (green) and patients with macular disease (blue). In controls, we predict higher FA and AD, and lower RD compared to patients. Lower FA and AD, and higher RD in patients may reflect structural abnormalities as a result of visual field defects.

3.3 Methods

3.3.1 Participants

13 individuals with macular disease were recruited from the Ophthalmology department at York Teaching Hospital and through advertisements in sight loss support groups in York (participant demographics included in Table 2.1). MD patients all had a diagnosis of bilateral macular disease; time since disease onset at the time of enrolment ranged from 9 months to 23 years, mean = 11.2 years. MD12 was excluded from longitudinal analyses due to ill health preventing participation in follow up MRI sessions. 18 sighted controls were recruited for this study through advertisements at the York Neuroimaging Centre (YNiC), University of York. Written informed consent was obtained from all participants. One control participant was excluded from the analysis due to poor data quality, leaving us with 17 in all analyses. This study followed the tenets of the Declaration of Helsinki with approval granted by YNiC Research, Ethics and Governance Committee and the NHS Research Ethics Committee (IRAS: 158456).

3.3.2 MRI data acquisition

Scanning was performed at the University of York Neuroimaging Centre using a 3 Tesla HD MRI system (GE Signa Excite 3.0T, High resolution brain array, MRI Devices Corp., Gainesville, FL) with an 8 channel whole head High Resolution Brain Array. Patients were

scanned between one and six times over a ~24-month period, whereas controls were scanned twice, approximately ~24 months apart. For full details of the high resolution T1 and T2 anatomical images, please refer to Section 2.3.2.

3.3.2.1 Diffusion MRI protocol 1 for MD1-MD12 and C1-C12

Two diffusion weighted MRI scans were acquired in each session, with opposing phase encoding directions. These were identical, with just the phase encoding direction changing (P/A to A/P). The duration of the individual dMRI scans was ~6 minutes. A single-shot pulsed gradient spin-echo echo-planar imaging sequence was used with the following parameters: b = 1000 s/mm^2, 21 unique diffusion directions, 47 slices, FOV = 192mm, TR = 12s, TE = 88.5ms (minimum full), voxel size = 2 x 2 x 2 mm^3, matrix= 96 × 96, flip angle = 90deg. 3 volumes without diffusion weighting (b0) were acquired at the start of each scan.

3.3.2.2 Diffusion MRI protocol 2 for MD7(2 time points), MD13 and C13-C18 (all time points)

Two diffusion scans were acquired in one session. The reversal scan was shorter (~2 minutes versus ~11 minutes) as it was used to correct for distortion only, hence only 6 diffusion sampling directions were acquired for this scan. Broadly, protocols were: b = 1000 s/mm^2, 45 directions, 58 slices, FOV = 192mm, TR = 12s, TE = 87.1ms (minimum full), voxel size = 2 x 2 x 2 mm^3, matrix size = 96 x 96, flip angle = 90deg. 3 volumes without diffusion (b0) were acquired at the start of the diffusion sequence. As we were replicating protocols from the first time points which were conducted by different research groups for one subgroup of participants, it was essential to keep protocols consistent within individuals to reduce the effect of scan type on the outcome measures. Due to an error in the first time point for the phase-encoding reversal scan whereby up-sampling was not turned off, two participants have slightly different parameters (voxel size 0.75 x 0.75 x 0.75mm^3 , matrix size = 256 x 256).

3.3.3 Longitudinal experiment design

As described in Section 2.3.3.1, participants were enrolled in the study for up to ~24 months with a maximum of 6 MRI scans during this time period. We acquired additional MRI data for two MD patients, referred to as patient MD7 and MD13. These are the individuals for whom we can make before versus after AMD diagnosis comparisons. All MD patients were given the option to opt in for the sessions they wished to attend, hence

not all participants completed all sessions. Control participants completed 2 MRI sessions over approximately 26 months.

3.3.4 Pre-processing diffusion data

Before running any pre-processing steps, any data with an odd number of slices had to be padded with an additional slice for the susceptibility- induced distortion correction to work. This affected 12 MD patients and 12 controls scanned under protocol 1. This was taken from the b0 image for each acquisition and applied to all subsequent b1000 images. Additionally, due to an error during data acquisition for two participants (described in Section 3.3.2.2), we have 2 scans within a session with a different field of view and different voxel size. To fix this, we applied a transformation to the DTI phase encoding reversal scan, bringing it into the same space as the main diffusion scan (using this as a reference image). Data could then be analysed in the same manner as all other data from this point forward.

All diffusion data were pre-processed which included using eddy-current distortion correction and motion correction with the FDT v5.0, part of FSL (v5.0) - FMRIB's Software Library (Smith et al., 2004). Data were split across time (Using FSLsplit) and the b0 volumes (with no diffusion) were extracted from the DTI files. The b0 volumes from each of the scans (A/P and P/A phase encoding directions) were combined into a single file to estimate the amount of distortion present in the two scans. Topup (Andersson, Skare, & Ashburner, 2003; Smith et al., 2004) was used to correct for the susceptibility-induced distortion which primarily affects the inferior frontal and inferior temporal regions – regions known for having air pockets present e.g. sinus cavities. Having a second scan which reads out the images in the opposite phase encoding direction also helps to correct for this distortion and improves anatomical accuracy. This distortion field is then applied to the original distorted DTI scans, which are then combined, giving us a single, undistorted set of images. After correction for distortion, BET (Smith, 2002) was used to exclude non-brain tissue. Finally, DTIFIT was used to apply the diffusion tensor model at each voxel and generate a fractional anisotropy (FA) map estimate and vector fits; FA, RD and AD were calculated by fitting a tensor model to each voxel; FA describes the coherence of diffusion, taking AD and RD into consideration. AD is measured along the primary axis of the model within each voxel, and the RD is average of the diffusivity measured in the two other (minor) axes of the tensor model. While DTIFIT is not necessary to run the probabilistic tractography, it allowed us to manually check to see if the data seemed sensible in relation to the anatomy before proceeding with tractography.

3.3.5 Region of interest (ROI) selection

Given findings from Yoshimine et al., (2018), we predicted that the fiber bundles in the optic radiations projecting to the anatomical representation of the visual field defect may be selectively impaired in our bilateral MD group, compared to sighted controls, whereas projections to the representation of the intact peripheral visual field may remain unaffected. To test this hypothesis, we used an anatomical atlas to define our ROIs - the occipital pole and the calcarine sulcus. These were taken from FreeSurfer's Destrieux Atlas (parcellation index 42 and 44 respectively - see Section 2.3.3.2 for details) whereby the occipital pole was used to capture central regions of the visual field (compromised in MD) and the calcarine sulcus was used to capture the more peripheral visual fields. These were first converted from fsaverage6 surface labels into a volume using FreeSurfer command mri_label2vol, before being transformed from the fsaverage space into MNI152 1mm space using FSL's FLIRT (Jenkinson, Bannister, Brady, & Smith, 2002).

3.3.6 Probabilistic tractography

Probabilistic fiber tracking allows for automatic extraction of the white matter tracts of interest in both hemispheres, and we did this using the FSL (v6.0) toolbox Xtract (Warrington et al., 2020). Before running Xtract, we fit the crossing fibers model (Jbabdi, Sotiropoulos, Savio, Graña, & Behrens, 2012) to the corrected diffusion data using FDT's bedpostx (Bayesian Estimation of Diffusion Parameters Obtained using Sampling Techniques). This calculates the number of crossing fibers within each voxel. All default parameters were used when running this model with the exception of drawing 10,000 streamlines (or samples) in each voxel (default is 5000). We then registered our FA data from the subject's native diffusion space to a standard $1mm^3$ space using FNIRT nonlinear registration (Andersson, Jenkinson, & Smith, 2007). The target image used was the FMRIB58_FA which is in the same space as the MNI152 standard space image. The registration steps that are part of the full Tract-Based Spatial Statistics (TBSS) (Smith et al., 2006), which is part of FSL (Smith et al., 2004), have been optimised, and so we used the TBSS scripts to avoid doing manual registrations. Xtract also requires the inverse warp that would allow data to go from MNI standard space back to the native diffusion space, so to generate this we used FSL's invwarp command on the transformation generated in the prior step.

Probabilistic tractography is run on the bedpostx output; the aim of probtrackx2 (Behrens, Berg, Jbabdi, Rushworth, & Woolrich, 2007; Behrens et al., 2003) is to produce streamlines that originate in a pre-defined seed region – the LGN for this study - that also

fulfil criteria such as passing through a waypoint (the occipital pole or calcarine sulcus). Exclusion points are also included to filter out any irrelevant projections. For our study, exclusion points included the midline sagittal plane to avoiding fibers crossing through the midline to the other hemisphere, the brainstem, a region posterior to the LGN to ensure only fibers that follow the signature curve up and away from the LGN are included, and regions anterior of the LGN to ensure fibers project in the posterior direction. It is possible that longitudinal fibers could be tracked without this exclusion criteria (Warrington et al., 2020). Our seed and exclusion points are shown in Figure 3.2.
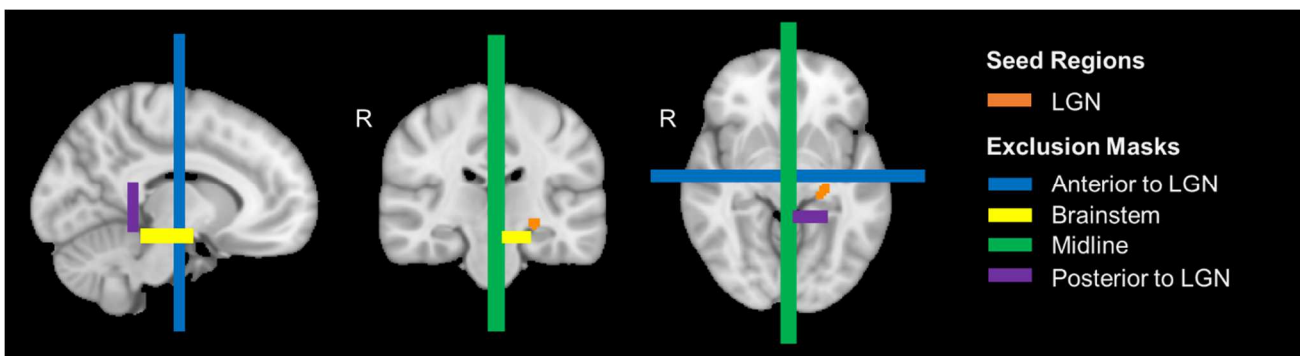
Figure 3.2. Example exclusion points and seed regions for the left optic radiations overlaid on the NI152_1mm standard brain. The lateral geniculate nucleus (LGN) was our seed region in each hemisphere (left shown in orange). Our exclusion masks included: Region anterior to the LGN to avoid longitudinal fibers being included (blue), the brainstem (yellow), the midline (green) and a region posterior to the LGN (purple) to help capture the curvature of the optic radiations close to the LGN. Exclusion points were the same for the right hemisphere.

3.3.7 Fiber tract cleaning

Before extracting our diffusion measures, we cleaned up the tracts to help reduce noise induced by complex fiber orientations. First, we set a threshold to exclude voxels where fewer than 20% of fibers passed through. Doing this gives us greater confidence that fibers are indeed part of a genuine white matter tract. We normalised our data and divided it into equally spaced bins (0-100) and extracted summary statistics from the central 80% of the tract; 10% of locations at the start (closer to the LGN) and end (early visual cortex) of the tracts were discarded to remove any noise and avoid partial-voluming effects. It is known that these locations have fibers going in many directions and the increased angle and/or curvature of the fibers adds to the noise. Similar methods have also been employed by previous work (Malania et al., 2017; Yeatman, Wandell, & Mezer, 2014; Yoshimine et al., 2018).

3.3.8 Calculating tract volume

In addition to FA, RD, and AD measures, we wanted to assess the volume of our two optic radiation bundles, projecting to the occipital pole and the calcarine sulcus. To normalise our data and make them more interpretable, we counted the number of voxels in the density files (which captures the fiber probability distribution) and divided this by the number of valid streamlines for a control tract - the forceps major - an easily identifiable posterior tract that runs through the corpus callosum, for which we did not anticipate any meaningful variation across subjects and time. The forceps major was identified using probabilistic tractography methods described above (Section 3.3.6). This was computed on an individual basis and within session e.g., Occipital pole tract for a given participant for their first time point was normalised using the forceps major identified in the same session for that individual. Normalisation is important because it helps to deal with the known differences in the ability to track white matter structures across subjects, scan sessions and even hemispheres, which can vary within subjects (Arrigo et al., 2016). Normalising to a control tract removes any broader differences in the ability to track without compromising any possible anatomical differences in our tract of interest, in this case, the two projections within the optic radiations. The resulting output is a more interpretable, scaled value. We did not trim the tract or threshold the tracts prior to normalisation. Both cross-sectional and longitudinal analyses were computed, to assess group differences, as well as changes over the period of the study. Normalised units for this measure are arbitrary, and therefore we will refer to this simply as normalised volume (Bartsch, Biller, & Homola, 2009).

3.3.9 Longitudinal analysis - linear mixed effects model

We wanted to determine if during the period of the study, there were any changes in FA over time in portions of the optic radiations that emerged significantly reduced in MD patients. In order to assess changes over time, we employed the same linear mixed effects model (Winter, 2013a, 2013b) as described in Section 2.3.5. The model used for each of our tracts (project to either occipital pole or calcarine sulcus) were as follows *(R syntax):*

Fractional Anisotropy ~ 1 + Age + Group:Time + (1 | Participant)

The FA value for each subject for each time point is entered into the model, which allows us to assess any changes over time. This model allows us to investigate the role of age (at baseline), group (MD patient versus controls) and any interactions between group and time, which were all included as fixed effects in the model. As before, participants were included as a random effect, allowing us to account for between-subject variability in FA.

The model for each of our tracts was evaluated using restricted maximum likelihood (REML) estimation to ensure the model was robust - this is the optimal method for studies such as this with smaller samples and uneven group sizes. The significance was assessed using t-tests which incorporated the Satterthwaite's method to calculate our degrees of freedom and in turn control for possible type-1 errors. This model was also applied to the volume data as described above.

3.4 Results

Tracts projecting from the LGN to the occipital pole and the LGN to the calcarine sulcus were identified in 12 MD patients and 17 control participants in both hemispheres. Fractional anisotropy (FA), axial diffusivity (AD) and radial diffusivity (RD) were plotted for multiple locations along each tract. Data were averaged across hemispheres.

3.4.1 Cross-sectional analysis of tract profiles

In Figure 3.3, tract profiles are plotted for each individual MD patient against the control group average. For each individual, we averaged across scans from all time points (between 1 and 6 across a ~24-month period) and plotted the mean FA for each location along the tract. What can be seen from most individuals is that a reduction in FA values emerges for both fiber bundles, and largely in the middle portion of the tract. There are a couple of exceptions, notably MD6, MD9 and MD11. MD6 and MD11 have the highest visual acuity scores (as shown in Table 2.1) and both have a form of JMD. MD9 seems to show this reduction in FA in the occipital pole bundle only.
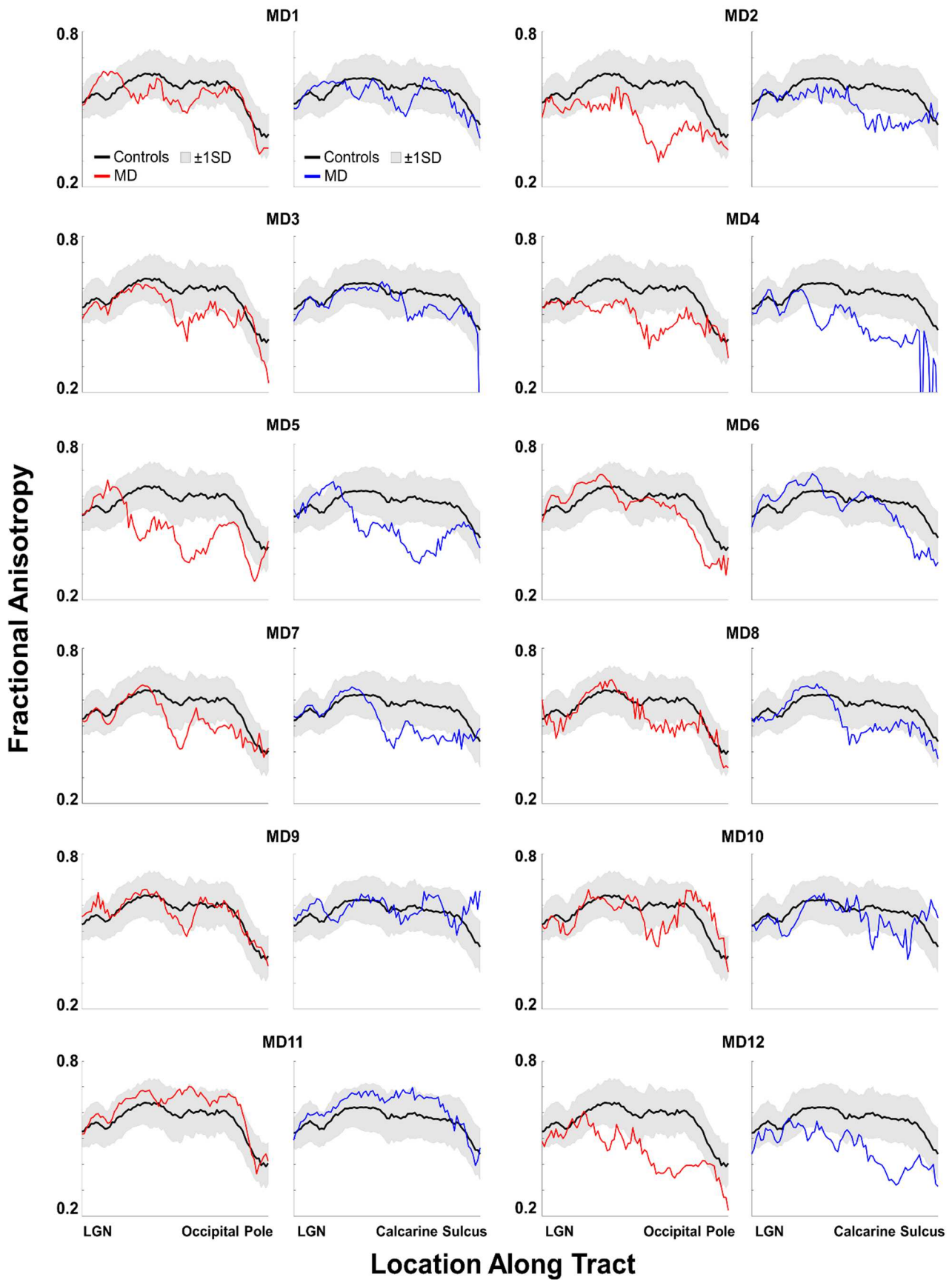
Figure 3.3. Cross sectional fractional anisotropy (FA) data averaged across all time points and hemispheres. Individual tract profiles for MD patients for fiber bundles projecting to the occipital pole (red) and calcarine sulcus (blue). Sighted control group mean FA (black line) and standard deviation (shaded grey region).

87

Next, we wanted to determine if there were group differences at certain locations along the tracts for our fiber bundles projecting to a) the occipital pole and b) the calcarine sulcus, and whether these would only occur in the former, given this captures the anatomical representation of the visual field defect. After averaging across time points (as shown in Figure 3.3), we then averaged across participants to generate group tract profiles for MD patients and sighted controls (Figure 3.4). A mixed ANOVA revealed a significant interaction between ROI (projecting to the occipital pole or calcarine sulcus), group (MD vs controls) and location along the tract ($F(80,2160) = 1.371$, $p = .018$) for our mean FA data. To tease apart these main effects, we ran two one-way ANOVAs correcting for multiple comparisons, reporting Welch's F values to accommodate unequal variances. For the tract projecting to the occipital pole, we found significant differences in 34 locations along the tract (all $p \leq .039$). For the tract projecting to the calcarine sulcus, we also observed significant differences in 39 locations (all $p \leq .049$). All significant locations are shown in Figure 3.4, indicated by the light grey blocks. Data suggest that there is a consistent drop in FA in a portion of the tracts closer to early visual cortex. For a detailed report of the inferential statistics for FA, AD and RD, see Appendix A (A1-A3).
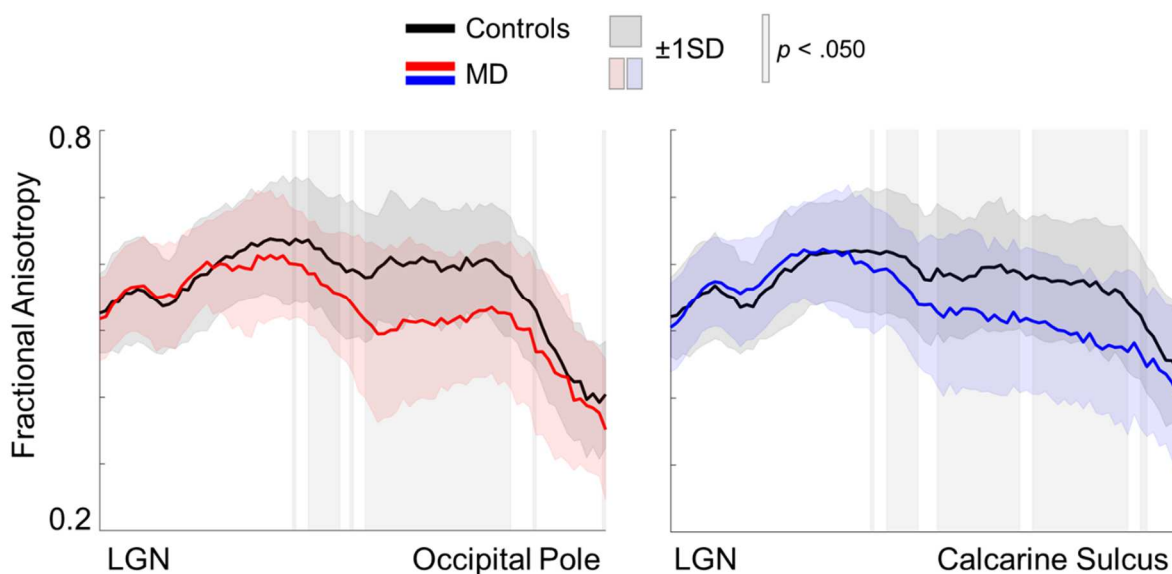
Figure 3.4. Mean fractional anisotropy (FA) measures for controls (black line) and MD patients (red and blue lines). Standard deviation is shown in the shaded region (grey for controls, red/blue for MD patients). Mean FA is significantly different between groups in the light grey blocks.

Whilst FA gives us a sense of the structural integrity of the tracts of interest, it cannot tell us about the nature of the changes observed. It is therefore important to also examine AD and RD to determine what may be driving the FA decrease observed in our patient group. As with FA measures, we ran two one-way ANOVAs, correcting for multiple comparisons and reporting Welch's F values. For AD, it appears there are few differences between sighted controls and MD patients; only 7 locations were significantly different between groups for the occipital pole projection (all $p \leq .044$), and for the calcarine sulcus projection, it was 2 locations ($p \leq .045$). All significant locations are illustrated by grey shaded blocks in Figure 3.5A.
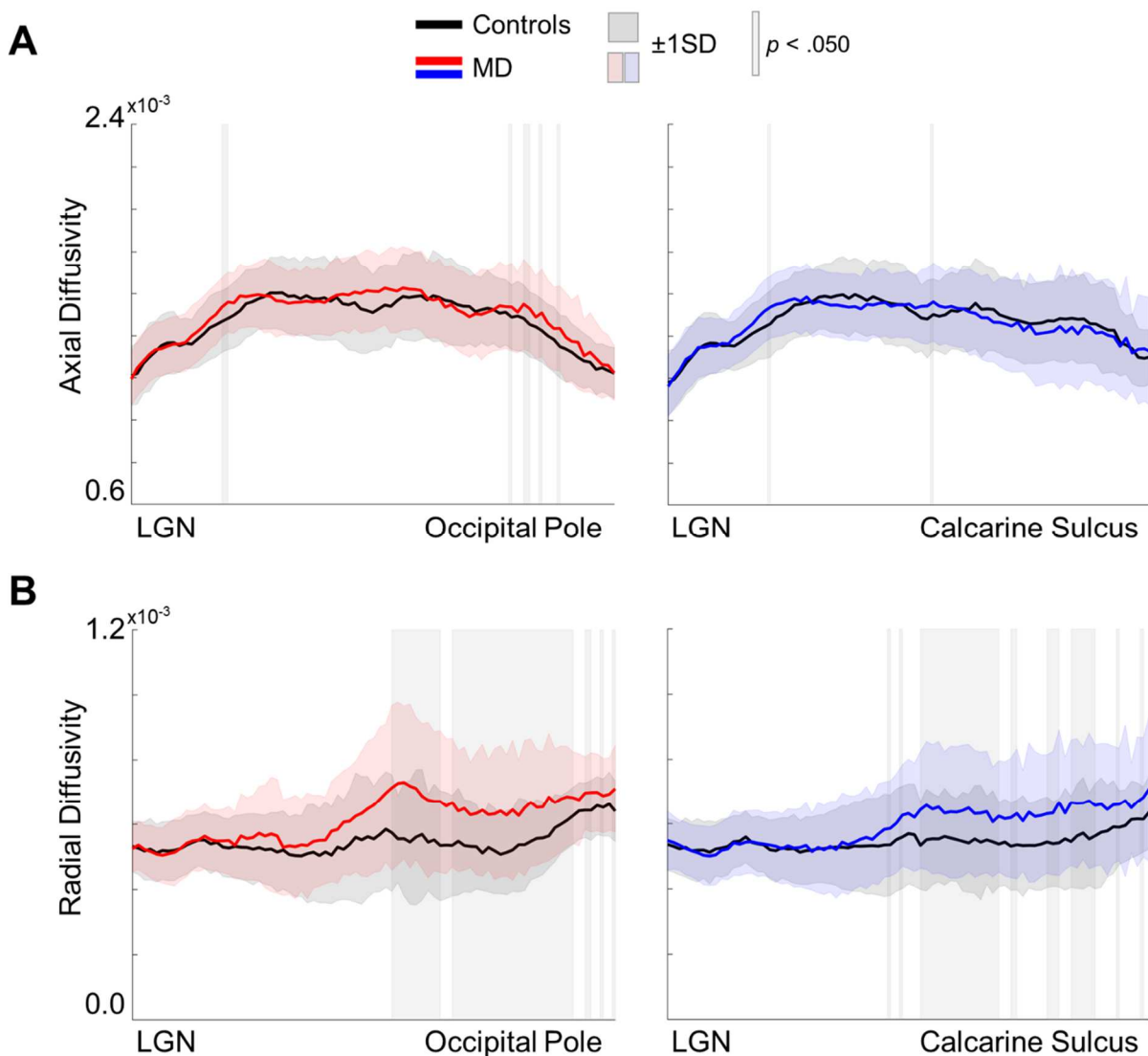
Figure 3.5. Mean axial anisotropy (AD) measures for controls (black line) and MD patients (red and blue lines). **B**: Mean radial diffusivity (RD) measures for controls and MD patients. Standard deviation is shown in the shaded region (grey for controls, red/blue for MD patients). Significant differences between groups emerged at locations with shaded blocks.

We observed significant differences in RD between groups in locations that largely overlapped with those which emerged significant when assessing FA; this is true for both the occipital pole projections (34 locations, all p≤.042) and the calcarine sulcus projections (28 locations, all p≤.048). Shaded blocks in Figure 3.5B show the locations where MD patients showed significantly greater RD measures compared to sighted controls.

3.4.2 Linear mixed effects model - assessing group changes over time

Having identified the location of the tract where FA was significantly lower in MD patients compared to sighted controls, we next wanted to determine whether we see a change in FA over time in this portion of the tract. To assess possible changes, we entered data for each individual time point into a linear mixed effects model in the same manner as described in Chapter 2 for cortical thickness and myelin density measures.

As shown in Table 3.1, age at baseline was as a significant predictor of FA for the subsection of the projections to the occipital pole, as well as the calcarine sulcus, however despite this, group also emerged as a significant predictor for both projections. There was no significant effect of time, nor were there any group x time interactions for either the occipital pole or calcarine sulcus projections, indicating that during the time window of the study (between 6 and 24months depending on number of sessions completed), there was not a significant change in FA in either group.

Table 3.1. Results for the linear mixed effects model, assessing changes in fractional anisotropy (FA) in the portion of the tract where groups significantly differed. All significant results are shown in bold.

	Occipital Pole		Calcarine Sulcus	
Predictor	b(SE)	t(df)	b(SE)	t(df)
Age	**-0.002 (0.0004)**	**-6.546 (24.994)*****	**-0.002 (0.0004)**	**-6.236 (25.126)*****
Group	**-0.030 (0.0138)**	**-2.208 (26.148)***	**-0.029 (0.0137)**	**-2.113 (26.376)***
Time	-0.002 (0.0015)	-1.258 (49.116)	-0.002 (0.0015)	-1.043 (49.258)
Group: Time	-0.004 (0.0031)	-1.284 (49.428)	-0.001 (0.0031)	-0.542 (49.594)

*** p<.001, * p<.050 from t-tests using Satterthwaite's method to correct for degrees of freedom (df).

3.4.3 Assessing the relationship between visual acuity fractional anisotropy

To assess if FA measures in our patient group (MD1 -11 only) could be predicted by acuity measures, we entered Early Treatments Diabetic Retinopathy Study (ETDRS) letter scores for the worse eye and the better eye into a hierarchical regression, with mean FA (for the portion of the tracts that emerged significantly different between groups) for both the occipital pole and calcarine sulcus projections. Despite a correlation between our two

visual acuity predictors (Pearson's R = .646, p=.016), collinearity statistics suggest this may not be problematic for our model (Tolerance = .582, VIF = 1.718). Worse eye was included in the model first as we deemed this a more likely predictor of FA.

Worse eye acuity scores did not significantly predict our mean FA measures for the occipital pole ($F(1,9)$ = 2.476, p=.150) or the calcarine sulcus projections ($F(1,9)$ = 3.063, p=.114). Adding in our better eye acuity score did not improve the model for either the occipital pole ($F(2,8)$ = 1.108, p=.376) or calcarine sulcus projections ($F(2,8)$ = 1.384, p=.305). Details of the linear model are shown in Table 3.2.

Table 3.2. Linear model of predictors of mean fractional anisotropy (FA) for a subsection of the occipital pole projections (upper) and calcarine sulcus projections (lower).

Occipital Pole

	b (95% CI)	Std Error b	b	p
Step 1				
Constant	.482 (.405, .559)	0.034		.000
Worse Eye VA	.001 (.000, .002)	0.001	0.464	.150
Step 2				
Constant	.489 (.315, .664)	0.076		.000
Worse Eye VA	.001 (-.001, .003)	0.001	0.494	.263
Better Eye VA	.000 (-.003, .003)	0.001	-0.045	.914

R^2 = .216 for Step 1, R^2 = .217 for Step 2. All p>.150

Calcarine Sulcus

	b (95% CI)	Std Error b	b	p
Step 1				
Constant	.469 (.397, .541)	0.032		.000
Worse Eye VA	.001 (.000, .002)	0.001	0.504	.114
Step 2				
Constant	.457 (.294, .621)	0.071		.000
Worse Eye VA	.001 (-.001, .003)	0.001	0.456	.286
Better Eye VA	.000 (-.003, .003)	0.001	0.074	.858

R^2 = .254 for Step 1, R^2 = .257 for Step 2. All p>.114

3.4.4 Assessing volumetric changes between groups and over time

The final metric we examined for our tracts was normalised volume. Generally, irrespective of group, the occipital pole bundle was lower than that of the calcarine sulcus, which is expected given the occipital pole ROI is smaller, therefore meaning there are likely fewer fibers reaching it compared to the calcarine sulcus (Figure 3.6A). To assess group

differences as well as changes over time, we again used a linear mixed effects model. There was no significant effect of age at baseline, group, time, and no group x time interactions for either the fiber bundle projecting to the occipital pole or the calcarine sulcus. All results from the linear mixed effects model are reported in Table 3.3. To visualise the data, the rate of change in normalised units per year was also computed using the slope of a regression line based on time measurements were taken with respect to the baseline (x-values) and the volume at each time point (y-values). This was calculated for each participant who are plotted as dots in Figure 3.6B. With the exception of one outlier in the MD patient group, it is clear that minimal change occurred within the time period of the study, and groups (as shown by the lack of group x time interactions in Table 3.3) did not differ in their rate of change.

Table 3.3. Linear mixed effects model for volume. Fixed effects reported with the standard error (SE) for predictors for each fiber bundle. Age = age at baseline, Group = MD patients and sighted controls. Volume is reported in arbitrary units following data normalisation.

	Occipital Pole		Calcarine Sulcus	
Predictor	b(SE)	t(df)	b(SE)	t(df)
Age	1.640e-04 (1.289e-04)	1.272 (26.58)	0.0007 (0.0005)	1.591 (25.33)
Group	2.462e-03 (4.909e-03)	0.502 (28.80)	0.0104 (0.0173)	0.602 (27.21)
Time	-2.157e-06 (8.694e-04)	-0.002 (49.83)	0.0012 (0.0023)	0.508 (49.53)
Group: Time	-9.108e-04 (1.785e-03)	-0.510 (50.74)	-0.0009 (0.0048)	-0.194 (50.04)

All t-tests using Satterthwaite's method to correct for degrees of freedom (df) are p>.124
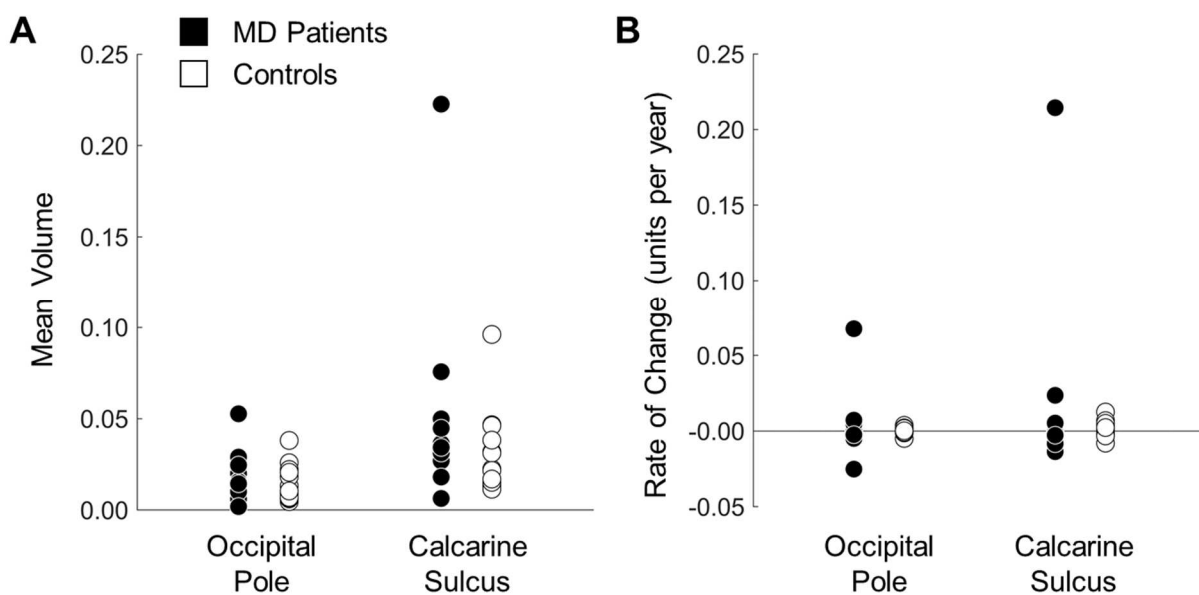
Figure 3.6. A: Cross sectional analysis of volume for MD patients (black dots) and sighted controls (white dots) for our fiber bundles projecting to the occipital pole and calcarine sulcus. **B:** Longitudinal analysis of the volume data. Rate of change (units per year) computed for both projections.

3.4.5 Assessing changes before and after sight loss

To give some insight into changes before and after a diagnosis of AMD, we have analysed data for MD7 for 7 time points - 1 prior to an AMD diagnosis and 6 post diagnosis (up to 2.5 years after diagnosis). For MD13 we have 2 time points – 1 before diagnosis and one 1.42 years after diagnosis. Figure 3.7 shows the time point before and latest time point after diagnosis for MD7 (Figure 3.7A) and MD13 (Figure 3.7B). What is interesting is that even at the time point before AMD diagnosis, MD7 appears to show reductions in FA in
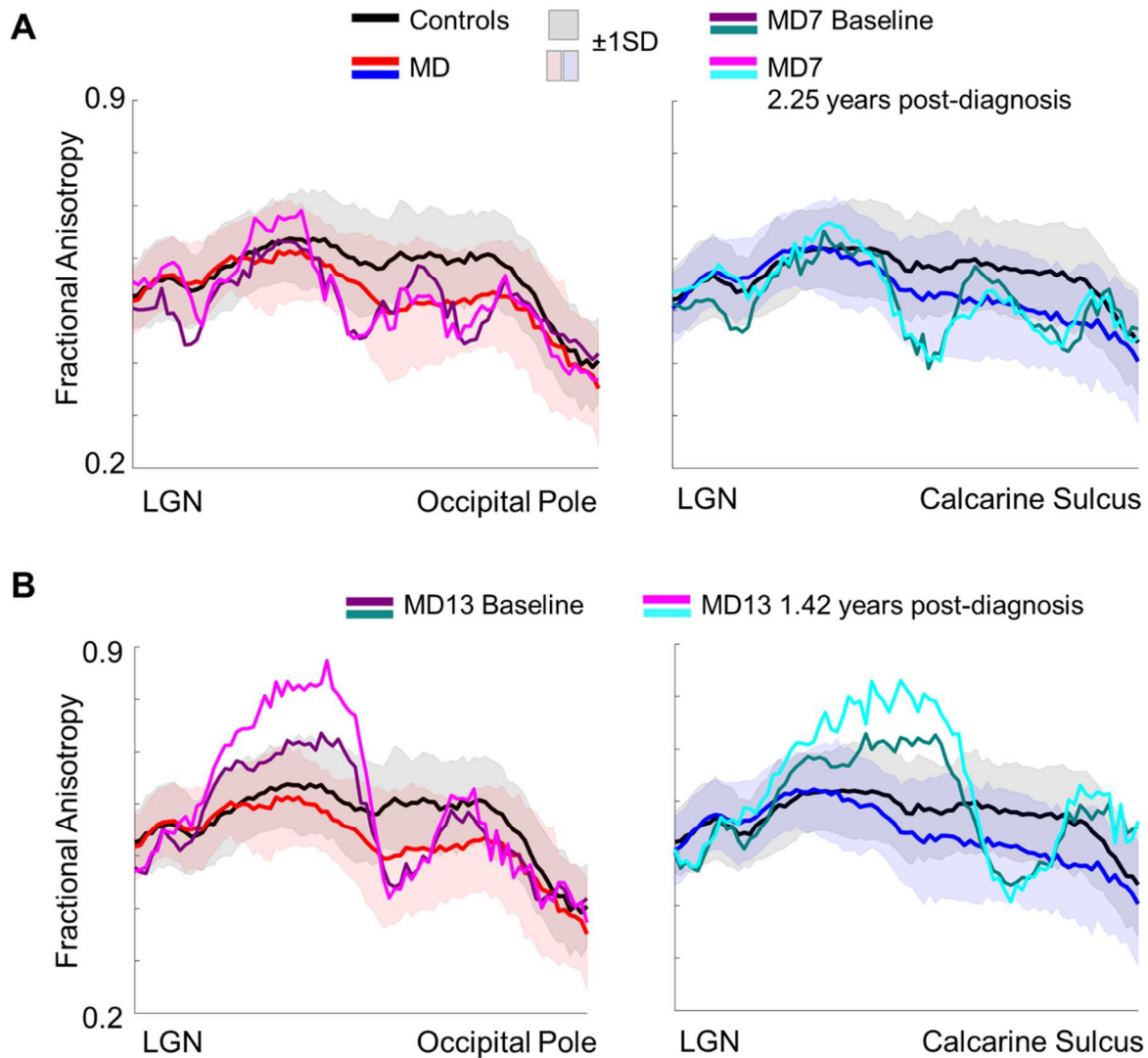
Figure 3.7. Comparing FA along the tracts for individual cases before and after diagnosis against sighted control and MD patient groups. **A:** Individual time point FA data for MD7 plotted against sighted control (black line) and MD group means (red for occipital pole projections, and blue for calcarine sulcus projections). Shaded regions represent 1 standard deviation for each group (grey = controls, red/blue = MD patient group). MD7 baseline data (before diagnosis) are shown in purple (left) and teal (right). Last time point (2.25 years after diagnosis) is shown in magenta (left) and cyan (right). **B:** Same as A, but for MD13 data. Second time point for MD13 (1.42 years post-diagnosis) is shown in magenta (left) and cyan (right).

various points along the tract, in the projections to both the occipital pole and the calcarine sulcus.

MD13 also follows this pattern despite not experiencing any functional vision loss. In line with our group data, we computed a mean FA score in the portion of the tracts where a significant reduction in FA was observed between our MD patient and control groups, and report values for each time point for both MD7 and MD13 alongside controls and a subset of the MD group in Table 3.4. Only 5 MD patients who all completed a baseline, 12 month and 18 month follow ups were included to ensure averages were computed from the same subset of individuals for each time point and making the changes across time more meaningful. It is interesting to see that at baseline, for both the occipital pole and calcarine sulcus projections, MD7 has a mean value lower than the control group, and similar to the MD group, whereas MD13 is closer to control group mean, particularly for the calcarine sulcus. With time, mean FA values seem relatively stable within this time window for all groups, with very little change. See Appendix A (A4-A5) for axial and radial diffusivity data along the tracts for MD7 and MD13.

Table 3.4. Mean fractional anisotropy (FA) for the locations along the tract that showed significant reductions in MD group. Mean FA at different time points between 0 and 2.25 years. Subset of MD patients has been reported here (n=5) that all had baseline, 1 year and 1.5-year data. For MD7 and MD13, time = 0 is the pre-diagnosis scan. For controls and MD group, time = 0 is the first scan undertaken for the study.

Occipital Pole

	Time (years)							
	0	0.69	1.00	1.17	1.50	1.75	2.00	2.25
Controls	0.592	-	-	-	-	-	0.589	-
MD group (n=5)	0.523	-	0.513	-	0.512	-	-	-
MD7	0.509	0.503	0.518	0.517	0.542	0.533	-	0.500
MD13	0.554	-	-	-	0.583	-	-	-

Calcarine Sulcus

	0	0.69	1.00	1.17	1.50	1.75	2.00	2.25
Controls	0.583	-	-	-	-	-	0.580	-
MD group (n=5)	0.509	-	0.497	-	0.501	-	-	-
MD7	0.504	0.502	0.512	0.505	0.533	0.521	-	0.494
MD13	0.588	-	-	-	0.627	-	-	-

Finally, we assessed the normalised volume of each of our optic radiation bundles in both cases, shown in Figure 3.8. For MD7, there is a noticeable downward trend for both occipital pole and calcarine sulcus projections, more so for the latter. MD13 shows a

different pattern, whereby no change is observed in the projection to the occipital pole, and a slight increase is seen for the calcarine sulcus projection, although only having two time points does limit interpretation somewhat, as some fluctuations can be seen in MD7's data.
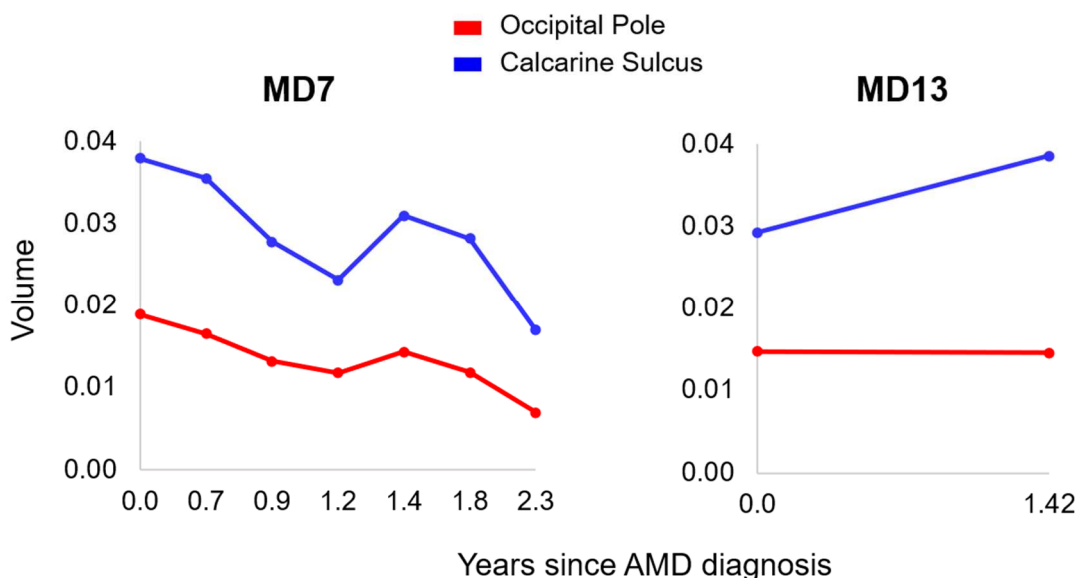
Figure 3.8. Volume measures for individual AMD cases (MD7 left, MD13 right) before and after diagnosis for projections to the occipital pole (red) and calcarine sulcus (blue).

3.5 Discussion

The aim of this study was to explore how bilateral MD impacts different fiber bundles within the optic radiations. Given our MD patients have partial vision loss, we divided the optic radiations into two bundles – one projecting to the occipital pole, the second projecting to the calcarine sulcus. For our cross-sectional analysis, we predicted that greater reductions in FA would be observed in the central projection (occipital pole), in line with findings from Yoshimine et al., (2018). We also predicted this would be accompanied by an increase in RD and possible decrease in AD. For our longitudinal analysis, while we predicted changes may be subtle in this short time window, we predicted a selective accelerated decline in FA over time in our patient group for the occipital pole projection. With our individual MD case data, we anticipated greater changes in FA, and perhaps RD and AD for MD7 compared to MD13, much like we have seen for our cortical thickness measures in Chapter 2. This was because of the difference in the severity of the visual loss between the two patients, with MD7 having more advanced AMD. In terms of volume, we predicted group differences in the same direction described for FA, whereby MD patients would

exhibit selective reductions in the occipital pole projection compared to controls, and this may also reveal a greater decline over time in the longitudinal analysis. Each of these predictions and corresponding results will be discussed in turn.

Our findings largely correspond with those reported by Yoshimine et al., (2018) whereby MD patients showed a significant reduction in FA in the optic radiations in a portion of the tract projecting to the central representation (occipital pole). We also show that this is likely driven by an increase in RD, which emerged significant in overlapping portions of the tract. However, one key difference is that we also observed this in the projection to the calcarine sulcus - capturing representations of peripheral (intact) vision. There are several reasons why this may be the case. Firstly, different atlases were used to divide up early visual cortex into central and peripheral representations. Yoshimine and colleagues used the Benson atlas (Benson, Butt, Brainard, & Aguirre, 2014; Benson et al., 2012), and divided V1 into 3 portions capturing the fovea, mid-peripheral and far periphery. as with the Benson atlas, there is more flexibility in that you can specify the eccentricity range of interest for your ROIs. The occipital pole and calcarine sulcus ROIs we used from the FreeSurfer Destrieux atlas are not restricted to V1 (as discussed in Chapter 2), but we also collapsed across a larger portion of the peripheral field representations, without leaving any gap between ROIs. Yoshimine and colleagues jumped from a foveal representation capturing 0°- 3° visual angle, to a mid-peripheral representation capturing 15°- 30°. Looking at their data more closely, it does appear that AMD patients on average exhibited lower FA in the peripheral representations in a portion of the tract, however it did not reach significance (Yoshimine et al., 2018). Our patient group, while larger, also consists of individuals with bilateral vision loss. The consensus within the literature is that severity of vision loss may affect the extent of changes observed. Malania et al., (2017) noted that it was not just the central projections that were showing a reduction in FA in patients with central loss in their cohort, suggesting more widespread changes to the visual white matter, as we have shown here. Finally, we opted for the Destrieux atlas ROIs to keep consistent across studies; in Chapter 2 we used the same ROIs to explore cortical thickness and myelin density changes in the same patient and control groups.

The reduction in FA observed in our MD group and individual cases seems to be driven by an increase in RD, where largely the same locations along the tract that were significantly lower for FA, were significantly higher for RD in patients. This pattern, alongside AD showing little change on average, coincides with findings from previous work on partial vision loss, for both central and peripheral affecting pathologies (Hofstetter et al., 2019;

Tellouck et al., 2016; Yoshimine et al., 2018; Zhou et al., 2017). For the rate of change in FA, no significant group x time interactions emerged, meaning the MD patient group did not show an accelerated rate of decline. This also applied to the individual MD case data shown in Table 3.4, where there was little change within the time window of the study for MD7, MD13, our MD patient subgroup and controls. Furthermore, we did not observe an accelerated decline in volume for the fiber bundles projecting to the occipital pole or the calcarine sulcus, highlighting the importance of exploring multiple metrics when determining the consequence of eye disease on the brain.

Volume measures can be difficult to interpret particularly in structures that are harder to track; discerning whether differences between groups or within individuals across several time points are meaningful can be a challenge. Diffusion measures are susceptible to many sources of noise, and so errors can result from poor quality dataset, distortions in the images, inadequate protocols, anatomy, poor preprocessing pipelines or models that do not represent the data well. These, and many other sources of error can all contribute to noisy data and correcting for this is not always straightforward (O'Donnell & Westin, 2011). At present there is no gold standard when it comes to measuring volume of white matter tracts, and it is important to remember that it is not possible to get quantitative measures of, for example, the number of axons in a fiber bundle (Nooij, Hoving, van Hulzen, Cornelissen, & Renken, 2015). Probabilistic tractography is shown to have superior reliability compared to deterministic tractography, particularly when resolving complex fiber orientations within individual voxels (Arrigo et al., 2016; Bartsch et al., 2009). Data acquired in patients with brain lesions is also better suited to probabilistic tractography when reconstructing tracts for this reason. The optic radiations can be tricky to reconstruct, especially when dividing it up into smaller bundles as we have in the current study. However, given that we know the structures exist, we can make our measurements more interpretable by normalising the data for each individual subject for the tracts of interest to a control tract. Doing this, we remove the differences in global trackability without affecting the possible structural differences in the optic radiations - this was particularly important for this study given we anticipated possible reductions in volume for our patient group. Going forward, one way to help interpret diffusion data more generally is by validating that which is acquired in vivo with post-mortem data ex vivo (Nooij et al., 2015).

MD7, having lost a lot of vision within a relatively short space of time, provides an interesting result, whereby all metrics explored appear to be reduced even at baseline -

approximately 9 months prior to diagnosis. MD13, who has no functional vision loss but a bilateral AMD diagnosis, follows suit but to a lesser extent, whereby mean FA values in the smaller portion of the two projections are more comparable to those observed in controls. However, for the occipital pole projection, while greater than values reported for MD7 and the MD subgroup, mean FA for MD13 is lower than that for the controls. For volume, MD7 shows a general downward trend over time for both projections, but MD13 seems to show no change for the occipital pole projection, and a slight increase for the calcarine sulcus. One must be wary with MD13 given they only have 2 data points, and as can be seen from MD7, individual data can fluctuate between time points. This seems to support our findings from Chapter 2, whereby MD7 showed greater decline in cortical thickness compared to MD13, and this appeared to happen in the early stages of the disease, after functional vision loss and more extensive structural decline in the retina. The timeline shown in Chapter 2 (Figure 2.1) highlights that while MD7 did not get diagnosed until May 2017, they did report noticing changes to their vision in the February of that year, ~6 months prior to the baseline scan. This, along with results from MD13, point to the idea that changes in the posterior visual pathway may be occurring earlier than expected, and that structural changes in the eye, even before functional vision loss, may be driving the changes observed in the brain. This has important implications for the timing at which potential neuroprotective strategies may be most effective.

In this study, we report the rate of change of specific metrics (FA versus volume), but Ogawa and colleagues have highlighted that there may also be differences in the rate of change for different diseases. Despite both LHON and CRD patients having comparable vision loss, the time since disease onset did differ between groups, whereby CRD patients had the condition for ~20 years, compared to ~5 years for LHON, indicating that changes happen faster in patients with LHON (Ogawa et al., 2014). This study would benefit from longitudinal assessments to see when changes emerge, much like we have started to do with our individual MD cases. As mentioned previously, timing of these structural changes is important to assess because there are implications for potential treatment strategies, but also this highlights that different disease types may benefit from different intervention times. For example, more comprehensive assessments of how JMD and AMD patients may be differently affected over time could be interesting, as these have largely been collapsed into one group, as in this study and Malania et al., (2017). Unfortunately having only two JMD patients recruited to this study means we do not have sufficient data to address this question.

Despite being frequently reported, it is not always clear what may be driving changes in diffusion measures. For example, FA can be affected by numerous things, such as RD and AD, but can also be influenced by volume, crossing fibers and partial voluming. To ensure it is not the latter two, it is important to apply preprocessing steps to deal with geometric distortions and use tools that can accurately and reliably determine if a white matter tract is genuine, and not a result of noise. It is also important to acknowledge that perhaps visual white matter tracts may be affected differently by visual deprivation. For the majority of the literature, a reduction in FA is typically coupled with an increase in RD in the optic radiations (Hofstetter et al., 2019; Tellouck et al., 2016; Yoshimine et al., 2018; Zhou et al., 2017), however for Malania et al., (2017) et al., this was not the case. Authors report reductions AD and no change in RD for the optic radiations, but the opposite was found for the optic tracts, whereby RD significantly increased, and AD remained unchanged. With the optic tract, others either report no significant differences between patient and control groups (Yoshimine et al., 2018) or find the FA reduction to be driven by a decrease in AD (Ogawa et al., 2014). The discrepancy seems to occur more for the optic tract assessments, which could be explained by the size; being much smaller than the optic radiations, only certain protocols may be sensitive enough to detect changes in such a small structure. It would be interesting to explore white matter connections between other visual areas, to determine just how widespread alterations may be following eye disease; we provide evidence in Chapter 5 that functional connections between primary visual cortex and higher level regions with known eccentricity biases (e.g. fusiform face complex) are compromised in MD patients and so complementary structural assessments would be valuable.

One important consideration with diffusion data is whether to calculate mean FA, RD, and AD measures for multiple locations along the tract, or whether to extract one measurement for the whole tract. The latter is not always useful but has been adopted by earlier work. For example, when exploring changes in the optic radiations in individuals with RP, Schoth et al., (2009) failed to find any significant differences between RP patients and sighted controls. While this study may lack sensitivity because of a small sample (n=5), generating tract profiles provides more meaningful data, particularly as not all fibers are of equal length and therefore may not extend fully between the seed and termination point in the grey matter, in turn reducing FA values. This is evident in the individual MD patient plots in Figure 3.3 – the end of the tract (even though we have trimmed 10% off) still drops off quite substantially in individuals. By trimming the start and end of the tracts (where fiber

orientation is more complex and crossing is more likely) and plotting multiple measures, we, and others, have been able to show that only specific portions of the tracts are impacted by eye disease (Malania et al., 2017; Ogawa et al., 2014; Ohno et al., 2015; Yeatman et al., 2012; Yoshimine et al., 2018). Treating any white matter tract as one single entity and averaging across the whole length loses valuable information.

While it is surprising that our visual acuity measures did not seem to correlate with our mean FA in the portions of the tracts that were significantly lower for our MD patients, there are some possible explanations for this. Not all the acuity measures were collected by the same researcher, meaning participants could be tested under different conditions (corrected or uncorrected) and using different charts. For 3 of our volunteers who did not come through the eye clinic at York Hospital, we were relying on self-reports of medical history, and so the measures given may not have been as accurate. We did however ask for their most recent assessments, but in some cases, this was some time before the baseline MRI appointment. More reliable and complete ophthalmic examinations to assess visual function (e.g. microperimetry), alongside detailed assessments of the scotoma size (using optical coherence tomography) would perhaps be better predictors of FA. It is also possible that the optic radiations genuinely do not correlate this with measure; Ohno et al., (2015) found that residual visual field area did not correlate with FA in the optic radiations in a group of RP patients. Authors note this may have been due to the fact patients were at various stages of the disease, had a broad age range and so the speed of disease progression may have varied heavily between patients. Collectively, these could be confounding factors, and it is not dissimilar to the current study in that regard – we too have a range of disease severity, age as well as having a combination of AMD and JMD patients. Time since disease onset could be a better predictor of FA in this instance. Unfortunately for this study, we do not have a disease duration information for all participants, and so we could only explore this in a subset of participants. An additional line of enquiry would be to see whether perhaps acuity measures correlated more with the metrics reported in the optic tracts. Malania et al., (2017) reported a lack of relationship between retinal nerve fiber layer (RNFL) thickness and diffusivity in the optic radiations, but RNFL thickness did correlate with optic tract diffusivity.

When considering the consequences of diseases such as macular degeneration, it is important to use techniques such as diffusion imaging to probe the consequences on microstructure in addition to cortical thickness, myelin density, surface area and overall volume. It is evident from this study that alterations in the white matter extend beyond

projections to the central representations in MD patients when examining FA, and these changes also appear at the earliest stages of the disease, as shown by our individual cases before and after diagnosis. With analysis techniques and protocols advancing rapidly, more sensitive measures of diffusion properties can be acquired, allowing for more reliable evaluation of the visual white matter, including the optic tracts which are more difficult to measure with lower resolution protocols. There is growing evidence suggesting that many additional visual disorders such as developmental prosopagnosia, amblyopia and cases with retinal ganglion cell damage are all associated with white matter changes (Millington, Ajina, & Bridge, 2014; Rokem et al., 2017). FA could potentially be used as a biomarker for disease severity, making it a useful clinical tool to help characterise eye disease alongside other standard ophthalmic measures. Understanding how visual disorders affect different parts of the visual pathway will allow for more targeted and refined potential treatment strategies. This may be particularly useful for neurodegenerative diseases such as glaucoma, as well as AMD (Li et al., 2014; Tellouck et al., 2016).

Chapter 4: Feasibility of a longitudinal neuroimaging and neurostimulation study with elderly, visually impaired participants

4.1 Summary

Longitudinal neuroimaging studies provide researchers an opportunity to collect highly valuable within-subject data which in patient populations, can offer new insights into disease progression that may not be possible to assess under current healthcare pathways. By monitoring structural and functional changes in the brain in a clinical population, alongside the changes occurring as a result of natural aging, we can tease apart what attributes are associated with the disease / pathology. This type of data could help determine at what point interventions would be most successful. Longitudinal research does however pose some additional difficulties including (and not restricted to) managing recruitment, building the relationships with returning participants and dealing with attrition rates. The aim of this chapter is to give an overview of the challenges faced when running a longitudinal neuroimaging study with neurostimulation procedures, exploring the issues faced during this project. Protocol amendments implemented to improve the recruitment rate will be discussed and evaluated in terms of how this impacted on the number of accruals. Next, neurostimulation procedures and contraindications will be discussed, focusing on medication use which appeared to be the most limiting factor (locally) for the neurostimulation procedures. Finally, it will discuss the wider implications for neuroimaging and neurostimulation studies and how they can be successfully implemented in the context of this study.

4.2 Overview of the research project

Chapters 2 and 3 describe findings from the longitudinal study discussed in this chapter. The study was very different at the outset and changed extensively due to recruitment barriers which will be discussed in turn. To recap, research in our lab following individuals with macular disease has reported a thinning of grey matter particularly in the occipital pole - the region representing the damaged retina - but reassuringly there is no evidence to suggest this region of visual cortex undergoes any large-scale remapping of function in cases of acquired retinal lesions (Baseler et al., 2011; Boucard et al., 2009; Hanson et al., 2019; Hernowo et al., 2014; Doety Prins et al., 2016). In Chapters 2 and 3 we have shown that as well as the grey matter, cortical myelin, and visual white matter show evidence of decline in individuals with macular disease. Whilst ophthalmological research is largely

focusing on restorative treatments of the retina, there is an assumption that visual cortex will be able to process the restored signals in an appropriate manner, which would in turn allow for functionally useful vision. Given that there is already evidence to suggest various forms of structural decline, the success of visual restoration may be compromised. For further discussion on neuroimaging research in the context of visual restoration, see Chapters 1 - 3.

The initial aims of our longitudinal project were twofold: First, we wanted to determine the time course of anatomical changes in visual cortex, and assess the functional consequences following macular disease. Second, we aimed to use a neurostimulation technique – transcranial direct current stimulation (tDCS) – to see if we could slow or possibly prevent the anatomical degeneration and loss of neural sensitivity in visual cortex, specifically in the region representing the damaged retina – the lesion projection zone (LPZ). The results of this project could provide valuable information; it would be one of the first longitudinal studies to examine changes in visual cortex in patients with age-related macular degeneration (AMD), characterising the time course of the reported decline in primary visual cortex. This is, we believe, fundamental to the success of restorative treatments as it will inform clinicians of the viability of visual cortex and potentially highlight the most suitable candidates for restoration treatments. The sensitivity of the regions that exhibit structural decline is not yet known and is an important question to address again within the context of visual restoration. We can use a non-invasive neurostimulation technique called transcranial magnetic stimulation (TMS) to determine this. By using TMS, we can bypass the damaged retina and stimulate visual cortex directly, causing a phosphene - artificial flash of light (Halko, Eldaief, & Pascual-Leone, 2013; Lang et al., 2007). Recording the minimum power required to induce a phosphene will inform us about the function of the LPZ – the less power required, the more functional the LPZ (Gothe et al., 2002). Finally, we aimed to assess the feasibility of tDCS as an intervention for patients with age-related macular disease. It has been widely used in rehabilitation of clinical populations for example, stroke patients experiencing language and motor difficulties (Baker, Rorden, & Fridriksson, 2010), however this was the first time to our knowledge that it was being used in macular degeneration research.

We aimed to recruit 30 participants with the dry form of AMD who would be enrolled in the study for ~12 months. The original inclusion and exclusion criteria are shown in Table 4.1.

Table 4.1. Inclusion and exclusion criteria for the original 12-month study.

Inclusion Criteria	Exclusion Criteria
• Aged 55 years or over • Foveal-involving atrophy in both eyes with the involvement of the second eye occurring within the last 18 months • Visual Acuity scores 35-70	• Contraindications for MRI • Contraindications for TMS • Contraindications for TDCS • Patients with neovascular AMD • Patients with other significant vision affecting pathology e.g. epiretinal membrane, cataracts, strokes

During the 12-month period, participants would have up to 29 research appointments. The clinical visits would take place at the hospital, the MRI, fMRI and TMS procedures would take place at the university, and the tDCS procedures could either take place at the university, or if the participant preferred, in their own home. As the tDCS kit is portable, we could reduce participant burden by having the researcher perform the procedures in their homes. The procedures included in the original protocol for this study are outlined in Table 4.2 and the proposed schedule of events is shown in Table 4.3.

Table 4.2. All procedures included in the original 12-month study protocol.

Clinical Visit	Magnetic Resonance Imaging (MRI)	Functional MRI (fMRI)	Transcranial Magnetic Stimulation (TMS)	Transcranial Direct Current Stimulation (tDCS)
• To acquire information about the functional and structural changes in the retina • ETDRS best corrected visual acuity • Microperimetry to map function of the retina • OCT to assess structural changes in the retina	• Used to acquire anatomical information, specifically to track changes in the structure of visual cortex (e.g. cortical thickness) • To provide a highly detailed anatomical image to overlay functional information on and to guide TMS	• Used to asses the sensitivity of visual cortex • Identify the Lesion Projection Zone (LPZ) which is the cortical representation of the part of vision that is now lost (central vision) • Identify Intact Projection Zone (IPZ) which is the cortical representation of parts of visual cortex still receiving input from the retina • The LPZ and IPZ are the target sites used for TMS	• Used to probe the sensitivity of target regions in the brain (LPZ and IPZ) • Deliver single pulses to target regions and determine minimum TMS power required to induce an artificial flash of light (phosphene) in the participants visual field	• Used to determine whether regular doses of tDCS can slow or prevent changes in structure in visual cortex • Each session included a 15 minute 'dose' of 1milliamp of electricity applied through saline-soaked sponge electrodes. One sponge should be placed over the occipital pole and reference electrode placed on the vertex (top of the head). Electrodes would be held in place with adjustable rubber straps • Participants divided into two groups: active stimulation and passive stimulation

By using multiple procedures to probe the state of the eye and the visual brain, we could track the rate of change in both the eye, but also monitor any neural consequences of macular disease; by having two groups, receiving either active stimulation or sham stimulation during the tDCS sessions, we could also assess the effectiveness of the intervention.

Table 4.3. Study timeline for each participant. Each procedure is listed as well as the frequency of visits. MRI and fMRI would be conducted in the same session whereas all other procedures would warrant a separate appointment. Maximum number of sessions involved is therefore 29.

	Baseline	Approximately fortnightly intervals	Month 3	Approximately fortnightly intervals	Month 6	Approximately fortnightly intervals	Month 9	Approximately fortnightly intervals	Month 12
Clinical Visit	✓				✓				✓
MRI	✓		✓		✓		✓		✓
fMRI	✓								✓
TMS	✓		✓		✓		✓		✓
tDCS		✓ ✓ ✓ ✓		✓ ✓ ✓ ✓		✓ ✓ ✓ ✓		✓ ✓ ✓ ✓	

4.3 Barriers for recruitment

4.3.1 Study Design

Multiple barriers for recruitment were identified throughout the recruitment phase of the study. This primarily included (but was not restricted to) the burden of the original study design and type of procedures used. Using the criteria described in Table 4.1 and the schedule outlined in Table 4.3, recruitment proved very difficult and participants were discouraged by the number of visits before even determining eligibility. It also proved very difficult to find individuals who fell into this narrow inclusion criteria. The dry form of AMD, despite being the most common and accounting for 85-90% of AMD cases, is not treatable (Singer & Bahadorani, 2017). This means the number of patients coming through the regular eye clinics at the hospital is far lower than the number attending with neovascular AMD. As described in Chapter 1, the neovascular or wet form of AMD can be treated with anti-vascular endothelial growth factor (anti-VEGF) injections every 4 - 12 weeks, depending on their treatment plan. Whilst this does not cure the disease, it does slow down the progression and help maintain visual function. A summary of the number of participants screened and their eligibility are in Figure 4.1B. Information has been grouped to show how amendments impacted on the recruitment rates – the timeline for key events

are outlined in Figure 4.1A. Our first amendment concerned the inclusion criteria. It was clear when screening potential participants that the narrow inclusion criteria were making recruitment difficult, as we rejected many volunteers.

A

B

	Participants Screened		
	Eligible & Recruited	Eligible & Not Recruited	Not Eligible or Declined
Pre-Amendment	0	0	57
Amendment Number — **Amendments**	Eligible & Recruited	Eligible & Not Recruited	Not Eligible or Declined
1 • Cut the study duration by 6 months • Reduced age limit to 18 years to include younger participants with similar forms of macular disease • VA score 20-80 • Include patients with Wet AMD (with stable vision)	1	48	159
2 • TMS removed from protocol • Recruitment target reduced from 30 to 10 • Remove sham stimulation group (for TDCS) • Extend recruitment window to March 2017			
3 • Extend the study until May 2017	11	27	118
4 • Gave participants the option to opt in or out of certain procedures so if they failed tDCS screening, they could still complete MRI and clinical visits.			
5 • Extend the study by 18 months			

Figure 4.1. Timeline for key milestones in the study, including amendments to the study protocol and documentation, as well as recruitment dates. **B:** Summary of the amendments to the study protocol and the number of volunteers screened. Volunteers were grouped into 3 categories: Eligible and recruited, eligible & not recruited, and ineligible or declined. For those who were eligible but not recruited, this was primarily because the participants seemed eligible at screening, but other contraindications emerged when speaking to volunteers, or the volunteer declined despite being eligible.

106

The final study procedures (Table 4.4) were significantly altered to successfully recruit for the study. As well as cutting the duration of the study by six months, TMS procedures were removed, and all other appointments (MRI, tDCS and hospital visits) became optional, allowing participants to just enrol in the MRI procedures, for example. Initially, we suspected it was due to the narrow criteria concerning the eye condition, however it was primarily due to the contraindications for neurostimulation procedures. Both issues will now be discussed in turn.

Table 4.4. Final study timeline after amendments to the study design and inclusion / exclusion criteria.

	Baseline	Approximately fortnightly intervals	Month 3	Approximately fortnightly intervals	Month 6
Clinical Visit	✓				✓
MRI	✓		✓		✓
fMRI	✓				
tDCS		✓ ✓ ✓ ✓		✓ ✓ ✓ ✓	

4.3.2 Inclusion criteria concerning the patient's eye condition

In the original study design (Table 4.1), the inclusion criteria were deliberately narrow as we were trying to recruit individuals who had recently been diagnosed with dry AMD in the second eye (within 18 months of diagnosis), and who did not exhibit any other forms of eye affecting diseases or injury. The rationale for this was that we wanted to establish the rate of change in visual cortex as close in time to the onset of visual loss, which would theoretically be the period in which changes would most likely be observed, as opposed to when patients have prolonged visual deprivation. Additionally, we hypothesised that this is the period during which tDCS might have the greatest impact in preventing or slowing any degeneration of visual cortex. In Figure 4.2 we outline the most common reasons for patients failing screening. The most frequent issues arising during screening were other eye-involving disease or injury, visual acuity falling outside of the desired range or patients having unstable vision, as determined by a change of more than 10 letters on the ETDRS chart within the three most recent clinic appointments.
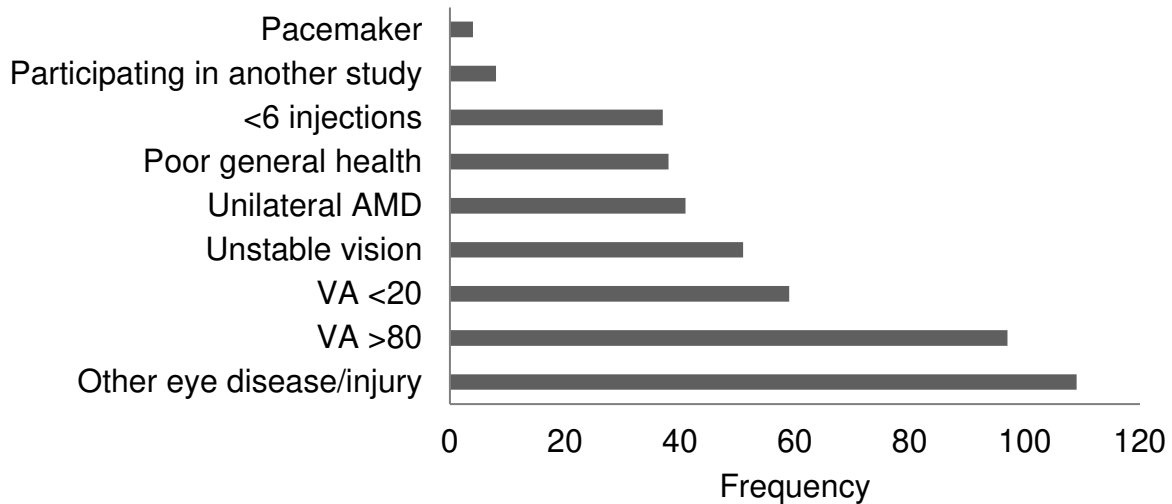
Figure 4.2. Reasons volunteers failed screening and classed ineligible for the study. *Unstable vision* was measured by reviewing visual acuity scores from the last three appointments at the eye clinic. Vision was deemed unstable if a change of >10 letters occurred in this time window. For more details about *Other eye disease/injury* criteria, see Appendix B1.

4.3.3 Contraindications for neurostimulation procedures

Transcranial magnetic stimulation (TMS) and transcranial direct current stimulation (tDCS) are non-invasive brain stimulation procedures that are used in multiple research groups in psychology and cognitive neuroscience, to probe the function of the brain by temporarily modifying the state of the brain (Halko et al., 2013). Stimulation can occur in two forms: online or offline. Online stimulation sessions constitute a task being performed while stimulation is being applied, whereas during offline stimulation, no task is performed (Filmer, Dux, & Mattingley, 2014).

TMS is a safe, non-invasive technique used to modulate cortical excitability using changing magnetic fields applied to the brain, which in turn causes an electric current in a region of interest (Rossi, Hallett, Rossini, & Pascual-Leone, 2009). TMS has been used to probe the function of different brain areas by either causing an increase in activity, or conversely, reducing activity by inducing a temporary cortical lesion.

TDCS delivers a constant low intensity electrical current to the brain, applied through the skull with small saline-soaked surface electrodes (Antal, Nitsche, & Paulus, 2006; Brunoni et al., 2012). Stimulation is delivered by a DC battery and can increase or decrease the cortical excitability in regions nearest the electrodes, depending on the type of stimulation used (Lang et al., 2007; Romero Lauro et al., 2014). Anodal stimulation increases the membrane potential of neurons and depolarises them, whereas cathodal stimulation

108

decreases the resting membrane potential, in turn hyperpolarising neurons (Poreisz, Boros, Antal, & Paulus, 2007). TDCS is a cheap form of brain stimulation, which is non-invasive, well tolerated with minimal adverse effects reported (Hummel & Cohen, 2006). However, protocols and safety guidelines can vary drastically between institutions and research groups. This in turn affects the feasibility of some studies as it will depend on the guidelines proposed by the host institution. This will be discussed in more detail later.

Both TMS and tDCS are increasingly being used to assess their effectiveness in rehabilitating patients with different clinical conditions who may be drug-resistant, for example. Over the last 20 years the number of studies using TMS for therapeutic applications has significantly increased and it has been used successfully in treating case of treatment-resistant depression (Cole et al., 2019; Concerto et al., 2015; Fox, Buckner, White, Greicius, & Pascual-Leone, 2012; Leggett et al., 2015; Pascual-Leone, Bartres-Faz, & Keenan, 1999; Pascual-Leone, Rubio, Pallardó, & Catalá, 1996; Philip, Barredo, Aiken, & Carpenter, 2018) and has shown promise for rehabilitating Parkinson's disease and stroke patients (Baker et al., 2010; Dionísio, Duarte, Patrício, & Castelo-Branco, 2018; Fregni et al., 2004; Fregni & Pascual-Leone, 2007; Gandiga, Hummel, & Cohen, 2006).

TDCS has also been adopted for a wide range of clinical studies not only because of the direct effects on cortical excitability, but also because it can be used in conjunction with other treatments (Brunoni et al., 2012). Historically, electrical currents have been utilised as a means of relieving epilepsy and headaches, but even as early as 1804, Aldini was the first to report using this method of treatment, particularly for psychological disorders (Stagg & Nitsche, 2011). Results were highly varied and often severe adverse effects were reported but this was prior to the establishment of more controlled protocols and rigorous safety testing; later studies adopted a similar method of treatment, using much lower DC currents. More recent work incorporating tDCS aims to use it as a means of treating various neurological and psychiatric conditions such as depression, epilepsy, chronic pain, Parkinson's disease, stroke rehabilitation and migraines (Berlim, Van den Eynde, & Daskalakis, 2013; Brunoni et al., 2011; Poreisz et al., 2007; Shiozawa et al., 2014). From a safety perspective, there is little evidence to suggest tDCS will lead to any serious adverse effects. For example, despite 20% of stroke patients reporting seizures during recovery, there is no direct evidence to suggest that tDCS would induce seizures even in compromised cases with atypical cerebrovascular structure (Bikson et al., 2016). Another consideration is the behavioural and psychological changes that occur during the recovery

phase post-stroke; understanding how tDCS may interact with these will help researchers to define what is actually a direct serious advert effect as a result of tDCS.

Arguably the biggest hurdle for recruitment to our study was finding individuals eligible for both neurostimulation procedures. Both procedures come with an extensive list of screening questions and safety checks to ensure an individual is safe to participate in such procedures, shown in Appendix B (B2-B3). For this reason, neurostimulation studies can also be difficult to implement in a clinical population outside of a hospital environment and without an M.D. present. The inclusion and exclusion criteria are virtually the same for both TMS and tDCS in our department and because of the two techniques being judged as largely identical in risk recruitment was limited. The main concern with neurostimulation is the safety of the participant, as the procedures present an increased risk of seizure, which is magnified if a participant is in a certain state, feeling unwell or taking a range of medications (Rossi et al., 2009). The effects are also dependent on the parameters set, such as the duration for which the stimulation is applied and the intensity of the stimulation.

Despite tDCS being deemed low risk and having an increasing number of clinical studies involving tDCS procedures in conjunction with drug treatments, the safety guidelines employed in our department do prohibit most of the elderly population from being recruited to a neurostimulation study. As part of the natural aging process, we do become more vulnerable to particular health conditions (e.g. neurodegenerative disease, respiratory disease, heart disease, cancer & diabetes (Age UK, n.d.), however evidence suggests comorbidities appear to be more prevalent in wet AMD patients compared to age-matched sight controls (Zlateva, Javitt, Shah, Zhou, & Murphy, 2007). Notwithstanding, it is important to disentangle the increased risk of seizure caused by pre-existing health conditions versus the overall risk of an adverse reaction to the neurostimulation itself in patient groups, as well as the elderly more generally, as this population would likely benefit most from such interventions. A recent review of the safety of tDCS concluded there is no current evidence from over 40 studies, which included testing of 600 older adults, that aging subjects have an increased risk of a serious adverse event (Bikson et al., 2016). This was also irrespective of their cognitive abilities or health status. Recent pilot data investigating the possible therapeutic effects of tDCS in individuals with a visual impairment who experience visual hallucinations caused by Charles Bonnet Syndrome (CBS) have shown some promising results; four of the six patients with CBS found the treatment alleviated the distressing symptoms (da Silva Morgan, Taylor, & ffytche, 2020).

CBS can occur in any form of visual impairment, but with AMD being the current leading cause of blindness in the UK, a large proportion of patients affected are elderly. This promising finding along with the success of other more established clinical studies warrants the re-evaluation of the site-specific tDCS guidelines, to allow for more research like this to be undertaken, where the possible therapeutic benefits are greater than the risk posed by tDCS.

The main reason for ineligibility in our study we believe concerned medication use. Our target population was initially just individuals with AMD and as the name suggests, it is an age-related disease and prevalent in the elderly. Approximately 2.4% of 50+ year olds, 4.8% of 60+ year olds and 12.2% of 80+ year olds are diagnosed with AMD (NICE, 2018). Furthermore, the older you get, the more likely you are to be taking one or more prescribed medications for other health conditions associated with aging as mentioned previously. A recent healthy survey for England highlighted the proportion of the population on prescribed medications, broken down into different age brackets (Moody, Mindell, & Faulding, 2016). Figure 4.3 illustrates the findings from the survey and highlights that even in the youngest age group (55-64 years), over 60% of individuals reported taking one or more prescribed medications. It should be noted that this does not include any over-the-counter medication. This data alone highlights how difficult it would be to conduct neurostimulation studies on AMD patients with such stringent safety criteria; older people are more likely to have AMD but are also highly likely to be on prescribed medications which are prohibited in the context of neurostimulation procedures. Figure 4.4 breaks down the most common forms of prescribed medications taken by individuals over 55 years of age, many of which render individuals ineligible for both TMS and tDCS (Rossi et al., 2009). It is at least encouraging to see this data support our recruitment data in Figure 4.1B, highlighting the vast amount volunteers excluded. Upon relaxing the criteria where participants could opt just for the MRI procedures, our successful recruitment increased nine-fold.
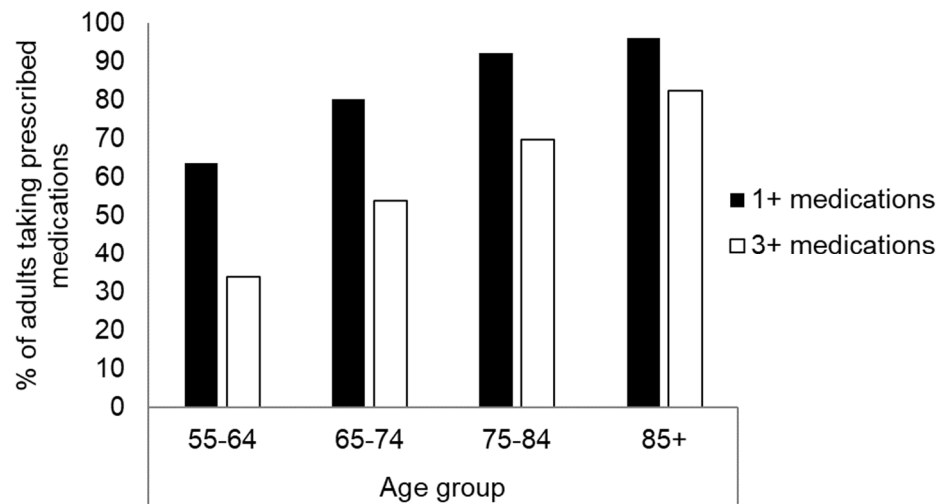
Figure 4.3. Data from Health Survey for England for 2016 on prescribed medicines. Percentage of the population taking prescribed medications in our target age groups. Black bars: percentage of population in each age bracket taking more 1+ prescribed medications. White bars: percentage taking more than three prescribed medications. Note this does not included any over-the-counter medication or non-prescribed medications. Prescribed medicines exclude smoking cessation products and contraceptives.
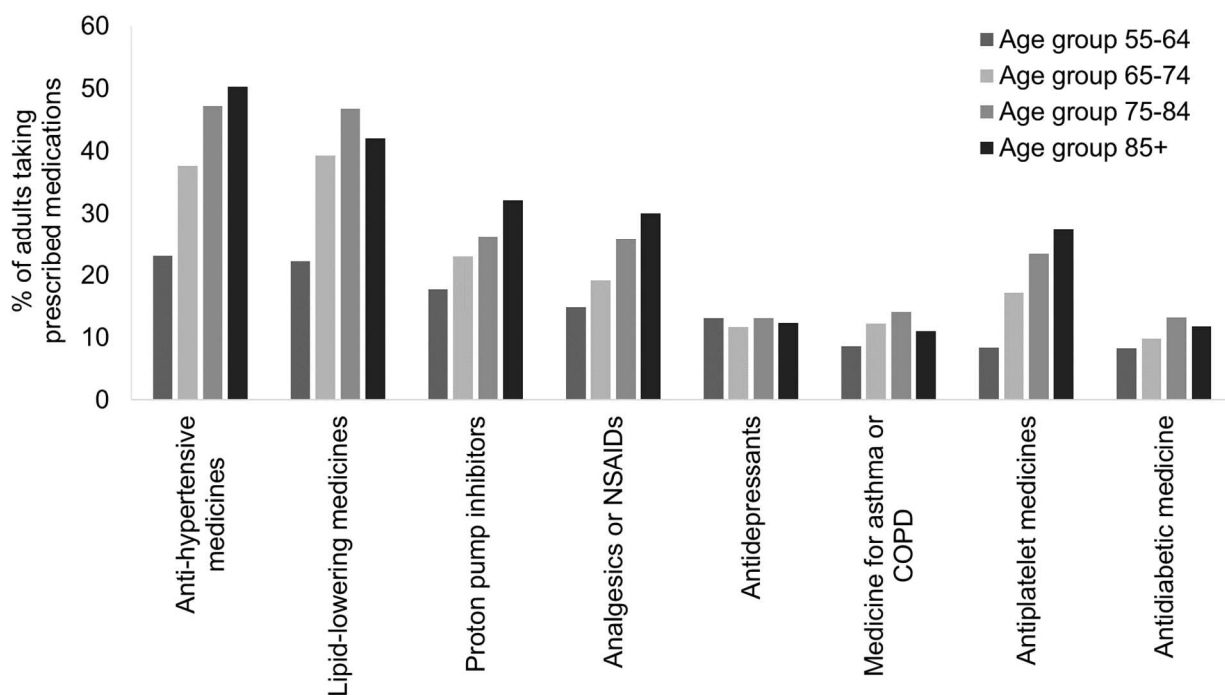
Figure 4.4: Data taken from the Health Survey for England 2016 on Prescribed medicines. Percentage of the population taking most prevalent forms of prescribed medications in the age range our study was targeting. Note this does not included any over the counter/non-prescribed medication. Anti-hypertensive medications lower blood pressure. Lipid-lowering medicines include statins to lower cholesterol, and fibrates which take care of fatty acids and triglycerides. Proton pump inhibitors are a group of drugs that reduce stomach acid production. Analgesics and NSAIDS (non-steroidal anti-inflammatory drugs) constitute painkillers. Antidepressants combat clinical depression. Medicines for asthma or COPD (chronic obstructive pulmonary disease) can include bronchodilaters which are usually combined with glucocorticosteroids. Antiplatelet medicines are a group of blood-thinning drugs to reduce chances of heart attack and stroke, for example. Antidiabetic medicines are used to control diabetes. See Appendix B4 for British National Formulary (BNF) codes.

4.4 Discussion

When conducting a longitudinal study with neurostimulation procedures, there are multiple factors that need to be considered for it to be successful. It is evident that stringent inclusion criteria, which includes the many contraindications listed for the neurostimulation procedures (notably medication), was by the far the most limiting factor when recruiting for this particular study. Evidence from our own observations in conjunction with data from the Health Survey England 2016 highlights the proportion of individuals on medications over the age of 55 years – our target population with age-related macular degeneration – is vast. Additionally, this only captures the prescribed medications and as such, the number of individuals taking over-the-counter medication will inflate the statistics further. Studies have been conducted in conjunction with drug treatments, and so in this instance, the main issues were the limitations imposed by the site-specific safety guidelines being stricter compared to other institutions. It appears that in order to successfully conduct studies examining the impact of neurostimulation procedures on clinical populations, it would require procedures to be undertaken where an M.D. is on site e.g. hospitals. Therefore, if this resource is not available, the design is unfortunately not feasible in such populations.

Establishing appropriate inclusion criteria is crucial to successful recruitment for any study. As discussed previously, our initial design was highly specific, to include individuals with dry AMD who were diagnosed in the second eye within the 18 months prior to recruitment. Dry AMD patients do not frequently attend the eye clinic, as there are currently no effective treatment plans compared to those with the wet form. In order to find such individuals, we were relying on them either attending clinics for an annual check-up at the time we were recruiting, or for them to have become members of local sight loss charities and support groups where we were also advertising our study in the later stages. Finding such individuals within such a tight time window was difficult without more help in the clinic.

To increase the chances of recruiting in clinic, we expanded our criteria to include wet-AMD patients. Despite being the less common form of AMD, we would encounter far more patients in the clinic since treatment is readily available. However, it was after this change in criteria that contraindications for neurostimulation procedures became the next hurdle to overcome. As we were still recruiting from the older population, medication issues were still prevalent. An additional factor to consider is a change in medication over the time course of the study, but also the use of temporary medications for example those who are taking medications for hay fever in the summer months. Antihistamines are named as an exclusion criterion under the TMS guidelines (Rossi et al., 2009). Timing of the study is

therefore also crucial to avoid undertaking data collection during the time of year where individuals will be on medication making them ineligible. Given longitudinal studies typically span more than 12 months, this is difficult to overcome. This is an important consideration for future neurostimulation studies because as a nation, we are an aging population. It is predicted that by 2037, almost a quarter of the population will be over 65 years of age (Office for National Statistics, 2018). With that, we will see an increase in the prevalence of AMD as well as other age-related diseases. Neurostimulation procedures are promising non-pharmacological interventions for conditions which largely affect the elderly, and yet it cannot always be utilised in the population who could benefit most.

Our final step to widen the inclusion criteria was to drop the age of the participants to 18 years of age and seek out individuals with any form of central vision loss. This would again increase the participant pool but also would help alleviate some of the problems faced with contraindications for the neurostimulation procedures. The important thing to consider in terms of the research question was that vision loss was bilateral and overlapping – age of onset or disease type would become irrelevant to the question at this stage. However, lowering the age unfortunately did not cause an influx of participants; individuals included were now of working age and therefore many of them in full time employment were unable to commit to a study that required multiple visits or testing within standard 9-5 working hours. While we broadened our pool, we did not necessarily increase recruitment opportunities. By the time recruitment had closed, we only had two individuals of working age enrolled in the study.

Upon reflection, it is clear our original study design was labour intensive for both participant and researcher. It is understandable that, particularly for the elderly, 29 visits within a 12-month period is burdensome, but also would have been difficult to manage for one researcher 29 visits for potentially 30 participants. Whilst this design was optimised for the research question, it was not inviting to the participants. Even with the option to have the tDCS procedures in the participant's home (which would make up 16 of the 29 visits), it is still a large time commitment. It is important to bear in mind that once the study opened up to wet AMD patients, we would have to fit in all the research visits around their regular eye clinic appointments which could be as often as once a month. Having multiple MRI appointments was less of an issue; of our original 12 patients enrolled in this study, 7 joined the extended project for between 6 and 18 months beyond the initial study period. Some have even gone on to participate in other experiments within our lab. The fact that

some participants consented to follow-up scans and attended an additional three appointments shows that multiple visits were acceptable within reason.

Since completing the study, we have conducted a short survey to establish what current participants' views on the number of required visits for future research. Results from the survey indicate that a design involving 8 visits over a 4-year period would be perfectly reasonable. Further to this, the acceptable duration of each individual visit was 1 to 2 hours for 5 out of 12 respondents, however the remaining 7 out of 12 thought 2+ hours an acceptable duration per appointment. The results of this survey also highlight the importance of incorporating patient and public involvement in our research at the very outset, to optimise the study and improve the quality of both the science and the experience for the participants themselves. See Appendix B (B5) for a summary of the survey.

The final iteration of our study was as follows: 12 MD patients (10 with AMD and 2 with juvenile MD) were recruited for the 6-month period, 3 of whom had tDCS procedures. Due to the small sample, we decided to focus on the MRI element of the study and applied for ethical approval to extend the MRI portion of the study to include 3 further appointments: 12, 18 and 24 months from baseline. We wanted to track the rate of change in anatomical measures (cortical thickness, myelin density and integrity of the white matter in visual cortex) over this time period in cases of established MD. We were also able to include a sighted control group by inviting back participants from a study which used the same MRI protocols, ensuring their data were comparable. We had 18 control participants of a similar age who were scanned between 22 and 26 months apart.

To conclude, this longitudinal neuroimaging and neurostimulation study proved a challenge, and several reasons for the difficulties faced have been discussed. Establishing a feasible inclusion and exclusion criteria is essential. Opting to include individuals who would be less likely to frequent the eye clinic was problematic, as was having such stringent criteria. The design of the study was deemed unfavourable by potential participants due to the frequency of appointments and burden, but also unachievable by the small research team at that time. The rate at which patients failed to pass the safety screening for neurostimulation procedures was a major concern. Due to many contraindications as determined by the safety questionnaires used, as well as the likelihood of finding AMD patients who were not taking any prescribed medication, protocol amendments had to be made to ensure we could recruit patients at least into the MRI

procedures and acquire useful data. Eventually, the study was altered to focus on the anatomical changes in the brain in a broader group of central vision loss patients. Our data still contribute new original findings to the field whilst also highlighting challenges faced in this field. Details of the final study are presented in Chapters 2 and 3.

Chapter 5: Assessing resting state functional connectivity between V1 and higher visual areas in cases of selective central or peripheral loss

5.1 Abstract

Previous studies have shown specific changes within visual cortex in cases of selective central or peripheral vision loss, notably reductions in cortical thickness and absence of functional responses in the region representing the lesioned retina. Here we used resting state fMRI to explore functional connectivity within visual cortex, examining specific connections between regions with matching eccentricity biases; (1) central visual field representations in V1 and foveal biased ventral visual areas (overlapping face-selective regions), and (2) peripheral visual field representation in V1 and peripheral biased ventral visual areas (overlapping place-selective regions). We tested individuals with selective central or peripheral vision loss as well as sighted controls, exploring connections between areas defined using atlas-based multimodal parcellations of cortex. Our second aim concerned viewing conditions; with known fixation instability in partially sighted populations, all participants completed the experiment twice, once with eyes closed and once with eyes open, fixating on a full screen fixation cross. Due to early termination of the study, our results focused on the central loss and sighted control groups only. Results revealed selective deficits in the central loss group, whereby the group showed reduced connectivity between regions with foveal biases (central V1 - face area) compared to sighted controls, whereas no such difference emerged in the peripheral biased regions (peripheral V1 - place area). This result was evident in both the eyes open and eyes closed conditions but was only observed in the right hemisphere, supporting the lateralisation of function of face processing.

5.2 Introduction

Resting state functional MRI allows for the opportunity to study the organisation of visual cortex in individuals with partial or complete blindness. It allows researchers to examine interactions between cortical regions and establish functional connectivity between regions of interest (ROI), without the need for stimuli or task demands. In cases of complete absence of vision, research has shown that the architecture underlying visual cortex remains largely the same, demonstrating typical retinotopic organisation despite no visual experience (Bock et al., 2015; Bridge et al., 2009; Striem-Amit et al., 2015). As described in Chapters 1 to 3, there is evidence of structural atrophy, or perhaps even degeneration, in visual cortex in cases of macular disease, affecting grey matter, cortical myelin and the visual white matter. A key study from Yoshimine and colleagues highlighted evidence of specific deficits in white matter projecting to the anatomical representation of the retinal deficit in individuals with age-related macular degeneration (Yoshimine et al., 2018). This begs the question of whether functional connectivity may follow suit, with observed changes being restricted to connections with the representation of damaged visual fields in partial vision loss. The function of the cortical representation of the lesion is also of interest; as discussed in Chapter 1 and later in Chapter 6, in cases of acquired vision loss there is debate over whether functional responses can be reliably detected in the cortical representation of the lesion at all, but also what this may represent. Assessing the functional connectivity between the cortical representation of the retinal lesion and higher-level visual areas may help give us some insight into the communication between visual areas.

Few studies have assessed functional connectivity in cases of partial vision loss, for which the onset is often later in life. Previous work has largely focused on individuals with complete blindness and been exploratory in nature, examining connectivity over the whole brain as opposed to focusing on functional connectivity within visual cortex (Frezzotti et al., 2014; Sabbah et al., 2017). However, there is evidence of decreased functional connectivity between the visual and working memory networks in individuals with advanced primary open-angle glaucoma, which, as described in Chapter 1, results in gradual peripheral vision loss. As well as reductions in functional connectivity, this study also found enhanced connections in visual and executive networks (Frezzotti et al., 2014). As for central vision loss, Sanda et al., (2018) explored changes in cortical entropy using resting state fMRI to explore connective properties in various parts of the occipital lobe. Results indicated a possible compensatory increase in cortical entropy in regions medial to

the mid fusiform sulcus (MFS) which are shown to have more of a peripheral bias (Sanda et al., 2018). The extent of the changes observed seemed to correlate with the severity of vision loss and this is important because it highlights the potential value of looking at other clinically relevant measures such as fMRI (Duncan et al., 2007; Frezzotti et al., 2014). There is some evidence suggesting higher-level face and scene processing are affected by sight loss, however, this is largely limited to behavioural studies (Peyrin, Ramanoël, Roux-Sibilon, Chokron, & Hera, 2017; Roux-Sibilon et al., 2018). As extrastriate regions receive input from earlier visual areas, it is important to understand how and whether information is fed forward to higher-order visual areas when earlier regions in the visual pathway no longer receive visual input. Likewise, understanding any remaining interaction between areas of deprived input and later processing stages is important.

Cortical regions in the ventral visual pathway that are selective for face and scene processing are known to have a central and peripheral eccentricity bias respectively (Glasser et al., 2016; Hasson, Levy, Behrmann, Hendler, & Malach, 2002; Levy et al., 2001; Malach, Levy, & Hasson, 2002; Striem-Amit et al., 2015). Neuroimaging studies examining the relationship between the functional representations (task-based fMRI & functional connectivity) and underlying architecture of cortex (myelin content, cortical thickness, cortical folding & white matter connectivity) have shown an overlap between domain specificity maps and eccentricity biases. Using a multi-modal approach, the Human Connectome Project (HCP) has identified 180 areas per hemisphere, which correspond with regions identified with post-mortem data (Glasser et al., 2016). In terms of the ventral visual stream, they have shown in a large participant group, that the regions referred to as the fusiform face complex (FFC) and the posterior inferotemporal (PIT) correspond with the two main clusters of activation in a face-based fMRI study; these largely capture the functional regions known as the fusiform face area (FFA) and the occipital face area (OFA). Grill-Spector and colleagues have also examined the structure of the ventral visual stream, exploring the relationship between anatomical and topographic representations (Grill-Spector & Weiner, 2014; Weiner et al., 2014; Weiner & Zilles, 2016). Divisions between face and/or foveal representations are shown to be separated from place and/or peripheral representations by the mid fusiform sulcus - MFS (Grill-Spector & Weiner, 2014; Weiner et al., 2014). Lateral to the MFS, Weiner and colleagues showed there are biases towards foveal representations, face-selectivity and animacy for example, whereas on the medial side, they observed a peripheral eccentricity bias, place-selectivity and a preference for inanimacy (Grill-Spector & Weiner, 2014;

Weiner & Zilles, 2016). The division also corresponded with transitions between white matter connectivity with faces (lateral) and places (medial), and myelin content. This coincides with the FFC and PIT regions identified by the HCP multi-modal parcellation (HCP-MMP1.0) described above, and the parahippocampal place area (PPA) ROI generated by Grill-Spector and colleagues - see Section 5.3.5.2 for more detail on how this was generated. Areal boundaries in the ventral visual pathway have been consistent with previous work focusing on just one property of cortex - typically functional organisation principles. Identifying these boundaries allows for identification of ROIs using parcellations of cortex that do not rely on having functional localiser data; this is particularly helpful in cases of partial or complete blindness.

Whilst previous work has shown that domain-specific connectivity is evident in sighted adults, how it develops over time and when this specificity emerges, is largely unknown. Kamps et al., (2020) provide greater insight after examining how portions of primary visual cortex connect with higher-level visual areas including the FFA, OFA, PPA and retrosplenial cortex (RSC), given that these areas are shown to have specific retinotopic biases (Hasson et al., 2002; Kamps et al., 2020; Levy et al., 2001) and retinotopic organisation is evident from birth (Arcaro, Schade, Vincent, Ponce, & Livingstone, 2017). Kamps et al have shown as early as 27-days old, stronger functional connectivity was observed between OFA and the central representation in V1, and for PPA and RSC, functional connectivity was strongest with peripheral V1. Interestingly, the FFA and central V1 functional connectivity was not significant, but authors note there was a trend in the direction of a foveal bias (Kamps et al., 2020). In cases of congenital blindness, functional connectivity analysis has also shown that FFA and PPA differ in terms of their eccentricity preferences, and this did not differ significantly between blind and sighted groups. Similarly, congenitally blind individuals do show FFA responses to auditory stimuli, for example expressing emotion through voice (van den Hurk, Van Baelen, & Op de Beeck, 2017) and to haptic stimuli, for example 3D printed faces (Murty et al., 2020). Collectively, the neonate and congenitally blind studies highlight that both retinotopic organisation as well as category selectivity in the occipital temporal cortex develop independently, and without visual experience. Whilst this division is evident in the absence of vision and visual experience, we do not know to what degree this may change in acquired or late-onset vision loss, particularly because connectivity with non-visual areas is where groups differed significantly (Striem-Amit et al., 2015).

As discussed in Chapter 1, one of the most common complaints from those with central vision loss, such as age-related macular degeneration (AMD) is difficulty identifying familiar faces and interpreting facial expressions. This is not surprising given that faces contain a lot of highly complex information which requires high acuity to scrutinise - something that is progressively lost with AMD. Considering visual deficits can be selective (as in AMD and glaucoma, affecting central and peripheral vision respectively), we want to know how the functional connections that are established early in life may be impacted by acquired sight loss. Determining whether higher-level visual areas with eccentricity biases matching the affected portion in V1 (anatomical representation of the retinal damage) also show reduced connectivity with this region was our main aim. Previous work using resting state functional connectivity with groups of selective central and peripheral loss found increased local connections from the unaffected early visual cortex, and increased remote connections with the portion of early visual cortex no longer receiving visual input (Sabbah et al., 2017). It is interesting to see perhaps there is a diversion to higher-order functions outside of the visual cortex, but how this would compensate areas with a loss of visual input is not clear. What happens to more specific functional connections within visual cortex is currently unknown, and something we aim to investigate in the current study.

When designing a resting state fMRI study, it is important to consider the state of the participant, and what will be expected of them during the scan. Typically, research will be conducted in one of three ways: 1) participants will be asked to close their eyes (2) participants are asked to keep their eyes open and (3) participants are asked to keep their eyes open but are presented with a simple fixation cross to help maintain attention (Patriat et al., 2013; Zhang et al., 2015; Zou & Long, 2009). The latter is generally considered optimal, as there is evidence of subtle improvements to the resting state functional connectivity compared to the alternatives, with the exception for visual networks showing a slight preference for eyes open without fixation (Patriat et al., 2013). Having something to attend to during the scan improves participant focus, however for visually impaired and/or completely blind participants, having a visual stimulus on which they fixate can be problematic, depending on the severity of the vision loss and fixation stability.

For this study we had two aims. First, we wanted to determine how much resting state fMRI is affected by having eyes open or closed in partially sighted populations, as well as sighted controls. In the eyes open condition, we opted for a large black fixation cross on a mid-grey screen which extended to the full width of the screen, ensuring the patients would be able to fixate on a part of the screen. This also was a way of reducing eye movements

which could modulate spontaneous activity within the visual network (Yang et al., 2007; D. Zhang et al., 2015; Zou & Long, 2009). We recruited participants from three groups in this study: sighted controls, individuals with central vision loss and individuals with peripheral vision loss. Following a similar set up to Kamps et al., we wanted to investigate whether the type of visual impairment (central vs peripheral loss) impacted on functional connections differently. Figure 5.1 illustrates the connections of interest. We predicted that connections between the V1 ROI capturing the anatomical representation of the affected visual field and the ventral visual area with the same eccentricity bias, will be most affected. For example, for central vision loss this would be central V1 and regions involving face processing, and for peripheral vision loss, this would be peripheral V1 and regions involving place processing. In the absence of functional localisers, we have opted to use atlas-based ROIs; the Benson atlas for portions of V1, the HCP-1.0MMP parcellations for FFC and OFA to create our face area and the PPA ROI from Grill-Spector's lab for our place area. There is evidence of a lateralisation of function for face processing, with the right hemisphere being more dominant in face processing (Kanwisher, McDermott, & Chun, 1997; McCarthy, Puce, Gore, & Allison, 1997) and therefore we have not collapsed across hemisphere in our analysis to determine whether functional lateralisation is evident in the functional connectivity data. In terms of our eyes open versus eyes closed condition, we predict that perhaps this will make the biggest difference to our patient groups, whereby eyes closed will yield more consistent results within sighted and visually impaired groups.
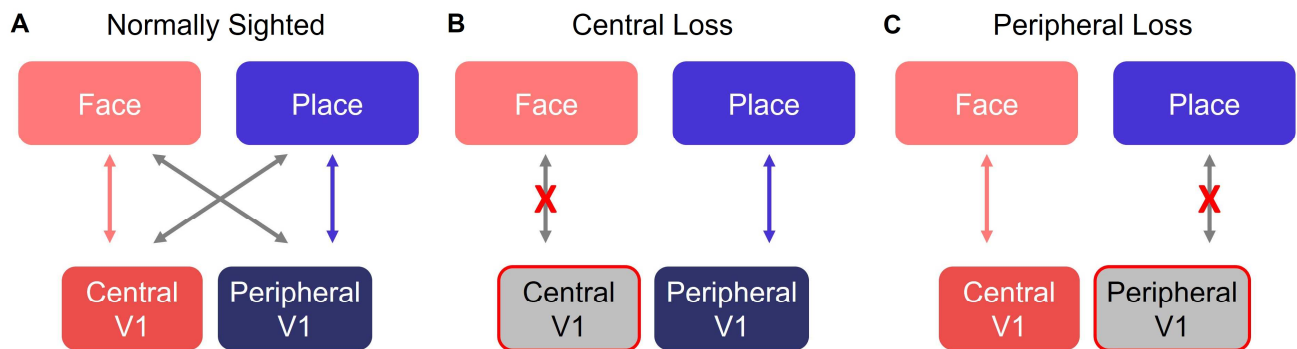
Figure 5.1. Illustration of functional connections of interest. **A:** Normally sighted representation. Kamps et al., 2020 showed within eccentricity correlations (e.g., Central V1 and face areas) are higher than between eccentricity correlations (e.g. central V1 and place areas). **B&C:** Predictions for central and peripheral vision loss groups only concern within eccentricity correlations – grey box indicates the region of V1 affected by vision loss, and the grey arrow with a red cross indicates the connection predicted to show a decrease in functional connectivity.

5.3 Methods

5.3.1 Participants

27 participants were recruited for this study; 16 sighted controls (6 females, mean age = 65.06 years, range = 47 - 82 years old), 7 individuals with central vision loss (2 females, mean age = 70.29 years, range = 53 to 84 years old) and 4 individuals with peripheral vision loss (4 females, mean age = 58.25 years, range = 48 to 65 years old) were recruited through advertisements in local sight loss support groups in York and the York Neuroimaging Centre (YNiC) Participant Pool, University of York. One sighted control was excluded due to poor image quality caused by dental braces, and 1 central vision loss participant was excluded due to poor quality structural images which FreeSurfer struggled to process despite further intervention. This left us with 15 sighted controls, 6 central loss and 4 peripheral loss participants. Written informed consent was obtained from all participants. This study followed the tenets of the Declaration of Helsinki with approval granted by YNiC Research, Ethics and Governance Committee.

5.3.2 Scanning Procedure

All participants took part in a single scanning session lasting ~45 minutes. The only instructions given to participants were for the two resting state scans (~6 minutes each), referred to as '*Eyes Closed*' and '*Eyes Open*'. For the first resting state scan, participants were instructed to close their eyes through the two-way communication system. For those

who were hard of hearing, written instructions were presented on the screen in the scanner and participants were asked not to open their eyes again until the sound of the scanner stopped – we confirmed they could indeed hear that the scans had finished. We determined an adequate size and style of font for the instructions prior to going into the scanner, which was particularly important for the visually impaired participants. Participants were also asked to verbally confirm when they had closed their eyes. For the second scan, participants were instructed to keep their eyes open for the duration of the scan and attend to the fixation cross presented on screen.

5.3.3 Stimulus Presentation

A black cross spanning the full width and height of the screen was presented on a mid-grey screen to participants during the '*Eyes Open*' condition; this was presented full screen using Microsoft PowerPoint. This is deemed the optimum set up for resting state scans to ensure participants are alert and have something to focus their attention on. The fixation cross was presented to participants using the PROPixx DLP LED Projector (VPixx Technologies), with 1920x1080 Native resolution (HD), 120 Hz refresh rate and a custom in-bore acrylic rear projection screen subtending 40 x 23 degrees of visual angle.

5.3.4 MRI Data acquisition

All structural and functional data were acquired at the University of York Neuroimaging Centre on the 3T Magnetom Prisma MR scanner (Siemens Healthineers, Erlangen, Germany), using the 20-channel head / neck receive-array coil. For T1 and T2-weighted structural scans, we opted for the Human Connectome Project (HCP) recommended protocols (Glasser & Van Essen, 2011).

One T1-weighted anatomical image was acquired using a 3D-MPRAGE sequence (TR = 2400ms, TE = 2.28ms, TI = 1010ms, voxel size = 0.8x0.8x0.8mm^3, flip angle = 8°, matrix size 320x320x208, FOV = 256mm) and one T2-weighted anatomical image was acquired (TR = 3200ms, TE = 563ms, voxel size = 0.8x0.8x0.8mm^3, flip angle = 120°, matrix size = 320x320x208, FOV = 256mm).

For the functional MRI, we acquired two resting state scans (each ~6 minutes in duration), along with a field map matching the resting state scan parameters (~2 minutes duration) to help correct distortions caused by inhomogeneity in the magnetic field and improve registration. Two scans using echo planar imaging (EPI) sequence (TR = 1500ms, TE = 31ms, voxel size = 2x2x2mm^3, flip angle = 52°, matrix size 120x120, 64 slices, FOV = 240mm, multiband acceleration factor = 4) were acquired.

5.3.5 Data Analysis

5.3.5.1 Structural data

T1 and T2-weighted anatomical scans were processed using the HCP minimal processing stream for structural data (HCP, version 4.0.0). The HCP MRI data pre-processing pipelines use tools from FreeSurfer (Van Essen et al., 2012) and FSL (Jenkinson et al., 2002) and are also described in Section 2.3.3.3.

5.3.5.2 Generating Regions of Interest (ROIs)

Primary Visual Cortex

For each hemisphere, we divided V1 into two parts: a central V1 ROI capturing <5 degrees of visual angle, and a peripheral V1 ROI capturing beyond 5 degrees (Figure 5.2A, B). We used a surface-based atlas approach which does not require any functional data, only a standard FreeSurfer output directory for each participant for the cortical surface registration. The retinotopic organisation of visual cortex (particularly V1 to V3) is consistent across individuals and when using the cortical surface topology alignment methods (to reduce geometric distortions), there is further evidence to suggests consistency in the size and location of V1 across subjects (Dougherty et al., 2003; Henriksson, Karvonen, Salminen-Vaparanta, Railo, & Vanni, 2012; Hinds et al., 2008). Benson and colleagues have developed a mapping approach that can accurately predict the organisation of visual cortex (primarily V1-V3) simply by registering anatomical data to the cortical surface atlas space (Benson et al., 2012). We applied the Benson atlas (Benson et al., 2014) and restricted V1 based on eccentricity templates provided.

Higher-level Visual Cortex:

To find anatomical ROIs capturing face-selective and place-selective regions, we have incorporated both the Human Connectome Project Multi-modal parcellation version 1.0 (HCP-MMP1.0 from Glasser et al., 2016) and used the version projected onto the FreeSurfer Average Surface Space (https://figshare.com/articles/HCP-MMP1_0_projected_on_fsaverage/3498446). Recent attempts using architectural (myelin content, cortical thickness, cortical folding) as well as functional (task-based fMRI, functional connectivity) information to find areal boundaries in the ventral visual pathway have been consistent with previous work focusing on just one property of cortex - typically functional organisation principles. Including a multi-modal approach, the HCP have identified 180 areas per hemisphere. In the ventral visual stream, they have shown regions referred to as the fusiform face complex (FFC) and the posterior inferotemporal (PIT)

correspond with the two main clusters of activation in a face-based fMRI study; these aim to capture the functional regions - the fusiform face area (FFA) and the occipital face area (OFA). For the place-selective and peripheral biased representation, we used a parahippocampal place area (PPA) ROI generated by the Grill-Spector group in the FreeSurfer average surface space (http://vpnl.stanford.edu/PlaceSelectivity/). Consistent with the functional literature, this ROI was situated on the collateral sulcus (CS), medial to the mid fusiform sulcus (MFS). This ROI also was consistent with the parahippocampal parcels identified in the HCP-MMP1.0 (Weiner et al., 2018). All ROIs were converted from FreeSurfer average surface space to each individual subject's native anatomical space and an example viewed on the inflated surface can be seen in Figure 5.2C.
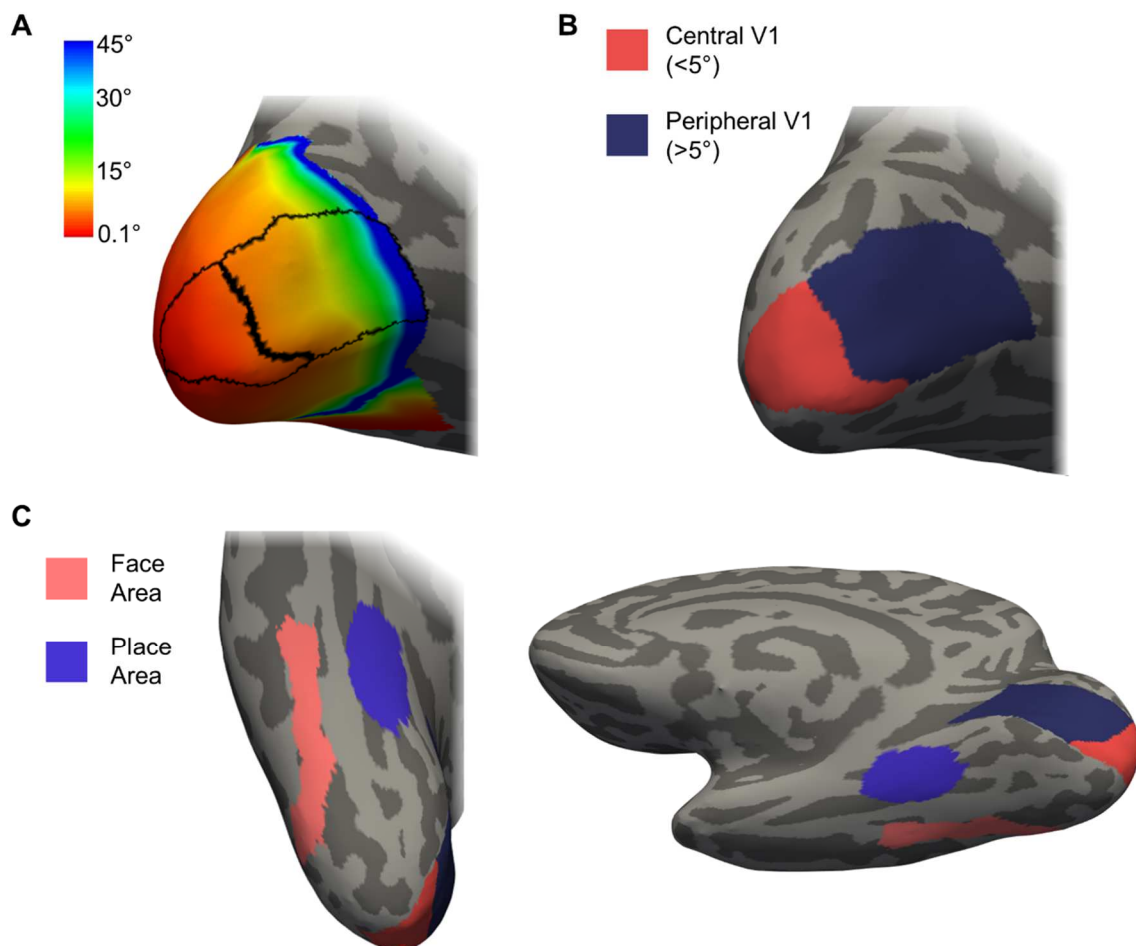
Figure 5.2. Regions of interest (ROIs) for one example participant, displayed on the FreeSurfer inflated cortical surface. **A:** Two V1 ROIs generated using the Benson Atlas, overlaid on the eccentricity map. **B:** The V1 ROIs in each hemisphere were divided in two – one portion capturing the central visual field (0-5deg) and one portion capturing the peripheral visual field (>5deg). **C:** Our higher-level visual ROIs shown on the ventral surface of the right hemisphere.

126

5.3.5.3 fMRI Preprocessing

Functional MRI data were analysed using FEAT (FMRI Expert Analysis Tool) Version 5.0, part of FSL (FMRIB's Software Library, www.fmrib.ox.ac.uk/fsl). First, given than functional data acquired with EPI sequences are susceptible to distortions caused by inhomogeneities in the magnetic fields, field maps were prepared by applying FUGUE - an FSL toolbox (https://fsl.fmrib.ox.ac.uk/fsl/fslwiki/FUGUE/Guide#SIEMENS_data). This process requires a magnitude image, phase image and the difference of echo times, which was 2.46ms for this protocol. Brain extraction was performed using BET (Smith, 2002) on the magnitude image to remove all non-brain voxels. It is important to get a conservative extraction, and so we eroded the image as an extra precaution. Examples of the various stages of analysis are shown in Figure 5.3.

Preprocessing in FEAT FSL (Worsley, 2001) included standard procedures: motion correction using MCFLIRT (Jenkinson et al., 2002), brain extraction using BET (Smith, 2002), grand-mean intensity normalisation, B0 unwarping (using field maps described above) and spatial smoothing (Gaussian kernel, 4mm (double voxel size) FWHM). The data were high pass filtered (gaussian-weighted least squares straight line fitting with sigma =50.0s) and registration to high resolution anatomical space was carried out using FLIRT (Jenkinson et al., 2002). Nuisance regressors were included to help clean up the signal. This included six motion parameter estimates and noise from the white matter and ventricles; to do this, we calculated the mean time series from the white matter and ventricles, creating masks converted to functional space from the FreeSurfer parcellation (Figure 5.4). These were then regressed out of the functional data using MATLAB (https://www.mathworks.com/products/matlab.html).
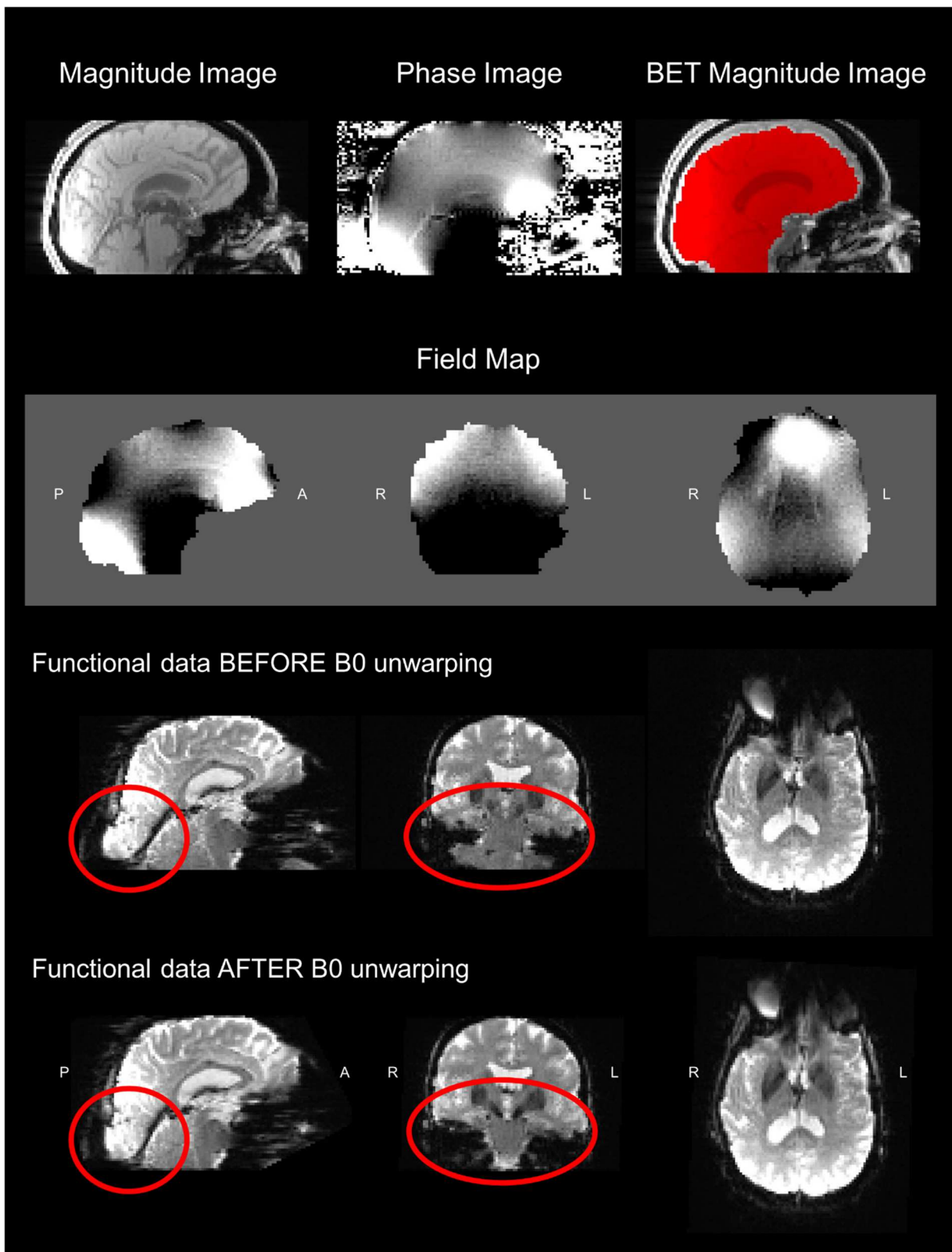
Figure 5.3. Preparing and applying a field map to fMRI data. **Top row:** Example magnitude and phase images, and brain extracted magnitude image overlaid onto the original magnitude image. This shows how it has been 'eroded' to ensure all non-brain tissue is excluded from the mask. **Second row:** Processed field map. Light colours highlight regions with greater inhomogeneity of the magnetic field. **Third row:** Example fMRI data before applying B0 unwarping with the field map. **Bottom row:** Example fMRI after B0 unwarping. Regions most improved are circled in red.
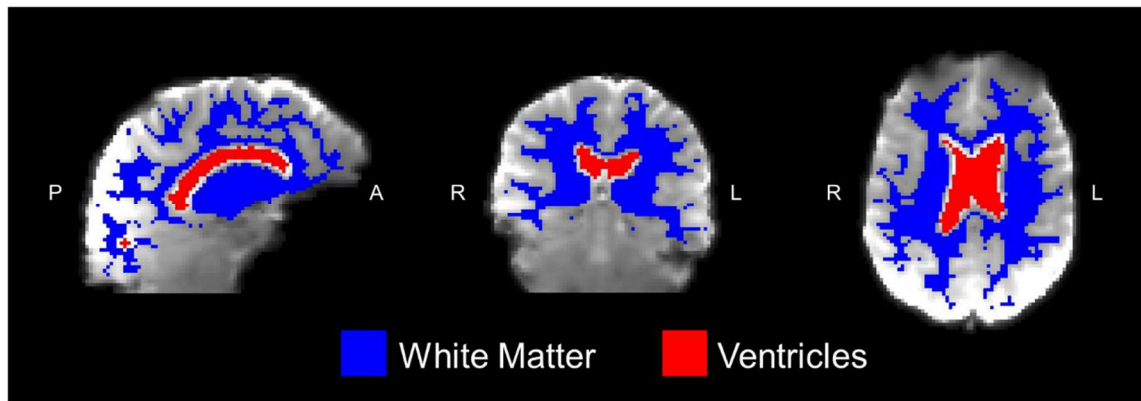
Figure 5.4. Example white matter and ventricle masks generated to remove noise from the functional data. The mean timeseries from each mask was calculated and included as a nuisance regressor to help improve the reliability of the signal.

Given our ROIs are generated on the surface, we projected the functional data volume onto the cortical surface as well, using bbregister to generate the appropriate registration file (Greve & Fischl, 2009).

5.3.5.4 Statistical Analysis

For each participant, the mean time series was extracted for each ROI (central V1, peripheral V1, face area and place area), hemisphere and for each condition (eyes open and eyes closed). 8 correlations were calculated for each participant in total - 4 correlations in each hemisphere. All correlations were transformed into Fisher's Z scores before running statistical analyses. Given our hypotheses concerned within eccentricity correlations and how they differ across group, only these were included in the statistical analysis.

5.4 Results

Recruitment for the study terminated early due to the global pandemic and having only recruited 4 individuals for the peripheral vision loss group, we decided not to include them in the statistical analysis. Here we report some of the descriptive statistics for each hemisphere in turn. One of our hypotheses was that we would see reductions in functional connectivity for specific within-eccentricity correlations in each patient group. For central loss patients, we expected to see the central V1 – face correlations to drop, whereas for peripheral loss patients, we expected to see a decline for the peripheral V1 – place correlations. While we acknowledge the lateralisation of face processing, seen repeatedly in the right hemisphere, there were no expectations concerning hemisphere for place

processing. Mean Fisher's Z scores and corresponding SEM are shown in Tables 5.1 and 5.2 for left and right hemispheres respectively.

In the left hemisphere, it appears that on average, our two patient groups are more similar, with sighted controls exhibiting higher Z scores compared to both patient groups for the central V1 – face correlations, with central loss patients showing the lowest values in the eyes open condition. For the peripheral V1 – place correlations, on average our peripheral loss group has higher Z scores compared to sighted controls, and similar to central loss in the eyes closed condition, but lower in the eyes open condition.

Table 5.1. Mean Fisher's Z scores for within eccentricity correlations, with SEM shown in brackets. Results for the *left* hemisphere for all participant groups, for both conditions (eyes closed and eyes open).

Left Hemisphere		Sighted Controls	Central Loss	Peripheral Loss
Central V1 – Face	Eyes Closed	0.412 (0.082)	0.370 (0.107)	0.391 (0.040)
	Eyes Open	0.473 (0.065)	0.280 (0.057)	0.377 (0.070)
Peripheral V1 – Place	Eyes Closed	0.526 (0.051)	0.538 (0.100)	0.532 (0.038)
	Eyes Open	0.372 (0.052)	0.559 (0.131)	0.466 (0.035)

For the right hemisphere, a similar pattern emerges with the two patient groups showing similar results for the central V1 – face correlations, with a lower average Z score compared to sighted controls. In the peripheral V1 – place correlations, we again see greater values for the central loss group, and while the peripheral loss group mean is higher than that of controls, it is important to note the larger SEM for both conditions in the peripheral loss group. Inferential statistical analyses are required to determine if any group differences in the descriptive statistics reported above are meaningful.

Table 5.2. Mean Fisher's Z scores for within eccentricity correlations, with SEM shown in brackets. Results for the *right* hemisphere for all participant groups, for both conditions (eyes closed and eyes open).

Right Hemisphere		Sighted Controls	Central Loss	Peripheral Loss
Central V1 – Face	Eyes Closed	0.231 (0.045)	0.103 (0.036)	0.133 (0.085)
	Eyes Open	0.421 (0.056)	0.155 (0.046)	0.083 (0.092)
Peripheral V1 – Place	Eyes Closed	0.180 (0.039)	0.307 (0.043)	0.240 (0.134)
	Eyes Open	0.410 (0.034)	0.445 (0.067)	0.435 (0.123)

In Table 5.3 we report the Z scores for each individual peripheral loss patient, calculated using the mean Fisher's Z scores and standard deviation for the sighted control group. We wanted to see if participants were indeed consistent. What we can see for both hemispheres is that the majority of the negative Z scores are reported for the central V1 - face correlations. This is interesting because our prediction was that we would observe this for the peripheral V1 - Place correlations instead. Possible reasons for this will be discussed later however, what we can see from Table 5.3 is that we do not have enough information to make any convincing conclusions, especially as RP4 seems to behave quite differently in the right hemisphere peripheral V1 - place correlations.

Table 5.3. Comparison of individual peripheral loss patients (labelled RP1-4) with the sighted control group data (mean fisher's Z score with standard deviation shown in brackets). Z scores of the Fisher's z transformed correlations were calculated to see how each individual peripheral loss patient compared. Greyed out boxes highlight negative z

			Z Scores			
Right Hemisphere		Sighted Controls	RP1	RP2	RP3	RP4
Central V1 – Face	Eyes Closed	0.231 (0.173)	-0.841	0.661	-0.101	-1.993
	Eyes Open	0.421 (0.217)	-1.852	-1.042	-0.550	-2.790
Peripheral V1 – Place	Eyes Closed	0.180 (0.150)	1.541	0.849	1.830	-2.624
	Eyes Open	0.410 (0.133)	1.093	0.082	2.310	-2.731
Left Hemisphere						
Central V1 – Face	Eyes Closed	0.412 (0.319)	-0.408	0.068	0.197	-0.287
	Eyes Open	0.473 (0.253)	-1.808	-1.093	-0.283	-0.782
Peripheral V1 – Place	Eyes Closed	0.526 (0.198)	1.352	0.328	1.045	1.095
	Eyes Open	0.372 (0.200)	1.296	1.018	1.982	1.322

We proceeded with a 2x2x2x2 mixed ANOVA to investigate effects of hemisphere (left vs right), condition (eyes open vs eyes closed), within eccentricity correlation (central V1 – face vs peripheral V1 – place) and group (sighted controls vs central loss). This highlighted a 4-way interaction between all of our factors listed above; $F(1,19) = 4.946$, $p=.038$, as well as an interaction between hemisphere and condition ($F(1,19) = 36.284$, $p<.001$) and main effects of hemisphere ($F(1,19) = 34.859$, $p<.001$) and condition ($F(1,19) = 4.493$, $p=.047$) as well. To investigate this further, we broke our analysis down into 4 separate 2x2 mixed ANOVAs to explore the results by hemisphere and condition separately. That way, we could determine if there were effects of within eccentricity correlation, or group for each condition and for each hemisphere. As mentioned previously, a functional lateralisation for face processing is also evident in the literature, whereby a bias for face processing is

consistently shown in the right hemisphere (Kanwisher et al., 1997; McCarthy et al., 1997), warranting the separate analysis for each hemisphere.

There were no significant main effects for **correlated ROI** or **group**, nor were there any interactions for either the eyes open (all p>.065) or eyes closed conditions (all p>.168) in the left hemisphere. For the right hemisphere, in the eyes closed condition we observed a **correlated ROI** x **group** interaction (F(1,19)=5.564, p=.029), but no main effect of either **group** or **correlated ROI** alone (both p>.174). For the eyes open condition in the right hemisphere, we observed a significant **correlated ROI** x **group** interaction again (F(1,19)=6.418, p=.020), a significant main effect of **correlated ROI** (F(1,19)=5.493, p=.030), but no significant main effect of **group** (F(1,19)=3.549, p=.078). Looking at Figure 5.5 and Table 5.2 , the interaction between **group** and **correlated ROI** shows central loss patients have lower overall Z scores in the central V1 – face correlation, whereas groups are similar for the peripheral V1 – place correlation, with central loss patients showing a slightly higher mean Z score. This applied to both the eyes open and eyes closed conditions with a greater difference in the peripheral V1 – place correlation in the eyes closed condition.
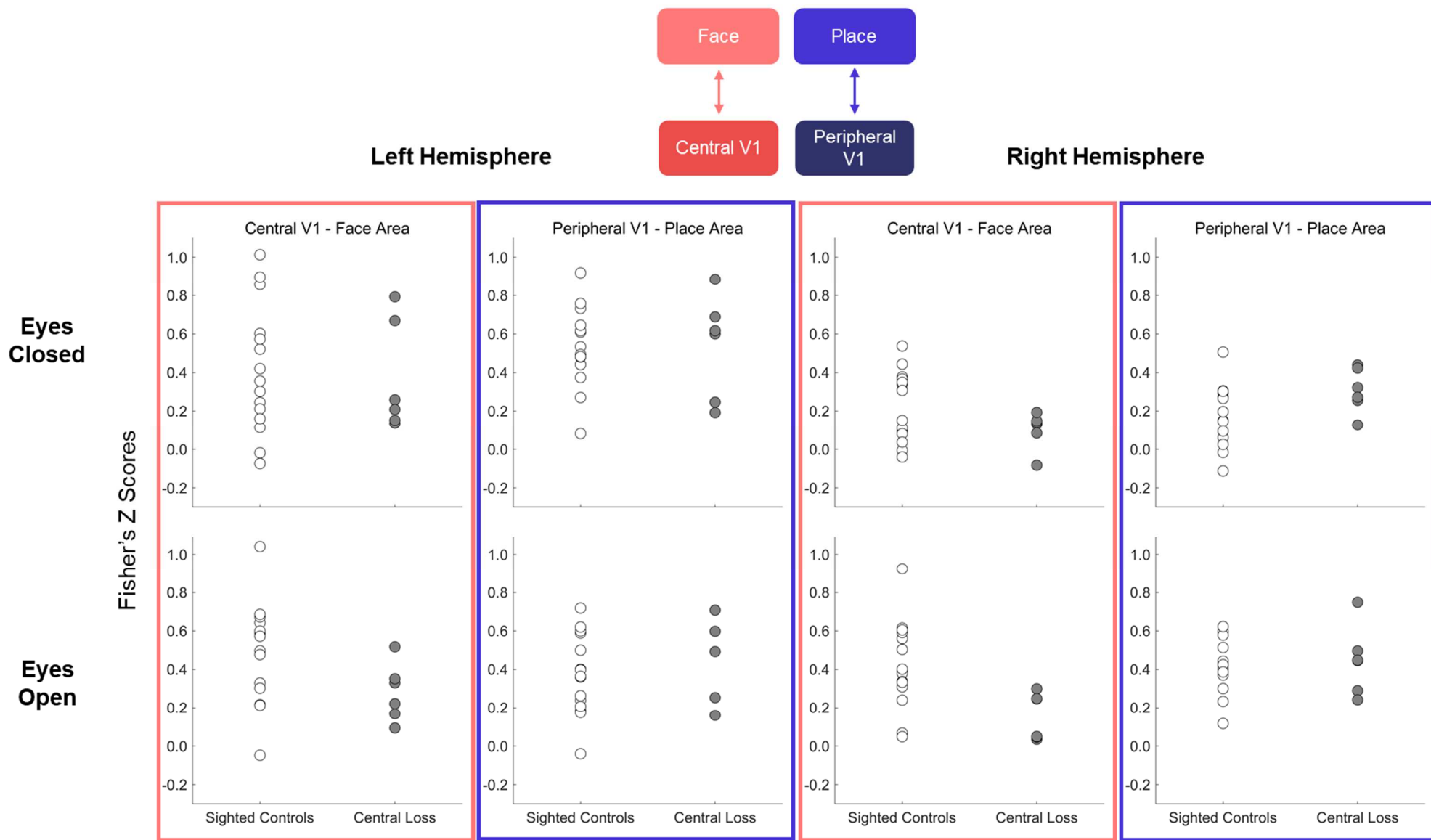
Figure 5.5. Correlations transformed into Fisher's Z scores. Each dot represents a single participant: white = sighted controls, grey = central loss. **Top row:** Results for the within eccentricity correlations for *Eyes Closed* condition. **Bottom row:** Results for within eccentricity correlations for *Eyes Open* condition. **Columns 1&2:** Results for left hemisphere. **Columns 3&4:** Results for right hemisphere.

5.5 Discussion

One of the aims for this study was to explore how selective visual field deficits impact on functional connectivity within visual cortex, by examining specific connections between areas with similar eccentricity biases. We predicted that those with central vision loss would show a deficit in functional connectivity between the central visual field representation in primary visual cortex (V1) and the atlas-based ROI capturing the foveal biased and face-selective region in the ventral visual pathway. We also predicted the corresponding Peripheral V1 and place-selective, peripheral biased region medial to the mid fusiform gyrus (MFS) would remain unaffected, since this represents the portion of the visual largely intact in this patient group. For the peripheral loss group, we expected to see the reverse, with the peripheral V1 – place connectivity being most affected, and central V1 – face connections remaining intact.

Kamps et al (2020) showed that functional connectivity seemed to precede visual experience in the developing brain, meaning that the connections between regions in visual cortex sharing the same eccentricity bias may be prewired. With this in mind, we have explored what happens to these well-established connections as a result of selective vision loss. For central vision loss at least, we have observed selective deficits in functional connectivity in the right hemisphere. The interaction observed between group and correlation was interesting; the central loss group showed a deficit in the central V1 – face area correlation as predicted, but for correlations between the peripheral V1 – place area, central loss patients were similar to the controls, and on average showed greater correlations. This supports findings from another resting state fMRI study which explored cortical entropy; greater cortical entropy was reported in a region named FG1 – situated medial to the MFS – in central loss patients compared to sighted controls (Sanda et al., 2018). This appears to overlap with peripheral biased representations described in our study and may be situated on or near our PPA ROI. Interestingly, this study seems to highlight possible compensation in the peripheral representations in the absence of central vision. Furthermore, both behavioural and neuroimaging literature suggest that scene processing is relatively well preserved in cases of age-related macular degeneration (AMD) (Peyrin et al., 2017; Tran et al., 2010) and the functional connectivity results seems to support this, further demonstrating that deficits are largely selective in visual cortex in cases of selective central vision loss. This also lends support to the structural literature and results from Chapter 2, showing a greater preservation of structure in the calcarine sulcus in later stages of the disease (rate of change closer to zero) – an anatomical ROI

capturing representation of the peripheral visual field – in individuals with macular disease (MD). In terms of compensation, continuing recruitment for this study would allow us to determine if patients show significantly greater functional connectivity between peripheral biased regions over time.

Unfortunately, due to unforeseen circumstances recruitment was terminated early limiting the number of patients in the peripheral loss group. In turn this made inferential statistical analyses largely irrelevant. It would be interesting to explore this hypothesis for a selective deficit further with a larger group of peripheral loss patients and determine if the reverse of what we observed in the central loss group could be observed, whereby peripheral V1 – place area correlations would be most affected in the peripheral loss group.

Whilst we only can comment on the descriptive statistics of a small cohort, it is interesting to see that the central and peripheral loss groups were fairly similar in the central V1 – face area correlations and although central loss patients showed the greatest deficit, the peripheral loss group had, on average, lower correlations compared to sighted controls. If this result were to be observed on a much larger scale study, it could be explained by the fact peripheral loss patients had retinitis pigmentosa (RP) which while largely affects peripheral vision, in the much more advanced stages of the disease, this can impact on central vision too (Ferreira et al., 2017). Behavioural work has shown that even in patients with glaucoma, face processing is affected, despite preserved central vision (Friedman et al., 1999; Glen et al., 2012; Roux-Sibilon et al., 2018). In addition to behavioural deficits, a recent fMRI study exploring functional properties of V1 in advanced cases of RP highlighted a possible remapping of visual field representations in V1, whereby regions formally representing peripheral visual fields took on the role of processing remaining central vision (Ferreira et al., 2017). This finding has implications for the functional connectivity we are exploring in the current study; if this remapping has indeed occurred in some or all our participants, we may not see the expected deficit in peripheral V1 – place correlations. Assessing individuals with RP at different stages of the disease may help to tease apart when and if remapping of V1 is occurring, and in turn how this may impact on the functional connections we are investigating here.

Previous work has also highlighted some interesting changes to connectivity within visual cortex that we have not explored for this study; another region of interest was the lateral occipital cortex (LOC) which is implicated in object and shape processing and is thought to have a more foveal bias. Whilst using slightly different methods for defining ROIs (external

functional localisers), similar findings emerged whereby more peripheral based representations in early visual cortex (not restricted to V1), showed greater connectivity with LOC in individuals with central vision loss as a result of Stargardt's disease (Sabbah et al., 2017). Similarly, Sanda et al., (2018) found that central loss patients showed an increase in cortical entropy in area hOc4la (using probabilistic cytoarchitectonic maps – this is thought to correspond with the functionally defined regions LO2) compared to sighted controls. This suggests an increase in the synaptic complexity points in a region also associated with object and shape processing. Again, authors collectively suggest this could be a compensatory increase as a result of selective vision loss, increasing connectivity to maintain effective processing of objects and shapes.

Determining how much resting state fMRI is affected by participant viewing conditions in partially sighted populations, as well as sighted controls was our second aim. The literature suggests asking participants to keep their eyes open is generally optimal, but this is in sighted populations (Patriat et al., 2013). Given potential fixation instability in partially sighted groups, for our 'Eyes Open' condition, we presented a large fixation cross occupying the full width and height of the screen to give participants a greater chance of finding something to fixate on. We predicted therefore that the biggest difference would emerge in our central loss group, since unstable viewing can lead to spontaneous activation, particularly in the visual network. Our results were very similar across eyes open and eyes closed conditions however, so in this particular cohort, it did not have a large effect. Despite little change, in order to guarantee spontaneous fluctuations are avoided, it seems opting to have participant's eyes closed is the best choice. Other studies exploring resting state fMRI in partially or completely blind individuals (with a sighted control group) do often report having eyes closed and sometimes blindfold participants to reduce any light perception (Aguirre et al., 2017; Dai et al., 2013; Sanda et al., 2018).

One issue in the way we recruited our participants was the fact we relied on volunteers to give us details of their visual impairment. An objective measure of the extent of the vision loss in both groups would have been ideal, acquired through visual field tests (perimetry or microperimetry). This could then guide our ROI selection and help refine it further. Having said this, Sabbah et al., (2017) also opted for a more general approach when selecting ROIs; their representations of early visual cortex were not restricted to V1, whereas ours were. For this study, we recruited participants through charities and sight loss support groups as opposed to through the NHS; given the time frame of the study and time needed to invest in NHS ethical approval, we opted to go down the volunteer route, since we had

very good connections with local organisations. Volunteers were asked about their diagnosis upon expressing interest in the study. While this is not the most desirable way of grouping our participants, it was the best solution during what became a short recruitment window. Going forward, any further work should include assessments of visual function to objectively measure the extent of vision loss in both groups and refine our V1 ROI definition.

In the absence of functional localiser scans, atlases such as the HCP-MMP1.0 provide an opportunity for researchers to examine functional properties in ROIs that can be generated easily in all participants, simply relying on a FreeSurfer output directory. The multi-modal approach to creating this atlas has highlighted a remarkably consistent organisation in the functional representations of faces and places relative to the mid fusiform sulcus (MFS) is therefore meaningful and reliable (Glasser et al., 2016); the surface ROI for the PPA generated by Grill-Spector's lab seemed to be aligned consistently with the collateral sulcus and medial to the MFS in all participants, and follow the cortical folding as predicted (Weiner et al., 2018). When time or funding is an issue and functional localisers are not possible, atlases prove to be an excellent resource.

In addition to highlighting any pathological changes in the function of visual cortex associated with vision loss, resting state fMRI may also help us to understand why some patients go on to develop Charles Bonnet Syndrome (CBS), and why some do not. CBS is characterised by the experience of visual hallucinations in individuals with visual impairment. It affects people with various forms of vision loss, both central and peripheral, and occurs in the absence of any psychological illness (Santhouse, Howard, & Ffytche, 2000). Approximately 50% of the visually impaired population experience hallucinations at some point in their lives, and experiences of it vary. For some, visual percepts are simple lines, patterns or geometric shapes of varying colours, while for others it can be more disturbing, featuring distorted and disembodied faces or figures in elaborate costumes (Santhouse et al., 2000). Alarmingly few people are aware of the condition, but once patients learn that what they are seeing is not real, the experience becomes significantly less distressing (Cox & Ffytche, 2014). Previous fMRI studies have shown that during active hallucinations, an increase in spontaneous activity is observed along the ventral visual stream; the content of the hallucinations determined which specific region showed a spike in percent signal change, for example perceiving colour elicited activation in area V4, whilst perceiving faces would elicit activity in the middle fusiform gyrus, in or around the FFA (Ffytche et al., 1998). As well as examining increases in the BOLD response across

visual cortex, further work examining the functional connectivity within visual cortex in those who do and those who do not experience CBS is important. In a recent study, a single case of CBS was compared against a group of sighted controls as well as late-blind subjects who did not report experiencing CBS; findings suggested changes in functional connectivity in the CBS patient, even when they were not actively hallucinating (Martial et al., 2019). Interestingly, the networks showing an increase in connectivity in the CBS patient compared to controls actually revealed a decrease in connectivity in the late-blind subjects; authors suggest this may link CBS to hyperactivity in the posterior visual pathway (Martial et al., 2019). Following how changes in function as well as structure link with CBS symptoms over time may help answer how and why some patients are affected by the condition.

The advent of resting state fMRI has allowed for greater exploration of visual cortex in individuals with partial or complete vision loss (Nir, Hasson, Levy, Yeshurun, & Malach, 2006). Assessing both the structure and function (both task based and resting state) of visual cortex in various forms of vision loss is important to understand how and when changes occur, which in turn will aid the efforts of visual restoration. It also provides another tool to help understand the relationship between structure and function in the posterior visual pathway; for example, whilst it is understood that the underlying architecture and retinotopic organisation in visual cortex remains intact even in cases of congenital vision loss, it does not mean that if vision were to be restored, that normal vision would be possible. Visual cortex has also elicited responses to other sensory modalities in congenitally blind cases, and so we do not know how visual cortex would respond if vision were restored. Similarly, CBS is another important consideration as described above, and understanding how it manifests may help to find ways of alleviating the symptoms, or at least manage them. Understanding why in some cases the condition resolves itself is also important. Finally, the differences observed in task based as well as resting state fMRI suggest functional properties are indeed altered in the absence of visual experience as well as in acquired or late-stage vision loss. The importance of understanding how and if reorganisation of visual function occurs in acquired vision loss will be discussed further in Chapter 6.

Chapter 6: Assessing functional reorganization in visual cortex with simulated retinal lesions

6.1 Abstract

Macular degeneration (MD) causes central vision loss, removing input to corresponding representations in the primary visual cortex. There is disagreement concerning whether the cortical regions deprived of input can remain responsive, and the source of reported cortical responses is still debated. To simulate MD, normally sighted participants viewed a bright central disk to adapt the retina, creating a transient 'retinal lesion' during a functional MRI experiment. Participants viewed blocks of faces, scrambled faces, and uniform grey stimuli, either passively or whilst performing a one-back task. To assess the impact of the simulated lesion, participants repeated the paradigm using a more conventional mean luminance simulated scotoma without adaptation. Our results suggest our attempt to create a more realistic simulation of a lesion did not impact on responses in the representation of the simulated lesion. While most participants showed no evidence of stimulus-driven activation within the lesion representation, a few individuals (22%) exhibited responses similar to a participant with juvenile MD who completed the same paradigm (without adaptation). Reliability analysis showed that responses in the representation of the lesion were generally consistent irrespective of whether positive or negative. We provide some evidence that peripheral visual stimulation can also produce responses in central representations in normally sighted participants while performing a task. This suggests that the 'signature of reorganization of visual processing', is not found solely in patients with retinal lesions, consistent with the idea that activity may be driven by unmasked top-down feedback.

6.2 Introduction

Macular degeneration (MD) is a progressive eye disease which causes the loss of vision in the central part of the visual field. Following degeneration of the retina, the corresponding representations in primary visual cortex (V1) are deprived of input. This has led to a number of studies exploring whether the region deprived of cortical input, known as the 'lesion projection zone' (LPZ), might reorganise and take on a new role, processing inputs from intact retina (Baker et al., 2008, 2005; Baseler et al., 2011; Dilks et al., 2009; Hoffmann, Tolhurst, Moore, & Morland, 2003; Sunness et al., 2004)(C. I. Baker et al., 2008, 2005; Baseler et al., 2011; Dilks et al., 2009; Hoffmann et al., 2003; Sunness et al., 2004). Determining the source of any LPZ responses is important; if there is evidence of remapping, or a more permanent reorganization of visual processing, this could interfere with the success of visual restoration (Baseler et al., 2011; Morland, 2015). Successful visual perception can only occur if the parts of the visual brain which previously processed input from the macula remain available, and capable of processing new incoming information. However, there is debate concerning the state of visual cortex following visual loss, primarily within the LPZ (for a review, see: Brown et al., 2016). The inconsistency within the literature is partly attributed to differences in how cortical reorganization is defined, but also by what mechanism it occurs (Morland, 2015). Reorganization can refer to structural changes occurring in the brain following acquired or congenital eye disease, but more frequently, it refers to functional changes, whereby patterns of neural activation differ from those observed in healthy individuals. For this study, reorganization refers to patterns of activity within the LPZ that cannot be explained by (a) known properties of the visual system and (b) the absence of visual input (Engel, Morland, & Haak, 2015; Morland, 2015).

Irrespective of the way in which reorganization is defined, there is also considerable variation in the proportion of patients that exhibit fMRI responses in the LPZ; estimates vary from zero to approximately 50% (Morland, 2015). Given this variability, we sought to determine whether this property is unique to patients, or whether similar response variability can also be found in a sample of individual sighted participants using a simulated LPZ.

A common approach to determining if reorganization occurs is to measure responses in the LPZ. In cases of congenital visual loss, e.g. rod achromats who have a small central scotoma from birth, there is evidence of remapping of visual inputs (Baseler et al., 2002). In cases of acquired vision loss, the results are mixed. Positive responses in the LPZ to

stimuli presented to intact peripheral visual field are frequently taken as a signature of reorganization of visual processing in MD (Baker et al., 2008, 2005). However, the mechanism underlying LPZ responses remains unknown. Furthermore, some studies report an absence of any positive responses in the LPZ, suggesting cortical reorganization does not occur in MD (Baseler et al., 2011; Smirnakis et al., 2005; Sunness et al., 2004).

One interpretation is that the LPZ starts to process information from the intact peripheral visual field not previously represented by this region of cortex (Baker et al., 2008, 2005; Dilks et al., 2009, 2014). An alternative view is that the signals observed in the LPZ reflect normal feedback to V1 from extrastriate areas, unmasked in partially blind individuals when engaged in a task (Masuda et al., 2008, 2010). Further evidence for the role of feedback mechanisms is provided in sighted individuals; when naturalistic scenes are partially occluded, stimulus-related information can be decoded in the unstimulated visual cortex which represents the occluded visual field (Petro, Vizioli, & Muckli, 2014; Smith & Muckli, 2010; Williams et al., 2008). It appears therefore that even in normally sighted participants, there is evidence of feedback in fMRI signals, although they are revealed in a consistent pattern of responses across voxels, rather than in a univariate increase in mean signal as found in patients.

Given that evidence of feedback to V1 can be found in sighted participants we asked whether it could be unmasked in univariate responses in V1. To answer this question, we used a more realistic simulation of a retinal lesion in normally sighted participants and measured their responses in V1's representation of the simulated lesion, the 'sLPZ'. Masuda and colleagues (2008) speculated that the sLPZ signals are not observed in sighted participants because retinal aftereffects signalled the presence of a uniform grey region, the 'simulated lesion'. Therefore, we simulated the loss of central vision physiologically, not by manipulating the viewed images, but instead by temporarily (and reversibly) compromising photoreceptor function in the macula in normally sighted individuals. We had participants adapt to a bright white disk, saturating signals from the eye and ensuring the simulated 'lesion' was in retinal coordinates, irrespective of eye movements. We reasoned that by making visual stimuli that were presented in the periphery also undetectable in the adapted region, we might unmask influences of cortical feedback on the mean signal measured in this simulated sLPZ. We hypothesised that under conditions of bright light adaptation of the macular, we would detect signals in the sLPZ, which would be absent when normally sighted participants viewed stimuli without prior adaptation. We also compared signals in the sLPZ during stimulus-related task and

passive viewing conditions, predicting that signals would be more likely to emerge under the stimulus-related task condition as found previously in patients (Masuda et al., 2008).

Finally, we asked whether responses in the sLPZ (sighted participants) and LPZ (patient) were consistent within individuals, or simply spurious or due to random chance. To do this we repeated our fMRI acquisitions for each condition, and for each participant assessed the average univariate response and its reliability across repeated acquisitions. These data allowed us to gauge whether the responses we obtained from a patient with longstanding loss of macula vision were similar in scale and reliability to those we obtained from sighted participants.

6.3 Methods

6.3.1 Participants
Eleven participants were recruited for the current study; 10 normally sighted participants (4 males; ages 23 – 37, average age = 26.8 years) and one participant with Juvenile Macular Degeneration (Referred to as JMD throughout, male, aged 40 years). JMD was diagnosed with Stargardt's disease, an inherited progressive disease, at 17 years old. JMD has bilateral absolute central scotomata (approximately 18 x 20 degrees of visual angle) and uses a preferred retinal locus (PRL) in the lower left visual field (fixating using an upper right retinal location at the edge of the scotoma). A visual representation of the scotoma, PRL and location of the stimulus is shown in Figure 6.1A. All participants participated in fMRI experiments, but JMD also completed an additional behavioural experiment and visual assessments at York Teaching Hospital. Written consent was obtained for all participants and the study was approved by the York Neuroimaging Centre ethics committee in accordance with the Declaration of Helsinki.

6.3.2 Imaging Parameters
Scanning was performed at the University of York Neuroimaging Centre using a GE 3 Tesla HDx Excite MRI scanner.

6.3.2.1 Structural MRI
One high-resolution 3D T1-weighted, Fast Spoiled Gradient Echo pulse sequence (FSPGR) anatomical image was acquired (TR = 7.8ms, TE = 2.9ms, TI = 450ms, voxel size = 1.13 x 1.13 x 1mm^3, flip angle = 20°, matrix size 256 x 256 x 176, FOV = 290mm) using the 8-channel whole head High Resolution Brain Array coil. Three T1-weighted anatomical images were acquired for each participant (TR = 7.8ms, TE = 3.0ms, TI = 600ms, voxel size = 1x1x1mm^3, flip angle = 12°, matrix size 256 x 256 x 176, FOV =

256mm) using a 16-channel Posterior Brain Array coil. One T2*-weighted fast gradient recalled echo scan was acquired (TR = 400ms, TE = 4.3ms, voxel size = 1 x 1 x 2mm^3, flip angle = 25°, matrix size 128 x 128, FOV = 260mm) using the 16-channel coil. Finally, an axial proton density scan was also acquired during the functional MRI experimental session using the 16-channel coil and the same slice prescription to aid alignment between functional and high-resolution structural data (TR = 2700ms, TE = 34.84ms, voxel size = 1 x 1 x 2mm, flip angle = 90°, matrix size 192 x 192 x 39, FOV = 192mm).

6.3.2.2 Functional MRI

All functional data were acquired on the 16-channel coil to improve the signal-to-noise in the occipital lobe. TR = 3000ms, TE = 30ms, voxel size = 2 x 2 x 2mm^3, flip angle = 90°, matrix size 96 x 96 x 39, FOV = 192mm. Data were acquired using a slice prescription with coverage including occipital and temporal lobes.

6.3.3 Stimulus generation

Stimuli were presented using a ProPixx LED projector (VPixx Technologies, Saint-Bruno, CA) and were rear-projected onto a textured screen in the bore of the MRI scanner, which could be viewed on the screen via a mirror attached to the head coil. To monitor participants' fixation stability, we used an eye tracker to record a video of the eye, allowing us to monitor eye movements in real time throughout the experiment (https://www.crsltd.com/tools-for-functional-imaging/mr-safe-eye-tracking-for-fmri/livetrack-fmri/).

PNG images of faces were processed in MATLAB (Mathworks). First, all images were converted to greyscale with flattened histograms, to control greyscale ranges across images. Following this, the mean luminance value of each image was set to 705cdm^{-2} so that they would be undetectable in regions of the retina that were adapted to bright light of ~15000cdm^{-2}. All images were rescaled to take up 50% of a 400 x 400-pixel size stimulus. Finally, all images were placed on a dark grey background matching mean luminance of the images.

To scramble the faces, each image was divided into a 20 x 20 square grid and each square was randomly shuffled through +/-90deg or 180deg. Finally, we applied a slight blurring to the intact and the scrambled images with a Gaussian filter (SD = 1px) to soften the lines created when scrambled.

6.3.3.1 JMD behavioural test

We devised a short behavioural experiment to confirm the location of JMD's PRL. Stimuli (mean size was ~7 x 9° of visual angle) comprised greyscale faces, scrambled faces, objects, and control trials containing no stimuli. Stimuli were presented for 800ms, appearing in any quadrant of the visual field, or in the centre of the screen. JMD was given an auditory cue when a stimulus was presented and was asked the following: (1) Did you see anything? (2) If yes, where was the stimulus? (3) Can you describe what the stimulus was? There were 40 trials (10 for each stimulus condition).

6.3.3.2 High light level adaptation experiment

Red fixation lines were centred vertically and horizontally, occupying 20 degrees of visual angle, to aid central fixation in the absence of an explicit central fixation marker (Figure 6.1B). During the 'adaptation' period, a white disk (12deg diameter, $15000cdm^{-2}$) was overlaid on the fixation lines. Previous work allowed us to estimate the level needed and to justify safe recovery after bleaching and $15000cdm^{-2}$ was the maximum we could achieve with the MRI projector and screen (Czeh, Casper, & Segraves, 1965; Stockman & Sharpe, 2006). In control blocks, the circle changed to uniform dark grey (mean luminance: $705cdm^{-2}$) to match the background. For all functional runs, the size of the adaptation circle, red fixation lines, and position of the stimulus remained the same. The size of individual face and scrambled stimuli varied slightly; the mean size was ~7 x 9° of visual angle. Images were positioned 10° of visual angle from the centre of the screen to the centre of the image. For sighted participants, stimuli were presented in the upper right quadrant of the visual field, abutting the edge of the adapted circle (Figure 6.1B). For JMD, they were presented in the lower left quadrant, corresponding with the PRL. Position differed due to JMD being recruited after the control participants.

6.3.3.3 Retinotopic Mapping

The travelling-wave method was used to acquire retinotopic maps to locate V1 in control participants (Engel, Glover, & Wandell, 1997). Stimuli were presented binocularly and consisted of high contrast (>98%, mean luminance = $400cdm^{-2}$) expanding checkerboard rings and 90° wedges rotating anti-clockwise. All checkerboards reversed at a rate of 6Hz. Stimuli were presented on a grey background (200cdm-2) with a red central fixation cross, traversing a circular region of radius 14.34deg. Each cycle lasted 36 seconds, with 8 cycles per run (Vernon, Morland, Wade, Lawrence, & Gouws, 2016).

6.3.3.4 LPZ and stimulus localiser

For sighted participants, a central radial checkerboard (12deg diameter, reversal rate = 6 Hz) was presented for 12 seconds, followed by a peripheral checkerboard annulus (radius extending from 6deg to 15deg radius) also presented for 12 seconds (Figure 6.1C, upper panel). This cycle was repeated 8 times to localise the representation of the simulated lesion. Using a similar paradigm, we used checkerboard stimuli to localise the region representing the stimulus (Figure 6.1C, lower panel). We isolated the region where the stimuli were presented (upper right quadrant) and alternated between a flickering checkerboard occupying this region and the surrounding region. For JMD, the same paradigm was used, however instead of a central radial checkerboard, a full field checkerboard alternated with uniform grey (mean luminance = 200cdm^{-2}). For all participants, stimuli were presented monocularly to the dominant eye only. Dominant eye was determined by having participants point to a corner of a room, then close each eye in turn and state during which interval their finger was closest to the corner.

6.3.4 Experimental design

Control participants completed three scanning sessions: one structural and two functional sessions, which included sLPZ/stimulus localiser scans and main functional scans (one with and one without the 'adaptation' disk). JMD completed two sessions: one structural and one functional session including LPZ localiser and main functional experiment without adaptation.

6.3.4.1 MRI protocol for lesion simulations and control conditions

All functional scans were completed under monocular viewing conditions, testing the dominant eye only. For each experiment (adaptation and no adaptation), all participants completed four functional runs; two passive viewing and two runs during which participants completed a one-back task. For the one-back tasks, participants were instructed to press a button when an image matched the previous one. For experiment 1, which included the 'adaptation' disk, each of the 4 functional runs were preceded by a 180 second adaptation period, followed by 12 stimulus blocks (4 blocks of each stimulus category: faces, scrambled faces and uniform grey control blocks, block duration = 6 seconds) interleaved with 11 top up adaptation blocks (18 seconds). See Figure 6.1B for further details. Stimulus blocks were presented in a pseudorandom order whereby each functional run had blocks presented in a different order, but the same four order sequences were presented to each participant. Six stimuli were presented per block (presented for 800ms, with 200ms inter-stimulus interval (ISI)). 18 seconds (uniform grey) were added at the end

of the scan to allow us to capture the full hemodynamic response to the last stimulus. Participants were instructed to fixate centrally, where they perceived the red fixation lines to intersect. For experiment 2, the same procedures were used, but the initial adaptation period was reduced to 18 seconds and the white central disk was changed to uniform grey. This experiment served as a control condition, replicating the conventional simulated lesions used in previous research (Baker et al., 2008, 2005; Baseler et al., 2011; Masuda et al., 2008) to contrast with our new approach that attempted to simulate a retinal lesion with adaptation. Top-up adaptation intervals were replaced with a uniform grey disk to keep the timings of the functional runs consistent with experiment 1.

JMD also completed 4 functional runs consistent with experiment 2, the 'no adaptation' paradigm. Given JMD has a PRL in the lower left visual field, the stimuli were positioned in the lower left quadrant. The red fixation lines were expanded to be the full width/height of the screen to guide fixation and help JMD position their eyes centrally on the screen.
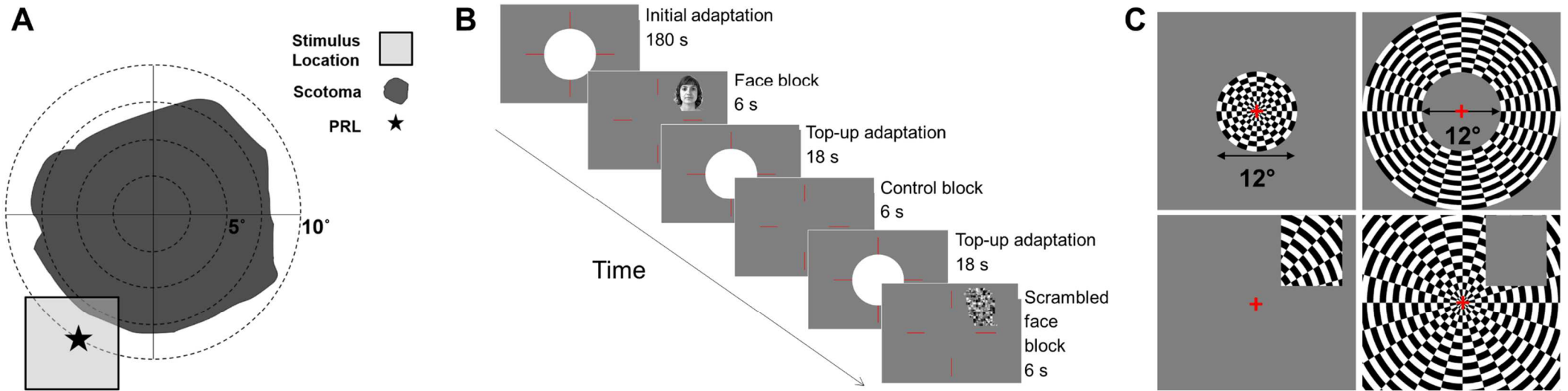
Figure 6.1. A: Schematic of JMD's central scotoma in the right eye. Preferred retinal locus (PRL) located in the lower left visual field, so stimuli were positioned here. The patient's scotoma was absolute, meaning no stimulus could be detected within the defined region. Only the right eye was tested in the functional MRI experiment. **B**: Schematic of main functional experiment (controls). Each run began with 180 second adaptation period; participants fixated centrally, using the red lines as a guide. 12 test blocks (6 seconds, comprising of either faces, scrambled faces or uniform grey) were presented, interleaved with top-up adaptation blocks (18seconds) to ensure adaptation was maintained. Each stimulus (faces or scrambled faces) were presented in the upper right quadrant of the visual field for 800ms, ISI of 200ms. For the first 2 runs, participants passively viewed the stimuli. For the last 2 runs, participants completed a one-back task. Participants were given a response box and were asked to indicate when an image was repeated by pressing a button. Each functional run lasted 7minutes 48seconds. For illustrative purposes, the RGB values are not the same as used in the experiment as images were too dark and very low contrast. **C**: Illustration of the sLPZ localiser (for controls only) and the stimulus localiser (for controls only).

6.3.5 Analysis
6.3.5.1 Anatomical data

Three high resolution T1 isotropic images were aligned and then averaged. This average was then divided by the T2* weighted data to correct for the gradient inhomogeneity caused by the 16-channel half head coil, and to improve the grey-white contrast. FreeSurfer software (http://surfer.nmr.mgh.harvard.edu/) was used to perform automatic segmentation of the averaged haem-corrected T1 scan. All automated segmentations were checked for quality and correctness and manual corrections were then performed where necessary to remove handles and bridges and fix poorly segmented white matter, using itkGrey software (https://web.stanford.edu/group/vista/cgi-bin/wiki/index.php/ItkGrey).

6.3.5.2 Retinotopic mapping:

For our sighted participants, we used the standard travelling wave method to analyse data using mrVista (http://web.stanford.edu/group/vista/cgi-bin/wiki/index/php/MrVista, Engel et al., 1997; Wandell, Dumoulin, & Brewer, 2007). The first 3 volumes were removed to minimize the effects of magnetic saturation. Between- and within-scan motion correction was applied. Data were aligned to the high-resolution T1-weighted image, and to reduce noise we averaged across wedge scans and across ring scans (Vernon et al., 2016). An 8-cycle sine wave was applied to each voxel in turn; the phase with the best fit was assigned to each voxel. Retinotopic maps were viewed on inflated cortical surfaces which were constrained to grey matter. The region of interest (ROI) V1 was manually drawn on the partially inflated cortical surfaces derived from the grey/white brain segmentation created using 'mrMesh' (part of the mrVista software package). ROIs were drawn using mrVista, using phase reversals to identify boundaries.

6.3.5.3 LPZ localiser Analysis

Individual participant fMRI data were analysed using FEAT (FMRI Expert Analysis Tool v4.1; Worsley, 2001). The first 3 volumes were removed, the high-pass filter cut-off point was 100sec (correcting for low frequency drift), FILM prewhitening and spatial smoothing (Gaussian kernel with 5mm FWHM spatial smoothing) were used, and motion was corrected for (motion parameters were also entered as confound covariates). Stimuli were entered as an explanatory variable, convolved with a gamma hemodynamic response function (HRF), and contrasts were run to compare stimuli to baseline. This allowed us to isolate responses to the central 12degree stimulus, and the surrounding annulus. We also included blink event files (derived from eye tracker data) as additional confound variables

as they can be an additional source of noise (Gouws et al., 2014). Data were cluster corrected (Z>2.3, *p*<0.05) and were registered to the high-resolution structural space, using the axial proton density scan to aid alignments.

6.3.5.4 High light level adaptation experiment analysis

Upon initial analysis we identified artefacts in some participants (including JMD) around the sagittal sinus and took additional measures to remove them and applied these steps to all participants. Functional data were first motion corrected. We then took the cumulative sum of absolute differences (CSAD) across volumes within a functional run in each participant. We then converted these values to Z scores. We reasoned that as fluid flow within the sagittal sinus would elicit rapid changes across volumes leading to larger CSAD values, any voxels with a CSAD value greater than 3 standard deviations should be excluded (de Zwart et al., 2005; Olman, Inati, & Heeger, 2007).

The remaining first level analyses were the same as for the LPZ localiser. The first 60 volumes from the adaptation runs were removed as this constituted the initial adaptation period. For experiment 2 (no-adaptation condition), the first 6 volumes were removed. We used spatial smoothing (Gaussian kernel with 4mm FWHM spatial smoothing) for both experiments. All three stimulus conditions were entered as separate explanatory variables (EVs), convolved with a double-gamma HRF, and two contrasts were run: faces versus control blocks, scrambled faces versus control blocks. This allowed us to isolate any possible effects of stimuli. Individual participant data were entered into a higher-level group analysis. The two task runs were combined, as were two passive runs for each participant using fixed-effects analysis with cluster correction (Z>2.3, p<.050).

6.3.5.5 ROI Analysis

V1 ROIs for all control participants were restricted to central and peripheral representations, using LPZ localiser data. Each participant therefore had an sLPZ ROI and surround (not used in subsequent analyses) in the hemisphere contralateral to the visual field where stimuli were presented. We also had a stimulus representation ROI for each control participant, derived in a similar manner using the stimulus localiser (see Figure 6.1, lower panel in part C). Due to the poor quality LPZ localiser data, we drew anatomical ROIs for JMD on the surface - one for the LPZ, and the other the remaining V1 (including stimulated and unstimulated peripheral representations). All ROI analysis was performed at the individual level using FSL's FEATquery. This was applied to the COPE (contrast of parameter estimates) statistics for each stimulus type, and subsequently converted into

mean percent signal change. This gave us a measure of mean response to each stimulus type and task condition in each ROI.

6.3.5.6 Data Visualisation

For each participant, a partially inflated surface derived from the grey/white brain segmentation was created using 'mrMesh' (part of the mrVista software package), and functional data (thresholded zstat images from FSL) were imported as parameter maps into mrVista to view on the inflated surface with ROIs.

6.3.5.7 Reliability Analysis

To interrogate the reliability of responses across functional runs for each viewing condition, multivoxel pattern analysis was used to characterise the pattern of responses across voxels within the LPZ, which were then correlated across two runs using Pearson's R. Values were subsequently converted into Fisher Z scores to ensure data were normally distributed. Each participant had four reliability scores: Faces with task, faces with passive viewing, scrambled faces with task, scrambled faces with passive viewing.

6.3.5.8 Classifier Analysis

We used the two measures from our fMRI data, response amplitude and the reliability of the response, to classify responses into two categories - those associated with the unstimulated LPZ or the stimulus representation. We applied linear discriminant analysis with leave one out cross-validation to train the classifier on adaptation and no-adaptation control data separately. Once the classifier had been trained on all of the control data, we applied it to JMD's data to establish whether the responses from his LPZ were best categorized as those originating from the LPZ or stimulus representation; exploring whether signals in JMD's LPZ were stimulus-driven or not.

6.4 Results

6.4.1 Individual LPZ BOLD responses

Given that stimuli were presented monocularly and appeared in one hemifield (right for sighted participants, left for JMD), we only report data from the left hemisphere in sighted participants, and the right hemisphere in JMD. This approach is consistent with that used by other researchers (Baker et al., 2005). In Figure 6.2 we provide thresholded statistical maps illustrating responses in the LPZ in JMD and three representative sighted participants, to highlight the variability in response patterns across individuals. When completing a task, JMD exhibited an increase in LPZ responses particularly when viewing faces (Figure 6.2). Whilst a slight increase is also observed when completing a task with scrambled faces, this effect was not as strong. JMD clearly shows a marked increase in BOLD in percent signal change within the LPZ in both experiments, typically taken as a signature of reorganisation of function. Sighted participant 1 behaves in a similar manner to JMD, exhibiting a task-related response to faces (z>2.3, p<.05). Sighted
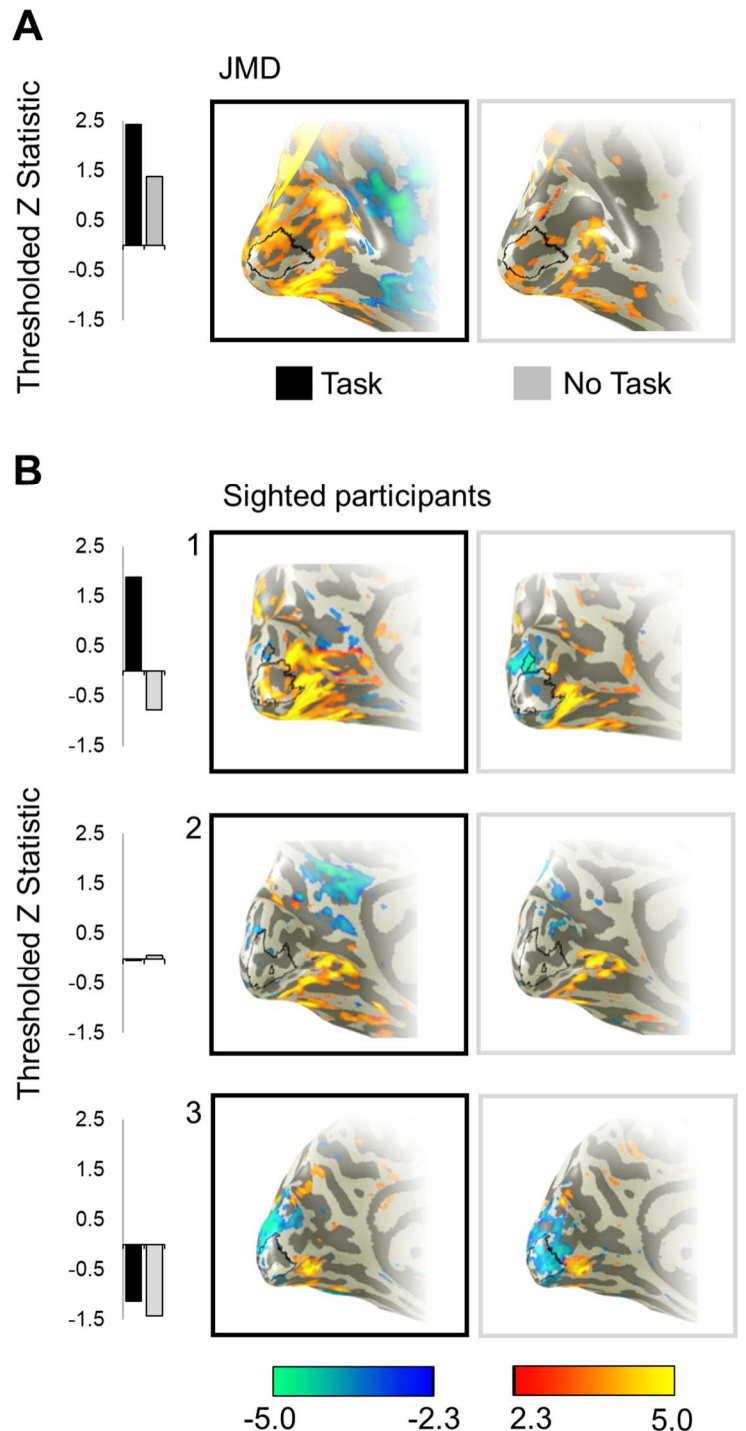
Figure 6.2. Examples of univariate responses to face stimuli on the inflated cortical surface for JMD (**A**) and 3 sighted participants (**B**) under two viewing conditions: task, no task. JMD data presented are from the right hemisphere and have been flipped for visualisation purposes. Data presented were obtained during adaptation (Sighted 2 and 3) and no adaptation (JMD and sighted 1). Data presented were obtained when sighted participants adapted to a bright light over the macula. Bar graphs illustrate thresholded z statistics to faces under task (black bars) and passive viewing (grey bars) conditions. LPZ (black line) is at the occipital pole.

participant 2 shows no marked increase or decrease in LPZ responses across all stimulus and task conditions. Finally, sighted participant 3 shows a large amount of negative BOLD for all stimulus and task conditions in terms of amplitude.

As patient studies focus on individual data, we plotted the percent signal change for each individual participant (coloured dots in Figure 6.3) for both adaptation and no adaptation experiments. Data for the sighted participants show that all individuals exhibit positive univariate responses in the cortical representation of the stimulus (irrespective of whether the stimuli were intact or scrambled faces – Figure 6.3 A&D). There is also a hint that a stimulus-related task may enhance these stimulus-driven responses (shaded bars are greater than open bars in three of the four conditions). The individual sighted participant responses from the sLPZ are distributed around a mean that is close to zero in all conditions. However, there are individuals that exhibited relatively large positive univariate responses in the sLPZ (Figure 6.3 B&E). Indeed, some of the sighted participant responses are as large as or exceed those found in the LPZ of JMD, who had visual loss. The patient, JMD, exhibits consistent positive responses in the LPZ that also appear to be modulated by the task, but little by the stimulus (Figure 6.3 C&F).
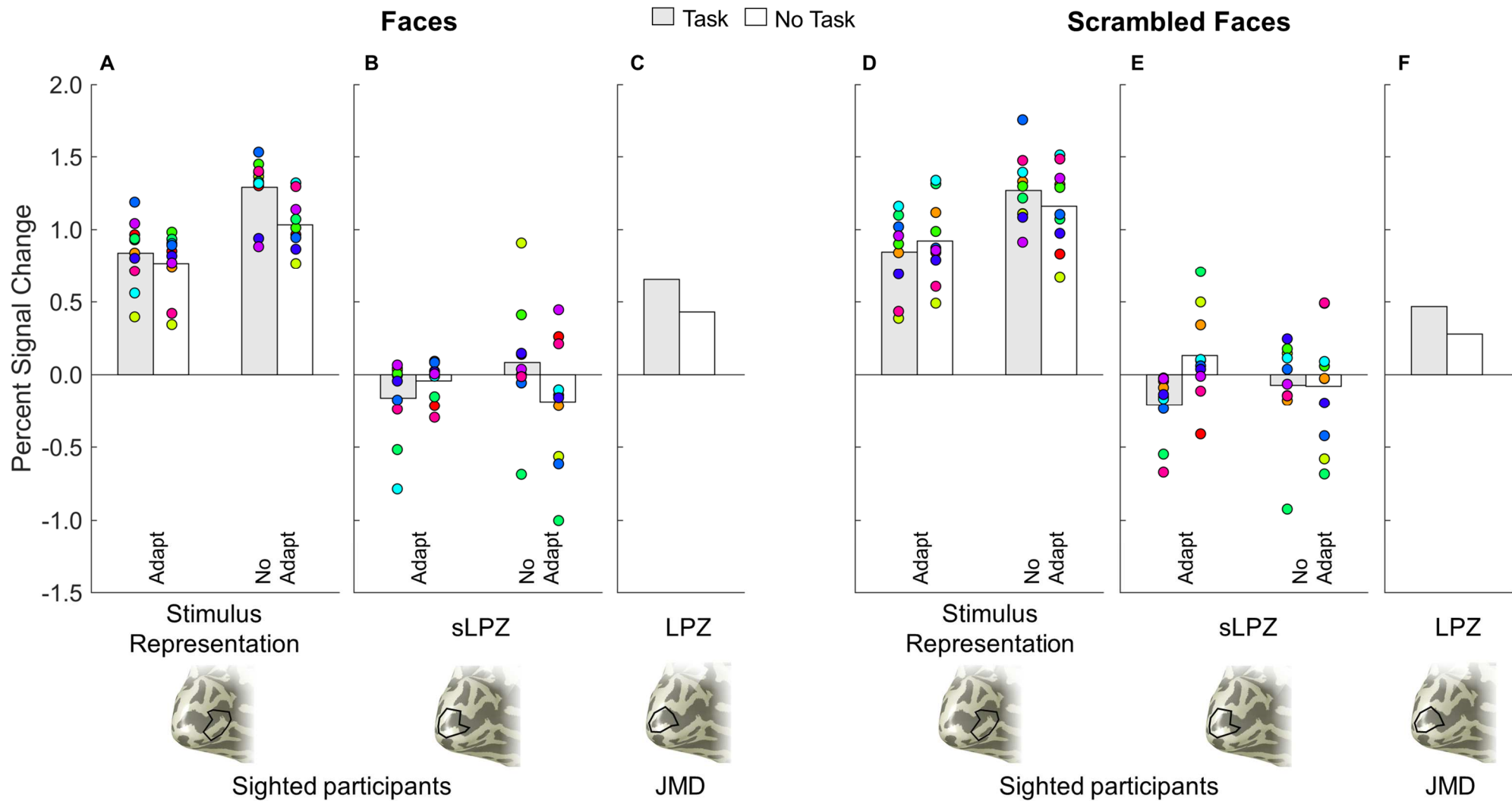
Figure 6.3. Summary statistics for sighted participants (**A,B,D,E**) and JMD (**C,F**), for faces (**A-C**) and scrambled faces (**D-F**) under two viewing conditions: task (shaded bars), no task (open bars). Sighted group average for adaptation and no adaptation for each ROI are represented by the bars – stimulus representation (**A** and **D**, lower bank of the calcarine, anterior to the sLPZ) and the simulated LPZ (**B** and **E**). Each sighted individual is represented by a coloured dot.

6.4.2 Group BOLD Responses
6.4.2.1 LPZ

We analysed the sighted group LPZ responses using a 2x2x2 (adaptation x task x stimulus) repeated measures ANOVA which confirmed there was no significant main effect of adaptation , $F(1,9) = 0.003$, $p=.957$, stimulus type, $F(1,9) = 0.187$, $p=.676$ or task condition, $F(1,9) = 0.328$, $p=.581$. Therefore, our hypothesis that a more realistic simulation of the retinal lesion would unmask feedback is not supported. We were also unable to detect any effect of task on responses that has previously been observed in the LPZ responses from patients. It is possible that responses could emerge as a result of adapting and performing a task which would be highlighted by an adaptation by task interaction. This two-way interaction was however not significant ($F(1,9) = 3.67$, $p=.088$). The results of this analysis are consistent with, but do not explicitly test for an absence of a positive mean univariate response in the sLPZ. To address this, we ran a series of one-sample t-tests – one for each condition - to assess whether we observe positive responses significantly above zero. For the sLPZ, there were no significant positive responses for any combination of adaptation, stimulus, or task ($t(9)$ ranged from -1.80 to 1.38, all $p>.105$). One result was significant (adaptation, scrambled faces, task), but this was a negative response in the sLPZ, indicative of an increase in negative BOLD ($t(9) = -2.958$, $p=.016$).

6.4.2.2 Stimulus Representation

The same ANOVA approach as described above was used to investigate the responses obtained from the stimulus representation in sighted participants. In this case, there was a significant main effect of adaptation on responses, $F(1,9) = 22.03$, $p=.001$, but no main effect of stimulus type, $F(1,9) = 3.38$, $p=.099$ or task, $F(1,9) = 2.947$, $p=.120$. While not reaching significance with an ANOVA, the one-tailed trend for larger responses elicited during a stimulus related task ($p=.060$) and for scrambled images ($p=.050$) are consistent with previous research. The plausible two-way interaction between adaptation and task was not significant ($F(1,9) = 4.00$, $p=.076$). To be consistent with the approach taken above, we also ran a series of one-sample t-tests to determine whether responses in the stimulus representation were significantly different from zero (in the positive direction). As expected, all combinations of adaptation, stimulus type and task emerged as significant in the positive direction ($t(9)$ ranged from 10.14 to 19.30, all $p<.001$).

6.4.3 Reliability analysis

Thus far we have examined the mean of the sighted group responses, which shows no evidence of being positive. At the same time, however, some individual sighted

participants exhibit responses in the sLPZ that exceed those responses from the JMD patient. To interrogate the reliability of the individual responses from the LPZ, patterns of response across voxels within the LPZ were correlated across experimental runs within each condition, for example run 1 no task with run 2 no task for faces. The reliability measure (correlation converted to a Fisher Z score) was plotted against the percent signal change observed in the univariate analysis (Figure 6.4). Results for the sLPZ indicate patterns of responses within individuals were more reliable across runs than expected by chance as indicated by the generally positive Z scores (blue data points in Figure 6.4). This contrasts with the distribution of the univariate response across the group being centred on zero (on the vertical axis). The responses from the stimulus representation of sighted participants are both largely reliable and have a positive mean.

Data for JMD lie on the fringe of the data 'cloud' consisting of all sighted participant data points for the sLPZ (JMD represented by black markers in Figure 6.4). Two data points represent task conditions for each stimulus type and two represent passive viewing of the same stimuli. The two most reliable responses are for the stimulus-related task, closely followed by the passive viewing of faces, with passive viewing of scrambled faces appearing least reliable. It is also true that by lying on the fringe of the distribution of sighted participant data originating from LPZ responses, JMD's data also lie near the fringe of the distribution of control data originating from the responses from stimulus representation. In the case of the patient therefore it is a challenge to categorise the responses from the LPZ as being consistent with either responses from the sLPZ or the stimulus representation in sighted participants.
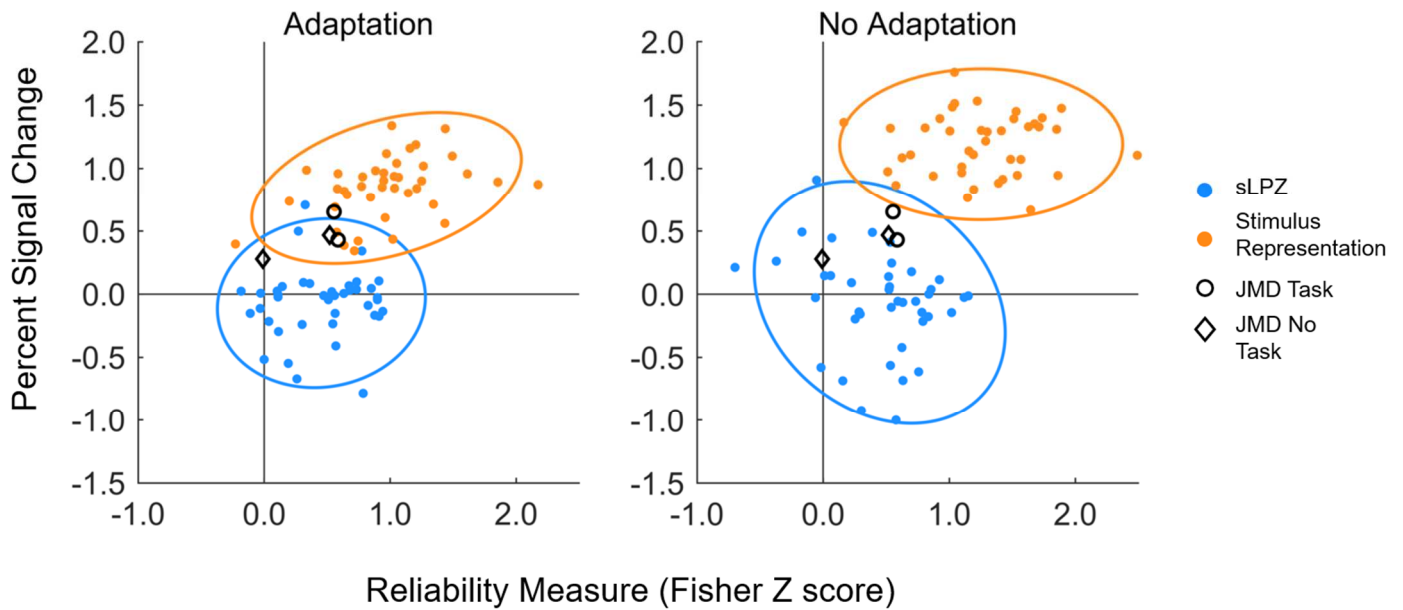
Figure 6.4. Reliability analysis: Scatterplots showing all data for all stimuli and viewing conditions (faces, scrambled faces, task, no task). Data from the bleaching experiment (left) and no bleaching (right) are plotted for both the LPZ (blue) and stimulus representation (orange) ROIs. Reliability measure (transformed to a Fisher Z score, with positive numbers indicating more reliable responses) is plotted against the univariate response, measured in percent signal change. Ellipses represent 95% confidence intervals. Despite the difference in the polarity of the responses in the sLPZ, responses seem largely reliable. JMD results (black) lie on the fringe of the data cloud, showing higher reliability and greater responses in the LPZ.

6.4.4 Classifier analysis

We combined the measures of amplitude and reliability to categorise responses in sighted participants. Using the leave one out cross-validation method, the linear discriminant analysis classified responses in the adaptation experiment as coming from the unstimulated zone (LPZ) and stimulus representation with 93.75% accuracy. For the no-adaptation condition, accuracy reached 98.75%. The LDA classifier trained on adaptation data for sighted participants, classified JMD responses as most comparable to the responses originating from the stimulus representation of sighted participants (3 of the 4 data points classified as stimulus representation). However, an LDA trained on no-adaptation data classified the same JMD responses as being most comparable to the unstimulated zone (LPZ) in sighted participants (all 4 data were classified as originating from the sLPZ). This supports data shown in Figure 6.4, illustrating that JMD responses fall largely within the 95% confidence intervals for the stimulus representation data in the adaptation condition, and all fall within 95% confidence intervals for the sLPZ for the no-adaptation condition.

6.5 Discussion

Our overall aim was to determine whether an fMRI signature of reorganisation of visual processing is unique to patients with retinal lesions or whether they can be detected in normally sighted individuals. To explore this, we asked whether we could (a) create a more realistic simulation of a retinal lesion that might unmask responses in the simulated LPZ, and (b) assess signals in the sLPZ under different viewing conditions (task vs passive viewing). We predicted that signals would be more likely to emerge during stimulus-related task conditions. Our results suggest that our attempt to create a more realistic simulation of a retinal lesion did not alter responses in the sLPZ. Additionally, whilst at the group level sighted participants did not mimic the LPZ response of a patient with retinal lesions, an fMRI signature of reorganisation of visual processing can be observed in some, but not all, normally sighted individuals. Given that only a minority of patients display responses in the LPZ too (Morland, 2015), careful consideration of evidence for reorganisation from LPZ signals is required.

We examined the sighted participants on an individual basis to be consistent with case / case series studies reported in the literature. Some sighted participants responded in a similar manner to JMD showing task-related modulations of positive responses in the sLPZ. These results are consistent with those reported by Masuda and colleagues, who found some patients exhibited the same task-related modulations of signals from the LPZ for visual, tactile and auditory stimuli (Masuda et al., 2008, 2010, 2021). The JMD patient we tested, therefore, exhibited the hallmark of reorganisation of visual processing that has been detected in many studies, but not all patients (Baker et al., 2008, 2005; Dilks et al., 2014). At the same time, however, the same signature of reorganisation of visual processing could be detected in individual sighted participants. The number of these sighted participants (22%) falls within the number of patients also showing sLPZ responses in the literature - between 0% and 50% (Morland, 2015). Therefore, responses in the LPZ may not be unique to patients. Our reliability analysis revealed that signals from the sLPZ of sighted participants are not random, and that some sighted participants exhibited responses from the sLPZ that were as large and reliable as those found in the patient.

Further to this, we analysed our sighted participants as a group which revealed a distribution of the univariate response that are centred around zero in the sLPZ for both adaptation and no-adaptation conditions, therefore suggesting that responses in the sLPZ observed in some individuals is not a general property of the group on average. With

regard to our aim to create a more realistic simulation of a retinal lesion, signals from the sLPZ were no greater when participants adapted to a bright light presented to the macula than when no adaptation occurred. Our second prediction that a stimulus related task could plausibly enhance signals from the sLPZ, particularly during adaptation conditions was also not supported by our results from sighted participants. Given previous work has focused on case / case series, it is clear that if group averages were computed for the patients assessed by Baker et al., (2005, 2008), Dilks et al., (2009), Masuda et al., (2008), a better assessment of the effect could be achieved. This highlights the need to shift from case and case series approaches to group studies. In an earlier group study, we found no evidence of responses in the LPZ of patients (Baseler et al., 2011), but it is noted that the stimulus and task conditions did not reproduce those used in studies that have detected responses in the LPZ (Baker et al., 2008, 2005; Dilks et al., 2009, 2014).

Our motivation to examine adaptation came from the framework put forward by Masuda et al. 2008 to explain signals in the LPZ of patients. They proposed that feedback was the source of responses in V1 and that in the absence of incoming signals to V1 from the retina, the feedback registered a significant positive response in V1's LPZ. Further, they reasoned that feedback to V1 would not register as a signal in the sLPZ of sighted participants because the retina would be signalling the presence of a zero contrast within the macula to V1, effectively cancelling out the feedback signals to V1. Our approach therefore was to assess the effect of dissociating macula signals to V1 from signals that would encode the stimulus. We did this by adapting the macula to bright light such that no stimulus contrast, whether it was zero or greater could be relayed to V1. Potentially, this adaptation could unmask, in sighted participants, the feedback signals that V1 receives. Our results however did not highlight an average positive response in the sLPZ during adaptation or during no adaptation and no significant differences between the signals from each condition emerged. The second aspect of Masuda et al's framework is that signals in the LPZ emerge only during a stimulus-related task, again consistent with the feedback hypothesis. We tested therefore whether an interaction with task and adaptation might underpin our results but found it did not.

The lack of a positive shift in the group mean of LPZ signals in the adaptation condition could indicate that the adaptation we used, while a better simulation of retinal lesions, did not match closely enough the total absence of retinal signalling found in patients. If that were the case, the cancellation of feedback signals by signalling along retinal afferents as

proposed by Masuda et al could still take place. Consistent with the presence of retinal signalling after adaptation was the report from participants of a strong visible afterimage with a sharp boundary. Our adaptation approach therefore can be thought of as saturating retinal stimulation rather than removing it. Our work contributes to the literature in so far as it shows that another manipulation to the experimental approach results in no detectable change in sLPZ responses at the group level. It is now established therefore that the use of a black (Lerner et al., 2006), uniform grey (Baker et al., 2008, 2005; Baseler et al., 2011; Dilks et al., 2009, 2014; Schumacher et al., 2008; Sunness et al., 2004) or adapted stimulus design generates largely equivalent results.

Finally, we have also shown that individual responses from the LPZ, despite varying in strength and polarity, are reliable. The reliability measure we computed provides some context. Overall, it seems responses were reliable for both adaptation and no-adaptation conditions, suggesting that perhaps the pattern of responses in the sLPZ, rather than the univariate response, contained some stimulus information. This is consistent with previous work reporting patterns of response in the representation of an unstimulated part of the visual field contained contextual information for the scenes presented to the surrounding regions (Smith & Muckli, 2010). It should be noted however that in such studies, there is an obvious missing component to the image that participants are presented, which is not the case in our study. Our results are perhaps more like the work of Williams et al (2008), who presented stimuli in peripheral locations and found reliable signals in central representations. The origin of such responses could be larger draining veins that register BOLD responses - and reliable ones (Olman et al., 2007; Turner, Howseman, Rees, Josephs, & Friston, 1998). However, these responses are not necessarily tied to the location of the neurons that may drive oxygen-level changes in these larger vessels. Using alternative imaging protocols that are less susceptible to large vessel artefacts, such as spin-echo sequences, would shed light on the origin of BOLD response patterns detected in the LPZ (Howseman & Bowtell, 1999; Yacoub et al., 2003).

Our approach to use both the univariate response along with the reliability of responses also has the potential to help understand whether a reorganisation of visual processing genuinely occurs in patients. As expected, responses from the stimulus representation in sighted participants are positive and reliable. Unequivocal evidence of reorganisation of visual processing following loss of visual input would register as similarly reliable and positive signals within the LPZ of patients (Morland, 2015). Whilst JMD does show reliable, positive signals overall, they do not appear to be entirely different from some responses

found in the sLPZ in sighted participants. Indeed, the use of response amplitude and reliability in classifying the LPZ responses of the patient resulted in a greater number of classifications being associated with normal responses from the LPZ rather than the stimulus representation.

Determining the source of LPZ responses is important; if there is evidence of reorganisation of visual processing, this will interfere with the success of visual restoration (Baseler et al., 2011; Morland, 2015). Even if the function of the eye were to be restored, it relies on the parts of the visual brain which previously processed input from the macula to remain capable of processing new incoming information. Effectively, cortex would have to reorganise again to resume its former role of processing information from central representation, to allow for some form of functionally useful vision. This clearly is not the desired outcome, and so the reliability of LPZ responses therefore needs to be considered in future work to determine if those responses represent genuine evidence of reorganisation of visual processing.

Chapter 7: General Discussion

The aim of this thesis was to use different neuroimaging methods to address one overarching question: How does eye disease, namely macular disease (MD), impact the structure and function of the posterior visual pathway? The focus of research has largely been on the physiological changes in the eye; the posterior visual pathway has not been studied as extensively, and so it is not surprising there are some inconsistencies within the neuroimaging literature concerning how the posterior pathway is affected in eye disease. There is an assumption that following restoration of function in the eye, the brain will be capable of processing new information, as it did prior to acquired vision loss. It is evident from studies presented in Chapters 2, 3, 5 and 6 that there are alterations to both the structure and function of the visual pathway in different forms of partial blindness. Difficulties faced when conducting longitudinal patient work were examined in Chapter 4, addressing some of the issues we faced for the studies presented in Chapters 2 and 3. Despite the challenges, we followed the same group of MD patients and sighted controls, exploring different anatomical measures in the posterior visual pathway over a ~24-month period. We have contributed some new insights on how MD affects the brain at both the earliest and later stages of the disease, and how this compares to natural aging. Chapters 5 and 6 explore more specific functional questions, examining how selective vision loss impacts on connectivity between early and higher-level visual areas with matching eccentricity biases, as well as trying to ascertain whether functional reorganisation in visual cortex can be observed in sighted individuals with simulated retinal lesions. Ultimately, we wanted to get a better understanding of how viable the brain may be in cases of MD.

In Chapters 2 and 3, we assessed changes in cortical thickness, myelin density and the integrity of the optic radiations across the same group of MD patients and sighted controls. We also had the unique opportunity to follow two individuals for whom we had MRI data before and after a diagnosis of bilateral age-related MD. This rich data set allowed us to tackle some of the more challenging questions concerning if and when changes occur in the brain, at what rate changes may occur in two individuals in the early stages of the disease, and how this compares to a cohort who have had bilateral MD for a number of years. Additionally, having data for sighted controls over a similar time period allowed us to directly compare the effects of natural aging against changes that may be associated with eye disease. Both studies provided confirmation that changes in both grey and white

matter tissues occur in individuals with some remaining vision, but two novel findings also emerged. The first was that changes in the posterior visual pathway may be occurring earlier in the disease progression than anticipated; for cortical thickness and myelin density measures, our cases showed a greater rate of decline for regions capturing the anatomical representation of the visual defect, but also regions capturing intact visual field representations. This suggests that broader changes occur within the first few years of AMD but following functional vision loss. For case MD13 - who had no loss of visual function despite a bilateral AMD diagnosis - there was evidence of a decline, but it was more akin to that observed in natural aging. For our white matter measurements in the two cases, there was evidence of a reduction in fractional anisotropy (FA) even in the time point prior to AMD diagnosis. Again, this was to a greater extent for MD7 we believe due to having loss of visual function. The second key finding was that there is evidence for a continued decline even in long-standing cases of bilateral vision loss. The majority of ophthalmic pathologies develop much later in life, and so plasticity is brought into question; will the mature brain be capable of responding appropriately if visual function were to be restored? This is especially important to consider, given the second finding of a continued decline in our MD cohort.

The anatomical studies presented in Chapters 2 and 3 also establish a broader point, that in order to determine how natural aging differs from aging with disease, both cross-sectional and longitudinal assessments should be adopted where possible. Longitudinal studies provide rich within subject data, and the measurements we have acquired for our two individual cases before and after an AMD diagnosis emphasise this point. We have shown how individuals with AMD can vary in terms of disease progression. Multiple assessments particularly in the earliest stages of AMD in a larger sample could point to possible biomarkers for the disease that precede functional vision loss. Assessing how these anatomical measures change within an individual therefore provide new insights that may be missed in group-based cross-sectional analyses (Schaie, 2005). For example, there are three instances in Chapters 2 and 3 where the cross-sectional and individual assessments over time were important. When examining myelin density in Chapter 2, cross-sectional data indicated that MD patients appeared to have a greater proportion of cortical myelin than our sighted control group. This could have been due to a number of factors as discussed in Section 2.5. What was interesting was that in spite of this, longitudinal assessments for both the MD group and our individual case MD7 suggest there is a decline in myelin density over time. Collectively, these results suggest that

cross-sectional data may be misleading, as a reduction in cortical thickness may lead to higher myelin density values being reported and indeed, this is what we found when examining cortical thickness. Furthermore, the longitudinal data show that myelin density appears to decline as well - something that would have been missed from cross-sectional analyses alone. The second instance where multiple time points proved valuable was in Chapter 3; while no significant changes emerged in white matter volume over the time period of the study for either MD patient or sighted control groups, our individual assessment particularly for MD7 - for whom we have multiple post-diagnosis data sets - indicates how early in the disease this may not be the case. Finally, we found that in both cases before AMD diagnosis, there was a dip in the structural integrity of the optic radiations in a particular portion of the tract, in both our projections to the occipital pole and the calcarine sulcus. This demonstrates that perhaps changes to the posterior pathway precede functional vision loss. Assessing more individuals in this early time window would be highly valuable, acquiring measurements at the earliest point following diagnosis, and even before if possible. Given the prevalence of AMD and the fact we are an aging population (Office for National Statistics, 2018), we may see more of the older volunteers who routinely participate in neuroimaging research go on to develop AMD. Like MD7 and MD13, we could follow individuals over time to build up a model of how AMD might progress. Assessing a group of age-matched controls in the same manner will also provide the necessary context for understanding how the posterior visual pathway responds to aging naturally.

As well as understanding why white matter shows signs of compromised structural integrity, as shown by the decline in FA, it is important to understand what is driving it. An increase in radial diffusivity (RD), as observed in Chapter 3, is thought to be indicative of myelin loss. Early mouse models have shown that white matter can be impaired through demyelination, axonal injury, or both. RD increases have repeatedly been reported in conjunction with demyelination, whilst only subtle changes emerged for axial diffusivity (Song et al., 2003; Song et al., 2002, 2005; Winklewski et al., 2018). Further support comes from the fact that during development, the inverse pattern emerges, whereby increases in FA are observed alongside increases in myelination (Natu et al., 2019; Rokem et al., 2017; Yeatman et al., 2012). Demyelination seems to fit with results reported in Chapter 2, where in the same patient group, there was evidence of cortical thinning and a reduction in myelin density over time in early visual cortex, in the same regions of interest (ROIs) that were used to guide our reconstructions of the optic radiation bundles.

As discussed in Chapter 2, we cannot say what this atrophy actually reflects, and with our diffusion measures we do not have a quantitative assessment of the number of axons for example, but we can make inferences based on the diffusion properties reported. This is where a combination of in vivo measurements would benefit us; assessing the neurochemistry with MR spectroscopy would help to identify whether cortical thinning is reflective of cell death, or whether tissue is shrinking in a manner that means, if signals from the eye were restored, atrophy could be reversed (Hanson et al., 2019). Post-mortem data has also provided support for in vivo results, also showing that retinal disease, affecting retinal ganglion cell layers, causes atrophy in early visual white and grey matter (Bartzokis et al., 2012; Ogawa et al., 2014).

Determining which features of the eye disease progression drives atrophy in the posterior visual pathway is of primary concern. It is possible that anatomical changes in the layers of the retina are not necessarily coupled with the functional changes captured by standard clinical assessments of visual function, such as perimetry and visual acuity. It is also possible that atrophy in the posterior pathway results from the degeneration of retinal ganglion cell axons (the inner layers of the retina), as observed in glaucoma. The latter would indicate that it is the late stages of AMD driving cortical changes. If it is driven by photoreceptor changes (the outer layers of the retina), then it suggests atrophy begins earlier in the disease progression. However, disease type may influence the time course of changes in the eye and brain. As discussed in Chapter 3, Ogawa et al., (2014) have shown that the optic radiations are affected in similar manner even across different eye diseases that cause progressive central vision loss; leber hereditary optic neuropathy (LHON) and cone-rod dystrophy (CRD) impact the retinal ganglion cell layer and the photoreceptor cell layer respectively, and while the outcome measures are similar for both acuity and white matter changes, the rate of change is what differs between the groups. LHON patients had the disease for ~5 years whereas for the CRD patients it was closer to 20 years. This suggests the progression is slower for the CRD patients and therefore managing the disease and determining the optimal time to implement treatment plans will vary for CRD and LHON patients. Most retinal pathologies develop later in life (Senthil, Khadka, Gilhotra, Simon, & Pesudovs, 2017), and given we are yet to fully understand the capacity of the posterior visual pathway to process newly restored retinal inputs, it is not clear how the brain will adapt, particularly in cases who are deprived of visual input for a number of years. This is again why determining the optimal timing of interventions with

further longitudinal studies may govern the success of restoration attempts, alongside understanding what is driving the observed cortical atrophy.

In Chapters 3 and 5, we have explored structural and functional connectivity within the posterior visual pathway respectively; one of the current goals in neuroscience research is to tease apart the biological underpinnings of communication within the brain and understand the relationship between structure and function. Evaluating well established connections at the earliest points in the posterior pathway - namely the optic radiations - is not sufficient going forward. Reliably reconstructing white matter tracts between different visual maps will allow for more specific assessments of how vision is affected in health and disease. In Chapter 5, we explored functional connectivity between portions of V1 and ventral visual areas with known eccentricity biases - the parahippocampal place area (PPA) and the fusiform face complex (FFC). We found specific deficits in patients with central vision loss, whereby the central V1 and FFC connectivity was selectively reduced in the right hemisphere only, compared to connectivity between peripheral V1 and PPA - areas with a peripheral visual field bias. Complementary structural assessments would allow us to build a more complete picture of how other white matter tracts beyond the optic tracts and radiations are impacted by disease, but also to understand this structure and function coupling. Other white matter structures of interest could be those projecting from the occipital cortex, through temporal regions and as far as the frontal lobe. The inferior longitudinal fasciculus (ILF) and inferior fronto-occipital fasciculus (IFOF) have been investigated in very few studies of acquired vision loss, and evidence is mixed. In cases of retinitis pigmentosa (RP) reductions in FA have been observed for both the IFOF and ILF, while others report an increase in functional connectivity in a different group of RP patients (Hofstetter et al., 2019; Rokem et al., 2017). Yoshimine et al., (2018) found no significant changes in a small group of AMD patients (most with unilateral loss). Given we have observed reduced functional connectivity between regions with a foveal bias, exploring white matter tracts implicated in more complex processing such as face perception may be fruitful in a larger group of patients. As discussed in Chapter 1, there is growing behavioural evidence highlighting poorer performance in face discrimination tasks in MD, but there is also a decline in face discrimination ability with natural aging (Rokem et al., 2017). Rokem and colleagues found that the size of a functionally defined fusiform face area (FFA) in the right hemisphere correlated with the volume of the right ILF, but also reported that performance on a face discrimination task correlated with FA and volume in the IFOF, highlighting a link between structure and function in this pathway. Furthermore,

age-related reductions in FA for the IFOF were more pronounced than ILF changes, which appeared to be more immune to age-related decline (Rokem et al., 2017). Cases of prosopagnosia - face blindness - also show compromised integrity of the right ILF (Grossi et al., 2014) and so it appears that ILF may be more vulnerable in clinical cases, whereas IFOF is more susceptible to age-related decline. Investigating how both structure and function changes in a group with an age-related visual pathology such as AMD would therefore be interesting.

When establishing the effects of pathological versus natural aging, sensory deprivation is a key model to study, as shown by the early work of Hubel and Wiesel (Hubel & Wiesel, 1965; Wiesel & Hubel, 1963, 1965). Exploring changes in different pathologies e.g. congenital versus late acquired, or partial versus complete vision loss, helps us to piece together when critical developmental periods occur and how plastic the brain might be throughout the lifespan. It is important to acknowledge that functional changes may be observed in the absence of structural changes in the brain. An example of this comes from research with congenitally blind individuals, who despite showing a reduction in FA, also showed an increase in the functional connectivity between visual and language regions (Bridge et al., 2009; Reislev et al., 2016). However, the link between structure and function may be impacted differently, depending on the type of vision loss. A consensus for what may happen in congenital versus acquired vision loss has yet to be reached, but age at disease onset may dictate how the brain is affected. Evidence of a typically developed structure in the occipital lobe in congenital vision loss, despite serving a different function suggests this coupling will differ compared to acquired cases, for whom the role of the occipital lobe for visual function has already been established prior to disease onset. For our studies of acquired vision loss, we have shown reduced functional and structural connectivity within the visual pathway; it is worth noting that we had some individuals with juvenile MD, but given the small number, AMD versus JMD comparisons were not conducted. The literature largely suggests that within visual cortex the outcomes are similar, but differences emerge when looking elsewhere, for example frontal regions (Hernowo et al., 2014). Assessing this plasticity across the lifespan would also address an important issue of when interventions might be most effective. Generally, the extent of vision loss seems to correlate with the changes in structure, as well as functional connectivity, highlighting that they may indeed be clinically relevant measures (Frezzotti et al., 2014). To advance this further, collecting both resting state fMRI and diffusion data in the same session for patients may be more fruitful and provide more opportunities to study

connectivity within the posterior visual pathway. With advances in both structural and functional imaging sequences, acquiring more data without needing to increase the scan duration using multiband protocols for example, will help to reduce participant burden - something of particular importance for vulnerable and/or aging participants.

The extent of changes observed in the brain, as shown in the literature, seems dependent on many factors including (but not limited to): pathology, age of disease onset, number of years since diagnosis, and severity of the vision loss. In terms of the research itself, variations in study design and analysis techniques may also contribute to the discrepancy in outcome measures. Establishing how these factors impact on findings requires a series of highly controlled studies, which presents challenges. In Chapter 4, the difficulties faced in our longitudinal neuroimaging and neurostimulation structural study reported in Chapters 2 and 3 were discussed. Using stringent inclusion criteria in order to control for variation within disease type can limit recruitment, making studies underpowered. However, without this, we face situations described previously whereby inconsistencies emerge within and between studies. For our research, we reasoned that disease aetiology was less relevant, but ensuring the patients had central-affecting bilateral vision loss was the most important factor when exploring changes in cortex. We did have to expand our criteria and recruit individuals with varying extents and types of central vision loss, for example allowing individuals with the wet form of AMD to enrol. This allowed us to recruit more individuals, primarily because these were the individuals routinely visiting the clinic for treatment, unlike patients with dry AMD who do not attend the clinic so frequently. Despite acquired vision loss such as AMD being common, it proved more difficult to recruit given the added contraindications associated with aging (e.g., more likely to have other ailments preventing them from participating in certain procedures). What we have learned in the process is that a delicate balance is required when considering longitudinal studies; balancing the participant burden - particularly if acquiring multiple measures on a smaller number of individuals - resources available and access to necessary equipment can be hard to achieve. Our studies suffered most with regard to ophthalmological assessments at the start and end of the study, due to lack of staff and equipment availability. Ensuring collaborations allow for sufficient and more reliable measures of visual function is important, especially when making inferences about the relationship between measures of structure and function in the eye and the brain.

The move towards more open science practises could be beneficial but is still more challenging in patient-based neuroimaging research; being more transparent about protocols, study design and analysis pipelines will allow for researchers to implement the same procedures in separate participant pools. With MRI studies, this can be more difficult given researchers will be limited by scanner type and so modifications to protocols may be required. Additionally, availability of software for analysis may also be a hindrance. Moving towards a more cohesive way of working, collaborating across research centres to build a larger database for patients may be the way forward. The human connectome project (HCP) protocols make consistency more achievable and were implemented in this thesis. They were adapted for our measures acquired in Chapter 2 as there was no guidance for setting it up on the GE scanner, but for Chapter 5 however, we could replicate the original HCP protocol for the Siemens scanner. Another issue identified in Chapters 2 and 3 which may explain part of the inconsistency in the literature, is the way in which cortex is parcellated and how ROIs are defined. Some researchers opt to explore V1 in its entirety, while others distinguish between central and peripheral representations using retinotopic mapping and anatomical or functional atlases. It is clear how different combinations of methods can lead to different results, especially when dealing with individuals with selective vision loss, but what was interesting for us is that we get very similar results in Chapter 2 when we used both the original anatomical parcellations for the occipital pole and calcarine sulcus, and those restricted to V1. An additional way to verify these results would be to use the Benson atlas, for example, where you can specify the degrees of visual angle you wish to restrict your ROI by. Having individuals with selective vision loss allows for participants to effectively act as their own control, by exploring representations of both lesioned and intact parts of the visual field; functionally defining which portions of early visual cortex are receiving visual input from the retina can therefore be highly valuable. Having said this, we have opted to use atlases for most of the work described in this thesis as it allowed for greater consistency across subjects (both patients and controls), as well as over time. Participant burden is also reduced this way as it means a shorter scanning session without a functional localiser.

Functional reorganisation of visual function has been a topic of interest for a number of years, and there is still some disagreement. As discussed in Chapters 1 and 6, part of the debate concerns differing definitions for functional reorganisation. The broader definition is that if a patient exhibits a response that cannot be shown in normally sighted populations, then it is indicative of a reorganisation of function. For this thesis, functional reorganisation

refers to a change from what we know about the organisation of the visual system in normally sighted individuals but observing abnormal signals does not necessarily mean that any cortical reorganisation has occurred (Morland, 2015). While there is evidence suggesting the brain is capable of some form of reorganisation of function in response to changes e.g. the natural aging process, disease or injury, some additional modifications may serve a purpose. This allows for some form of compensation of function following a change, for example visual deprivation. Cross-modal plasticity, while useful in congenital blindness, may be more inconvenient in cases of acquired vision loss, particularly when visual restoration is the ultimate goal. The brain would effectively have to undergo reorganization for a second time, to revert to its former role of processing visual information from the central visual field (Baseler et al., 2011; Morland, 2015). In Chapter 6 we wanted to investigate functional reorganisation further, by focusing more on whether we could observe responses in a simulated lesion projection zone (LPZ) in sighted participants when presenting images to the periphery, after inducing a transient retinal lesion - something that had not been done before. Previous work failed to report any responses in the simulated LPZ in sighted participants, for whom the central visual field was simply greyed out. Whilst at the group level we did not observe patient-like LPZ responses, and our more realistic simulation of a retinal lesion did not alter responses in the simulated LPZ, individual assessments were interesting. Given that in the literature, only a minority of patients display responses in the LPZ (Morland, 2015), it is important to determine whether the responses observed in this subset of individuals is genuine or not. In a small number of sighted participants, task-related responses in the simulated LPZ could be observed. An important addition to our study was an assessment of the reliability of these responses. Previous work has reported the presence or absence of response, but not the reliability within individuals. Our results suggest that despite individual responses in the simulated LPZ varying in strength and polarity, they are indeed reliable, and perhaps the pattern of responses within the simulated LPZ contained some stimulus information, as opposed to the univariate responses. Our work lends support to the idea that responses in the LPZ may not be unique to patients with retinal defects, and is likely that responses are a result of the unmasking of top-down feedback as proposed by Masuda and colleagues, described in more detail in Section 1.5.1 (Masuda et al., 2008, 2010, 2021). This additional information about the reliability of the responses observed gives the results some context and other patient-based work would benefit from adopting this type of analysis.

Concluding comments:

Vision plays an important role in our overall health and well-being; it is essential for many everyday activities and so the consequences of vision loss, particularly if acquired later in life, can have a detrimental effect. Not being able to read, drive, accurately recognise familiar faces, or navigate round your home can make basic tasks much more challenging, in turn reducing independence. This is just one of the many justifications for investigating the full extent of MD and the consequences beyond the eye. To fully understand the disease progression in MD, a multi-pronged approach must be taken, to explore both ophthalmological and neural consequences of sensory deprivation. Combining ophthalmic measures with structural and functional MRI to further understand the relationship between the eye and brain could allow for reliable and earlier detection of biomarkers for disease, but also inform research focused on developing therapeutic and neuroprotective strategies. Glaucoma is a good example of how something originally thought to be a purely ophthalmological disease may indeed fall under neurodegenerative conditions. It has been reported that only 40% of individuals with wet AMD who are undergoing anti-VEGF treatment successfully regain some visual function (Gonzalez, 2011; Heier et al., 2012; Yoshimine et al., 2018), and so it is important to acknowledge that the viability of the visual brain may limit the success of current treatments as well as future attempts at visual restoration. Research focused on treating the eye is currently gaining pace, examining the effects of gene therapy, stem cell therapy, as well as retinal prostheses, in a bid to restore functionally useful vision in conditions such as MD. There is an assumption that visual areas will be able to process the restored retinal signals in an appropriate manner, but if the visual brain is no longer viable due to prolonged sensory deprivation, or if there is evidence of reorganisation of function, success will likely be limited. Previous work has demonstrated that following restoration of visual input using retinal implants, brain responses are not immediate, and it needs time to recalibrate and resume responding appropriately to the newly restored visual input (Castaldi et al., 2016). What has been highlighted in this thesis is that changes in the posterior visual pathway are broad. Using various MRI protocols as shown throughout this thesis, we can non-invasively tease apart the consequences of sight loss on both the structure and function of the entire visual pathway, from retina to cortex, in various stages of eye disease. It may also be a useful tool for identifying who may be better candidates for restoration based on the status of visual cortex. The fact we are an aging population further highlights the need to get a broader understanding of how age-related decline associated with a particular eye disease

may be different to natural aging, as the prevalence of the age-related form of MD will undoubtedly rise in the coming years.

Appendices

Appendix A

A1. Results from one-way ANOVAs for the occipital pole and calcarine sulcus fiber bundles for fractional anisotropy for Chapter 3. Locations along the tract where significant group differences emerge ($p<.050$). Full range of locations = 10 to 90.

	Fractional Anisotropy				
Occipital Pole			Calcarine Sulcus		
Location	F (df)	p	Location	F (df)	p
41	5.75 (1, 24.84)	.024	42	5.35 (1,21.50)	.031
43	7.89 (1,26.90)	.009	44	4.47 (1,24.04)	.045
44	4.87 (1,24.77)	.037	45	6.28 (1,24.57)	.019
45	7.62 (1,23.50)	.011	46	5.60 (1,24.84)	.026
46	5.77 (1,23.01)	.025	47	7.50 (1,23.20)	.012
47	5.84 (1,21.21)	.025	48	4.63 (1,21.99)	.043
48	5.65 (1,23.86)	.026	49	8.35 (1,23.52)	.008
50	4.81 (1,21.66)	.039	52	6.47 (1,22.77)	.018
52	5.21 (1,17.57)	.035	53	5.15 (1,22.36)	.033
53	6.44 (1,16.17)	.022	54	5.84 (1,21.23)	.025
54	13.25 (1,14.24)	.003	55	4.61 (1,19.78)	.044
55	15.65 (1,16.58)	.001	56	4.47 (1,17.22)	.049
56	12.91 (1,16.62)	.002	57	6.36 (1,18.93)	.021
57	11.55 (1,17.24)	.003	58	7.81 (1,18.47)	.012
58	9.13 (1,16.97)	.008	59	10.04 (1,18.88)	.005
59	11.05 (1,15.18)	.005	60	11.00 (1,22.62)	.003
60	11.31 (1,15.88)	.004	61	10.51 (1,19.55)	.004
61	8.93 (1,17.09)	.008	62	11.48 (1,21.14)	.003
62	8.41 (1,17.90)	.010	63	11.70 (1,17.72)	.003
63	9.33 (1,17.45)	.007	64	10.19 (1,17.28)	.005
64	8.88 (1,19.60)	.008	65	7.02 (1,16.84)	.017
65	9.76 (1,19.17)	.006	67	5.61 (1,16.80)	.030
66	9.88 (1,18.15)	.006	68	5.11 (1,15.73)	.038
67	8.02 (1,18.83)	.011	69	4.62 (15.79)	.048
68	16.43 (1,19.84)	.001	70	5.33 (1,15.53)	.035
69	7.64 (1,16.60)	.014	71	6.07 (1,14.98)	.026
70	10.16 (1,18.79)	.005	72	5.89 (1,15.07)	.028
71	10.47 (1,17.42)	.005	73	8.26 (1,16.53)	.011
72	7.53 (1,19.16)	.013	74	9.08 (1,17.89)	.007
73	6.62 (1,18.33)	.019	75	15.31 (1,19.25)	.001
74	4.94 (1,19.06)	.039	76	9.03 (1,24.06)	.006
75	7.29 (1,17.95)	.015	77	22.32 (1,21.64)	.000
79	5.09 (1,19.34)	.036	78	22.88 (1,23.11)	.000
90	6.82 (1,20.82)	.016	79	12.35 (1,23.58)	.002
			80	14.13 (1,21.70)	.001
			81	12.94 (1,26.17)	.001
			82	8.16 (1,22.91)	.009
			84	4.42 (1,24.95)	.046
			85	5.09 (1,25.04)	.033

A2. Results from one-way ANOVAs for the occipital pole and calcarine sulcus fiber bundles for axial diffusivity for Chapter 3. Locations along the tract where significant group differences emerge ($p<.050$). Full range of locations = 10 to 90.

| Axial Diffusivity					
Occipital Pole			**Calcarine Sulcus**		
Location	**F (df)**	**p**	**Location**	**F (df)**	**p**
25	5.75 (1,20.62)	.026	27	4.60 (1,19.41)	.045
26	10.23 (1,26.00)	.004	54	4.83 (1,24.07)	.038
73	5.29 (1,20.52)	.032			
75	7.96 (1,18.41)	.011			
76	8.35 (1,19.57)	.009			
78	6.54 (1,13.45)	.023			
81	4.60 (1,20.58)	.044			

A3. Results from one-way ANOVAs for the occipital pole and calcarine sulcus fiber bundles for radial diffusivity for Chapter 3. Locations along the tract where significant group differences emerge ($p<.050$). Full range of locations = 10 to 90.

Radial Diffusivity					
Occipital Pole			**Calcarine Sulcus**		
Location	**F (df)**	**p**	**Location**	**F (df)**	**p**
53	4.74 (1,18.84)	.042	47	4.46 (1,23.68)	.045
54	8.38 (1,15.52)	.011	49	5.17 (1,23.43)	.032
55	8.53 (1,18.94)	.009	52	8.18 (1,19.85)	.010
56	6.82 (1,19.28)	.017	53	5.34 (1,21.77)	.031
57	6.27 (1,18.36)	.022	54	7.11 (1,17.87)	.016
58	5.45 (1,17.61)	.032	55	6.22 (1,15.14)	.025
59	6.31 (1,14.55)	.024	56	4.57 (1,19.83)	.045
60	5.75 (1,16.95)	.028	57	5.91 (1,16.72)	.027
61	5.66 (1,16.72)	.030	58	6.17 (1,18.50)	.023
63	5.88 (1,17.46)	.026	59	5.94 (1,17.77)	.026
64	4.97 (1,21.15)	.037	60	7.18 (1,17.90)	.015
65	5.42 (1,19.74)	.031	61	5.81 (1,19.75)	.026
66	6.31 (1,17.09)	.022	62	5.85 (1,22.37)	.024
67	6.40 (1,18.33)	.021	63	6.61 (1,17.16)	.020
68	11.90 (1,15.57)	.003	64	5.43 (1,20.07)	.030
69	5.66 (1,17.70)	.029	65	5.20 (1,18.53)	.035
70	9.19 (1,16.62)	.008	67	4.64 (1,17.70)	.045
71	11.01 (1,15.20)	.005	68	4.89 (1,14.71)	.043
72	9.99 (1,17.03)	.006	73	5.28 (1,14.96)	.036
73	9.94 (1,16.18)	.006	74	5.04 (1,16.98)	.038
74	5.54 (1,16.45)	.031	75	6.60 (1,16.15)	.021
75	12.03 (1,16.56)	.003	77	7.82 (1,18.02)	.012
76	7.92 (1,13.85)	.014	78	6.35 (1,20.13)	.020
77	6.09 (1,15.52)	.026	79	4.40 (1,21.60)	.048
78	9.49 (1,15.50)	.007	80	5.79 (1,17.59)	.027
79	9.42 (1,14.29)	.008	81	4.62 (1,19.73)	.044
80	7.10 (1,16.08)	.017	85	5.56 (1,20.31)	.029
81	7.41 (1,17.07)	.014	89	4.31 (1,26.93)	.048
82	5.40 (1,16.51)	.033			
83	6.21 (1,16.50)	.024			
85	5.48 (1,17.20)	.032			
86	5.04 (1,20.01)	.036			
88	4.47 (1,20.85)	.047			
90	6.87 (1,22.11)	.016			

A4. Tract profiles for our individual AMD cases MD7 (**A**) and MD13 (**B**) for axial diffusivity for Chapter 3.
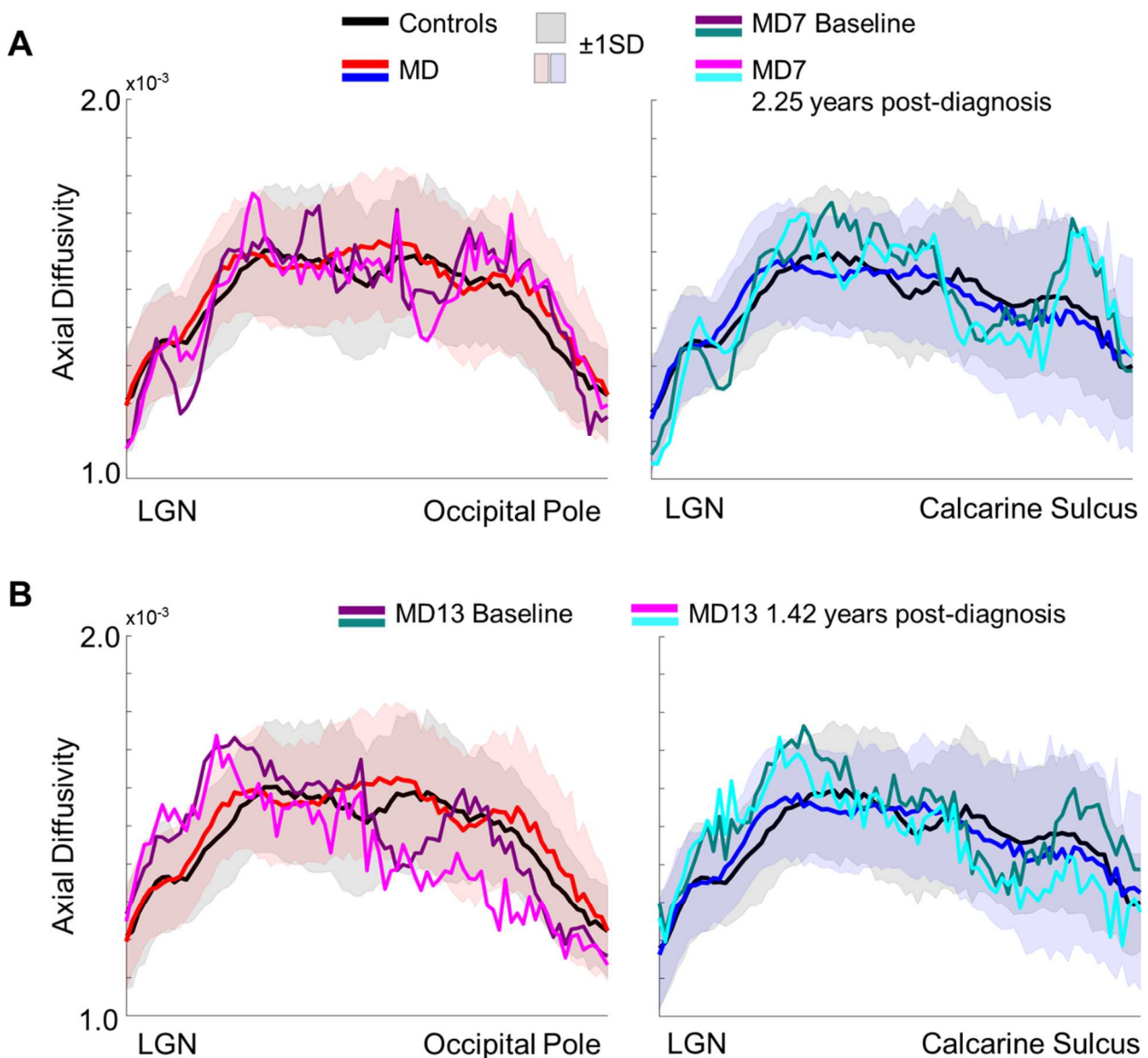
Comparing AD along the tracts for individual cases before and after diagnosis against sighted control and MD patient groups. **A***:* Individual time point AD data for MD7 plotted against sighted control (black line) and MD group means (red for occipital pole projections, and blue for calcarine sulcus projections. Shaded regions represent 1 standard deviation for each group (grey = controls, red/blue = MD patient group). MD7 baseline data (before diagnosis) are shown in purple (left) and teal (right). Last time point (2.25 years after diagnosis) is shown in magenta (left) and cyan (right). **B**: Same as A, but for MD13 data. Second time point for MD13 (1.42 years post-diagnosis) is shown in magenta (left) and cyan (right).

A5. Tract profiles for our individual AMD cases MD7 (upper) and MD13 (lower) for radial diffusivity for Chapter 3.
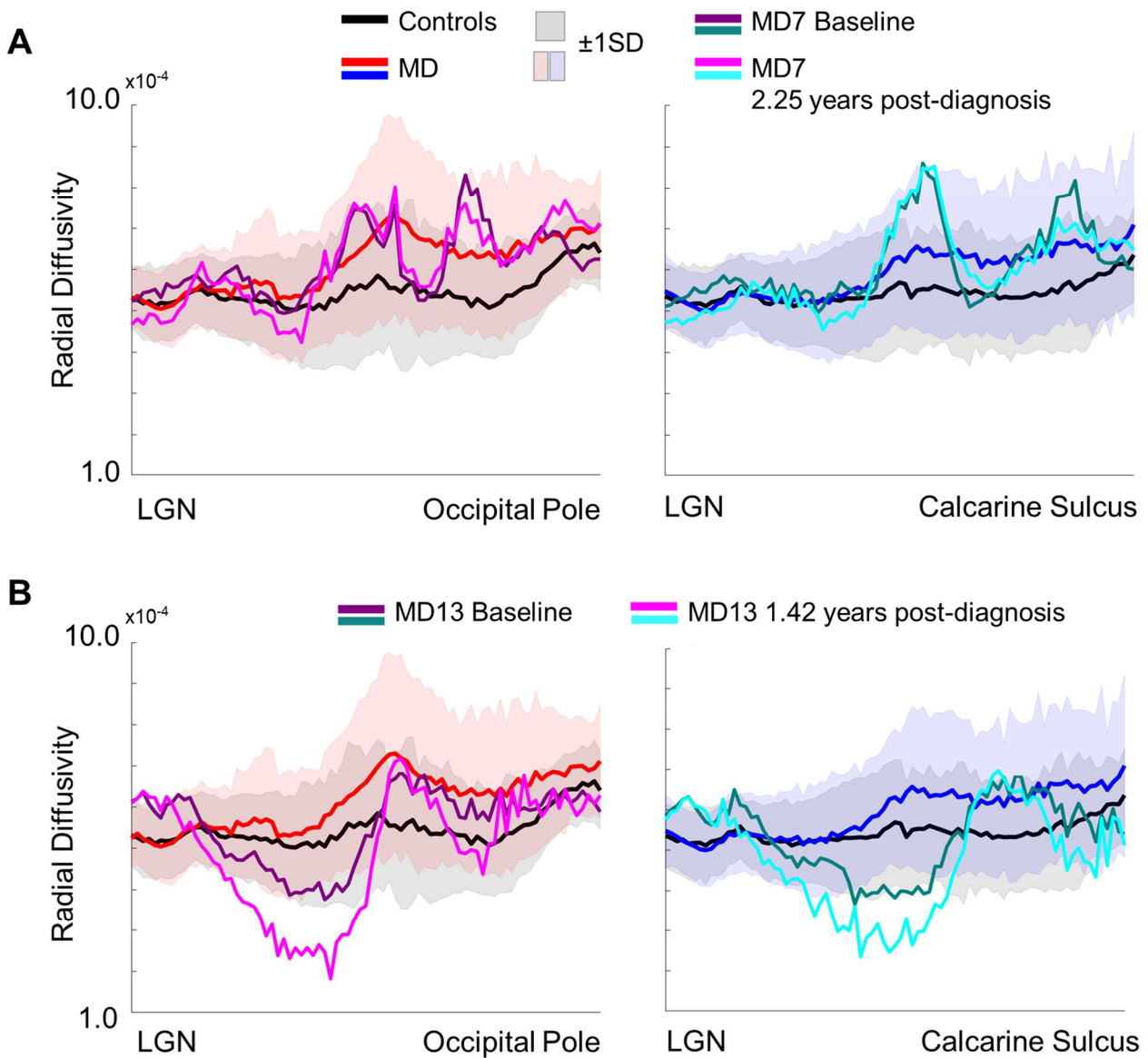
Comparing RD along the tracts for individual cases before and after diagnosis against sighted control and MD patient groups. **A***:* Individual time point RD data for MD7 plotted against sighted control (black line) and MD group means (red for occipital pole projections, and blue for calcarine sulcus projections. Shaded regions represent 1 standard deviation for each group (grey = controls, red/blue = MD patient group). MD7 baseline data (before diagnosis) are shown in purple (left) and teal (right). Last time point (2.25 years after diagnosis) is shown in magenta (left) and cyan (right). **B**: Same as A, but for MD13 data. Second time point for MD13 (1.42 years post-diagnosis) is shown in magenta (left) and cyan (right).

Appendix B

B1. Full list of other eye affecting pathologies – Chapter 4

Eye Disease / Injury	Definition
Retinal Pigment Epithelial Rip	Rip in the RPE developed from an RPE detachment or caused by intravitreal injection. Associated with vascularised RPE detachment due to AMD.
Retinal Detachment	When retina pulls away from the blood vessels supplying it with oxygen
Chronic branch retinal vein occlusion	Second most common retinal vascular disorder (after diabetic retinopathy). Main symptom includes visual floaters from a vitreous haemorrhage (blood vessels leaking into the vitreous gel of the eye). Essentially a blockage of the small veins in the retina.
Degeneration of Posterior Pole	Degeneration of the retina between the macula and the optic disc.
Central Serous Retinopathy /chorioretinopathy (CSR/CSCR)	Fluid collects in the macula, causing it to swell, affecting central vision, usually temporary but can reoccur. Largely unknown cause, but could be Type A personality, steroid use, pregnancy, Cushing Syndrome.
Pigment epithelial detachment	Fluid beneath the RPE (layer of cells beneath the retina), usually caused by AMD and CSR
Adult Vitelliform (Pattern Dystrophy)	Genetic form of macular dystrophy with onset in mid-adulthood.
Choroidal Neovascularisation	Growth of new blood vessels that originate from the choroid through a break in the Bruch membrane into the sub-retinal pigment epithelium or subretinal space.
Pseudophakia	Replacement lens following cataract removal surgery
Corneal Surface Break	Damage to the cornea resulting in blocking or distortion of light
Fuch's Endothelial Dystrophy	inherited eye condition causing the cornea to become cloudy
Ocular Hypertension	Increased intraocular pressure if left untreated can lead to glaucoma and permanent vision loss
Amblyopia	Lazy eye. Developmental eye disorder - eye fails to achieve normal visual acuity even with prescription glasses or contact lenses. Usually only one eye affected.
Corneal epithelial membrane dystrophy	Affects the anterior cornea, causing blurry vision, pain, sensitivity to light, excessive tearing, and a feeling of something being in the eye
Polypoidal Choroidal Vasculopathy	Loss of central vision caused by bleeding, leakage, and scar tissue formation.
Band Keratopathy	calcific degeneration of the superficial cornea that involves mainly the bowman layer. Appearance of calcium in the central cornea.
Glaucoma	Caused by elevated intraocular pressure. Progressive disease-causing loss of central vision.

Retinitis Pigmentosa	Rare genetic disorders that cause a breakdown of cells in the retina. Peripheral vision loss and difficulty seeing at night.
Optic Disc Pit	Congenital anomaly of the optic disc complicated by intraretinal and subretinal fluid at the macula.

B2. TDCS safety questionnaire

THE UNIVERSITY *of York*

York Neuroimaging Centre

The Biocentre, York Science Park, Heslington, York, YO10 5DG

Tel. 01904 435329, Fax 01904 435356

Confidential

SAFETY SCREENING FORM

(version 1.1 – 9th February 2015)

If you agree to take part in this study, please answer the following questions. It is essential that you answer truthfully. The information you provide is for safety screening purposes only and will be kept completely confidential.

1. Have you ever suffered from any neurological or psychiatric conditions?	YES / NO
If YES please give details (nature of condition, duration, current medication, etc).	
2. Have you ever suffered from epilepsy, febrile convulsions in infancy, had a fit or seizure or recurrent fainting spells?	YES / NO
3. Does anyone in your immediate or distant family suffer from epilepsy?	YES / NO
If YES please state your relationship to the affected family member.	
4. Have you ever had an operation on your head or spine (including eye surgery)?	YES / NO
If YES please give details.	
5. Do you currently have any of the following fitted to your body?	YES / NO

- Heart pacemaker
- Cochlear (ear) implant
- Medication pump
- Surgical clips
- Any other biomechanical implant

6. Have you ever had an injury to your eye involving metal fragments?	YES / NO

7. Do you have any skin damage or disease affecting your scalp or face?	YES / NO
• 8. Do you suffer from recurrent headaches or migraines?	YES / NO
9. Are you currently taking any unprescribed or prescribed medication?	YES / NO
If YES please give details.	
10. Are you currently undergoing anti-malarial treatment?	YES / NO
11. Have you drunk more than 3 units of alcohol, or used recreational drugs in the last 24 hours?	YES / NO
12. Have you already drunk alcohol today?	YES / NO
13. Have you had more than one cup of coffee, or other sources of caffeine, in the last hour?	YES / NO
14. Did you have very little sleep last night?	YES / NO
15. Have you already participated in a TMS/tDCS experiment today?	YES / NO
16. Are you or could you be pregnant?	YES / NO

Participant details:

16. Are you left or right handed?
    Left / Right

17. Date of birth
__/__/__

I understand that the above questions check for serious risk factors. I CONFIRM THAT I HAVE READ, UNDERSTOOD AND CORRECTLY ANSWERED THE ABOVE QUESTIONS
IN CASE OF ANY DOUBT, please inform the researcher before signing this form.

Participant Name:…………………………………………… Signature:………………………

Date…………………………………..

Researcher Name:…………………………………………… Signature:………………………

Date…………………………………..

B3. TMS safety questionnaire and consent form

Safety Questionnaire and Consent for Participants

Version: 2 - 2014-04-01

Modality - TMS

Participant ID: R	Surname:	Forename:	Date of Birth:	Contact No:
Address			**GP Address**	
Verified			**Verified**	

If your, or your GP's, address are different to those shown above please cross out the old address and write the new one next to it.
Please do not assume we will accept you for an experiment on the basis that you have participated in TMS elsewhere (regardless of whether it was for research or clinical reasons).
It is essential that all questions on this sheet are answered truthfully. This information is essential in order to ensure your safety and will be kept completely confidential.

Please answer the following questions accurately by ticking the appropriate box. **Safety**	Answer		Please answer the following questions accurately by ticking the appropriate box. **Safety**	Answer	
	Yes	No		Yes	No
Have you ever suffered from any neurological or psychiatric conditions?			Have you already participated in a TMS or tDCS experiment today?		
Have you ever suffered from epilepsy?			Have you had more than 1 cup of coffee or other sources of caffeine, in the last hour?		
Does anyone in your family (immediate or distant) suffer from epilepsy?			Have you drunk any alcohol today?		
Have you experienced febrile convulsions (fits associated with a high fever) at any time in your life?			Have you drunk more than 3 units of alcohol or used **any** recreational drugs in the last 24 hours?		
Have you ever suffered from a fit or a seizure?			**Consent**		
Have you fainted more than once?					
Have you fainted in the last 12 months?			I understand that this questionnaire checks for serious risk factors		
Have you ever suffered a head trauma that was diagnosed as a concussion or was associated with a loss of consciousness?			I have fully understood and correctly answered all the questions on this form.		
Do you suffer from regular headaches or migraines?			**If in any doubt please inform the Investigator before signing this form**		
Do you suffer from anxiety?			I have been fully informed and understand the nature of the procedure(s) to be carried out		
Are you feeling unduly anxious about the experiment today?			I have been able to ask questions regarding the procedure(s)		
Have you ever had any surgery on your head (including eyes), or spine?			I confirm that I give my full consent to the TMS procedure(s) being performed on me		
Do you have a cardiac pacemaker?			I am aware that I may end the procedure(s) at any time by informing a member of staff		
Do you have any medication pumps?			**Signatures**		
Do you have a cochlear implant?			Only sign if you are in **no doubt** about the participant's suitability for TMS		
Do you have hearing problems or ringing in your ears?			Project ID: -		Date
Are you currently taking any prescribed or un-prescribed medication other than the contraceptive pill?			**Participant** (I confirm that I am over 18 years of age)		
Are you currently undergoing anti-malarial treatment?					
Do you have any other bio-medical implants?					
Did you have very little sleep last night?			**Approved investigator**	*Signature:*	
Do you have any surgical clips?				*Print Name:*	
Have you ever had an injury to your eye(s) involving metal fragments?			**Approved operator**	*Signature:*	
Female Participants Only: Are you, or could you be pregnant?				*Print Name:*	

B4. Notes on medications described in Figure 4.4.

1 Anti-hypertensive medicines are defined as BNF codes 2.2, 2.4, 2.5 and 2.6.2.

2 Lipid-lowering medicines are defined as BNF codes 2.12.

3 Proton pump inhibitors are defined as BNF code 1.3.5.

4 Analgesics and/or NSAIDs (non-steroidal anti-inflammatory drugs) are defined as BNF codes 4.7, 10.1.1 and 10.3.2

5 Antidepressants medicines are defined as BNF code 4.3.

6 Medicine for asthma or COPD are defined as BNF codes 3.1, 3.2, 3.3, and 3.6.

7 Antiplatelet medicines are defined as BNF code 2.9.

8 Antidiabetic medicines are defined as BNF codes 6.1.1 and 6.1.2.

B5. Participant survey results – future research into the consequences of sight loss on the visual pathway – Chapter 4.

Methods:

Survey was sent out attached to an email to participants who had signed up to our Vision Research Mailing list. Participants had the option of filling out the survey themselves and returning electronically, by post or the survey could be completed over the phone with the researcher. Where electronic signatures were not possible, written consent was obtained from participants by posting out the study information. 12 participants responded to the survey (Age range 54 – 90 years, mean age = 66.75 years). 9 out of 12 participants reported having a visual impairment (3 sighted controls, 4 with retinitis pigmentosa, 4 with age-related macular degeneration, 1 with juvenile macular degeneration).

The short study was devised to get some participant feedback on ideas for an upcoming grant application. This study followed the tenets of the Declaration of Helsinki with approval granted by YNiC Research, Ethics and Governance Committee.

Summary of the survey:

The Vision Research Group at York Neuroimaging Centre are hoping to secure funding to continue working on vision loss research, examining the consequences of vision loss on the entire visual pathway, from eye to brain. The aim for this survey is to engage with individuals with and without visual impairment and get some feedback on future research project ideas, as well as feedback on previous research experience.

The relevant questions to the point made on page 13 are as follows:

Did you find the multiple research visits problematic?

5 out of 12 responded N/A due to the fact they have only participated in single session studies so far. The remaining 7 out of 12 had completed a multi-visit study, all of whom responded '*No*'.

For one of our future studies examining potential changes in the brain in sight loss, we anticipate having 8 visits for each participant over 4 years. This would include 1 visit to the University for the MRI scans, and 1 visit to a clinic to acquire images of the eye each year. We would pay for all travel costs/expenses incurred. Does this seem reasonable?

All 12 responded '*Yes*'.

Typically, an MRI session itself would last no longer than 1 hour, plus 30 minutes of paperwork in advance of the session. Does this seem reasonable?

All 12 responded '*Yes*'.

How much time would you be willing to give up for a research session (MRI or otherwise, EXCLUDING travel time)?

1 – 1.5 hours	2
1.5 -2 hours	3
Beyond 2 hours	7

References

Age UK. (n.d.). Age related conditions, illnesses and diseases | Age UK. Retrieved September 1, 2020, from https://www.ageuk.org.uk/information-advice/health-wellbeing/conditions-illnesses/

Aguirre, G. K., Butt, O. H., Datta, R., Roman, A. J., Sumaroka, A., Schwartz, S. B., … Jacobson, S. G. (2017). Postretinal structure and function in severe congenital photoreceptor blindness caused by mutations in the GUCY2D gene. *Investigative Ophthalmology and Visual Science*, *58*(2), 959–973. https://doi.org/10.1167/iovs.16-20413

Andersson, J. L. R., Skare, S., & Ashburner, J. (2003). How to correct susceptibility distortions in spin-echo echo-planar images: Application to diffusion tensor imaging. *NeuroImage*, *20*(2), 870–888. https://doi.org/10.1016/S1053-8119(03)00336-7

Antal, a, Nitsche, M., & Paulus, W. (2006). Transcranial direct current stimulation and the visual cortex. *Brain Research Bulletin*, *68*(6), 459–463. https://doi.org/10.1016/j.brainresbull.2005.10.006

Arcaro, M. J., Schade, P. F., Vincent, J. L., Ponce, C. R., & Livingstone, M. S. (2017). Seeing faces is necessary for face-domain formation. *Nature Neuroscience*, *20*(10), 1404–1412. https://doi.org/10.1038/nn.4635

Arrigo, A., Calamuneri, A., Mormina, E., Gaeta, M., Quartarone, A., Marino, S., … Aragona, P. (2016). New insights in the optic radiations connectivity in the human brain. *Investigative Ophthalmology and Visual Science*, *57*(1), 1–5. https://doi.org/10.1167/iovs.15-18082

Baker, C. I., Dilks, D. D., Peli, E., & Kanwisher, N. (2008). Reorganization of visual processing in macular degeneration: Replication and clues about the role of foveal loss. *Vision Research*, *48*(18), 1910–1919. https://doi.org/10.1016/j.visres.2008.05.020

Baker, C. I., Peli, E., Knouf, N., & Kanwisher, N. G. (2005). Reorganization of visual processing in macular degeneration. *The Journal of Neuroscience : The Official Journal of the Society for Neuroscience*, *25*(3), 614–618. https://doi.org/10.1523/JNEUROSCI.3476-04.2005

Baker, J., Rorden, C., & Fridriksson, J. (2010). Using transcranial direct current stimulation

(tDCS) to treat stroke patients with aphasia. *Stroke*, *41*(6), 1229–1236. https://doi.org/10.1161/STROKEAHA.109.576785.Using

Ball, K., Edwards, J. D., & Ross, L. A. (2007). The Impact of Speed of Processing Training on Cognitive and Everyday Functions. *The Journals of Gerontology: Series B*, *62*(Special_Issue_1), 19–31. https://doi.org/10.1093/geronb/62.special_issue_1.19

Bartsch, A. J., Biller, A., & Homola, G. A. (2009). Tractography for surgical targeting. In *Diffusion MRI* (pp. 415–444). Elsevier Inc. https://doi.org/10.1016/B978-0-12-374709-9.00019-5

Bartzokis, G. (2004, January 1). Age-related myelin breakdown: A developmental model of cognitive decline and Alzheimer's disease. *Neurobiology of Aging*. Elsevier Inc. https://doi.org/10.1016/j.neurobiolaging.2003.03.001

Bartzokis, G., Lu, P. H., Raven, E. P., Amar, C. P., Detore, N. R., Couvrette, A. J., … Nuechterlein, K. H. (2012). Impact on intracortical myelination trajectory of long acting injection versus oral risperidone in first-episode schizophrenia. *Schizophrenia Research*, *140*(1–3), 122–128. https://doi.org/10.1016/j.schres.2012.06.036

Baseler, H. a, Brewer, A. a, Sharpe, L. T., Morland, A. B., Jägle, H., & Wandell, B. a. (2002). Reorganization of human cortical maps caused by inherited photoreceptor abnormalities. *Nature Neuroscience*, *5*(4), 364–370. https://doi.org/10.1038/nn817

Baseler, H. a, Gouws, A., Haak, K. V, Racey, C., Crossland, M. D., Tufail, A., … Morland, A. B. (2011). Large-scale remapping of visual cortex is absent in adult humans with macular degeneration. *Nature Neuroscience*, *14*(5), 649–655. https://doi.org/10.1038/nn.2793

Beer, A. L., Plank, T., & Greenlee, M. W. (2020). Aging and central vision loss: Relationship between the cortical macro-structure and micro-structure. *NeuroImage*, *212*, 116670. https://doi.org/10.1016/j.neuroimage.2020.116670

Behrens, T. E.J., Berg, H. J., Jbabdi, S., Rushworth, M. F. S., & Woolrich, M. W. (2007). Probabilistic diffusion tractography with multiple fibre orientations: What can we gain? *NeuroImage*, *34*(1), 144–155. https://doi.org/10.1016/j.neuroimage.2006.09.018

Behrens, Timothy E.J., Woolrich, M. W., Jenkinson, M., Johansen-Berg, H., Nunes, R. G., Clare, S., … Smith, S. M. (2003). Characterization and Propagation of Uncertainty in Diffusion-Weighted MR Imaging. *Magnetic Resonance in Medicine*, *50*(5), 1077–1088.

https://doi.org/10.1002/mrm.10609

Benson, N. C., Butt, O. H., Brainard, D. H., & Aguirre, G. K. (2014). Correction of Distortion in Flattened Representations of the Cortical Surface Allows Prediction of V1-V3 Functional Organization from Anatomy. *PLoS Computational Biology*, *10*(3). https://doi.org/10.1371/journal.pcbi.1003538

Benson, N. C., Butt, O. H., Datta, R., Radoeva, P. D., Brainard, D. H., & Aguirre, G. K. (2012). The retinotopic organization of striate cortex is well predicted by surface topology. *Current Biology*, *22*(21), 2081–2085. https://doi.org/10.1016/j.cub.2012.09.014

Berlim, M. T., Van den Eynde, F., & Daskalakis, Z. J. (2013). Clinical utility of transcranial direct current stimulation (tDCS) for treating major depression: A systematic review and meta-analysis of randomized, double-blind and sham-controlled trials. *Journal of Psychiatric Research*. Elsevier Ltd. https://doi.org/10.1016/j.jpsychires.2012.09.025

Berson, E. L. (1993). Retinitis pigmentosa: The Friedenwald lecture. *Investigative Ophthalmology and Visual Science*, *34*(5), 1659–1676.

Bikson, M., Grossman, P., Thomas, C., Zannou, A. L., Jiang, J., Adnan, T., … Woods, A. J. (2016). Safety of Transcranial Direct Current Stimulation: Evidence Based Update 2016. *Brain Stimulation*, *9*(5), 641–661. https://doi.org/10.1016/j.brs.2016.06.004

Bø, L. (2009). The histopathology of grey matter demyelination in multiple sclerosis. *Acta Neurologica Scandinavica*, *120*(SUPPL. 189), 51–57. https://doi.org/10.1111/j.1600-0404.2009.01216.x

Bock, A. S., Binda, P., Benson, N. C., Bridge, H., Watkins, K. E., & Fine, I. (2015). Resting-State Retinotopic Organization in the Absence of Retinal Input and Visual Experience. *Journal of Neuroscience*, *35*(36), 12366–12382. https://doi.org/10.1523/JNEUROSCI.4715-14.2015

Borges, V. M., Danesh-Meyer, H. V, Black, J. M., & Thompson, B. (2015). Functional effects of unilateral open-angle glaucoma on the primary and extrastriate visual cortex. *Journal of Vision*, *15*(15), 1–14. https://doi.org/10.1167/15.15.9

Boucard, C. C., Hernowo, A. T., Maguire, R. P., Jansonius, N. M., Roerdink, J. B. T. M., Hooymans, J. M. M., & Cornelissen, F. W. (2009). Changes in cortical grey matter density associated with long-standing retinal visual field defects. *Brain : A Journal of*

Neurology, *132*(Pt 7), 1898–1906. https://doi.org/10.1093/brain/awp119

Boucart, M., Dinon, J.-F., Despretz, P., Desmettre, T., Hladiuk, K., & Oliva, A. (2008). Recognition of facial emotion in low vision: a flexible usage of facial features. *Visual Neuroscience*, *25*(4), 603–609. https://doi.org/10.1017/S0952523808080656

Boucart, M., Moroni, C., Szaffarczyk, S., & Tran, T. H. C. (2013). Implicit processing of scene context in macular degeneration. *Investigative Ophthalmology and Visual Science*, *54*(3), 1950–1957. https://doi.org/10.1167/iovs.12-9680

Bridge, H., Cowey, A., Ragge, N., & Watkins, K. (2009). Imaging studies in congenital anophthalmia reveal preservation of brain architecture in "visual" cortex. *Brain : A Journal of Neurology*, *132*(Pt 12), 3467–3480. https://doi.org/10.1093/brain/awp279

Brown, H. D. H., Woodall, R. L., Kitching, R. E., Baseler, H. A., & Morland, A. B. (2016). Using magnetic resonance imaging to assess visual deficits: A review. *Ophthalmic and Physiological Optics*. https://doi.org/10.1111/opo.12293

Brunoni, A. R., Amadera, J., Berbel, B., Volz, M. S., Rizzerio, B. G., & Fregni, F. (2011). A systematic review on reporting and assessment of adverse effects associated with transcranial direct current stimulation. *The International Journal of Neuropsychopharmacology / Official Scientific Journal of the Collegium Internationale Neuropsychopharmacologicum (CINP)*, *14*(8), 1133–1145. https://doi.org/10.1017/S1461145710001690

Brunoni, A. R., Nitsche, M. a, Bolognini, N., Bikson, M., Wagner, T., Merabet, L., … Fregni, F. (2012). Clinical research with transcranial direct current stimulation (tDCS): challenges and future directions. *Brain Stimulation*, *5*(3), 175–195. https://doi.org/10.1016/j.brs.2011.03.002

Burge, W. K., Griffis, J. C., Nenert, R., Elkhetali, A., DeCarlo, D. K., ver Hoef, L. W., … Visscher, K. M. (2016). Cortical thickness in human V1 associated with central vision loss. *Scientific Reports*, *6*(1), 23268. https://doi.org/10.1038/srep23268

Castaldi, E., Cicchini, G. M., Cinelli, L., Biagi, L., Rizzo, S., & Morrone, M. C. (2016). Visual BOLD Response in Late Blind Subjects with Argus II Retinal Prosthesis. *PLOS Biology*, *14*(10), e1002569. https://doi.org/10.1371/journal.pbio.1002569

Castaldi, Elisa, Cicchini, G. M., Falsini, B., Binda, P., & Morrone, M. C. (2019). Residual visual responses in patients with retinitis pigmentosa revealed by functional magnetic

resonance imaging. *Translational Vision Science and Technology*, *8*(6), 44. https://doi.org/10.1167/tvst.8.6.44

Chen, W. W., Wang, N., Cai, S., Fang, Z., Yu, M., Wu, Q., … Gong, Q. (2013). Structural brain abnormalities in patients with primary open-angle glaucoma: A study with 3T MR imaging. *Investigative Ophthalmology and Visual Science*, *54*(1), 545–554. https://doi.org/10.1167/iovs.12-9893

Cheung, S.-H., & Legge, G. E. (2005). Functional and cortical adaptations to central vision loss. *Visual Neuroscience*, *22*(2), 187–201. https://doi.org/10.1017/S0952523805222071

Chow, A Y, Packo, K. H., Pollack, J. S., & Schuchard, R. A. (2003). Subretinal artificial silicon retina microchip implantation in retinitis pigmentosa patients: long term follow-up. *Investigative Ophthalmology & Visual Science*, *44*(13), 4205.

Chow, Alan Y, Chow, V. Y., Packo, K. H., Pollack, J. S., Peyman, G. A., & Schuchard, R. (2004). The artificial silicon retina microchip for the treatment of visionloss from retinitis pigmentosa. *Archives of Ophthalmology*, *122*(4), 460–469.

Cole, E., Gulser, M., Stimpson, K., Bentzley, B., Hawkins, J., Xiao, X., … Williams, N. (2019). Stanford accelerated intelligent neuromodulation therapy for treatment-resistant depression (SAINT-TRD). *Brain Stimulation*, *12*(2), 402. https://doi.org/10.1016/j.brs.2018.12.299

Concerto, C., Lanza, G., Cantone, M., Ferri, R., Pennisi, G., Bella, R., & Aguglia, E. (2015). Repetitive transcranial magnetic stimulation in patients with drug-resistant major depression: A six-month clinical follow-up study. *International Journal of Psychiatry in Clinical Practice*, *19*(4), 252–258. https://doi.org/10.3109/13651501.2015.1084329

Cox, T. M., & Ffytche, D. H. (2014). Negative outcome Charles Bonnet syndrome. *British Journal of Ophthalmology*, *98*(9), 1236–1239. https://doi.org/10.1136/bjophthalmol-2014-304920

Cunningham, S. I., Shi, Y., Weiland, J. D., Falabella, P., Olmos de Koo, L. C., Zacks, D. N., & Tjan, B. S. (2015). Feasibility of Structural and Functional MRI Acquisition with Unpowered Implants in Argus II Retinal Prosthesis Patients: A Case Study. *Translational Vision Science & Technology*, *4*(6), 6. https://doi.org/10.1167/tvst.4.6.6

Czeh, R. S., Casper, A. W., & Segraves, E. C. (1965). A Mathematical Model of Flashblindness, *70*(October), 447–459. https://doi.org/10.1007/BF00639569

da Silva Morgan, K., Taylor, J. P., & ffytche, D. (2020). P9 Treating visual hallucinations in the visually impaired: A non-invasive stimulation pilot study. *Clinical Neurophysiology*, *131*(4), e14–e15. https://doi.org/10.1016/j.clinph.2019.12.120

Dai, H., Morelli, J. N., Ai, F., Yin, D., Hu, C., Xu, D., & Li, Y. (2013). Resting-state functional MRI: Functional connectivity analysis of the visual cortex in primary open-angle glaucoma patients. *Human Brain Mapping*, *34*(10), 2455–2463. https://doi.org/10.1002/hbm.22079

Davis, S. W., Dennis, N. A., Buchler, N. G., White, L. E., Madden, D. J., & Cabeza, R. (2009). Assessing the effects of age on long white matter tracts using diffusion tensor tractography. *NeuroImage*, *46*(2), 530–541. https://doi.org/10.1016/j.neuroimage.2009.01.068

de Hoz, L., & Simons, M. (2015). The emerging functions of oligodendrocytes in regulating neuronal network behaviour. *BioEssays*, *37*(1), 60–69. https://doi.org/10.1002/BIES.201400127

de Zwart, J. A., Silva, A. C., van Gelderen, P., Kellman, P., Fukunaga, M., Chu, R., … Duyn, J. H. (2005). Temporal dynamics of the BOLD fMRI impulse response. *NeuroImage*, *24*(3), 667–677. https://doi.org/10.1016/J.NEUROIMAGE.2004.09.013

Destrieux, C., Fischl, B., Dale, A., & Halgren, E. (2010). Automatic parcellation of human cortical gyri and sulci using standard anatomical nomenclature. *NeuroImage*, *53*(1), 1–15. https://doi.org/10.1016/j.neuroimage.2010.06.010

Dietrich, S., Hertrich, I., Kumar, V., & Ackermann, H. (2015). Experience-related structural changes of degenerated occipital white matter in late-blind Humans-A diffusion tensor imaging study. *PLoS ONE*, *10*(4), e0122863. https://doi.org/10.1371/journal.pone.0122863

Dilks, D. D., Baker, C. I., Peli, E., & Kanwisher, N. (2009). Reorganization of visual processing in macular degeneration is not specific to the "preferred retinal locus". *The Journal of Neuroscience : The Official Journal of the Society for Neuroscience*, *29*(9), 2768–2773. https://doi.org/10.1523/JNEUROSCI.5258-08.2009

Dilks, D. D., Julian, J. B., Peli, E., & Kanwisher, N. (2014). Reorganization of visual

processing in age-related macular degeneration depends on foveal loss. *Optometry and Vision Science : Official Publication of the American Academy of Optometry*, *91*(8), e199-206. https://doi.org/10.1097/OPX.0000000000000325

Dionísio, A., Duarte, I. C., Patrício, M., & Castelo-Branco, M. (2018, January 1). The Use of Repetitive Transcranial Magnetic Stimulation for Stroke Rehabilitation: A Systematic Review. *Journal of Stroke and Cerebrovascular Diseases*. W.B. Saunders. https://doi.org/10.1016/j.jstrokecerebrovasdis.2017.09.008

Dougherty, R. F., Koch, V. M., Brewer, A. A., Fischer, B., Modersitzki, J., & Wandell, B. A. (2003). Visual field representations and locations of visual areas v1/2/3 in human visual cortex. *Journal of Vision*, *3*(10), 586–598. https://doi.org/10.1167/3.10.1

Duncan, R. O., Sample, P. A., Weinreb, R. N., Bowd, C., & Zangwill, L. M. (2007). Retinotopic organization of primary visual cortex in glaucoma: Comparing fMRI measurements of cortical function with visual field loss. *Progress in Retinal and Eye Research*, *26*(1), 38–56. https://doi.org/10.1016/j.preteyeres.2006.10.001

Elbert, T., & Flor, H. (1999). *Magnetoencephalographic investigations of cortical reorganization in humans. Functional Neuroscience: Evoked potentials and magnetic fields (EEG Supplement 49)*.

Engel, S. a., Glover, G. H., & Wandell, B. a. (1997). Retinotopic organization in human visual cortex and the spatial precision of functional MRI. *Cerebral Cortex*, *7*(2), 181–192. https://doi.org/10.1093/cercor/7.2.181

Engel, S. a., Morland, A. B., & Haak, K. V. (2015). Plasticity, and Its Limits, in Adult Human Primary Visual Cortex. *Multisensory Research*, *28*(3–4), 297–307. https://doi.org/10.1163/22134808-00002496

Epstein, R. A. (2008). Parahippocampal and retrosplenial contributions to human spatial navigation. *Trends in Cognitive Sciences*, *12*(10), 388–396. https://doi.org/10.1016/J.TICS.2008.07.004

Epstein, R., & Kanwisher, N. (1998). A cortical representation of the local visual environment. *Nature*, *392*(6676), 598–601. https://doi.org/10.1038/33402

Ferreira, S., Pereira, A. C., Quendera, B., Reis, A., Silva, E. D., & Castelo-Branco, M. (2017). Primary visual cortical remapping in patients with inherited peripheral retinal degeneration. *NeuroImage: Clinical*. https://doi.org/10.1016/j.nicl.2016.12.013

Ffytche, D. H., Howard, R. J., Brammer, M. J., David, A., Woodruff, P., & Williams, S. (1998). The anatomy of conscious vision: An fMRI study of visual hallucinations. *Nature Neuroscience*, *1*(8), 738–742. https://doi.org/10.1038/3738

Filmer, H. L., Dux, P. E., & Mattingley, J. B. (2014). Applications of transcranial direct current stimulation for understanding brain function. *Trends in Neurosciences*, *37*(12), 742–753. https://doi.org/10.1016/j.tins.2014.08.003

Fischl, B., Rajendran, N., Busa, E., Augustinack, J., Hinds, O., Yeo, B. T. T., … Zilles, K. (2008). Cortical Folding Patterns and Predicting Cytoarchitecture. *Cerebral Cortex August*, *18*, 1973–1980. https://doi.org/10.1093/cercor/bhm225

Fjell, A. M., & Walhovd, K. B. (2010). Structural brain changes in aging: Courses, causes and cognitive consequences. *Reviews in the Neurosciences*. https://doi.org/10.1515/REVNEURO.2010.21.3.187

Fjell, A. M., Westlye, L. T., Amlien, I., Espeseth, T., Reinvang, I., Raz, N., … Walhovd, K. B. (2009). High Consistency of Regional Cortical Thinning in Aging across Multiple Samples. https://doi.org/10.1093/cercor/bhn232

Flor, H., Elbertt, T., Knechtt, S., Wienbrucht, C., Pantevt, C., Birbaumer, N., … Taubll, E. (1994). *LETTERS TO NATURE Phantom-limb pain as a perceptual correlate of cortical reorganization following arm amputation. Tulloch, A. J. & Kimbrough, D. I. Tectonics* (Vol. 1). Kiuwer Academic.

Fox, M. D., Buckner, R. L., White, M. P., Greicius, M. D., & Pascual-Leone, A. (2012). Efficacy of Transcranial Magnetic Stimulation Targets for Depression Is Related to Intrinsic Functional Connectivity with the Subgenual Cingulate. *Biological Psychiatry*, *72*(7), 595–603. https://doi.org/10.1016/J.BIOPSYCH.2012.04.028

Fregni, F., Santos, C. M., Myczkowski, M. L., Rigolino, R., Gallucci-Neto, J., Barbosa, E. R., … Marcolin, M. A. (2004). Repetitive transcranial magnetic stimulation is as effective as fluoxetine in the treatment of depression in patients with Parkinson's disease. *Journal of Neurology, Neurosurgery and Psychiatry*, *75*(8), 1171–1174. https://doi.org/10.1136/jnnp.2003.027060

Fregni, Felipe, & Pascual-Leone, A. (2007). Technology insight: noninvasive brain stimulation in neurology-perspectives on the therapeutic potential of rTMS and tDCS. *Nature Clinical Practice. Neurology*, *3*(7), 383–393.

https://doi.org/10.1038/ncpneuro0530

Frezzotti, P., Giorgio, A., Motolese, I., De Leucio, A., Iester, M., Motolese, E., … De Stefano, N. (2014). Structural and functional brain changes beyond visual system in patients with advanced glaucoma. *PLoS ONE*, *9*(8). https://doi.org/10.1371/journal.pone.0105931

Friedman, S. M., Munoz, B., Rubin, G. S., West, S. K., Bandeen-Roche, K., & Fried, L. P. (1999). Characteristics of discrepancies between self-reported visual function and measured reading speed. Salisbury Eye Evaluation Project Team. *Investigative Ophthalmology & Visual Science*, *40*(5), 858–864.

Gandiga, P. C., Hummel, F. C., & Cohen, L. G. (2006). Transcranial DC stimulation (tDCS): A tool for double-blind sham-controlled clinical studies in brain stimulation. *Clinical Neurophysiology*, *117*, 845–850. https://doi.org/10.1016/j.clinph.2005.12.003

Gill, J. S., Georgiou, M., Kalitzeos, A., Moore, A. T., & Michaelides, M. (2019). Progressive cone and cone-rod dystrophies: Clinical features, molecular genetics and prospects for therapy. *British Journal of Ophthalmology*, *103*(5), 711–720. https://doi.org/10.1136/bjophthalmol-2018-313278

Glasser, M. F., Coalson, T. S., Robinson, E. C., Hacker, C. D., Harwell, J., Yacoub, E., … Van Essen, D. C. (2016). A multi-modal parcellation of human cerebral cortex. *Nature*, *536*(7615), 171–178. https://doi.org/10.1038/nature18933

Glasser, M. F., Goyal, M. S., Preuss, T. M., Raichle, M. E., & Van Essen, D. C. (2014). Trends and properties of human cerebral cortex: Correlations with cortical myelin content. *NeuroImage*, *93*, 165–175. https://doi.org/10.1016/j.neuroimage.2013.03.060

Glasser, M. F., & Van Essen, D. C. (2011). Mapping human cortical areas in vivo based on myelin content as revealed by t1- and t2-weighted MRI. *The Journal of Neuroscience : The Official Journal of the Society for Neuroscience*, *31*(32), 11597–11616. https://doi.org/10.1523/JNEUROSCI.2180-11.2011

Glen, F. C., Crabb, D. P., Smith, N. D., Burton, R., & Garway-Heath, D. F. (2012). Do patients with glaucoma have difficulty recognizing faces? *Investigative Ophthalmology and Visual Science*, *53*(7), 3629–3637. https://doi.org/10.1167/iovs.11-8538

Gonzalez, C. (2011). Intravitreal Ranibizumab for retrofoveolar neovascular Age Related Macular Degeneration, in Pseudo vitelliform and/or Drusenoid pigment epithelium

detachment shape. *Acta Ophthalmologica*, *89*(s248), 0–0.
https://doi.org/10.1111/j.1755-3768.2011.344.x

Gothe, J., Brandt, S. A., Irlbacher, K., Röricht, S., Sabel, B. A., & Meyer, B. U. (2002).
Changes in visual cortex excitability in blind subjects as demonstrated by transcranial
magnetic stimulation. *Brain*, *125*(3), 479–490. https://doi.org/10.1093/brain/awf045

Gouws, A. D., Alvarez, I., Watson, D. M., Uesaki, M., Rodgers, J., Rogers, J., & Morland,
A. B. (2014). On the role of suppression in spatial attention: evidence from negative
BOLD in human subcortical and cortical structures. *The Journal of Neuroscience : The
Official Journal of the Society for Neuroscience*, *34*(31), 10347–10360.
https://doi.org/10.1523/JNEUROSCI.0164-14.2014

Graham, S. L., & Klistorner, A. (2013). New magnetic resonance imaging techniques
identify cortical changes in glaucoma. *Clinical & Experimental Ophthalmology*, *41*(1),
3–5. https://doi.org/10.1111/ceo.12043

Greve, D. N., & Fischl, B. (2009). Accurate and robust brain image alignment using
boundary-based registration. *NeuroImage*, *48*(1), 63–72.
https://doi.org/10.1016/j.neuroimage.2009.06.060

Griffis, J. C., Burge, W. K., & Visscher, K. M. (2016). Age-dependent cortical thinning of
peripheral visual field representations in primary visual cortex. *Frontiers in Aging
Neuroscience*, *8*(OCT), 1–7. https://doi.org/10.3389/fnagi.2016.00248

Grill-Spector, K., & Weiner, K. S. (2014). The functional architecture of the ventral
temporal cortex and its role in categorization. *Nature Reviews Neuroscience*, *15*(8),
536–548. https://doi.org/10.1038/nrn3747

Grossi, D., Soricelli, A., Ponari, M., Salvatore, E., Quarantelli, M., Prinster, A., & Trojano,
L. (2014). Structural connectivity in a single case of progressive prosopagnosia: The
role of the right inferior longitudinal fasciculus. *Cortex*, *56*, 111–120.
https://doi.org/10.1016/j.cortex.2012.09.010

Gupta, N, Greenberg, G., de Tilly, L. N., Gray, B., Polemidiotis, M., Yucel, Y. H., & Yücel,
Y. H. (2009). Atrophy of the lateral geniculate nucleus in human glaucoma detected
by magnetic resonance imaging. *The British Journal of Ophthalmology*, *93*(1), 56–60.
https://doi.org/10.1136/bjo.2008.138172

Gupta, Neeru, & Yücel, Y. H. (2007). What Changes Can We Expect in the Brain of

Glaucoma Patients? *Survey of Ophthalmology*, *52*(6 SUPPL.), 122–126. https://doi.org/10.1016/j.survophthal.2007.08.006

Halko, M. A., Eldaief, M. C., & Pascual-Leone, A. (2013). Noninvasive brain stimulation in the study of the human visual system. In *Journal of Glaucoma* (Vol. 22, pp. 1–5). https://doi.org/10.1097/IJG.0b013e3182934b31

Hanson, R. L. W., Gale, R. P., Gouws, A. D., Airody, A., Scott, M. T. W., Akthar, F., … Morland, A. B. (2019). Following the status of visual cortex over time in patients with macular degeneration reveals atrophy of visually deprived brain regions. *Investigative Ophthalmology and Visual Science*, *60*(15), 5045–5051. https://doi.org/10.1167/iovs.18-25823

Hasson, U., Andric, M., Atilgan, H., & Collignon, O. (2016). Congenital blindness is associated with large-scale reorganization of anatomical networks. *NeuroImage*, *128*, 362–372. https://doi.org/10.1016/j.neuroimage.2015.12.048

Hasson, U., Levy, I., Behrmann, M., Hendler, T., & Malach, R. (2002). Eccentricity bias as an organizing principle for human high-order object areas. *Neuron*, *34*(3), 479–490. https://doi.org/10.1016/S0896-6273(02)00662-1

Haxby, J. V., Hoffman, E. A., & Gobbini, M. I. (2000). The distributed human neural system for face perception. *Trends in Cognitive Sciences*, *4*(6), 223–233. https://doi.org/10.1016/S1364-6613(00)01482-0

Heier, J. S., Brown, D. M., Chong, V., Korobelnik, J. F., Kaiser, P. K., Nguyen, Q. D., … Schmidt-Erfurth, U. (2012). Intravitreal aflibercept (VEGF trap-eye) in wet age-related macular degeneration. *Ophthalmology*, *119*(12), 2537–2548. https://doi.org/10.1016/j.ophtha.2012.09.006

Henriksson, L., Karvonen, J., Salminen-Vaparanta, N., Railo, H., & Vanni, S. (2012). Retinotopic Maps, Spatial Tuning, and Locations of Human Visual Areas in Surface Coordinates Characterized with Multifocal and Blocked fMRI Designs. *PLoS ONE*, *7*(5), e36859. https://doi.org/10.1371/journal.pone.0036859

Hernowo, A. T., Boucard, C. C., Jansonius, N. M., Hooymans, J. M. M., & Cornelissen, F. W. (2011). Automated morphometry of the visual pathway in primary open-angle glaucoma. *Investigative Ophthalmology and Visual Science*, *52*(5), 2758–2766. https://doi.org/10.1167/iovs.10-5682

Hernowo, A. T., Prins, D., Baseler, H. a., Plank, T., Gouws, A. D., Hooymans, J. M. M., … Cornelissen, F. W. (2014). Morphometric analyses of the visual pathways in macular degeneration. *Cortex; a Journal Devoted to the Study of the Nervous System and Behavior*, *56*, 99–110. https://doi.org/10.1016/j.cortex.2013.01.003

Hill, R. A., Patel, K. D., Goncalves, C. M., Grutzendler, J., & Nishiyama, A. (2014). Modulation of oligodendrocyte generation during a critical temporal window after NG2 cell division. *Nature Neuroscience*, *17*(11), 1518–1527. https://doi.org/10.1038/nn.3815

Hinds, O. P., Rajendran, N., Polimeni, J. R., Augustinack, J. C., Wiggins, G., Wald, L. L., … Fischl, B. (2008). Accurate prediction of V1 location from cortical folds in a surface coordinate system. *NeuroImage*, *39*(4), 1585–1599. https://doi.org/10.1016/j.neuroimage.2007.10.033

Hoffmann, M. B., & Dumoulin, S. O. (2015). Congenital visual pathway abnormalities: a window onto cortical stability and plasticity. *Trends in Neurosciences, 38*(1), 55–65. https://doi.org/10.1016/j.tins.2014.09.005

Hoffmann, M. B., Tolhurst, D. J., Moore, A. T., & Morland, A. B. (2003). Organization of the visual cortex in human albinism. *The Journal of Neuroscience : The Official Journal of the Society for Neuroscience*, *23*(26), 8921–8930.

Hofstetter, S., Sabbah, N., Mohand-Saïd, S., Sahel, J.-A., Habas, C., Safran, A. B., & Amedi, A. (2019). The development of white matter structural changes during the process of deterioration of the visual field. *Scientific Reports*, *9*(1), 2085. https://doi.org/10.1038/s41598-018-38430-5

Howseman, a M., & Bowtell, R. W. (1999). Functional magnetic resonance imaging: imaging techniques and contrast mechanisms. *Philosophical Transactions of the Royal Society of London. Series B, Biological Sciences*, *354*(1387), 1179–1194. https://doi.org/10.1098/rstb.1999.0473

Hubel, D. H., & Wiesel, T. N. (1965). Binocular interaction in striate cortex of kittens reared with artificial squint. *Journal of Neurophysiology*, *28*(6), 1041–1059. https://doi.org/10.1152/jn.1965.28.6.1041

Hummel, F. C., & Cohen, L. G. (2006). Non-invasive brain stimulation: a new strategy to improve neurorehabilitation after stroke? *Lancet Neurology*, *5*(August), 708–712.

https://doi.org/10.1016/S1474-4422(06)70525-7

Ikram, M. K., Cheung, C. Y., Wong, T. Y., & Chen, C. P. L. H. (2012). Retinal pathology as biomarker for cognitive impairment and Alzheimer's disease. *Journal of Neurology, Neurosurgery and Psychiatry*, *83*(9), 917–922. https://doi.org/10.1136/jnnp-2011-301628

Jbabdi, S., Sotiropoulos, S. N., Savio, A. M., Graña, M., & Behrens, T. E. J. (2012). Model-based analysis of multishell diffusion MR data for tractography: How to get over fitting problems. *Magnetic Resonance in Medicine*, *68*(6), 1846–1855. https://doi.org/10.1002/mrm.24204

Jenkinson, M., Bannister, P., Brady, M., & Smith, S. (2002). Improved optimization for the robust and accurate linear registration and motion correction of brain images. *NeuroImage*, *17*(2), 825–841. https://doi.org/10.1016/S1053-8119(02)91132-8

Jenkinson, M., Beckmann, C. F., Behrens, T. E. J., Woolrich, M. W., & Smith, S. M. (2012). Review FSL. *NeuroImage*, *62*(2), 782–790. https://doi.org/10.1016/j.neuroimage.2011.09.015

Kamps, F. S., Hendrix, C. L., Brennan, P. A., & Dilks, D. D. (2020). Connectivity at the origins of domain specificity in the cortical face and place networks. *Proceedings of the National Academy of Sciences*, 201911359. https://doi.org/10.1073/pnas.1911359117

Kanwisher, N., McDermott, J., & Chun, M. M. (1997). The fusiform face area: a module in human extrastriate cortex specialized for face perception. *The Journal of Neuroscience : The Official Journal of the Society for Neuroscience*, *17*(11), 4302–4311. https://doi.org/10.1098/Rstb.2006.1934

Karl, A., Birbaumer, N., Lutzenberger, W., Cohen, L. G., & Flor, H. (2001). Reorganization of Motor and Somatosensory Cortex in Upper Extremity Amputees with Phantom Limb Pain. *Journal of Neuroscience*, *21*(10), 3609–3618. https://doi.org/10.1523/JNEUROSCI.21-10-03609.2001

Lang, N., Siebner, H. R., Chadaide, Z., Boros, K., Nitsche, M. A., Rothwell, J. C., … Antal, A. (2007). Bidirectional modulation of primary visual cortex excitability: A combined tDCS and rTMS study. *Investigative Ophthalmology and Visual Science*, *48*(12), 5782–5787. https://doi.org/10.1167/iovs.07-0706

Leggett, L. E., Soril, L. J. J., Coward, S., Lorenzetti, D. L., MacKean, G., & Clement, F. M. (2015). Repetitive Transcranial Magnetic Stimulation for Treatment-Resistant Depression in Adult and Youth Populations: A Systematic Literature Review and Meta-Analysis. *The Primary Care Companion for CNS Disorders*, *17*(6). https://doi.org/10.4088/PCC.15r01807

Lemaitre, H., Goldman, A., Sambataro, F., Verchinski, B., Meyer-Lindenberg, A., Weinberger, D., & Mattay, V. (2012). Normal age-related brain morphometric changes: Nonuniformity across cortical thickness, surface area and grey matter volume? *Neurobiology of Aging*, *33*(3), 617.e1. https://doi.org/10.1016/J.NEUROBIOLAGING.2010.07.013

Lenoble, Q., Lek, J. J., & Mckendrick, A. M. (2016). Visual object categorisation in people with glaucoma. *British Journal of Ophthalmology*, *100*(11), 1585–1590. https://doi.org/10.1136/bjophthalmol-2015-308289

Lerner, Y., Hendler, T., Malach, R., Harel, M., Leiba, H., Stolovitch, C., & Pianka, P. (2006). Selective fovea-related deprived activation in retinotopic and high-order visual cortex of human amblyopes. *NeuroImage*, *33*(1), 169–179. https://doi.org/10.1016/j.neuroimage.2006.06.026

Levy, I., Hasson, U., Avidan, G., Hendler, T., & Malach, R. (2001). Center–periphery organization of human object areas. *Nature Neuroscience*, *4*(5), 533–539. https://doi.org/10.1038/87490

Li, K., Lu, C., Huang, Y., Yuan, L., Zeng, D., & Wu, K. (2014). Alteration of Fractional Anisotropy and Mean Diffusivity in Glaucoma: Novel Results of a Meta-Analysis of Diffusion Tensor Imaging Studies. *PLoS ONE*, *9*(5), e97445. https://doi.org/10.1371/journal.pone.0097445

Lim, L. S., Mitchell, P., Seddon, J. M., Holz, F. G., & Wong, T. Y. (2012). Age-related macular degeneration. *The Lancet*, *379*(9827), 1728–1738. https://doi.org/10.1016/S0140-6736(12)60282-7

Lipinski, D. M., Thake, M., & MacLaren, R. E. (2013). Clinical applications of retinal gene therapy. *Progress in Retinal and Eye Research*, *32*(1), 22–47. https://doi.org/10.1016/j.preteyeres.2012.09.001

Logan, A. J., Wilkinson, F., Wilson, H. R., Gordon, G. E., & Loffler, G. (2016). The

Caledonian face test: A new test of face discrimination. *Vision Research*, *119*, 29–41. https://doi.org/10.1016/j.visres.2015.11.003

Lois, N., Halfyard, A. S., Bird, A. C., Holder, G. E., & Fitzke, F. W. (2004). Fundus autofluorescence in stargardt macular dystrophy-fundus flavimaculatus. *American Journal of Ophthalmology*, *138*(1), 55–63. https://doi.org/10.1016/j.ajo.2004.02.056

Lu, P. H., Lee, G. J., Raven, E. P., Tingus, K., Khoo, T., Thompson, P. M., & Bartzokis, G. (2011). Age-related slowing in cognitive processing speed is associated with myelin integrity in a very healthy elderly sample. *Journal of Clinical and Experimental Neuropsychology*, *33*(10), 1059–1068. https://doi.org/10.1080/13803395.2011.595397

Machado, A., Carvalho Pereira, A., Ferreira, F., Ferreira, S., Quendera, B., Silva, E., & Castelo-Branco, M. (2017). Structure-function correlations in Retinitis Pigmentosa patients with partially preserved vision: A voxel-based morphometry study. *Scientific Reports*, *7*(1), 1–10. https://doi.org/10.1038/s41598-017-11317-7

Maguire, E. (2001). The retrosplenial contribution to human navigation: A review of lesion and neuroimaging findings. *Scandinavian Journal of Psychology*, *42*(3), 225–238. https://doi.org/10.1111/1467-9450.00233

Maguire, E. A., Burgess, N., Donnett, J. G., Frackowiak, R. S. J., Frith, C. D., & O'keefe, J. (1998). *Knowing Where and Getting There: A Human Navigation. Source: Science, New Series* (Vol. 280).

Mäkelä, P., Näsänen, R., Rovamo, J., Melmoth, D., Makela, P., & Ma, P. (2001). Identification of facial images in peripheral vision. *Vision Research*, *41*(5), 599–610. https://doi.org/10.1016/S0042-6989(00)00259-5

Malach, R., Levy, I., & Hasson, U. (2002, April 1). The topography of high-order human object areas. *Trends in Cognitive Sciences.* Trends Cogn Sci. https://doi.org/10.1016/S1364-6613(02)01870-3

Malania, M., Konra, J., Jägle, H., Werner, J. S., & Greenlee, M. W. (2017). Compromised integrity of central visual pathways in patients with macular degeneration. *Investigative Ophthalmology and Visual Science*, *58*(7), 2939–2947. https://doi.org/10.1167/iovs.16-21191

Martial, C., Larroque, S. K., Cavaliere, C., Wannez, S., Annen, J., Kupers, R., … Perri, C. Di. (2019). Resting-state functional connectivity and cortical thickness characterization

of a patient with Charles Bonnet syndrome. *PLoS ONE*, *14*(7), e0219656.
https://doi.org/10.1371/journal.pone.0219656

Masuda, Y., Dumoulin, S. O., Nakadomari, S., & Wandell, B. a. (2008). V1 projection zone
signals in human macular degeneration depend on task, not stimulus. *Cerebral
Cortex*, *18*(11), 2483–2493. https://doi.org/10.1093/cercor/bhm256

Masuda, Y., Horiguchi, H., Dumoulin, S. O., Furuta, A., Miyauchi, S., Nakadomari, S., &
Wandell, B. a. (2010). Task-dependent V1 responses in human retinitis pigmentosa.
Investigative Ophthalmology and Visual Science, *51*(10), 5356–5364.
https://doi.org/10.1167/iovs.09-4775

Masuda, Y., Takemura, H., Terao, M., Miyazaki, A., Ogawa, S., Horiguchi, H., … Amano,
K. (2021). V1 Projection Zone Signals in Human Macular Degeneration Depend on
Task Despite Absence of Visual Stimulus. *Current Biology*, *31*(2), 406-412.e3.
https://doi.org/10.1016/j.cub.2020.10.034

McCarthy, G., Puce, A., Gore, J. C., & Allison, T. (1997). Face-specific processing in the
human fusiform gyrus. *Journal of Cognitive Neuroscience*, *9*(5), 605–610.
https://doi.org/10.1162/jocn.1997.9.5.605

McGinnis, S. M., Brickhouse, M., Pascual, B., & Dickerson, B. C. (2011). Age-Related
Changes in the Thickness of Cortical Zones in Humans. *Brain Topography*, *24*(3–4),
279–291. https://doi.org/10.1007/s10548-011-0198-6

Miki, A., Nakajima, T., Takagi, M., Shirakashi, M., & Abe, H. (1996). Detection of visual
dysfunction in optic atrophy by functional magnetic resonance imaging during
monocular visual stimulation. *American Journal of Ophthalmology*, *122*(3), 404–415.
https://doi.org/10.1016/S0002-9394(14)72067-7

Millington, R. S., Ajina, S., & Bridge, H. (2014). Novel brain imaging approaches to
understand acquired and congenital neuro-ophthalmological conditions. *Current
Opinion in Neurology*, *27*(1), 92–97. https://doi.org/10.1097/WCO.0000000000000050

Moody, A., Mindell, J., & Faulding, S. (2016). Health Survey for England 2016 Prescribed
medicines. *NHS Digital*, (December), 1–28.

Morland, A. B. (2015). Organization of the Central Visual Pathways Following Field
Defects Arising from Congenital, Inherited, and Acquired Eye Disease. *Annual Review
of Vision Science*, *1*(1), 329–350. https://doi.org/10.1146/annurev-vision-082114-

035600

Muckli, L., De Martino, F., Vizioli, L., Petro, L. S., Smith, F. W., Ugurbil, K., … Yacoub, E. (2015). Contextual Feedback to Superficial Layers of V1. *Current Biology*, *25*(20), 2690–2695. https://doi.org/10.1016/j.cub.2015.08.057

Murphy, K. M., Mancini, S. J., Clayworth, K. V., Arbabi, K., & Beshara, S. (2020). Experience-Dependent Changes in Myelin Basic Protein Expression in Adult Visual and Somatosensory Cortex. *Frontiers in Cellular Neuroscience*, *14*(March), 1–9. https://doi.org/10.3389/fncel.2020.00056

Murphy, M. C., Conner, I. P., Teng, C. Y., Lawrence, J. D., Safiullah, Z., Wang, B., … Chan, K. C. (2016). Retinal Structures and Visual Cortex Activity are Impaired Prior to Clinical Vision Loss in Glaucoma. *Scientific Reports*, *6*(1), 31464. https://doi.org/10.1038/srep31464

Murty, N. A. R., Teng, S., Beeler, D., Mynick, A., Oliva, A., & Kanwisher, N. (2020). Visual experience is not necessary for the development of face-selectivity in the lateral fusiform gyrus. *Proceedings of the National Academy of Sciences of the United States of America*, *117*(37), 23011–23020. https://doi.org/10.1073/pnas.2004607117

Nakamura, K., Kawashima, R., Sato, N., Nakamura, A., Sugiura, M., Kato, T., … Zilles, K. (2000). Functional delineation of the human occipito-temporal areas related to face and scene processing. A PET study. *Brain : A Journal of Neurology*, *123 (Pt 9)*, 1903–1912.

Natu, V. S., Gomez, J., Barnett, M., Jeska, B., Kirilina, E., Jaeger, C., … Grill-Spector, K. (2019). Apparent thinning of human visual cortex during childhood is associated with myelination. *Proceedings of the National Academy of Sciences of the United States of America*, *116*(41), 20750–20759. https://doi.org/10.1073/pnas.1904931116

NICE. (2018). Age-related macular degeneration, (January 2018).

Nir, Y., Hasson, U., Levy, I., Yeshurun, Y., & Malach, R. (2006). Widespread functional connectivity and fMRI fluctuations in human visual cortex in the absence of visual stimulation. *NeuroImage*, *30*(4), 1313–1324. https://doi.org/10.1016/j.neuroimage.2005.11.018

Nooij, R. P., Hoving, E. W., van Hulzen, A. L. J., Cornelissen, F. W., & Renken, R. J. (2015). Preservation of the optic radiations based on comparative analysis of diffusion

tensor imaging tractography and anatomical dissection. *Frontiers in Neuroanatomy*, *9*(AUGUST), 96. https://doi.org/10.3389/fnana.2015.00096

O'Donnell, L. J., & Westin, C. F. (2011, April). An introduction to diffusion tensor image analysis. *Neurosurgery Clinics of North America*. NIH Public Access. https://doi.org/10.1016/j.nec.2010.12.004

Office for National Statistics. (2018). Overview of the UK Population: November 2018, (November), 14.

Ogawa, S., Takemura, H., Horiguchi, H., Terao, M., Haji, T., Pestilli, F., … Masuda, Y. (2014). White matter consequences of retinal receptor and ganglion cell damage. *Investigative Ophthalmology & Visual Science*, *55*(10), 6976–6986. https://doi.org/10.1167/iovs.14-14737

Ohno, N., Murai, H., Suzuki, Y., Kiyosawa, M., Tokumaru, A. M., Ishii, K., & Ohno-Matsui, K. (2015). Alteration of the optic radiations using diffusiontensor MRI in patients with retinitis pigmentosa. *British Journal of Ophthalmology*, *99*(8), 1051–1054. https://doi.org/10.1136/bjophthalmol-2014-305809

Olivo, G., Melillo, P., Cocozza, S., D'Alterio, F. M., Prinster, A., Testa, F., … Quarantelli, M. (2015). Cerebral involvement in stargardt's disease: A VBM and TBSS study. *Investigative Ophthalmology and Visual Science*, *56*(12), 7388–7397. https://doi.org/10.1167/iovs.15-16899

Olman, C. A., Inati, S., & Heeger, D. J. (2007). The effect of large veins on spatial localization with GE BOLD at 3 T: Displacement, not blurring. *NeuroImage*, *34*(3), 1126–1135. https://doi.org/10.1016/J.NEUROIMAGE.2006.08.045

Owsley, C. (2011). Aging and Vision. *Vision Research*, *51*(13), 1610. https://doi.org/10.1016/J.VISRES.2010.10.020

Pan, W. J., Wu, G., Li, C. X., Lin, F., Sun, J., & Lei, H. (2007). Progressive atrophy in the optic pathway and visual cortex of early blind Chinese adults: A voxel-based morphometry magnetic resonance imaging study. *NeuroImage*, *37*(1), 212–220. https://doi.org/10.1016/j.neuroimage.2007.05.014

Park, H. J., Lee, J. D., Kim, E. Y., Park, B., Oh, M. K., Lee, S. C., & Kim, J. J. (2009). Morphological alterations in the congenital blind based on the analysis of cortical thickness and surface area. *NeuroImage*, *47*(1), 98–106.

https://doi.org/10.1016/j.neuroimage.2009.03.076

Pascual-Leone, A., Bartres-Faz, D., & Keenan, J. P. (1999). Transcranial magnetic stimulation: Studying the brain-behaviour relationship by induction of "virtual lesions." *Philosophical Transactions of the Royal Society B: Biological Sciences*, *354*(1387), 1229–1238. https://doi.org/10.1098/rstb.1999.0476

Pascual-Leone, A., Rubio, B., Pallardó, F., & Catalá, M. D. (1996). Rapid-rate transcranial magnetic stimulation of left dorsolateral prefrontal cortex in drug-resistant depression. *Lancet*, *348*(9022), 233–237. https://doi.org/10.1016/S0140-6736(96)01219-6

Patriat, R., Molloy, E. K., Meier, T. B., Kirk, G. R., Nair, V. A., Meyerand, M. E., … Birn, R. M. (2013). The effect of resting condition on resting-state fMRI reliability and consistency: A comparison between resting with eyes open, closed, and fixated. *NeuroImage*, *78*, 463–473. https://doi.org/10.1016/j.neuroimage.2013.04.013

Peters, A. (2002). The effects of normal aging on myelin and nerve fibers: A review - 2002 Peters JNeurocytol Review.pdf. *Journal of Neurocytology*, *31*(8–9), 581–593.

Petro, L. S., Vizioli, L., & Muckli, L. (2014). Contributions of cortical feedback to sensory processing in primary visual cortex. *Frontiers in Psychology*, *5*(OCT), 1–8. https://doi.org/10.3389/fpsyg.2014.01223

Peyrin, C., Ramanoël, S., Roux-Sibilon, A., Chokron, S., & Hera, R. (2017). Scene perception in age-related macular degeneration: Effect of spatial frequencies and contrast in residual vision. *Vision Research*, *130*, 36–47. https://doi.org/10.1016/j.visres.2016.11.004

Philip, N. S., Barredo, J., Aiken, E., & Carpenter, L. L. (2018). Neuroimaging Mechanisms of Therapeutic Transcranial Magnetic Stimulation for Major Depressive Disorder. *Biological Psychiatry: Cognitive Neuroscience and Neuroimaging*, *3*(3), 211–222. https://doi.org/10.1016/J.BPSC.2017.10.007

Plank, T., Frolo, J., Brandl-Rühle, S., Renner, A. B., Hufendiek, K., Helbig, H., & Greenlee, M. W. (2011). Gray matter alterations in visual cortex of patients with loss of central vision due to hereditary retinal dystrophies. *NeuroImage*, *56*(3), 1556–1565. https://doi.org/10.1016/j.neuroimage.2011.02.055

Plank, T., Frolo, J., Brandl-Rühle, S., Renner, A. B., Jägle, H., & Greenlee, M. W. (2017). FMRI with central vision loss: Effects of fixation locus and stimulus type. *Optometry*

and Vision Science. https://doi.org/10.1097/OPX.0000000000001047

Poreisz, C., Boros, K., Antal, A., & Paulus, W. (2007). Safety aspects of transcranial direct current stimulation concerning healthy subjects and patients. *Brain Research Bulletin*, *72*(4–6), 208–214. https://doi.org/10.1016/j.brainresbull.2007.01.004

Prins, D., Hernowo, A., Baseler, H., Plank, T., Greenlee, M., Morland, T., & Cornelissen, F. (2011). White matter in early visual pathway structures is reduced in patients with macular degeneration. In *Perception* (Vol. 40, pp. 48–48). Pion Ltd.

Prins, Doety, Plank, T., Baseler, H. A., Gouws, A. D., Beer, A., Morland, A. B., … Cornelissen, F. W. (2016). Surface-based analyses of anatomical properties of the visual cortex in macular degeneration. *PLoS ONE*, *11*(1), 1–14. https://doi.org/10.1371/journal.pone.0146684

Quigley, H. A. (2006). The number of people with glaucoma worldwide in 2010 and 2020. *British Journal of Ophthalmology*, *90*(3), 262–267. https://doi.org/10.1136/bjo.2005.081224

Ramanoël, S., Chokron, S., Hera, R., Kauffmann, L., Chiquet, C., Krainik, A., & Peyrin, C. (2018). Age-related macular degeneration changes the processing of visual scenes in the brain. *Visual Neuroscience*, *35*, E006. https://doi.org/10.1017/S0952523817000372

Raz, N., Shear-Yashuv, G., Backner, Y., Bick, A. S., & Levin, N. (2015). Temporal aspects of visual perception in demyelinative diseases. *Journal of the Neurological Sciences*, *357*(1–2), 235–239. https://doi.org/10.1016/j.jns.2015.07.037

Raz, Naftali, Lindenberger, U., Rodrigue, K. M., Kennedy, K. M., Head, D., Williamson, A., … Acker, J. D. (2005). Regional brain changes in aging healthy adults: General trends, individual differences and modifiers. *Cerebral Cortex*, *15*(11), 1676–1689. https://doi.org/10.1093/cercor/bhi044

Reislev, N. L., Dyrby, T. B., Siebner, H. R., Kupers, R., & Ptito, M. (2016). Simultaneous Assessment of White Matter Changes in Microstructure and Connectedness in the Blind Brain. *Neural Plasticity*, *2016*. https://doi.org/10.1155/2016/6029241

Reuter, M., & Fischl, B. (2011). Avoiding asymmetry-induced bias in longitudinal image processing. *NeuroImage*, *57*(1), 19–21. https://doi.org/10.1016/j.neuroimage.2011.02.076

Reuter, M., Rosas, H. D., & Fischl, B. (2010). Accurate Inverse Consistent Robust Registration. *NeuroImage*, *53*(4), 1181–1196. https://doi.org/10.1016/j.neuroimage.2010.07.020

Reuter, M., Schmansky, N. J., Rosas, H. D., & Fischl, B. (2012). Within-subject template estimation for unbiased longitudinal image analysis. *NeuroImage*, *61*(4), 1402–1418. https://doi.org/10.1016/J.NEUROIMAGE.2012.02.084

Rokem, A., Bock, A. S., Scherf, K. S., Wandell, B. A., Bridge, H., Takemura, H., … Pestilli, F. (2017). The visual white matter : The application of diffusion MRI and fiber tractography to vision science. *Journal of Vision*, *17*(2), 1–30. https://doi.org/10.1167/17.2.4.doi

Romero Lauro, L. J., Rosanova, M., Mattavelli, G., Convento, S., Pisoni, A., Opitz, A., … Vallar, G. (2014). TDCS increases cortical excitability: Direct evidence from TMS-EEG. *Cortex; a Journal Devoted to the Study of the Nervous System and Behavior*, *58*, 99–111. https://doi.org/10.1016/j.cortex.2014.05.003

Rossi, S., Hallett, M., Rossini, P. M., & Pascual-Leone, A. (2009). Safety, ethical considerations, and application guidelines for the use of transcranial magnetic stimulation in clinical practice and research. *Clinical Neurophysiology : Official Journal of the International Federation of Clinical Neurophysiology*, *120*(12), 2008–2039. https://doi.org/10.1016/j.clinph.2009.08.016

Rostron, E., & McKibbin, M. (2012). Visual impairment certification secondary to ARMD in Leeds, 2005-2010: is the incidence falling? *Eye (London, England)*, *26*(7), 933–936. https://doi.org/10.1038/eye.2012.61

Roux-Sibilon, A., Rutgé, F., Aptel, F., Attye, A., Guyader, N., Boucart, M., … Peyrin, C. (2018). Scene and human face recognition in the central vision of patients with glaucoma. *PLoS ONE*, *13*(2), 1–19. https://doi.org/10.1371/journal.pone.0193465

Sabbah, N., Sanda, N., Authié, C. N., Mohand-Saïd, S., Sahel, J.-A., Habas, C., … Safran, A. B. (2017). Reorganization of early visual cortex functional connectivity following selective peripheral and central visual loss. *Scientific Reports*, *7*(August 2016), 43223. https://doi.org/10.1038/srep43223

Sabeti, F., James, A. C., Essex, R. W., & Maddess, T. (2013). Dichoptic multifocal visual evoked potentials identify local retinal dysfunction in age-related macular

degeneration. *Documenta Ophthalmologica*, *126*(2), 125–136.
https://doi.org/10.1007/s10633-012-9366-6

Salat, D. H., Buckner, R. L., Snyder, A. Z., Greve, D. N., Desikan, R. S. R., Busa, E., …
Fischl, B. (2004). Thinning of the cerebral cortex in aging. *Cerebral Cortex*, *14*(7),
721–730. https://doi.org/10.1093/cercor/bhh032

Sanda, N., Cerliani, L., Authié, C. N., Sabbah, N., Sahel, J. A., Habas, C., … Thiebaut de
Schotten, M. (2018). Visual brain plasticity induced by central and peripheral visual
field loss. *Brain Structure and Function*, *223*(7). https://doi.org/10.1007/s00429-018-
1700-7

Santhouse, A. M., Howard, R. J., & Ffytche, D. H. (2000). Visual hallucinatory syndromes
and the anatomy of the visual brain. *Brain*, *123*(10), 2055–2064.
https://doi.org/10.1093/brain/123.10.2055

Schaie, K. W. (2005). What Can We Learn From Longitudinal Studies of Adult
Development? *Research in Human Development*, *2*(3), 133–158.
https://doi.org/10.1207/s15427617rhd0203_4

Schoth, F., Burgel, U., Dorsch, R., Reinges, M. H. T., & Krings, T. (2006). Diffusion tensor
imaging in acquired blind humans. *Neuroscience Letters*, *398*(3), 178–182.
https://doi.org/10.1016/j.neulet.2005.12.088

Schumacher, E. H., Jacko, J. a, Primo, S. a, Main, K. L., Moloney, K. P., Kinzel, E. N., &
Ginn, J. (2008). Reorganization of visual processing is related to eccentric viewing in
patients with macular degeneration. *Restorative Neurology and Neuroscience*, *26*(4–
5), 391–402.

Senthil, M. P., Khadka, J., Gilhotra, J. S., Simon, S., & Pesudovs, K. (2017). Exploring the
quality of life issues in people with retinal diseases: A qualitative study. *Journal of
Patient-Reported Outcomes*, *1*(2017). https://doi.org/10.1186/s41687-017-0023-4

Shiozawa, P., Fregni, F., Benseñor, I. M., Lotufo, P. A., Berlim, M. T., Daskalakis, J. Z., …
Brunoni, A. R. (2014). Transcranial direct current stimulation for major depression: an
updated systematic review and meta-analysis. *The International Journal of
Neuropsychopharmacology*, *17*(09), 1443–1452.
https://doi.org/10.1017/S1461145714000418

Shu, N., Li, J., Li, K., Yu, C., & Jiang, T. (2009). Abnormal diffusion of cerebral white

matter in early blindness. *Human Brain Mapping*, *30*(1), 220–227. https://doi.org/10.1002/hbm.20507

Simons, M., & Nave, K. A. (2016, January 1). Oligodendrocytes: Myelination and axonal support. *Cold Spring Harbor Perspectives in Biology*. Cold Spring Harbor Laboratory Press. https://doi.org/10.1101/cshperspect.a020479

Singer, M., & Bahadorani, S. (2017). Recent advances in the management and understanding of macular degeneration. *F1000Research*. Faculty of 1000 Ltd. https://doi.org/10.12688/f1000research.10998.1

Smirnakis, S. M., Brewer, A. a, Schmid, M. C., Tolias, A. S., Schüz, A., Augath, M., … Logothetis, N. K. (2005). Lack of long-term cortical reorganization after macaque retinal lesions. *Nature*, *435*(7040), 300–307. https://doi.org/10.1038/nature03495

Smith, F. W., & Muckli, L. (2010). Nonstimulated early visual areas carry information about surrounding context. *Proceedings of the National Academy of Sciences*, *107*(46), 20099–20103. https://doi.org/10.1073/pnas.1000233107

Smith, S. M. (2002). Fast robust automated brain extraction. *Human Brain Mapping*, *17*(3), 143–155. https://doi.org/10.1002/hbm.10062

Smith, S. M., Jenkinson, M., Johansen-Berg, H., Rueckert, D., Nichols, T. E., Mackay, C. E., … Behrens, T. E. J. (2006). Tract-based spatial statistics: Voxelwise analysis of multi-subject diffusion data. *NeuroImage*, *31*(4), 1487–1505. https://doi.org/10.1016/j.neuroimage.2006.02.024

Smith, S. M., Jenkinson, M., Woolrich, M. W., Beckmann, C. F., Behrens, T. E. J., Johansen-Berg, H., … Matthews, P. M. (2004). Advances in functional and structural MR image analysis and implementation as FSL. In *NeuroImage* (Vol. 23). https://doi.org/10.1016/j.neuroimage.2004.07.051

Song, S.-K., Sun, S.-W., Ju, W.-K., Lin, S.-J., Cross, A. H., & Neufeld, A. H. (2003). Diffusion tensor imaging detects and differentiates axon and myelin degeneration in mouse optic nerve after retinal ischemia. *Neuroimage*, *20*(3), 1714–1722.

Song, S. K., Sun, S. W., Ramsbottom, M. J., Chang, C., Russell, J., & Cross, A. H. (2002). Dysmyelination revealed through MRI as increased radial (but unchanged axial) diffusion of water. *NeuroImage*, *17*(3), 1429–1436. https://doi.org/10.1006/nimg.2002.1267

Song, S. K., Yoshino, J., Le, T. Q., Lin, S. J., Sun, S. W., Cross, A. H., & Armstrong, R. C. (2005). Demyelination increases radial diffusivity in corpus callosum of mouse brain. *NeuroImage*, *26*(1), 132–140. https://doi.org/10.1016/j.neuroimage.2005.01.028

Stagg, C., & Nitsche, M. (2011). Physiological basis of transcranial direct current stimulation. *The Neuroscientist : A Review Journal Bringing Neurobiology, Neurology and Psychiatry*, *17*(1), 37–53. https://doi.org/10.1177/1073858410386614

Stingl, K., Bartz-Schmidt, K. U., Besch, D., Chee, C. K., Cottriall, C. L., Gekeler, F., … Zrenner, E. (2015). Subretinal Visual Implant Alpha IMS--Clinical trial interim report. *Vision Research*, *111*(Pt B), 149–160. https://doi.org/10.1016/j.visres.2015.03.001

Stockman, A., & Sharpe, L. T. (2006). Into the twilight zone: The complexities of mesopic vision and luminous efficiency. *Ophthalmic and Physiological Optics*, *26*(3), 225–239. https://doi.org/10.1111/j.1475-1313.2006.00325.x

Striem-Amit, E., Ovadia-Caro, S., Caramazza, a., Margulies, D. S., Villringer, a., & Amedi, a. (2015). Functional connectivity of visual cortex in the blind follows retinotopic organization principles. *Brain*, 1679–1695. https://doi.org/10.1093/brain/awv083

Sullivan, E. V., Rohlfing, T., & Pfefferbaum, A. (2010). Quantitative fiber tracking of lateral and interhemispheric white matter systems in normal aging: Relations to timed performance. *Neurobiology of Aging*, *31*(3), 464–481. https://doi.org/10.1016/j.neurobiolaging.2008.04.007

Sunness, J. S., Liu, T., & Yantis, S. (2004). Retinotopic mapping of the visual cortex using functional magnetic resonance imaging in a patient with central scotomas from atrophic macular degeneration. *Ophthalmology*, *111*(8), 1595–1598. https://doi.org/10.1016/j.ophtha.2003.12.050

Tejeria, L., Harper, R. A., Artes, P. H., & Dickinson, C. M. (2002). Face recognition in age related macular degeneration: perceived disability, measured disability, and performance with a bioptic device. *The British Journal of Ophthalmology*, *86*(9), 1019–1026. https://doi.org/10.1136/bjo.86.9.1019

Tellouck, L., Durieux, M., Coupé, P., Cougnard-Grégoire, A., Tellouck, J., Tourdias, T., … Schweitzer, C. (2016). Optic radiations microstructural changes in glaucoma and association with severity: A study using 3tesla-magnetic resonance diffusion tensor

imaging. *Investigative Ophthalmology and Visual Science*, *57*(15), 6539–6547. https://doi.org/10.1167/iovs.16-19838

Thambisetty, M., Wan, J., Carass, A., An, Y., Prince, J. L., & Resnick, S. M. (2010). Longitudinal changes in cortical thickness associated with normal aging. *NeuroImage*, *52*(4), 1215–1223. https://doi.org/10.1016/j.neuroimage.2010.04.258

Thibaut, M., Delerue, C., Boucart, M., & Tran, T. H. C. (2016). Visual exploration of objects and scenes in patients with age-related macular degeneration. *Journal Français d'ophtalmologie*, *39*(1), 82–89. https://doi.org/10.1016/j.jfo.2015.08.010

Thomason, M. E., & Thompson, P. M. (2011). Diffusion Imaging, White Matter, and Psychopathology. *Annual Review of Clinical Psychology*, *7*(1), 63–85. https://doi.org/10.1146/annurev-clinpsy-032210-104507

Timmler, S., & Simons, M. (2019). Grey matter myelination. *Glia*, *67*(11), 2063–2070. https://doi.org/10.1002/glia.23614

Tran, T. H. C., Rambaud, C., Despretz, P., & Boucart, M. (2010). Scene Perception in Age-Related Macular Degeneration. *Investigative Opthalmology & Visual Science*, *51*(12), 6868. https://doi.org/10.1167/iovs.10-5517

Tschernutter, M., Schlichtenbrede, F. C., Howe, S., Balaggan, K. S., Munro, P. M., Bainbridge, J. W. B., … Ali, R. R. (2005). Long-term preservation of retinal function in the RCS rat model of retinitis pigmentosa following lentivirus-mediated gene therapy. *Gene Therapy*, *12*(8), 694–701.

Turner, R., Howseman, A., Rees, G. E., Josephs, O., & Friston, K. (1998). Functional magnetic resonance imaging of the human brain: data acquisition and analysis. *Exp Brain Res*, *123*(1–2), 5–12. https://doi.org/10.1007/s002210050538

van den Hurk, J., Van Baelen, M., & Op de Beeck, H. P. (2017). Development of visual category selectivity in ventral visual cortex does not require visual experience. *Proceedings of the National Academy of Sciences*, *114*(22), E4501–E4510. https://doi.org/10.1073/pnas.1612862114

Van Essen, D. C., Glasser, M. F., Dierker, D. L., Harwell, J., & Coalson, T. (2012). Parcellations and Hemispheric Asymmetries of Human Cerebral Cortex Analyzed on Surface-Based Atlases. *Cerebral Cortex*, *22*(10), 2241–2262. https://doi.org/10.1093/cercor/bhr291

Vernon, R. J. W., Morland, A. B., Wade, A. R., Lawrence, S. J. D., & Gouws, A. D. (2016). Multivariate Patterns in the Human Object-Processing Pathway Reveal a Shift from Retinotopic to Shape Curvature Representations in Lateral Occipital Areas, LO-1 and LO-2. *Journal of Neuroscience, 36*(21), 5763–5774. https://doi.org/10.1523/jneurosci.3603-15.2016

Wandell, B. A., Dumoulin, S. O., & Brewer, A. A. (2007). Visual Field Maps in Human Cortex. *Neuron, 56*(2), 366–383. https://doi.org/10.1016/j.neuron.2007.10.012

Wang, M. Y., Wu, K., Xu, J. M., Dai, J., Qin, W., Liu, J., … Shi, D. (2013). Quantitative 3-T diffusion tensor imaging in detecting optic nerve degeneration in patients with glaucoma: Association with retinal nerve fiber layer thickness and clinical severity. *Neuroradiology, 55*, 493–498. https://doi.org/10.1007/s00234-013-1133-1

Warrington, S., Bryant, K. L., Khrapitchev, A. A., Sallet, J., Charquero-Ballester, M., Douaud, G., … Sotiropoulos, S. N. (2020). XTRACT - Standardised protocols for automated tractography in the human and macaque brain. *NeuroImage, 217*, 116923. https://doi.org/10.1016/j.neuroimage.2020.116923

Weiner, K. S., Barnett, M. A., Witthoft, N., Golarai, G., Stigliani, A., Kay, K. N., … Grill-Spector, K. (2018). Defining the most probable location of the parahippocampal place area using cortex-based alignment and cross-validation. *NeuroImage, 170*, 373–384. https://doi.org/10.1016/j.neuroimage.2017.04.040

Weiner, K. S., Golarai, G., Caspers, J., Chuapoco, M. R., Mohlberg, H., Zilles, K., … Grill-Spector, K. (2014). The mid-fusiform sulcus: A landmark identifying both cytoarchitectonic and functional divisions of human ventral temporal cortex. *NeuroImage, 84*, 453–465. https://doi.org/10.1016/j.neuroimage.2013.08.068

Weiner, K. S., & Zilles, K. (2016). The anatomical and functional specialization of the fusiform gyrus. *Neuropsychologia, 83*, 48–62. https://doi.org/10.1016/j.neuropsychologia.2015.06.033

Wiesel, T. N., & Hubel, D. H. (1963). EFFECTS OF VISUAL DEPRIVATION ON MORPHOLOGY AND PHYSIOLOGY OF CELLS IN THE CATS LATERAL GENICULATE BODY. *Journal of Neurophysiology, 26*, 978–993. https://doi.org/10.1152/jn.1963.26.6.978

Wiesel, T. N., & Hubel, D. H. (1965). Comparison of the effects of unilateral and bilateral

eye closure on cortical unit responses in kittens. *Journal of Neurophysiology*, *28*(6), 1029–1040. https://doi.org/10.1152/jn.1965.28.6.1029

Williams, A. L., Lackey, J., Wizov, S. S., Chia, T. M. T., Gatla, S., Moster, M. L., … Lai, S. (2013). Evidence for widespread structural brain changes in glaucoma: A preliminary voxel-based MRI study. *Investigative Ophthalmology and Visual Science*, *54*(8), 5880–5887. https://doi.org/10.1167/iovs.13-11776

Williams, M. a, Baker, C. I., Op de Beeck, H. P., Shim, W. M., Dang, S., Triantafyllou, C., & Kanwisher, N. (2008). Feedback of visual object information to foveal retinotopic cortex. *Nature Neuroscience*, *11*(12), 1439–1445. https://doi.org/10.1038/nn.2218

Williamson, J. M., & Lyons, D. A. (2018). Myelin Dynamics Throughout Life: An Ever-Changing Landscape? *Frontiers in Cellular Neuroscience*, *12*, 424. https://doi.org/10.3389/fncel.2018.00424

Winklewski, P. J., Sabisz, A., Naumczyk, P., Jodzio, K., Szurowska, E., & Szarmach, A. (2018). Understanding the physiopathology behind axial and radial diffusivity changes-what do we Know? *Frontiers in Neurology*. https://doi.org/10.3389/fneur.2018.00092

Winter, B. (2013a). Linear models and linear mixed effects models in R: Tutorial 1, 1–22.

Winter, B. (2013b). Linear models and linear mixed effects models in R: Tutorial 2, (Tutorial 2), 1–22.

Worsley, K. J. (2001). Statistical analysis of activation images. In *Functional Magnetic Resonance Imaging* (Vol. 17, pp. 251–270). Oxford University Press. https://doi.org/10.1093/acprof:oso/9780192630711.003.0014

Xin, W., & Chan, J. R. (2020). Myelin plasticity: sculpting circuits in learning and memory. *Nature Reviews Neuroscience*. https://doi.org/10.1038/s41583-020-00379-8

Yacoub, E., Duong, T. Q., Van De Moortele, P. F., Lindquist, M., Adriany, G., Kim, S. G., … Hu, X. (2003). Spin-echo fMRI in humans using high spatial resolutions and high magnetic fields. *Magnetic Resonance in Medicine*, *49*(4), 655–664. https://doi.org/10.1002/mrm.10433

Yang, H., Long, X.-Y., Yang, Y., Yan, H., Zhu, C.-Z., Zhou, X.-P., … Gong, Q.-Y. (2007). Amplitude of low frequency fluctuation within visual areas revealed by resting-state functional MRI. *NeuroImage*, *36*(1), 144–152.

https://doi.org/10.1016/j.neuroimage.2007.01.054

Yeatman, J. D., Dougherty, R. F., Myall, N. J., Wandell, B. A., & Feldman, H. M. (2012). Tract Profiles of White Matter Properties: Automating Fiber-Tract Quantification. *PLoS ONE*, *7*(11), e49790. https://doi.org/10.1371/journal.pone.0049790

Yeatman, J. D., Wandell, B. A., & Mezer, A. A. (2014). Lifespan maturation and degeneration of human brain white matter. *Nature Communications*, *5*(1), 1–12. https://doi.org/10.1038/ncomms5932

Yoshimine, S., Ogawa, S., Horiguchi, H., Terao, M., Miyazaki, A., Matsumoto, K., … Pestilli, F. (2018). Age-related macular degeneration affects the optic radiation white matter projecting to locations of retinal damage. *Brain Structure and Function*, *223*(8), 3889–3900. https://doi.org/10.1007/s00429-018-1702-5

Young, M. T., Braich, P. S., & Haines, S. R. (2018). Critical flicker fusion frequency in demyelinating and ischemic optic neuropathies. *International Ophthalmology*, *38*(3), 1069–1077. https://doi.org/10.1007/s10792-017-0561-z

Zhang, D., Liang, B., Wu, X., Wang, Z., Xu, P., Chang, S., … Huang, R. (2015). Directionality of large-scale resting-state brain networks during eyes open and eyes closed conditions. *Frontiers in Human Neuroscience*, *9*(February), 1–10. https://doi.org/10.3389/fnhum.2015.00081

Zhang, Y. Q., Li, J., Xu, L., Zhang, L., Wang, Z. C., Yang, H., … Jonas, J. B. (2012). Anterior visual pathway assessment by magnetic resonance imaging in normal-pressure glaucoma. *Acta Ophthalmologica*, *90*(4), e295–e302.

Zhou, W., Muir, E. R., Nagi, K. S., Chalfin, S., Rodriguez, P., & Duong, T. Q. (2017). Retinotopic fMRI Reveals Visual Dysfunction and Functional Reorganization in the Visual Cortex of Mild to Moderate Glaucoma Patients. *Journal of Glaucoma*, *26*(5), 430–437. https://doi.org/10.1097/IJG.0000000000000641

Zlateva, G. P., Javitt, J. C., Shah, S. N., Zhou, Z., & Murphy, J. G. (2007). Comparison of comorbid conditions between neovascular age-related macular degeneration patients and a control cohort in the medicare population. *Retina*, *27*(9), 1292–1299. https://doi.org/10.1097/01.iae.0000300915.81866.b8

Zou, Q., & Long, X. (2009). Functional Connectivity under Eyes Closed and Eyes Open: Resting State. *Pmc*, *30*(9), 3066–3078. https://doi.org/10.1002/hbm.20728.Functional